LEUPHANA
UNIVERSITÄT LÜNEBURG

The Reactions of Mixed Salts in Advanced Heat Storage Systems

---

A Dissertation for obtaining a Doctorate degree in Natural Sciences

(Dr. rer. nat.)

presented by

Dipl.-Min., Dipl.-Met. Mona-Maria Druske

June, 2018

The Reactions of Mixed Salts in Advanced Heat Storage Systems

---

Eine Dissertation der Fakultät Nachhaltigkeit der Leuphana Universität Lüneburg zur Erlangung des Grades Doktorin der Naturwissenschaften

(Dr. rer. nat.)

Vorgelegte Dissertation von

Dipl.-Min., Dipl.-Met. Mona-Maria Druske

Geb.: 11.01.1974 In: Eutin, Germany

Eingereicht am:

Betreuer und Gutachter

Gutachter

Gutachter

Tag der Disputation:

Summary

To improve the properties of thermochemical heat storage materials, salt mixtures were evaluated for their heat storage capacity and cycle stability as part of the innovation incubator project “Thermochemical battery” of the Leuphana university Lüneburg. Based on naturally occurring compound minerals, 16 sulfates, 18 chlorides and 5 chloride multi-mixtures, 18 bromides and 5 intermixtures between sulfates, chlorides and bromides were synthesized either from liquid solution or by dry mixing for TGA/DSC screening before continuing the heat storage evaluation with five different measurement setups at a laboratory scale.

The TGA/DSC analysis served as a screening process to reduce the number of testing materials for the upscaled experiments. The evaluation process consisted of a three-cycle dehydration/hydration measurement at T_{max} = 100°C and T_{max} = 200°C. In case of the bromide samples a measurement of hydration conditions with T_{max} = 110°C and a water flow at e = 18.68mbar, were added to the procedure to detect the maximum water uptake temperature. Also, a single dehydration to a temperature of T_{max} = 500°C was implemented to observe melting behavior and to easier calculate the samples’ stages of hydration from the remaining anhydrous mass. Materials which showed high energy storage density and improved cycle stability during this first evaluation were cleared for multi-cycle measurements of 10 to 25 dehydration and hydration cycles at T_{max} = 100 to 120°C and the evaluations at m = 20 to 100g scale. An estimate for the specific heat capacities at different temperatures of the materials which passed the initial stage was calculated from the TGA/DSC results as well.

The laboratory scale measurement setup went through five stages of refining, which led to reducing the intended maximum sample mass from m = 100g to m = 20g. A switch from supplied liquid water to water vapor as the used reactant was also implemented in exchange for improved dehydration conditions. Introducing a vacuum pump for evaporating the water limited the influence of outside heat sources during hydration and in-situ dehydration was enabled as to not disturb the state the samples were settling in between measurements. Baseline calculation from blanc measurements with glass powder and attempts to calculate the specific heat capacity c_p of the tested materials by

applying the Joule-Lenz-law to the measurement apparatus was another step of method development.

The evaluation process of the laboratory scale tests at the final setting consisted of 1 to 5 cycle measurements of in-situ dehydration and hydrations with applied vacuum for t = 30 minutes at p ~ 30mbar.

Upscaling the sample mass to m = 20g allowed for a close observation of different material behaviors. Agglomeration, melting and dissolving of the m = 10mg samples during the TGA/DSC analysis can be deducted from the recorded measurement curves and the state of the sample after measurement. However, at laboratory scale the visible volume changes, observed sample consistency after agglomeration and an automatic removal of molten and dissolved sample mass during the measurement allowed for a better characterization and understanding of the magnitude of the actual changes. This was done for the first time, particularly for mixed salts.

Of the original number of 62 samples, 4 mixtures which passed the initial TGA/DSC screening namely {$2MgCl_2$+ KCl}, {$2MgCl_2$+$CaCl_2$}, {$5SrBr_2$+$8CaCl_2$} and {$2ZnCl_2$ + $CaCl_2$} were chosen for further evaluation. The multi-cycle TGA/DSC measurements of {$2MgCl_2$+ KCl}, {$2MgCl_2$+$CaCl_2$} and {$5SrBr_2$+$8CaCl_2$} showed an improved cycle stability for all three materials over the untreated educts.

Of the four materials {$2ZnCl_2$ + $CaCl_2$} displayed the strongest deliquescence during hydration in the upscaled experimental setup.

{$2MgCl_2$+$CaCl_2$} proved to be the most stable material regarding the heat storage density. The {$MgCl_2$} content of the mixture is likely to partially or completely react to {Mg(OH)Cl} at temperatures of T > 110°C, which however does not impede the heat storage density.

{$5SrBr_2$+$8CaCl_2$} displayed a low melting point in hydrated state, causing a fast material loss. This makes it an undesirable storage material. A lower heating rate may still help to avoid an early melting.

The {$2MgCl_2$+KCl} mixture was the most temperature stable of the mixtures showing no melting or dissolving behavior. A reaction of the {$MgCl_2$} component of the mixture to {Mg(OH)Cl} was not observed within the applied temperature range of T = 25 to 200°C.

Table of contents

Formula symbols

T temperature in [°C] or [K] as required by applied formula.

t time [s]

m sample mass in [g]

p pressure in [bar]

e partial water vapor pressure [bar]

$\dot{V}$ volume flow of N_2 in [ml min^{-1}]

I electric current [A]

U electric voltage [V]

Q heat [J]

ϕ heat flow in [W]

β heating rate in [Kmin^{-1}]

H reaction enthalpy in [Jg^{-1}]

c_p specific heat capacity at constant pressure in [J(gK)$^{-1}$]

C_p specific heat capacity for 1 mol at constant pressure in [JK^{-1}]

C_a heat capacity of a measurement apparatus [JK^{-1}]

2Θ scattering angle of x-ray beams in powder diffraction in [°]

Ø diameter in [m]

1. Introduction

While there are many different methods to conserve excess electricity, the storage of heat energy in the modern context of energy transition (i.e. Power-to-heat and heat storages for flexibilization of combined heat and power (chp) units) is a relatively new concept which sets new goals in regards of system requirements and the properties of the storage materials to be used.

The choice of the method has a great influence on the overall heat loss during storage, the available temperature range, the size of the storage system, expenditure on maintenance and the overall material costs.

The necessity for energy- and cost-efficiency speaks for itself but the other factors also play a role in the successful implementation. Too large a system size will prevent its use in older flats and buildings where the available space is limited, while charging and discharging temperatures exceeding T_{max} = 100°C or the necessity of constant maintenance and supervision may render a system useless for anything but industrial applications.

Of the different storage methods, thermochemical storage is attractive because it avoids a continuous loss of heat and can be used for long term storage efficiently. Thermochemical storage materials also come with higher storage densities than sensible heat storage materials and some of the lowest material costs compared to latent or adhesion-based heat storage systems. But the materials also bring many challenges that need to be overcome before an efficient battery system can be created.

Thermochemical storage in particular needs materials which will not decompose, melt, dissolve, agglomerate or emit corrosive or otherwise dangerous byproducts within the expected temperature conditions, to allow for a cost-efficient battery that can be used over many charging and discharging cycles without additional maintenance.

1.1. Temperature ranges

As mentioned above, heat storage systems have to be distinguished into household and industrial applications. The main difference is the temperature range a system is operating within. For industrial settings heat storage systems are of interest which are

providing a temperature range of T = 400 to 1000°C. The transport of the heat in such a high temperature range to a battery and the redistribution from that same battery, require specialized transport media and systems.

To stay cost efficient, Household systems have to rely on water for the heat transfer to and from the battery and thus ideally should not exceed a charging temperature of T_{max} = 100°C which marks the boiling point of water at normal pressure of p = 1 bar. Additionally, heat sources of T > 100°C are not easily available in typical household settings either. A combined heat and power unit (CHP) operates at T_{max} = 80 to 95°C (Messerschmid-Energiesysteme, 2011), (EC POWER A/S, 2016), (Energiewerkstatt, 2017), while solar heat exchangers operate within a temperature range of T = 30 to 75°C (Wolf-Heiztechnik, 2005), (Wagner&Co, 2007).

However, operating temperatures below T_{max} = 150°C are still considered as low temperature applications for heat storage systems (Scapino, Zondag, Van Bael, Diriken, & Rindt, 2017).

2. Heat storage Systems – an overview

2.1. Systems

2.1.1. Sensible heat storage

Due to continuous loss of heat, sensible heat storage systems are mainly useable for short term storage.

Their basic construction is relatively simple only requiring an insulated tank filled with the chosen storage material. The material is then heated up for the remaining heat to be retrieved again several hours or days later. The insulation is supposed to slow the continuous loss of heat down to a minimum as shown in the schematic in Figure 1. At temperatures below T_{max} = 100°C water is a cost-efficient, environmentally compatible material-choice for storage.

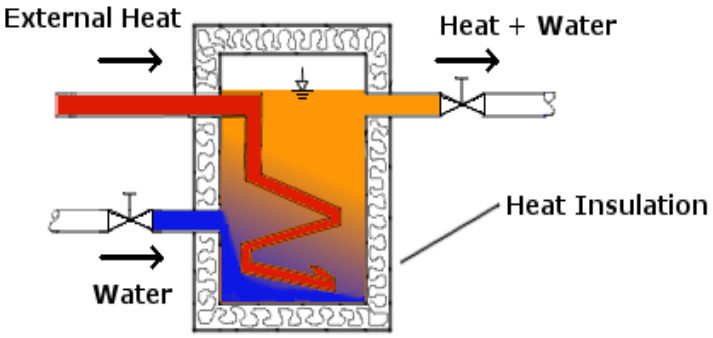

Figure 1 Sensible heat storage system based on water as storage material. The water is heated by an external heat source. The tank is insulated to slow down the heat loss during storage. Hot water can be stored until retrieval for a few hours up to days depending on the volume of the stored water and the efficiency of the insulation.

By optimizing the insulation and heating a huge body of storage material, the efficient storage duration can be extended. However, the increase in volume of the storage tanks makes the system unattractive for households with limited available storage space.

Aside from household applications, there are large scale district heating solutions using sensible heat storage.

In regions where subterranean aquifers are available, underground thermal energy storage (UTES) becomes an option with the surrounding rock layers

serving as the insulation which allows for effective storage times of several months.

The next large-scale option is a solar pond system, where a gradient in salinity separates the body of the water into different layers of different temperatures, with the upper layers serving as the insulation for the lower layers. (Kalaiselvam & Parameshwaran, 2014)

Another form of sensible heat storage is the rock bed thermal storage, where instead of water, rock is loosely packed into a bed-formation to serve as the storage material and air as the heat transport medium (Kalaiselvam & Parameshwaran, 2014).

2.1.2. Latent heat storage

Latent heat storage avoids the continuous loss of heat which is the main drawback of sensible heat storage. Charge and discharge of the battery are caused by changing the phase of the storage material from solid to liquid and back as seen as a schematic in Figure 2. The charged material can be stored indefinitely until the solidification and with it the discharge is triggered. Latent heat storage materials can be organic (paraffins, non-paraffins), inorganic salt hydrates or eutectic materials and the latent heat storage is separated into external and internal melt-ITES systems or chilled water-PCM TES systems, where each of those has different merits and drawbacks. (Kalaiselvam & Parameshwaran, 2014)

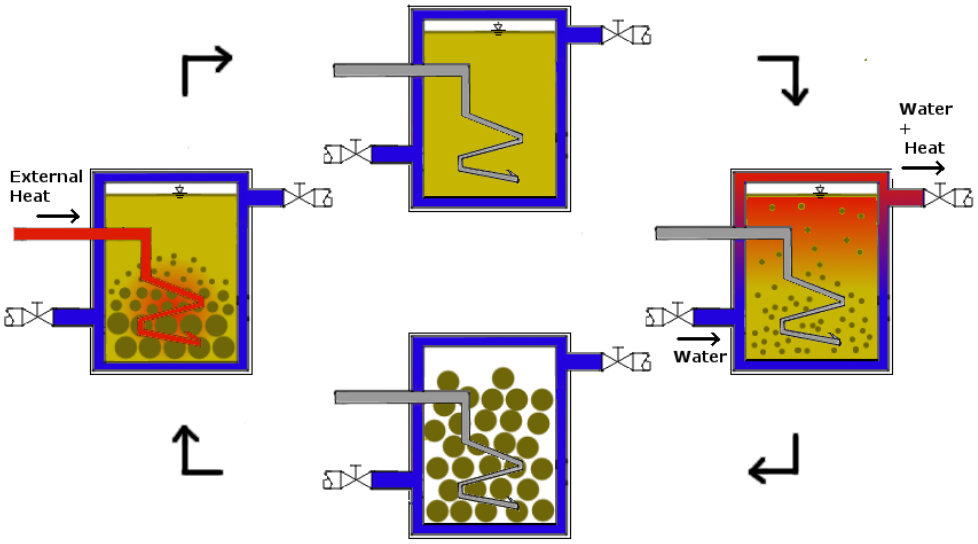

Figure 2 Schematics of a latent heat storage system. The solid storage material is molten by an external heat source and stored in its cooled down liquid form until the recrystallization is mechanically triggered. During the formation of the solid phase heat is released. The material is then stored in solid form until the battery is recharged.

2.1.3. Adhesive heat storage materials

Drying agents, which bind solvent molecules (such as water {H_2O}, ammoniac {NH_3}, ethanol {C_2H_6O} or methanol {CH_4O}) to their surface without a phase change or continuous loss of heat are some of the most cycle-stable and efficient heat storage materials available. Upon charging, the material is heated until the solvent breaks away from its surface. However drying agents such as zeolites come at relatively high cost and are not cost-efficient for household applications.

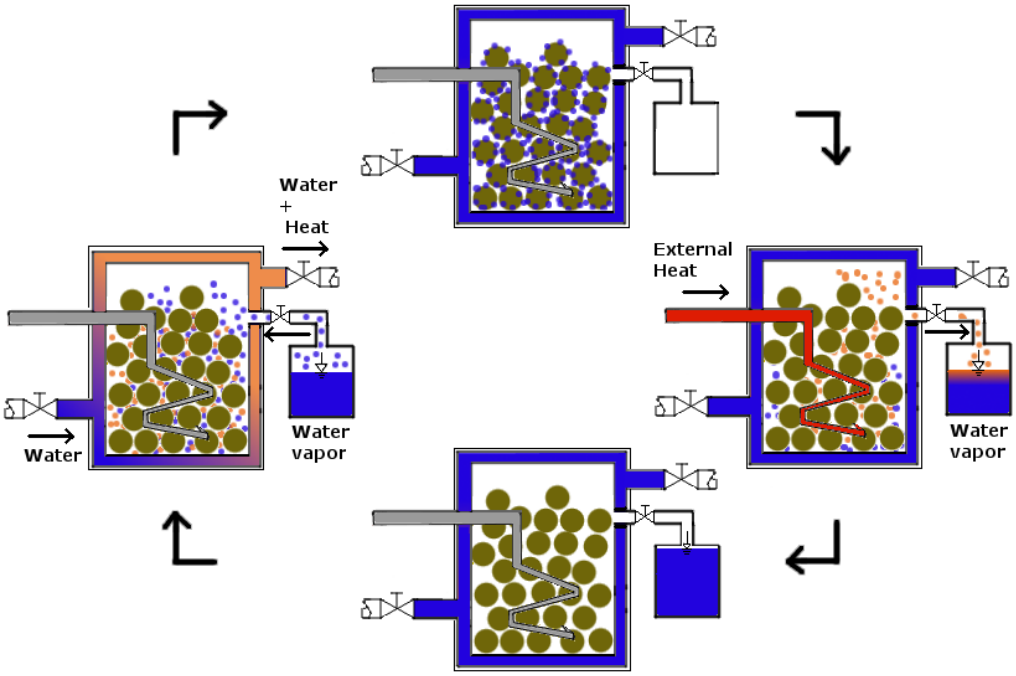

Figure 3 Heat storage based on adhesive or chemically reacting storage materials. A solid storage material is brought into contact with a gaseous solvent such as water, alcohol or ammoniac. An adhesive material binds the solvent to its surface, while a thermochemical material incorporates the solvent into its crystal structure. In both cases heat is released until the material can't adsorb or absorb more solvent. The heat is transported away by a separate current of a transport liquid (water, oil, etc.). To recharge the battery, external heat is applied until the solvent breaks free and is stored in an extra storage space separated from the solid material. In dried state, the solid material can be stored indefinitely before the battery is discharged again.

2.1.4. Thermochemically reacting storage materials

Thermochemical storage systems are set up similar as adhesive systems. The solid storage material however incorporates a gaseous solvent into its crystal lattice in a reversible thermochemical reaction (Donkers, 2015):

$$A \cdot nB[s] \overset{Heat}{\Longleftrightarrow} A \cdot (n-x)B[s] + xB[g]$$

$$with$$

$A := Storage\ material$

$B := Solvent$

$n := amount\ of\ solvent\ within\ the\ crystal\ lattice$

$x := amount\ of\ released\ or\ to\ be\ incorporated\ solvent$

$[s] := solid$

$[g] := gaseous$

Said gaseous solvents can be water-vapor {H_2O}, ammoniac {NH_3}, ethanol {C_2H_6O} or methanol {CH_4O}) similar as in adhesion-based heat storage systems. The solid storage materials of interest are salts due to their good availability and their (generally) low costs.

The salts can be stored in charged state for an indefinite span of time, as long as they are kept from contact to solvents. Due to the high heat storage density of the thermochemical reacting salts, a battery system of a compact volume can be constructed, to fit into buildings with limited space.

However, in practical application there are several unwanted properties of those salts considered as storage materials, which need to be mitigated before a battery system can be fitted with them efficiently.

2.2. Challenges of chemical heat storage systems

For several materials which show the necessary heat storage capacity to be considered as storage materials, the temperature ranges required for dehydration exceed what is practical for household applications (T_{max} = 100°C) as seen in the results taken from literature (Kerkes & et al., 2011) in Table 1.

Furthermore, as a chemical reaction takes place within the storage material by adding the solvent or heat, alterations in its phase or macroscopic structure like melting, dissolving, decomposition or agglomeration may occur.

Reaction	Temperature interval [°C]
$MgSO_4 \cdot 7H_2O \underset{heat}{\Longleftrightarrow} MgSO_4 \cdot H_2O + 6H_2O$	100 to 150
$MgCl_2 \cdot 6H_2O \underset{heat}{\Longleftrightarrow} MgCl_2 \cdot H_2O + 5H_2O$	100 to 130
$CaCl_2 \cdot 6H_2O \underset{heat}{\Longleftrightarrow} CaCl_2 \cdot H_2O + 5H_2O$	150 to 200
$CuSO_4 \cdot 5H_2O \underset{heat}{\Longleftrightarrow} CuSO_4 \cdot H_2O + 4H_2O$	120 to 160

Table 1 Reversible reactions and temperature intervals (Kerkes & et al., 2011) for salts considered as thermochemical storage materials.

The unwanted melting leads to an incomplete recrystallization and the solidification as a non-permeable layer of amorphous material. Such a layer blocks the solvent from reaching any storage material below, which may have preserved its crystalline structure. Since such amorphous phases do not have a crystal-lattice to incorporate solvents into, this leads to an overall decrease of the heat storage capacity of the material with every cycle. As the melting point decreases with the degree of hydration, especially hydrated phases need to be exposed slowly to the heat during the charging process, so excess water may escape before melting or dissolving can occur. Another way of reducing the occurrence of melting is to limit the supply of solvent during discharge to avoid the formation of the higher hydrated phases and keep the material's melting point within a high temperature range which is not met during charge.

A deliquescent material will also dissolve when exposed to too high amounts of solvent or when the exposure is extended over too long a timespan. While such materials may share the same issues with incomplete recrystallization as those of a low melting point, here the effect can be mitigated by strict regulation of the amount of solvents added and the duration of exposure.

Another issue to bear in mind is the thermal conductivity of the used salts. If the temperature within the material rises over a certain threshold during the hydration, the discharge may come to a hold until the heat can be conducted away. This can be circumvented by the battery design incorporating metallic components of high heat conductivity but can easier be dealt with by choosing materials which are still

able to incorporate solvents at elated temperatures. If used, metallic conductor components can be costly as they need to be treated against corrosion. They also take up extra volume better used for storage material and increase the overall weight of the battery.

As the solvent to be used in thermochemical heat storage, water is the most cost-efficient choice. Not only is it widely available, it is also non-flammable, non-poisonous, non-corrosive on its own and environmentally neutral. However, many of the unwanted material properties such as agglomeration, deliquescence and decomposition combined with production of unwanted byproducts (HCl, $Fe^{3+}{}_2O_3$) can be observed during the hydration or dehydration of the salts. Also, metal parts of the battery may corrode over time when in continuous contact with saltwater.

The drawback of using ammoniates or alcoholates as solvents is that any salt that may be used as a material will firstly integrate water into its crystal structure before absorbing other supplied solvents, as long as any form of water-source is available. This means that the storage material needs to be prepared and stored under exclusion of air humidity to prevent unwanted chemical alterations. Furthermore, ammoniac is poisonous, noxious and corrosive. While of the alcohols for example ethanol is easily flammable and methanol is flammable, poisonous and a health hazard.

An advantage is that there is no reported melting/dissolving during heating at low temperatures for ammoniates or alcoholates as is observed for some hydrates ({$CaCl_2 \cdot 4H_2O$}, $T_{melt/dissolve}$ = 35 to 45.5°C (IFA Institut für Arbeitsschutz Datenbank), (Ropp, 2012)).

2.3. Related studies and material evaluations

Within the innovation incubator project “Thermochemical battery” of the Leuphana university Lüneburg which this work is also a part of, several studies were and are still published about the thermochemical storage performance of different salt hydrates.

The dissertation paper (Fopah Lele, 2016) provides an introduction into the economic and ecologic merits of heat storage applications, as well as a detailed overview of the different types of sorption-based storage methods. It is focused on linking up combined heat and power (CHP) systems with thermochemical storage systems for higher energy efficiency and the significant heat and mass transfer mechanics for the related processes.

Especially calcium chloride and calcium oxide were screened for their heat storage capacities in different system setups, with the goal to increase the cycle stability of the reversible processes.

A full study of the performance of {$CaCl_2$}-hydrates as PCM (phase changing materials), sorption and the possible thermochemical application was performed by (N'Tsoukpoe, et al., 2015).

The reversible hydration and dehydration reactions of {CaO} and {$CaCl_2$}, observed with TGA/DSC were exemplified during the IRES conference 2011 (Rammelberg, Opel, Ross, & Ruck, 2011).

(Fopah Lele, et al., 2013) covered methods to measure and improve the relatively low thermal conductivity and cycle stability of salt hydrates by impregnating matrix materials, such as Silica Gel and Expanded Vermiculite, with brines of the salt {$CaCl_2$}.

The thermodynamic storage performance, cycle stability and thermal conductivity of mixed salt hydrates of {$CaCl_2$ + KCl}, which were crystallized from a brine and different $CaCl_2$-impregnated matrices were compared and discussed at the ICAE conference 2014 (Druske, et al., 2014). The afore mentioned properties of the materials were then elaborated later in an extended article (Korhammer, et al., 2015).

As an alternative for water, alcoholates were tested for their qualities as solvents in sorption-based heat storage systems, based on TGA/DSC evaluations.

Ethanol as a solvent in combination with calcium chloride and magnesium chloride as well as mixed calcium-magnesium chlorides was the focus of the article (Korhammer, Apel, Osterland, & Ruck, 2016), showing that systems with the materials {$CaCl_2$ + C_2H_5OH} and {$2CaCl_2 \cdot MgCl_2$ + C_2H_5OH} showed improved sorption properties and cycle stability compared to systems using {H_2O} as a solvent.

A combination of methanol as the solvent and calcium chloride as the storage material showed not only possible application in heat storage systems but also possibilities for implementation in evaporation-based cooling systems (Korhammer, Neumann, Opel, & Ruck, 2017).

The cumulative thesis paper (Rammelberg, 2015), includes the articles

- (Opel, Rammelberg, Gérard, & Ruck, 2011) which describes method development and experimental setups for TGA/DSC evaluations with the goal to observe the hydration and dehydration cycles of thermochemical storage materials.

- (Rammelberg, Schmidt (Osterland), & Ruck, 2012) where the thermochemical hydration and dehydration behavior, heat storage capacity and cycle stability of {$Ca(OH)_2$} ↔ {$CaO + H_2O$}, {$CaCl_2 \cdot 6H_2O$} ↔ {$CaCl_2 + 6H_2O$} and {$MgCl_2 \cdot 6H_2O$} ↔ {$MgCl_2 \cdot 2H_2O + 4H_2O$} were analyzed.

- (Khutia, Rammelberg, Schmidt (Osterland), Henniger, & Janiak, 2013), which investigates materials for adsorption-based heat storage systems, namely the water uptake and cycle stability of four nitro- or amino-functionalized MIL-101(Cr) materials (Highly Porous Metal-Organic

Framework) {$Cr_3O(OH)(H_2O)_2(bdc)_3$}, which were tested over 40 adsorption- and desorption-cycles.

- (N'Tsoukpoe, Schmidt (Osterland), Rammelberg, Watts, & Ruck, 2014), which contained an evaluation of operability, energy storage density and storage efficiency for 125 different salt hydrates based on TGA/DSC analysis data. This study did not yet include any mechanical mixtures or compounds of two or more salts.

- (Rammelberg, Myrau, Schmidt (Osterland), & Ruck, 2013) took the first steps into analyzing the properties of mechanically mixed {$MgCl_2$ + $CaCl_2$} samples by TGA/DSC. The results were published then during the IMPRESS conference 2013.

- (Rammelberg, Osterland, Priehs, Opel, & Ruck, 2015), which picked up on the properties of mechanically mixed {$MgCl_2$ + $CaCl_2$} samples, measured by TGA/DSC, with the conclusion that a distinct improvement of the cycle stability of the material was observed.

However, whilst Rammelberg et al. experimented with mixed materials, there were no attempts made, to systematically grow compound salts from brines, nor were differences in cycle stability and heat storage capacity linked to the crystal lattices of the materials nor were larger material units than mg-scale samples evaluated. Therefore, the present study will cover those issues.

2.4. Improving material properties by changes in the crystal structure

As the material behavior is tied to the crystal structure (for example how much water a crystal may draw in before its structure breaks down and the material

dissolves) a complete monitoring of the different changes of phase within the structures would be necessary, to predict the development of the desired properties.

Controlling the crystal-structure is possible by either regulating the amount of water available or by adding a second material to create a compound of a specific spacegroup.

Determining which phases or compounds are formed requires an x-ray-powder diffraction analysis (XRPD), while cycles of TGA/DSC measurements for the material behavior are necessary for the determining the heat storage density and calculate the water content. If a correlation between the changes in the crystal structures and the changes of the material properties are found, suitable materials can be searched for or created specifically by their crystal structure.

However, while there are materials such as {KCl} which will only occur in one phase ($Pm\bar{3}m$) as seen in Figure 4, most crystals will occur in multiple stages of hydration as seen for {$CaCl_2$} in Figure 5.

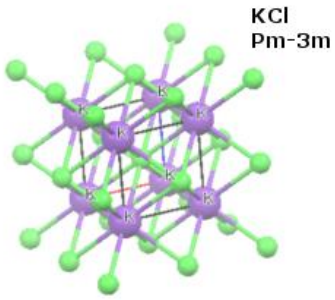

Figure 4 Crystal structure of {KCl} (P m $\bar{3}$ m) (Will, 1981), no hydrated forms are known. (Created with Mercury 3.1, 2015)

And even at the same state of hydration, a material may have more than one possible alignment as for example the {$MgCl_2$} in Figure 6 a) (R $\bar{\mathbf{3}}$ m) and b) (P $\bar{\mathbf{3}}$ m 1) which is opening up an even wider range of different material behaviors.

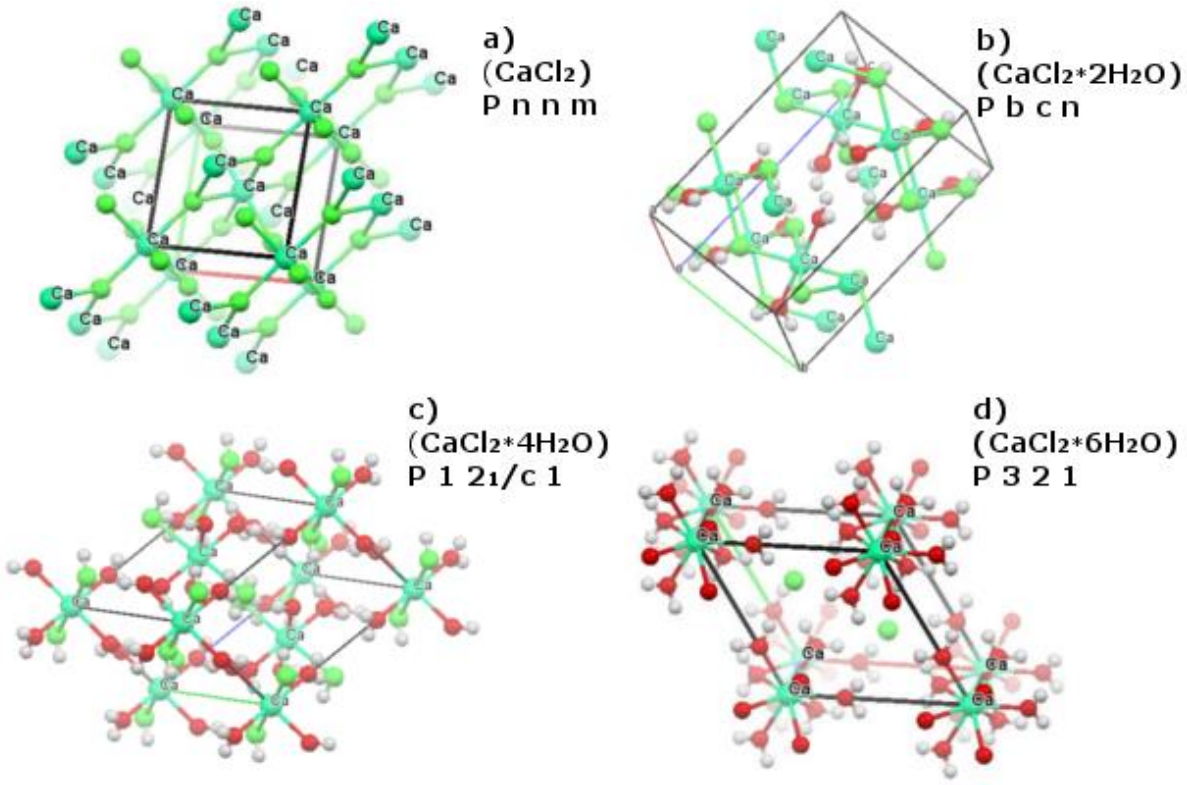

Figure 5 Changes in the crystal structure of $CaCl_2$ during hydration: a) {$CaCl_2$} ($P\ n\ n\ m$) (Wyckoff R. W., 1963), b) {$CaCl_2 \cdot 2H_2O$} ($P\ b\ c\ n$) (Leclair & Borel, 1977), c) {$CaCl_2 \cdot 4H_2O$} ($P\ 1\ \frac{2_1}{c}\ 1$) (Leclaire & Borel, 1980), d) {$CaCl_2 \cdot 6H_2O$} ($P\ 3\ 2\ 1$) (Leclaire & Borel, 1977); (Created with Mercury 3.1)

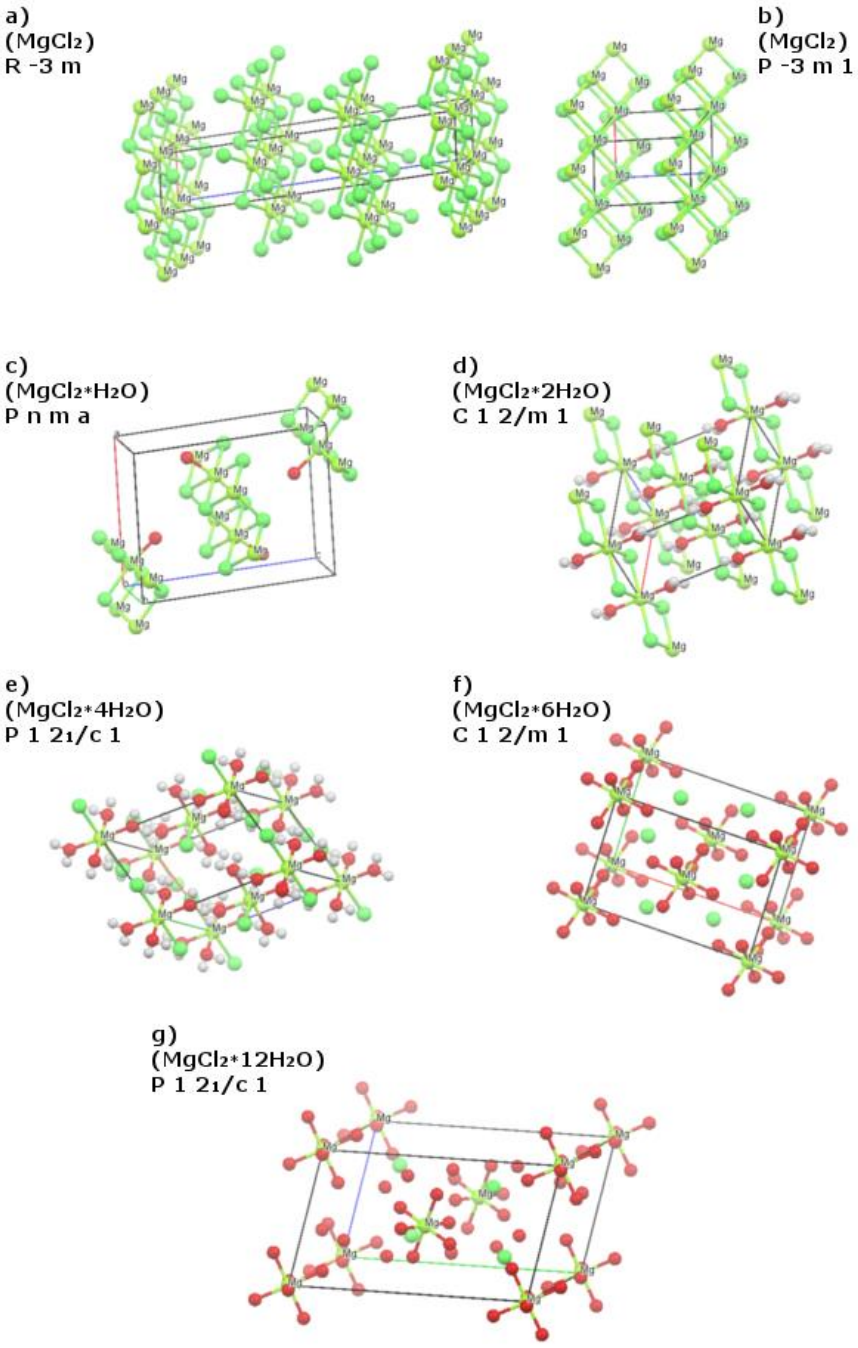

Figure 6 a) Changes in the crystal structure of {$MgCl_2$} during hydration: {$MgCl_2$} ($R\ \bar{3}\ m$) (Busing, 1970), b) {$MgCl_2$} ($P\ \bar{3}\ m\ 1$) (Bassi, Polanto, Calcaterra, & Bart, 1982), c) {$MgCl_2 \cdot H_2O$} ($P\ n\ m\ a$) (Kaduk, 2002), d) {$MgCl_2 \cdot 2H_2O$} ($C\ 1\ \frac{2}{m}\ 1$) (Kaduk, 2002), e) {$MgCl_2 \cdot 4H_2O$} ($P\ 1\ \frac{2_1}{c}\ 1$) (Kaduk, 2002), f) {$MgCl_2 \cdot 6H_2O$} ($C\ 1\ \frac{2}{m}\ 1$) (Andress & Gundermann, 1934), g) {$MgCl_2 \cdot 12H_2O$} ($P\ 1\ \frac{2_1}{c}\ 1$) (Sasvari & Jeffrey, 1966) As seen in a) and b) the anhydrate may occur in two different spacegroups. (Created with Mercury 3.1)

The crystal structures of naturally occurring compounds and synthetic copies of naturally occurring compounds (as for example Tachyhydrite {$CaMg_2Cl_6 \cdot 12H_2O$} or Carnallite {$KMgCl_3 \cdot 6H_2O$}) have been researched before (Clark, Evans, & Erd, 1980), (Leclaire, Borel, & Monier, 1980), (Fischer, 1973), (Schlemper, Sen Gupta, & Zoltai, 1985) but stable deviations of their natural compositions with different concentrations and variations of cations may exist, which have not yet been observed.

Even if no compound is formed within a mixture, the presence of two or more materials with different properties may stabilize the material over several cycles of hydration and dehydration by offering a base for recrystallization to a molten component, keeping neighboring grains from agglomerating or by acting as a secondary drying agent and drawing away excess water, preventing over-hydration. In that case a validation of the phases of each of the educts should reveal whether and how the two materials in the mixture balance each other's properties out.

3. Materials and methods

Chlorides, Sulfates and Bromides of Na, K, Li, Sr, Ca, Mg, Zn, Fe^{2+}, Fe^{3+} or Al are storage material candidates.

3.1. Educts used for synthesis

3.1.1. Sulfates

- Thenardite (Na_2SO_4) (Hawthorne & Ferguson, 1975), (Anthony, Bideaux, Bladh, & Nichols, 2003) it is orthorhombic and easily soluble in water. Thenardite hydrates at normal temperatures to Mirabilite ($Na_2SO_4 \cdot 10H_2O$) (Ericksen, Mrose, & Fahey, 1970); (Anthony, Bideaux, Bladh, & Nichols, 2003).

- Arcanite (K_2SO_4) (Mc Ginnety, 1972), (Anthony, Bideaux, Bladh, & Nichols, 2003) it is orthorhombic and easily soluble in water.

- Magnesium sulfate {$MgSO_4$} can occur naturally in different states of hydration as seen in Table 2.

- Zinc sulfate {$ZnSO_4$} occurs in several states of hydration of which the heptahydrate is known as the orthorhombic mineral Goslarite ($ZnSO_4 \cdot 7H_2O$) (Swanson, Gilfrich, Cook, Stinchfield, & Parks, 1959); (Anthony, Bideaux, Bladh, & Nichols, 2003).

- Iron-sulfate {$Fe^{2+}SO_4$} has several different hydration stages as seen in Table 3.

- Anhydrous aluminum sulfate {$Al_2(SO_4)_3$} does not occur naturally but there are minerals of two hydrated stages, the anorthic (triclinic) Alunogen ($Al_2(SO_4)_3 \cdot 17H_2O$) (Cesbron & Sadrzadeh, 1973), (Anthony, Bideaux,

Bladh, & Nichols, 2003) and the monoclinic Meta-alunogen ($Al_4(SO_4)_6 \cdot 27H_2O$) (Fleischer, 1943), (Anthony, Bideaux, Bladh, & Nichols, 2003), (Burke, 2008). For laboratory use it is sold as ($Al_2(SO_4)_3 \cdot 18H_2O$) (CAS #: 7784-31-8).

Table 2 Hydrated states of magnesium sulfate and their crystal systems. (Perroud, 2016)

Mineral	Formula	Crystal System	References
Magnesium sulfate	$MgSO_4$	Orthorhombic	(Lide, 2006)
Kieserite	$MgSO_4 \cdot H_2O$	Monoclinic	(Hawthorne, Groat, Raudsepp, & Ercit, 1987), (Anthony, Bideaux, Bladh, & Nichols, 2003)
Sanderite	$MgSO_4 \cdot 2H_2O$	(unknown)	(Fleischer, 1952), (Kali und Steinsalz 4, 1967)
Starkeyite	$MgSO_4 \cdot 4H_2O$	Monoclinic	(Snetsinger, 1975), (Anthony, Bideaux, Bladh, & Nichols, 2003)
Cranswickite	$MgSO_4 \cdot 4H_2O$	Monoclinic	(Weiß, 2010), (Williams, Hatert, Pasero, & Mills, 2010)
Pentahydrate	$MgSO_4 \cdot 5H_2O$	Anorthic (Triclinic)	(Baur & Rolin, 1972), (Anthony, Bideaux, Bladh, & Nichols, 2003)
Hexahydrate	$MgSO_4 \cdot 6H_2O$	Monoclinic	(Zalkin, Ruben, & Templeton, 1964), (Anthony, Bideaux, Bladh, & Nichols, 2003)
Epsomite	$MgSO_4 \cdot 7H_2O$	Orthorhombic	(Calleri, Gavetti, Ivaldi, & Rubbo, 1984), (Anthony, Bideaux, Bladh, & Nichols, 2003)
Meridianiite	$MgSO_4 \cdot 11H_2O$	Anorthic (Triclinic)	(Peterson, Nelson, Madu, & Shurvell, 2007)

Table 3 Hydrated states of iron sulfate and their crystal systems. (Perroud, 2016)

Mineral	Formula	Crystal System	Reference
Szomolnokite	$Fe^{2+}SO_4 \cdot H_2O$	monoclinic	(Wildner & Giester, 1991), (Sabelli & Trosti-Ferroni, 1985), (Anthony, Bideaux, Bladh, & Nichols, 2003)
Rozenite	$Fe^{2+}SO_4 \cdot 4H_2O$	monoclinic	(Jambor & Traill, 1963), (Anthony, Bideaux, Bladh, & Nichols, 2003)
Ferrohexahydrite	$Fe^{2+}SO_4 \cdot 6H_2O$	monoclinic	(Vlassov & Kusnetzov, 1962), (Fleischer, 1963), (Anthony, Bideaux, Bladh, & Nichols, 2003)
Melanterite	$Fe^{2+}SO_4 \cdot 7H_2O$	monoclinic	(Baur, 1964), (Anthony, Bideaux, Bladh, & Nichols, 2003)

3.1.2. Chlorides

- Naturally occurring calcium-chloride minerals are the tetragonal Sinjarite ($CaCl_2 \cdot 2H_2O$) (Aljubouri & Aldabbach, 1980), (Anthony, Bideaux, Bladh, & Nichols, 1997) and the rhombohedral (trigonal) Antarcticite ($CaCl_2 \cdot 6H_2O$) (Torii & Ossaka, 1965), (Anthony, Bideaux, Bladh, & Nichols, 1997). It can also appear as the monoclinic tetrahydrate ($CaCl_2 \cdot 4H_2O$) (Leclaire & Borel, 1980) as can be seen in Figure 5.
  The tetrahydrate has been observed to melt at T_{melt} = 35 to 45.5°C (IFA Institut für Arbeitsschutz Datenbank), (Ropp, 2012), while the hexahydrate has a reported melting temperature of T_{melt} = 30°C (Ropp, 2012).

- Untreated potassium-chloride occurs naturally as the cubic mineral Sylvite (KCl) (Mineralogical Magazine 29, 1951); (Anthony, Bideaux, Bladh, &

Nichols, 1997) with no known hydrated stages. It's melting point is reported as T_{melt} = 773°C (Merck & Co., Inc., 2006).

The naturally occurring magnesium-chloride minerals are trigonal Chloromagnesite ($MgCl_2$) (Busing, 1970), (Bassi, Polanto, Calcaterra, & Bart, 1982) and monoclinic Bischofite ($MgCl_2 \cdot 6H_2O$) (Andress & Gundermann, 1934), (Swanson, et al., 1974), (Anthony, Bideaux, Bladh, & Nichols, 1997). As depicted in Figure 6 it can also appear as mono-, bi-, tetra- or dodeca-hydrate. Which of those phases are the predominant hydration stages is depending on temperature as can be seen in Figure 7. The magnesium chloride is known to be thermally instable in its hydrated form, reported reacting to ($Mg(OH,Cl)_2$) at T > 167°C or (MgO) at T > 415°C (Qiong-Zhu Huang, Gui-Min Lu, Jin Wang, & Jian-Guo Yu, 2010), though (HCl) emissions have been observed already at temperatures of T > 110°C (Institut für Arbeitsschutz der Deutschen Gesetzlichen Unfallversicherung, 2017). A thermal decomposition at T > 110°C concurs with the phase change to {$MgCl_2 \cdot 4H_2O$}, while a decomposition at T > 167°C concurs with the phase change to {$MgCl_2 \cdot 2H_2O$} (Kipouros & Sadoway, 2001).

The different hydrated stages and some known hydroxides are listed in Table 4.

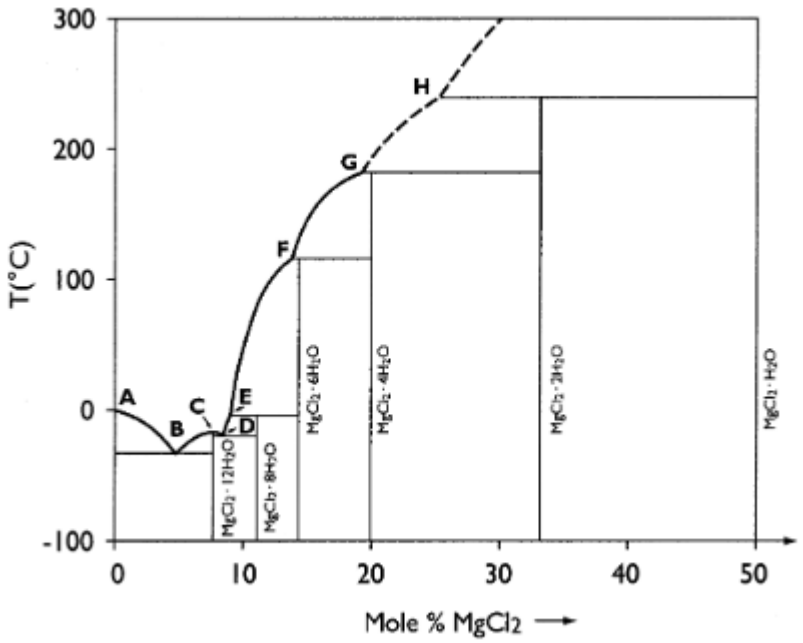

Figure 7 Phase diagram of the hydration stages of {$MgCl_2$} (Kipouros & Sadoway, 2001)

- Anhydrate Zinc-chloride {$ZnCl_2$} does not occur naturally but a synthetic anhydrate can occur in two different tetragonal stages (α and β), one monoclinic (γ) and one orthorhombic crystalline form (δ) (Wells, 1984). The monoclinic form was analyzed by (Černý, et al., 2012), (Winkler & Brehler, 1959) and (Brehler, 1977), the tetragonal forms by (Oswald & Jaggi, 1960), (Brehler, 1977), (Brynestad & Yakel, 1978) analyzed the orthorhombic form and an additional trigonal (rhombohedral) form was reported by (Wyckoff R. W., 1931). There are six stages of hydration of ($ZnCl_2 \cdot nH_2O$), with n = 1, 1.5, 2.5, 3, 4 and 4.5 (Holleman & Wiberg, 2001), (Hennings, Schmidt, & Voigt, 2014). Known crystal structures for the hydrates are monoclinic ($ZnCl_2 \cdot 2.5H_2O$), triclinic ($ZnCl_2 \cdot 2.5H_2O$), triclinic ($ZnCl_2 \cdot 3H_2O$) and orthorhombic ($ZnCl_2 \cdot 4.5H_2O$) (Hennings, Schmidt, & Voigt, 2014), (Wilcox, et al., 2015).

Table 4 Hydrated states of magnesium chloride and magnesium hydroxide salts and their crystal systems

Mineral	Formula	Crystal System	References
Chloromagnesite	$MgCl_2$	trigonal	(Busing, 1970)
	$MgCl_2$	trigonal	(Bassi, Polanto, Calcaterra, & Bart, 1982)
	$MgCl_2 \cdot H_2O$	orthorhombic	(Kaduk, 2002)
	$MgCl_2 \cdot 2H_2O$	monoclinic	(Kaduk, 2002)
	$MgCl_2 \cdot 4H_2O$	monoclinic	(Kaduk, 2002)
Bischofite	$MgCl_2 \cdot 6H_2O$	monoclinic	(Andress & Gundermann, 1934)
	$MgCl_2 \cdot 12H_2O$	monoclinic	(Sasvari & Jeffrey, 1966)
Korshunovskite	$Mg_2(OH)_3Cl \cdot 3.5\text{-}4H_2O$	triclinic	(Malinko, Lisitsin, Purusova, Fitsev, & Khruleva, 1982), (Anthony, Bideaux, Bladh, & Nichols, 1997)
	$Mg_3(OH)_5Cl \cdot 4H_2O$	monoclinic	(Kunihisa, Dinnebier, & Schlecht, 2007)
	$9Mg(OH)_2 \cdot MgCl_2 \cdot 4H_2O$	monoclinic	(Dinnebier, Freyer, Bette, & Oestreich, 2010)

3.1.3. Bromides

- Strontium bromide occurs as the anhydrate {$SrBr_2$} in orthorhombic form with the spacegroup $Pbnm$ (Kamermans, 1939), (Wyckoff R. W., 1963) and tetragonal with the spacegroup $P\frac{4}{n}$ (Sass, Brackett, & Brackett, 1963), (Smeggil & Eick, 1971). The melting point of the anhydrate is found at T_{melt} = 643°C (Galan, Labrador, & Alvarez, 1980).

  It can also occur as the trigonal hexahydrate {$SrBr_2 \cdot 6H_2O$} with the spacegroup $P321$ (Abrahams & Vordemvenne, 1995) with the melting point

at T_{melt} = 88°C (Gardner, Finch, Steadman, & Crosby, 1971), (Harris & Rusch, 2013).

- Sodium bromide has no known hydrated phases. {NaBr} occurs cubic with the spacegroup $Fm\bar{3}m$ (Wyckoff R. W., 1963) and has a melting temperature of T_{melt} = 755°C (IFA Institut für Arbeitsschutz Datenbank).

- Potassium bromide {KBr} does not have any known hydrated phases and occurs cubic with the spacegroup $Fm\bar{3}m$ (Ott, 1926), (Wyckoff R. W., 1963), (Ahtee, 1969). The material melts at T_{melt} = 732°C (IFA Institut für Arbeitsschutz Datenbank).

- Lithium bromide can occur as the anhydrate {LiBr} in cubic form with the spacegroup $Fm\bar{3}m$ (Ott, 1923), (Wyckoff R. W., 1963), and a melting temperature of T_{melt} = 550°C (Maiti, Kundu, & Guin, 2003), (Meek, Sharick, Winey, & Elabd, 2015) or as the orthorhombic monohydrate {LiBr·H_2O} with the spacegroup $Cmcm$ (Hoennerscheid, Jansen, Nuss, & Muehle, 2003) and a melting temperature of approximately T_{melt} = 162 to 167 °C (Matsuo, Oguchi, Maekawa, Takamura, & Orimo, 2007).

- Magnesium bromide occurs as the trigonal anhydrate {$MgBr_2$} with the spacegroup $P\bar{3}m1$ (Wyckoff R. W., 1963) and a melting temperature of T_{melt} = 711°C (Merck (formerly Sigma-Aldrich), 2017), as the monoclinic hexahydrate {$MgBr_2$·$6H_2O$} with the spacegroup $C1\frac{2}{m}1$ (Andress & Gundermann, 1934), (Hennings, Schmidt, & Voigt, 2013), and a melting temperature of T_{melt} = 146°C (ChemicalBook, 2017) to 165°C (American Elements, 2017) and the monoclinic nonahydrate {$MgBr_2$·$9H_2O$} $C1\frac{2}{c}1$ (Hennings, Schmidt, & Voigt, 2013) with an unknown melting point.

- Calcium bromide occurs as the orthorhombic anhydrate {$CaBr_2$} with the spacegroup $Pnnm$ (Brackett, Brackett, & Sass, 1963) and a melting temperature of T_{melt} = 730°C (International Programme on Chemical Safety and the European Commission, 2012)

  Or as the trigonal hexahydrate {$CaBr_2 \cdot 6H_2O$} with a spacegroup of $P321$ and a melting point of T_{melt} = 38°C where the material dehydrates (Winter, 2017). It is sold as {$CaBr_2 \cdot xH_2O$} (Merck (formerly Sigma Aldrich)).

3.2. Heat capacities for selected educts

For the planned analysis on laboratory scale, the specific heat capacity or specific heat c_p of the evaluated materials is required, to calculate the heat output during hydration. Literature offers values for most of the anhydrates of untreated salts at T = 298K (T= 25°C) as can be seen in Table 6. While (Biermann, et al., 1989) published calculation-tables for c_p values at changing heat, studies by (Warren, 2017) of the {$CaCl_2$}-hydrates show that the values vary stronger by water content than the change in temperature.

The specific heat capacities were calculated from spot samples of the dehydration curves of those materials considered for the laboratory scale evaluations and the used starting materials necessary for comparison, using the formulas:

$$c_p = \frac{\phi_{sample} - \phi_{blanc}}{m_{sample} \cdot \beta_s}, \text{ (Riesen, 2008)}$$

$$\lim_{T \to 0} \left(\frac{\delta H}{\delta T}\right)_p = \lim_{T \to 0} c_p\,(T) = 0, \quad \text{(Cemič, 2005)}$$

Table 5 Specific heat capacities c_p [kJ(kgK)$^{-1}$] from different literature sources.

Material	T_1 [K]	cp (T_1) [kJ(kgK)$^{-1}$]	T_2 [K]	cp (T_2) [kJ(kgK)$^{-1}$]	Literature
{$CaCl_2$}	298	0.654 0.67			(Georgia State University, 2017); (Warren, 2017)
{$CaCl_2 \cdot H_2O$}	298	0.84			(Warren, 2017)
{$CaCl_2 \cdot 2H_2O$}	298	1.17			(Warren, 2017)
{$CaCl_2 \cdot 4H_2O$}	298	1.35			(Warren, 2017)
{$CaCl_2 \cdot 6H_2O$}	298	1.66			(Warren, 2017)
{KCl}	298	0.691	1043	0.863	(Biermann, et al., 1989)
{$MgCl_2$}	298	0.747	987	0.882	(Biermann, et al., 1989)
{MgO}	298	0.923			(Haynes, 2011)
{$SrBr_2$}	298	0.304			(MatWeb, LLC, 2017)
{$ZnCl_2$}	298	0.523			(Hargittai, Tremmel, & Hargittai, 1986)
{KCl+$MgCl_2$}	298	0.768	760	0.969	(Biermann, et al., 1989)
Glass	298	0.80			(Kopp Glass; Galbraith, J., 2016)

Since the materials went through several phase changes during dehydration, the spot samples could only be taken from intervals between dehydration peaks, this resulted in missing data for different temperature ranges. The data from the literature sources was added to fill those blanks when available, despite the literature data referring mostly to anhydrate salts.

3.3. Material synthesis

To encourage the forming of compounds within the mixtures, first naturally occurring compounds with hydrated phases were chosen to be replicated. The mixing ratios of the cations of those compounds were then altered to try to create synthetic compounds with a different chemical setup but similar crystal structures. The minerals were chosen from the online database ATHENA (Perroud, 2016), the list of the materials considered for evaluation can be found in the appendix (Table 54 Naturally occurring sulfate evaporate minerals considered for synthesis and material evaluation. Cation-variations were added to Changoite and Mereiterite. Table 54 to Table 57).

However, the presence of Fe^{2+} and Fe^{3+} can cause the development of the unwanted not soluble byproduct $\{Fe^{3+}{}_2O_3\}$. Furthermore, since the mixed salts were grown from a brine solution, the exact grade of oxidization of the iron in the mixture was unknown, which left the identification of the resulting products to the XRPD-analysis.

Since Anhydrite ($CaSO_4$) is not soluble in water after dehydration and does not rehydrate, minerals with $\{CaSO_4\}$ components were excluded from the synthesis.

Li- and Sr-containing salts tend to be too expensive for cost-efficient heat storage systems within a household setting but a series of Sr-bromide mixtures was synthesized, since $\{SrBr_2\}$ is known for its good heat storage capacity and high cycle stability. However, there are no known naturally occurring bromide minerals which incorporate Sr along other cations.

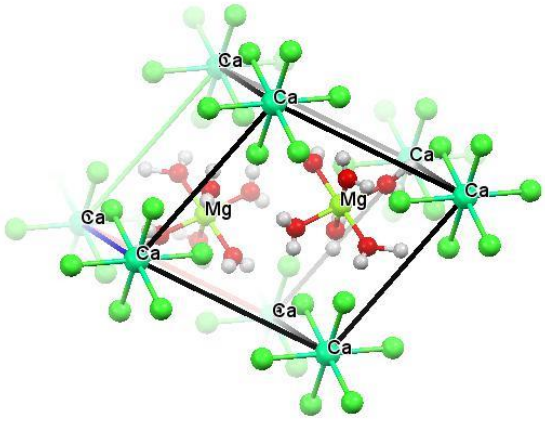

Figure 8 $\{CaMg_2Cl_{16}\cdot 12H_2O\}$ ($R\bar{3}$) (Leclaire, Borel, & Monier, 1980); (Created with Mercury 3.1) Tachyhydrite is a naturally occurring evaporate mineral which incorporates water in its crystal structure.

For several naturally occurring salt minerals methods are confirmed to create synthetic compound crystals.

Carnallite has been synthesized by evaporation from a brine solution at T = 23°C (Podder, Gao, Evitts, Besant, & Matthews, 2014). Likewise, Tachyhydrite has been created synthetically by (Erd, Clynne, Clark, & Potter, 1979), first heating a brine solution to T= 65°C and then cooling it down to T = 25°C for t = 12 to 18h under constant stirring.

A similar method to the approach of Podder et al. was used to synthesize samples for the TGA/DSC analysis.

The educts were dissolved in H_2O_{dest} at a ratio of 1g to 10ml and then mixed to match the desired compound at individually calculated ratios. The liquid solutions were then dried slowly in a desiccator to encourage crystal growth. Drying agents of varying efficiency such as silica gel $\{SiO_2\}$, $\{CaCl_2\}$, $\{ZnCl_2\}$ or Köstrolith (see Appendix 7 for the material information) were applied within the desiccator, depending on sample composition and expected or observed grade of deliquescence. Chloride samples were dried by using $\{CaCl_2\}$, excluding chloride samples containing $\{CaCl_2\}$ which were dried with $\{ZnCl_2\}$ or Köstrolith in case the samples contained $\{ZnCl_2\}$. Parallel to drying the material in the desiccator, half of the solutions were dried in an oven at T_{max} = 110°C as a backup. However, for the TGA analysis only the desiccator dried samples were used due to their superior crystallization.

For the later laboratory scale tests, a similar method to that of Erd et al. was picked to crystallize samples within the m = 20 to 100g range. The salts were first mixed at the desired ratios and then dissolved within H_2O_{dest} to a saturated solution before being dried quickly in an oven at T_{max} = 120°C.

As it was observed that several of the solutions were developing a solid crystal layer at the surface which prevented the remaining brine below from drying properly, they were further dehydrated on a hotplate under constant stirring, where necessary.

The {$2ZnCl_2 + CaCl_2$} mixture samples for the tests on laboratory scale additionally had to be cooled within a fridge at T_{max} = 5°C after the heating to initialize solidification, hinting towards a very low melting point of the mixture. Still the samples proved to remain solid during dry-storage at an average room temperature of T = 25°C.

3.4. Mixed salt samples in X-ray-Powder-Diffractometry (XRPD)

In powder diffraction, an x-ray beam is shot at a powdered sample of a crystal to read the interval lengths between layers of the crystal lattice by the ray's angle of scattering 2Θ (also written sometimes as 2theta). As each crystalline material has an individual set pattern of scattering-peaks, the formation of compounds in a mixture can be either validated or disproved and the crystal lattice of mixture variants or unknown mixtures can be determined.

The powder diffraction analysis was done in cooperation with the University of Düsseldorf and the University of Bremen. Spot samples of the mixture batches that were prepared for the initial TGA/DSC evaluation were sent for identification, for later comparison of crystal structure influence on heat storage capacity and cycle stability. A list of the chosen materials can be found in Table 6.

Table 6 Salt mixtures sent for XRPD-evaluation.

Mixture	Naturally occurring mineral	Evaluated at
{KCl + $MgCl_2$}	Carnallite	Uni Düsseldorf
{3$MgSO_4 \cdot 7H_2O$ + 16KCL}	Kainite	Uni Düsseldorf
{2Na_2SO_4 + $Al_2(SO_4)_3 \cdot 18H_2O$}	Na-Alumn	Uni Düsseldorf
{$MgSO_4 \cdot 7H_2O$ + $Al_2(SO_4)_3 \cdot 18H_2O$}	Pickeringite	Uni Düsseldorf
{17$MgSO_4 \cdot 7H_2O$ + 3$Al_2(SO_4)_3 \cdot 18H_2O$}	(Aromite)	Uni Düsseldorf
{2$CaCl_2$ + $MgCl_2$}	---	Uni Düsseldorf
{$CaCl_2$ + $MgCl_2$}	---	Uni Düsseldorf
{$CaCl_2$ + 2$MgCl_2$}	Tachyhydrite	Uni Düsseldorf
{$CaCl_2$ + 2$ZnCl_2$}	---	Uni Düsseldorf
{2$MgCl_2$ + $ZnCl_2$}	---	Uni Düsseldorf
{$MgBr_2 \cdot 6H_2O$ + $SrBr_2 \cdot 6H_2O$}	---	Uni Bremen
{5$CaBr_2 \cdot xH_2O$ + 16$SrBr_2 \cdot 6H_2O$}	---	Uni Bremen

Known powder patterns of natural and synthetic minerals were chosen as a base for comparison and identification of potentially formed compounds or unreacted educts. The mineral powder patterns were selected from the Crystallography open Database (Day & Murray-Rust, 2017), while the powder patterns of the educts were provided by the University of Düsseldorf (Heinrich Heine Universität Düsseldorf , 2013).

3.4.1. Naturally occurring minerals for powder pattern comparison

- Carnallite ($KMgCl_3 \cdot 6H_2O$) occurs in orthorhombic form, interpreted as $P\ n\ n\ a$ by (Schlemper, Sen Gupta, & Zoltai, 1985) though the axes had previously been labeled as $P\ b\ n\ n$ by (Fischer, 1973).
- Kainite (4($KMg(SO_4)Cl \cdot 11H_2O$) occurs monoclinic with the crystal system $C\ 1\ \frac{2}{m}\ 1$ (Robinson, Fang, & Ohya, 1972).

- Na-Alumn has been observed as monoclinic ($NaAl(SO_4)_2 \cdot 6H_2O$) with the crystal system $P\ 1\ \frac{2_1}{a}\ 1$ (Mereiter, 2013), (Robinson & Fang, 1969), monoclinic ($NaAl(SO_4)_2 \cdot 11H_2O$) with the crystal system $C\ 1\ \frac{2}{c}\ 1$ (Fang & Robinson, 1972) and trigonal ($NaAl(SO_4)_2 \cdot 12H_2O$) with the crystal system $P\ a\ \bar{3}$ (Cromer, Kay, & Larson, 1967).
- Pickeringite occurs naturally as monoclinic ($(Mg_{0.93},Mn_{0.07})Al_2(SO_4)_4 \cdot 22H_2O$) with the crystal system $P\ 1\ \frac{2_1}{c}\ 1$ (Quartieri, Triscari, & Viani, 2000).
- Aromite is a variety of Epsomite and may be a mixture of Epsomite and Pickeringite with the structure formula ($Mg_6Al_2(SO_4)_9 \cdot 54H_2O$). It was treated as Pickeringite when discovered (Darapsky, 1890), (Palache, Berman, & Frondel, 1951) and is not officially acknowledged as a mineral (Hudson Institute of Mineralogy 1993-2017, 2017).
- Tachyhydrite occurs naturally as rhombohedral ($CaMg_2Cl_6 \cdot 12H_2O$) in the crystal system $R\ \bar{3}$ (Clark, Evans, & Erd, 1980), (Leclaire, Borel, & Monier, 1980).

3.5. TGA/DSC screening of sulfates, chlorides and bromides

3.5.1. Reaction heat and Enthalpy measurements with the TGA/DSC evaluation

The analyzation and recording of the reaction enthalpy and change in sample mass during hydration and dehydration was handled by a TGA/DSC1 (Mettler) system which was implemented by (Rammelberg, Opel, Ruck, & Ross, 2011). This system allows for releasing two separate reaction gases and a purge gas into the furnace with the sample during measurement. Nitrogen, which is used as the purge gas, is being dried in two steps by the drying agents {$CaCl_2$} and Silica Gel (Roth, 2017) and released into the furnace at a flow rate of $\dot{V} = 50\text{ml min}^{-1}$. The TGA/DSC controlled a gas box which offered two separate mass flow regulators to supply the furnace with either the dried N_2 purge gas or humidified N_2 as reaction gas. The

humidification of the reaction gas was accomplished by a bubble flask in a thermostat water bath. The schematics of the setup can be seen in Figure 9.

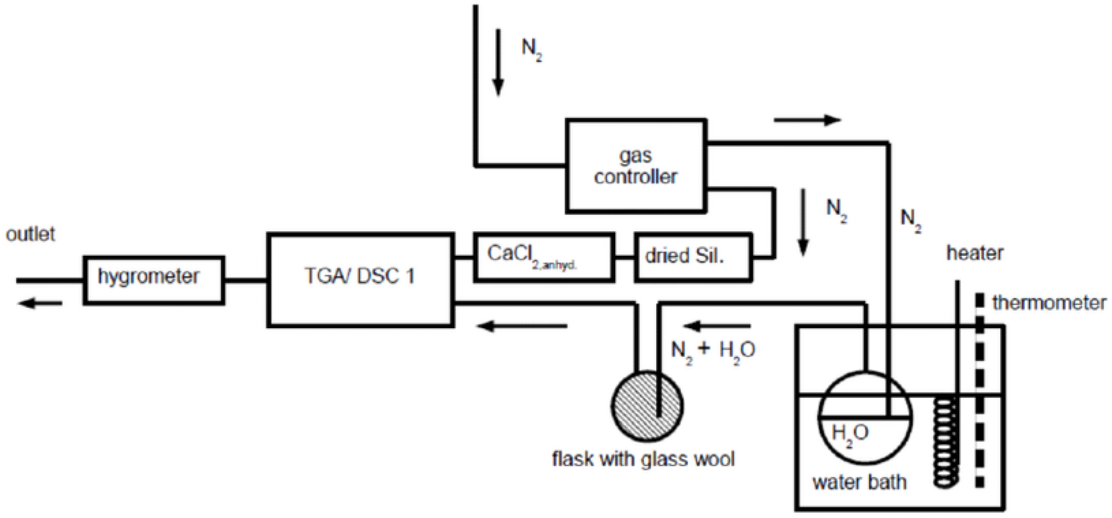

Figure 9 TGA/DSC setup, Leuphana University Lüneburg (Rammelberg, Opel, Ruck, & Ross, 2011).

During the initial TGA/DSC measurements, salt samples of m ~ 10mg were sent through three cycles of dehydration and hydration. Since several of the samples showed deliquescence during storage and even weight gain due to absorbing water from the atmosphere while waiting on the sample tray for their first measurement, the 1st cycle had a low temperature dehydration at T_{max} = 100°C with a slow heating rate of β = 1 $Kmin^{-1}$ to dry off excess water and recrystallize potentially liquefied samples. As the desiccator-dried materials had not been exposed to heat during their synthesis, the heat gained during the following hydration still represented the storage capacity of a low temperature charge.

The next two dehydrations reached a maximum temperature of T_{max} = 200°C to show a broader range of the sample behavior. As factors like agglomeration and partial recrystallization play a lesser role with small sample sizes as those used in the TGA analysis, materials which already displayed a clear degeneration in cycle stability during this stage of testing were excluded from further experiments – an improvement of stability with a larger sample size was not to be expected.

Two additional TGA measurement settings were implemented later with a new batch of samples of the respective materials.

The first of those measurements was a combination of heating the samples up to T_{max} = 110°C for t_1 = 90 min, while keeping up a steady supply of water and lowering the temperature later to T = 62.5°C for t_2 = 60min to determine, at which temperatures the samples were still able to take up water and release heat.

The second new measurement cycle served to discern potential low melting temperatures of the mixtures and to turn them into anhydrates by heating the samples up to T_{max} = 500°C.

The detailed methods used for the TGA/DSC analysis can be found in the appendix.

3.5.2. Evaluation of the specific heat capacity of materials with the TGA/DSC

The specific heat capacity or simply specific heat of a material is a necessary value to calculate temperature readings into reaction heat or enthalpy. The specific heat capacity can be applied for a constant volume or a constant pressure. As the materials are expected to undergo phase changes and with them volume changes but the pressure p can be controlled during the experiments with the TGA/DSC as well as during the later laboratory scale measurements, c_p [kJ(kgK)$^{-1}$] is chosen over c_v [kJ(kgK)$^{-1}$] for calculation with:

$$C_p = (\frac{\delta H}{\delta T})_p, \text{ (Cemič, 2005)}$$

$Where\ C_p\ is\ the\ specific\ heat\ capacity\ for\ 1mol\ of\ substance.$

$$c_p m = \left(\frac{\delta H}{\delta T}\right)_p$$

$with$

$m :=\ sample\ mass\ [g]$

Literature offers c_p values for anhydrate salts at T = 25°C as seen in Table 5 but the specific heat c_p varies by temperature and hydration stage of a material (Cemič, 2005). With complex mixed salts, temperature ranges planned to go up to T_{max} = 200 to 500°C and changing hydration stages during evaluations instead of anhydrates, the specific heat needed to be calculated from measurements.

The TGA/DSC analysis offers values for temperature, heat, mass and time at any point of the recorded hydration and dehydration curves, as well as substracting a blanc curve measured with an empty crucible from the measured curve. With this data, the so called 'direct' method (Riesen, 2008) can be used:

$$c_p = \frac{\phi_{sample} - \phi_{blanc}}{m_{sample} \cdot \beta_s}$$

$with$

$$\beta_s = \frac{\Delta T}{\Delta t}\ [Ks^{-1}]$$

and

$\phi_{sample} := heatflow\ measured\ for\ the\ sample\ [mW]$

$\phi_{blanc} := heatflow\ measured\ for\ a\ blanc\ curve\ with\ an\ empty\ crucible\ [mW]$
$\phi_{sample}\ and\ \phi_{blanc}\ are\ entered\ as\ positive\ values\ into\ the\ formula\ for\ both\ endothermic\ and\ exothermic\ events.$
$m_{sample} := sample\ mass\ [g]$
$\Delta T := temperature\ change\ within\ the\ sample\ since\ start\ of\ the\ measurement\ [K]$
$\Delta t := time\ interval\ since\ start\ of\ the\ measurement\ [s]$

However, the formula only applies, while no phase change takes place within a tested material, as the additional reaction heat of the phase change will create a phantom value.

Since the enthalpy H of a solid nears constant values when reaching absolute zero temperature T = 0K, δH will approach zero as well:

$$\lim_{T\to 0}\left(\frac{\delta H}{\delta T}\right)_p = \lim_{T\to 0} c_p\,(T) = 0, \quad \text{(Cemič, 2005)}$$

With these two formulas, $c_p(T)$ trends were calculated from spot samples which were taken in between reaction peaks of the dehydration curves. Chosen for $c_p(T)$ trend calculations were materials which were used later in the laboratory scale analysis. The trends calculated by this method do not represent the anhydrous materials but the average values for the varying hydrated stages of the materials, observed at certain temperatures between phase changes.

3.6. Development of a measurement method for upscaled sample size

The main drawback of the TGA/DSC measurements is the small sample size of m ~ 10mg. Material behavior such as agglomeration or water- and heat-distribution may be altered by the small sample amounts used and the small samples hydrate or even overhydrate and dissolve easily at average air humidity before the measurements. To simulate material behavior in an actual battery system, a method needed to be implemented, which allowed for a larger sample mass.

3.6.1. Experimental setups with a supply of liquid water

a) Setup #01 (with liquid water supply)

The sample size was first increased to m = 50g. During discharge the sample was mixed with liquid water within a flask. The temperature of the sample and of the air in that sample bottle were measured with two thermometers and recorded manually during Charge and discharge. An oil bath below the sample bottle served as a heat source during the charging stage and was supposed to drive the water out of the sample into a simple cooling trap as seen in Figure

10. Aside from the temperature the pH value of the water vapor was monitored during the charging stage with a strip of litmus paper.

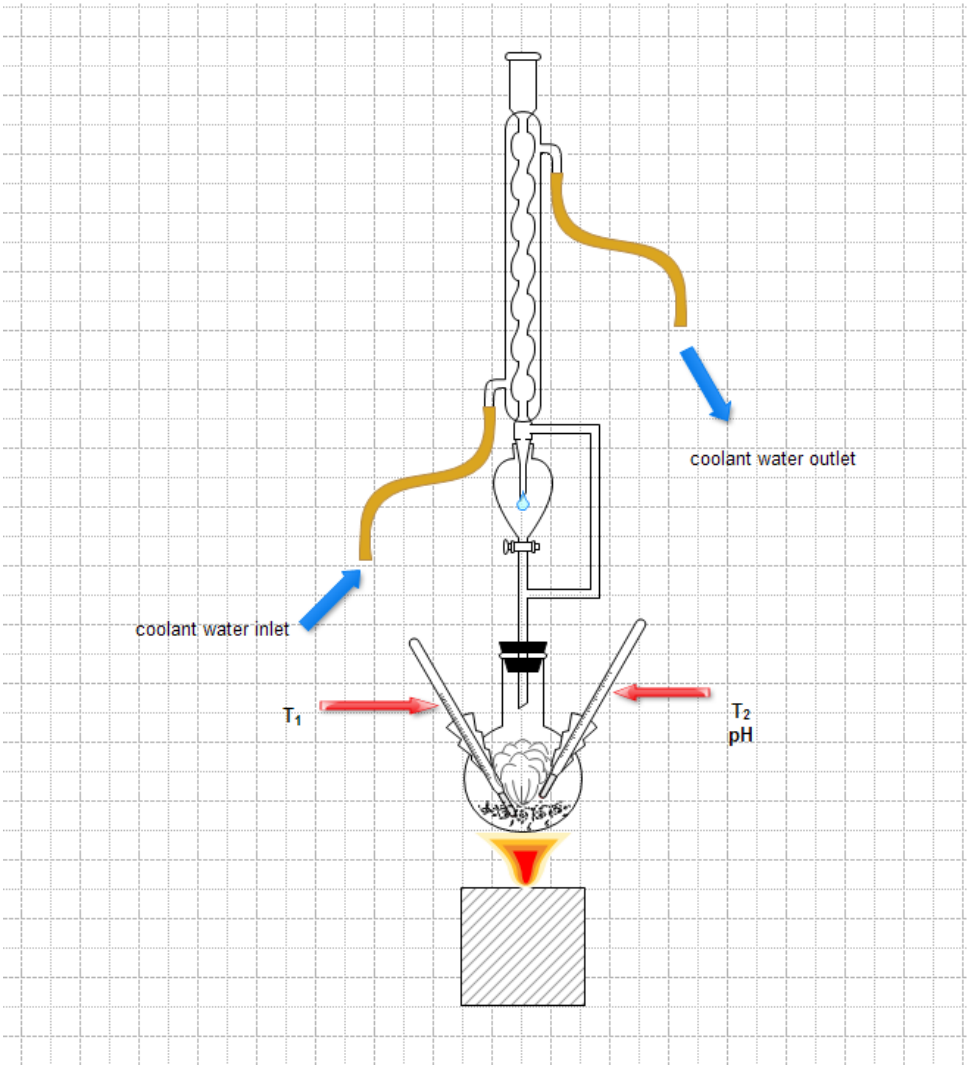

Figure 10 First setup for cycle measurements of m = 50g samples discharged with liquid water

b) Setup #02 (with liquid water supply)

The second experimental setup had an additional heating unit, to keep the water in the gaseous phase during charge, and a vacuum pump to improve the flow of the water vapor out of the sample bottle. Since the measured air temperature within the bottle did not provide crucial data, the second thermometer was removed. The schematic of the 2nd setup can be seen in Figure 11.

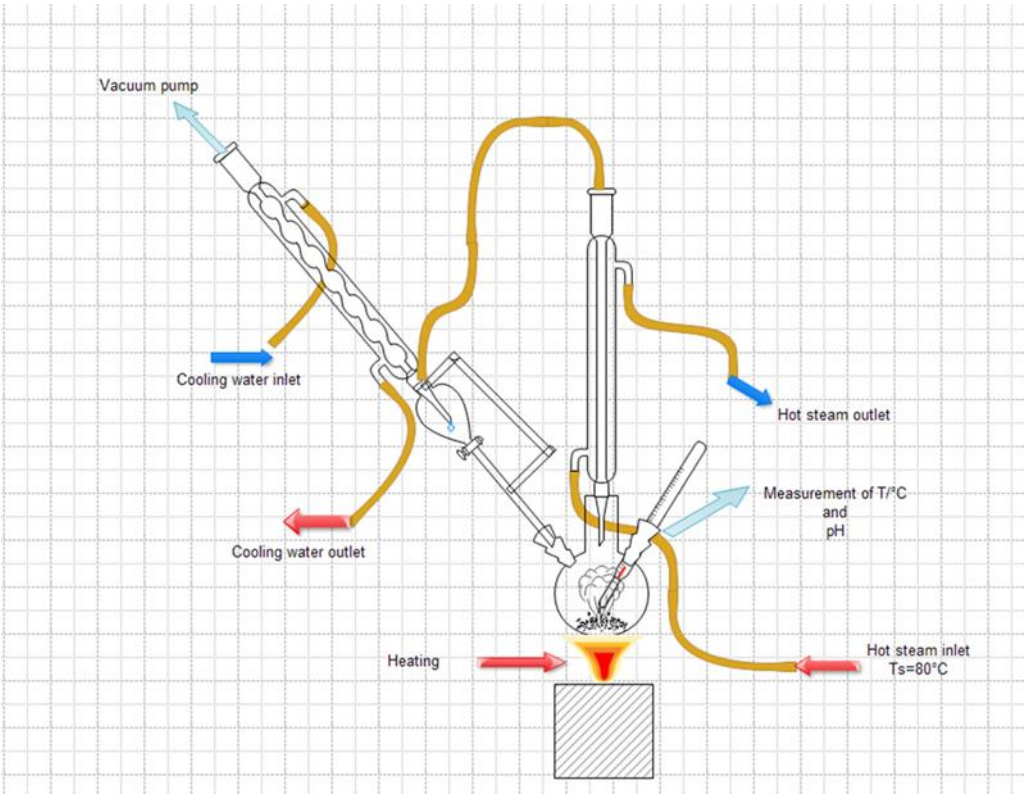

Figure 11 Schematics of the second setup for cycle measurements of m = 50g samples discharged with liquid water.

3.6.2. Experimental setups with a water vapor supply

To prevent the complete dissolving of the samples during hydration measurements, material relocation caused by recrystallization as well as limiting the influence of adding varying amounts of cold, liquid water to the temperature readings within the sample bottle during ongoing measurements, a complete new experimental setup, working with water vapor instead of liquid water, was implemented. Two thermo-elements took over the automatic recording of the temperature change within the sample and the water reservoir. The sample holder was a modified glass tube with an inwrought wire mesh to allow for the passage of gaseous and liquid substances but not the solid sample material. For the planned in-situ dehydration of the samples, adhesive heating foils were attached to the outside of the tube.

The sample size was reduced to m = 20g since the perimeter of the tube was limited by what the used heating coils were covering, to heat up the samples within evenly. In favor of future setup upgrades for the planned cycle measurements, the idea of using a tube of increased length for storing a larger sample was discarded. The flow of water vapor out of the sample holder would have been influenced negatively during the dehydration step, as had already been an issue of the two previous setups with liquid water supply.

a) Setup #01(with water vapor supply)

The first setup as seen in Figure 12 was used for measuring the temperature change of a sample during a single hydration stage each. As not to falsify the measurement of the sample temperature T_1 during hydration and assisting the flow of water vapor through the sample, instead of heating the water reservoir to $T_{boiling}$ = 100°C, the water vapor was generated by applying a vacuum, lowering the pressure within the apparatus to p_{min} ~ 33mbar which causes water to boil at room temperature of T_2 ~ 25°C. However, since the energy for that phase change is drawn from the water's heat, an extra water bath was necessary to keep the temperature in the reservoir as stable around T_2 ~ 25°C as possible. While applying the vacuum caused a lag between heat loss within the reservoir and reheating, the water bath was still able to provide the necessary extra energy to keep the phase change to water vapor up for the time of the measurement. Another side-effect of applying a vacuum instead of using heated water vapor was the low pressure of the water vapor itself, but by channeling it directly through the samples, enough water was absorbed by the tested materials for starting a chemical reaction.

The samples were prepared for hydration by drying them in an oven at T= 120°C for t = 2h and letting them cool back down in a desiccator before filling them into the sample holder.

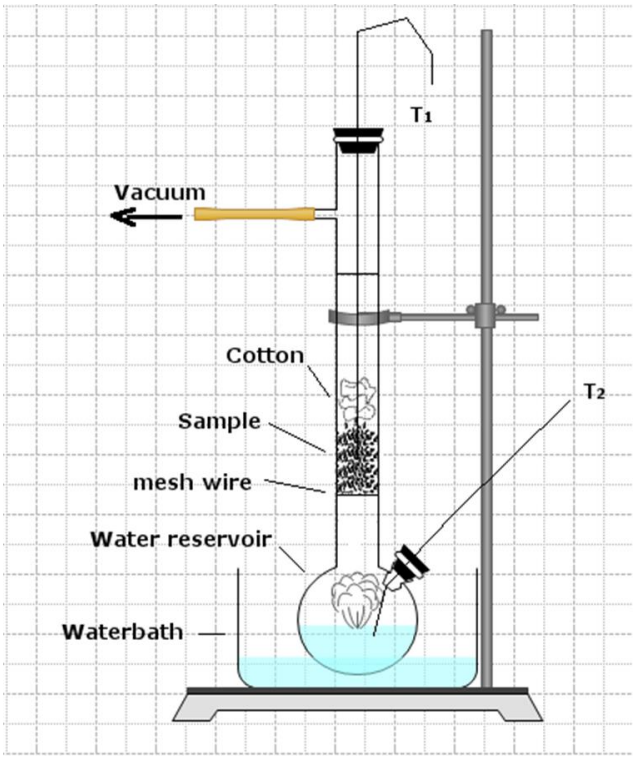

Figure 12 First experimental setup with a supply of water vapor and m = 20g sample size. The sample is held in a vertical drying rod and rests in a wrap of filter paper on a wire mesh over a water supply. A piece of cotton above the sample ensures that applying a vacuum does not suck the sample out of the sample holder during measurements. The temperature is measured directly within the sample (T_1) and in the water supply (T_2) with thermo-elements. The vacuum lowers the pressure inside the setup to about p ~ 33mbar and serves to generate water vapor at room temperature T_2 ~ 25°C. The water bath is to keep the temperature of the water reservoir at approximately T_2 ~ 25°C during the entire measurement.

Since the material could not be dried in situ with this setup, the samples were removed, dried in the oven again at T = 120°C for t = 2h and stored dry within a desiccator between the measurements.

Measuring just a single hydration event for a material was not yielding conclusive results, as any untreated materials may have been factory dried at unknown, higher temperatures than T = 120°C beforehand and the resulting values were not directly comparable to those of the mixed salts crystallized from liquid solution.

Removing the material from the sample holder for oven drying disturbed any changes caused by the chemical reaction such as agglomeration or dissolving and recrystallization and may also lead to a significant loss of material during the removal and refilling processes from and to the sample holder, the setup upgrade with the heating foils was implemented next to dry the samples within the sample holder without removing them from the apparatus.

Lastly, while the temperature curves even out over time, differences between the starting and the end temperatures can be observed in some of the curves. They were caused by a change of the surrounding temperature in the lab.

Therefor a baseline, calculated from the measured water temperature, the temperature difference between sample- and water-temperature at the beginning of the hydration and temperature changes within a nonreactive material sample of comparable mass during a hydration is also required, to take those outside temperature changes into account and make the results of the different materials comparable to each other.

b) Setup #02 (with water vapor supply)

The original setup was supplemented by two self-adhesive heating-foils attached to the outside of the sample holder, a cooler and a secondary water reservoir for catching the excess water during dehydration and two valves to shut the sample holder (Ø = 21mm) off from the water supply, resulting in the second experimental setup as depicted in Figure 13.

With both heating foils activated, the salt sample in the holder can be heated up to a temperature of T_{max} ~ 120°C. The drying temperature can be further increased by wrapping the heated sample holder with an extra layer of tinfoil.

Contrary to setup #2 with liquid water, no vacuum was applied during the dehydration process, as the timeframe of the dehydration was exceeding what was observed to be the safe maximum operation time of the vacuum pump of $t_{vac\text{-}max}$ = 30 min.

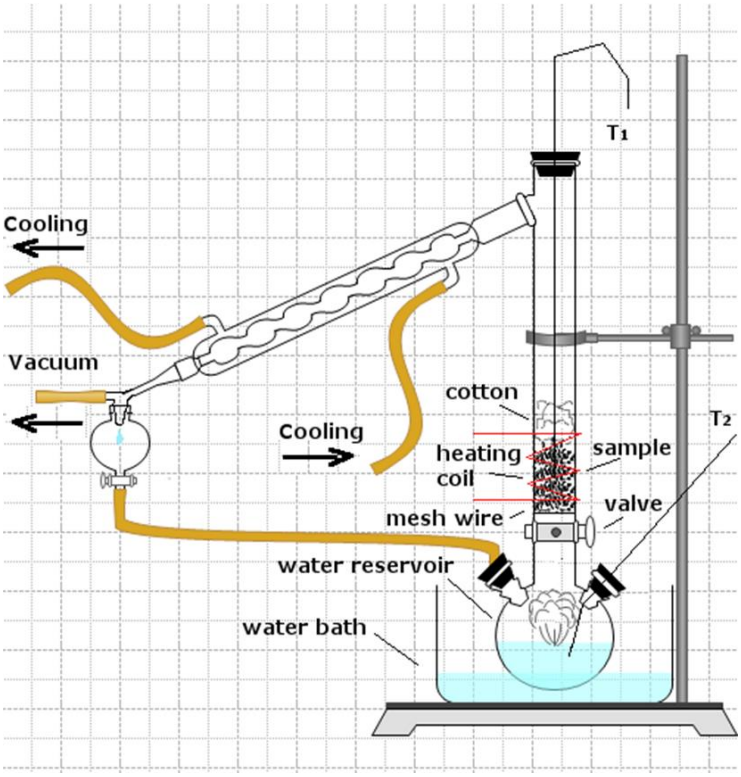

Figure 13 Experimental setup #02 with a supply of water vapor. In addition to the heating foils wrapped around the outside of the sample holder, a cooler and a water trap were added to setup #1 to enable cycle measurements with in-situ dehydration of the samples.

Since the setup of the sample holder did not allow for a liquid standard sample, powdered glass was chosen over the more commonly used water as the nonreactive material for the baseline calculation.

The hydration measurement with glass powder, the recorded water temperatures during the measurements of the salt mixtures and the temperature difference between the temperature of the cold sample at the start of the hydration measurement and the cooled off sample at the end of each hydration were used in the calculation:

$$T_{Baseline}(x) = T_{x\,water} + \Delta T_{x\,g} - \Delta T_{1\,sample}$$

$T_{Baseline} := baseline\ temperature\ [°C]$

$T_{x\,water} := temperature\ measured\ within\ the\ water\ reservoir\ [°C]$

$with$

$x = 1, 2, 3, \dots n$

and

$$n = \frac{t_{max}\,[s]}{5}$$

$as\ the\ thermoelements\ recorded\ the\ temperature\ in\ intervals\ of\ \Delta t = 5s.$

$$\Delta T_{x\,g} = \left(T_{x\,glass} - T_{x\,gwater}\right)$$

$T_{x\,glass} := temperature\ of\ powdered\ glass, measured\ within$

$the\ sample\ holder\ [°C]$

$T_{x\,gwater} := temperature\ within\ the\ water\ reservoir\ during$

$the\ glass\ measurement\ [°C]$

$$\Delta T_x = \left(T_{x\,water} + \Delta T_{xg}\right) - T_{x\,sample}$$

$with$

$T_{x\,sample} := temperature\ of\ the\ sample\ [°C]$

$And\ with\ \Delta T_{1\,sample}\ compensating\ for\ diferences\ in\ starting$

$temperature\ between\ glass - standard\ measurement\ and$

$measurement\ of\ a\ sample.$

$$\Delta T_{1\,sample} = (T_{1\,water} + \Delta T_{1\,g}) - T_{1\,sample}$$

Fitting the baseline to the corresponding temperature curve, required some interpretation of the data to compensate for temperature changes in the laboratory in a few cases. If the temperature increase is linear, a term for a linear trend was added:

$$T_{Baseline}(x) = T_{x\,water} + \Delta T_{x\,g} - \Delta T_{1\,sample} + (x-1) \cdot \left(\frac{\Delta T_{n\,sample} - \Delta T_{1\,sample}}{n-1}\right)$$

In other cases, the curve of the water temperature indicated increased activity of the water bath' s heater at the end of the time interval where the vacuum

pump was active as the source of a sudden temperature rise, then a negative modificatory needed to be added to the curve after the vacuum shutdown instead of the linear modification:

$$T_{Baseline}(a) = T_{a\,water} + \Delta T_{a\,g} - \Delta T_{1\,sample}$$

$for\ a = \{1, \dots y\},$

$$T_{Baseline}(b) = T_{b\,water} + \Delta T_{b\,g} - \Delta T_{1\,sample} - \left(\Delta T_{y\,sample} - \Delta T_{1\,sample}\right)$$

$for\ b = \{y, \dots x\}$

$and\ with\ t(y) := time\ of\ vacuum\ shut\ down.$

The change in the water temperature leading up to the discrepancy between baseline and temperature reading at the end of the measurement may also originate in a period of inactivity of the water bath' s heater at the start of the measurement, when the vacuum was initiated, causing a steeper drop in temperature than being compensated for by the baseline adjustment. In that case, the modification needs to be added to the curve at the beginning, when the vacuum pump is activated. As the sudden drop in temperature can also be an indication for a phase change of the material causing an endothermic event, those modifications need to be applied carefully as not to falsify the results.

With fitted baselines and specific heat capacity $c_p(T)$ trends of the materials the reaction enthalpy ΔH can be calculated for the recorded temperature curves by applying Kirchhoff's law:

$$\left(\frac{\delta \Delta_r H}{\delta T}\right)_p = \Delta_r C_p \text{ , (Cemič, 2005)}$$

The trends of $c_p(T)$ calculated for the tested materials already take the average states of hydration-phase for the materials into account. The enthalpy H can be replaced by the heat flow ϕ:

$$(\phi_{sample} - \phi_{blanc})\Delta t = (H_{sample} - H_{blanc}) = \delta H$$

This formula can be changed to:

$$(\frac{\Delta_r(\phi_{sample} - \phi_{blanc})}{\delta T}\Delta t)_p = mc_p(T)$$

or:

$$((\phi_{sample}(T) - \phi_{blanc}(T))_p = \frac{mc_p(T)}{\Delta t}\delta T$$

$$\phi_{sample}(T) = \phi_{blanc} + mc_p(T)\beta$$

c) Setup #03 (with water vapor supply)

To improve the flow of water-vapor out of and through the sample, the glass rod serving as the sample holder was replaced by a similar one with a larger diameter (Ø = 25.9mm).

Setup #3 also allowed for the entire sample holder to be removed for weight recording without disturbing the sample within, to monitor the water uptake and possible material losses from melting or dissolving, between hydration and dehydration stages.

With the mass m of the sample known, a baseline provided by calculation from a measurement with glass powder and the temperature difference ΔT [°C]

monitored during the hydration stage, the heat ΔQ [J], heat flow Δϕ [W] or the enthalpy ΔH [Jg^{-1}] of the reaction can be calculated, if the material's heat capacity is also known. Instead of relying solely on the values provided by literature as seen in section 3.2, Table 5 and the $c_p(T)$ trends calculated from the TGA/DSC curves in section 3.2, Setup #3 of the apparatus was tested for possible application of in-situ measurements of the test-materials' heat capacities to be able to take changes in temperature as well as changes in the hydration stages into account more accurately.

To first determine how much heat ΔQ the apparatus and the samples are exposed to by activating the heating coil, the Joule-Lenz law was applied:

$$\Delta Q = I \cdot U \cdot \Delta t \; [AVs]$$

$$1 \; [AVs] \triangleq 1 \; [Ws] \triangleq 1[J \,]$$

$$\Delta Q := \; Change \; in \; heat \; [J]$$

$I := \; electric \; current \; through \; the \; heating \; coil \; [A]$

$U := \; electric \; voltage \; applied \; to \; the \; heating \; coil \; [V]$

$\Delta t := \; applied \; heating \; time \; [s]$

The heat is directly correlated to the change in temperature by a factor C

$$\Delta Q = C \cdot \Delta T \; [J]$$

Where C is the heat capacity of sample and apparatus multiplied with their respective masses:

$$C = c_{p\,sample} \cdot \; m_{sample} + c_{p\,apparatus} \; \cdot \; m_{apparatus} \; [JK^{-1}]$$

As the effective mass of the apparatus was unknown the apparatus specific factor C_a was used instead in the following calculations with:

$$C_a = c_{apparatus} \cdot m_{apparatus}\,[JK^{-1}]$$

$$I \cdot U \cdot \Delta t = \left(C_a + c_{p\,sample} \cdot m_{sample}\right) \cdot \Delta T$$

$$C_a = \frac{I \cdot U \cdot \Delta t}{\Delta T} - c_{sample} \cdot m_{sample}$$

Heating a material with a known specific heat capacity c_p in place of the sample, allows for calculating C_a for the apparatus. Once C_a is known, the heat capacities $c_{p\ sample}$ for the mixed salts can be determined by:

$$c_{p\,sample} = \frac{I \cdot U \cdot \Delta t}{\Delta T \cdot m_{sample}} - \frac{C_a}{m_{sample}}\,[Jg^{-1}K^{-1}]$$

d) Setup #4 (with water vapor supply) – unrealized

As taking measurements for the calculation of the heat capacity c_p is not the main objective of experimental setup #4, a calorimeter or an improved TGA/DSC measurement will be required to complement the necessary material information for the enthalpy calculations.

One source for error in setup #3 was the required interpretation of the applied baselines. Since the baselines were not recorded at the same time, temperature shifts within the surrounding laboratory area and discrepancies in measurement time had to be corrected, while discrepancies due to loss of sample mass could not be corrected.

For the 4th experimental apparatus, a setup is suggested, where the temperature of a sample of a non-reactive material standard like glass powder can be monitored and recorded parallel to the temperature within the salt-sample.

This would require a U-adapter separating the water vapor to flow into two sample holders. One of those sample holders would contain the material and be wrapped with a heating coil like implemented in setup #2 and #3, while the second, holding the standard, requires an insulation cover to avoid outside heat influencing the baseline measurement. A second U-adapter would lead the water vapor streaming out of the sample holders back together again and towards the cooling trap like in setup #2 and #3. Additional heat insulation of the second U-adapter would keep hot water vapor during dehydration from condensing before it enters the cooling trap. While this does not allow for the glass sample to be dried in situ, it has the advantage, that the standard mass can be adapted to match the material mass within the other sample holder after dehydration, in case melting or dissolving has caused a decrease. And since the standard is supposed to be non-reactive, disturbing the standard sample by removing it for oven-drying does not lead to additional errors in measurement.

However, opening a second route for the water vapor to flow, might decrease the amount of water vapor passing through the sample significantly, especially in the case that strong agglomeration within a sample occurs. No pressure-gradient would build up to force the water vapor through a cemented salt sample, while the easier route of passage through the holder with the glass-standard is available.

The 4th setup was not realized within the frame of this thesis but can be implemented for future investigations.

4. Results of the XRPD analysis

The materials were reported to be prone to liquefaction while in storage as well as during the crushing process of the crystals into powders for analysis, due to their deliquescent nature. In the attempt to dry the chloride salts for recrystallization before starting the measurements, a too high heating rate was chosen at the Heinrich Heine University of Düsseldorf. As a result, several of the salts turned partially or completely into amorphous solids and the XRPD analysis was incomplete or failed.

The same issue was encountered later with the bromide salts at the University of Bremen where no valid results were reported.

With the high deliquescence of the salts and the low melting points in their hydrated states of phase, the validations of the crystal structures were not conclusive for all mixtures, though it was found that the salt samples were composed of more than one phase and contained traces of the educts as well as the expected compounds.

The 2Θ curve-comparisons of the powder diffraction analysis with literature data can be found in part 3 of the appendix.

4.1. {$MgCl_2$ + KCl}

The sample appears to be partially recrystallized after having been molten or dissolved previous to the measurement, there are several refraction peaks (2Θ = 25 to 30.5° and 2Θ = 38 to 46.5°) which match the powder patterns of Carnallite ($KMgCl_3 \cdot 6H_2O$) $P\ b\ n\ n$ (Fischer, 1973), (Cambridge Crystallographic Data Centre (CCDC), 2016) or $P\ n\ n\ a$ (Schlemper, Sen Gupta, & Zoltai, 1985), (Cambridge Crystallographic Data Centre (CCDC), 2016) and one of the educts Sylvite (KCl) ($F\ m\ \bar{3}\ m$) (Heinrich Heine Universität Düsseldorf , 2013).

4.2. {$3MgSO_4 \cdot 7H_2O$ + 16KCl}

The observed powder pattern curve shows amorphous behavior, indicating a partial dissolving or melting of the sample, which didn't recrystallize completely upon solidifying. The sample's refraction peaks between 2Θ = 28 to 36° match with

those of Kainite ($4(KMg(SO_4)Cl)\cdot 11H_2O$) $C\ 1\ \frac{2}{m}\ 1$ (Robinson, Fang, & Ohya, 1972), (Cambridge Crystallographic Data Centre (CCDC), 2016) and the peaks at (2Θ = 28, 40.5, 58 and 67°) with Sylvite (KCl) $F\ m\ \bar{3}\ m$ (Heinrich Heine Universität Düsseldorf , 2013).

4.3. $\{2Na_2SO_4+Al2(SO_4)_3\cdot 18H_2O\}$

The mixture appears mostly crystallized. The sample peaks match with those of monoclinic $(NaAl(SO_4)_2\cdot 6H_2O)$ $P\ 1\ \frac{2_1}{a}\ 1$ (Robinson & Fang, 1969), (Cambridge Crystallographic Data Centre (CCDC), 2016) and monoclinic $(NaAl(SO_4)_2\cdot 11H_2O)$ $C\ 1\ \frac{2}{c}\ 1$ (Fang & Robinson, 1972), (Cambridge Crystallographic Data Centre (CCDC), 2016) with no confirmed traces of the educts (Heinrich Heine Universität Düsseldorf , 2013).

4.4. $\{MgSO_4\cdot 7H_2O + Al_2(SO_4)_3\cdot 18H_2O\}$

The material appears partially amorphous but the refraction peaks at 2Θ = 19, 21, 22 and 26° match with the powder-pattern of the mineral Pickeringite $((Mg_{0.93},Mn_{0.07})Al_2(SO_4)_4\cdot 22H_2O)$ $P\ 1\ \frac{2_1}{c}\ 1$ (Quartieri, Triscari, & Viani, 2000), (Cambridge Crystallographic Data Centre (CCDC), 2016). No peak matches with the powder patterns of the educts were confirmed (Heinrich Heine Universität Düsseldorf , 2013).

4.5. $\{17MgSO_4\cdot 7H_2O + 3Al_2(SO_4)_3\cdot 18H_2O\}$

While similarities to the refraction peaks of Pickeringite $((Mg_{0.93},Mn_{0.07})Al_2(SO_4)_4\cdot 22H_2O)$ $P\ 1\ \frac{2_1}{c}\ 1$ (Quartieri, Triscari, & Viani, 2000), (Cambridge Crystallographic Data Centre (CCDC), 2016) can be seen, the powder pattern of the sample reads as too amorphous for a validation or for a comparison

with the refraction peaks of the educts (Heinrich Heine Universität Düsseldorf , 2013).

4.6. {$MgCl_2$ + 2$CaCl_2$}

The sample shows amorphous readings, indicating that the mixture recrystallized incompletely. The refraction peaks at 2Θ = 15, 17, 23, 23.5, 26, 28, 31.5, 34 and 43.5°match those of the powder pattern of Tachyhydrite ($CaMg_2Cl_6 \cdot 12H_2O$) $R\,\bar{3}$ (Leclaire, Borel, & Monier, 1980), (Clark, Evans, & Erd, 1980), (Cambridge Crystallographic Data Centre (CCDC), 2016). No match was found with the powder patterns of different phases of the educts (Heinrich Heine Universität Düsseldorf , 2013).

4.7. {$MgCl_2$ + $CaCl_2$}

The sample shows mainly amorphous readings, with only few refraction peaks. This indicates that the sample either dissolved or melted completely during storage, preparation or heating in the oven respectively and did not crystallize when solidifying after drying. No matching peaks to the powder pattern of Tachyhydrite ($CaMg_2Cl_6 \cdot 12H_2O$) $R\,\bar{3}$ (Leclaire, Borel, & Monier, 1980), (Clark, Evans, & Erd, 1980), (Cambridge Crystallographic Data Centre (CCDC), 2016) or different phases of the educts (Heinrich Heine Universität Düsseldorf , 2013) were found.

4.8. {2$MgCl_2$ + $CaCl_2$}

The sample shows amorphous readings indicating partial melting or dissolving and incomplete recrystallisation when oven-dried. The crystalline part of the mixture has matching refraction peaks at 2Θ = 29, 32, 35 and 47.5° with Tachyhydrite ($CaMg_2Cl_6 \cdot 12H_2O$) $R\,\bar{3}$ (Leclaire, Borel, & Monier, 1980), (Clark, Evans, & Erd, 1980), (Cambridge Crystallographic Data Centre (CCDC), 2016) and three possibly matching peaks with anhydrate {$CaCl_2$} (Heinrich Heine Universität Düsseldorf ,

2013) which however fall together with the matching peaks of Tachyhydrite at 2Θ = 29, 32 and 47.5°.

4.9. {$CaCl_2$+2$ZnCl_2$}

This synthetic sample has a mixing ratio similar to that of the synthetic Tachyhydrite mixtures but has no naturally occurring minerals for comparison. The sample appears to have melted or dissolved almost completely and not recrystallized, as most of the mixture reads as amorphous mass. Due to the lack of enough refraction peaks for analysis neither the presence of a potential compound nor that of excess educts was validated.

4.10. {2$MgCl_2$ + $ZnCl_2$}

This synthetic sample has a mixing ratio like that of the synthetic Tachyhydrite mixtures but has no similar naturally occurring minerals for comparison. The sample shows only amorphous readings due to dissolving or melting and re-solidification without recrystallisation. No matching peaks for the educts or possible compounds were confirmed.

5. Results of the TGA/DSC analysis

5.1. Sulfates

The following16 different sulfate mixtures were tested for their heat storage properties:

5.1.1. {$3Na_2SO_4 + K_2SO_4$}, {$Na_2SO_4 + K_2SO_4$}, {$Na_2SO_4 + 3K_2SO_4$}

Aphthitalite was the naturally occurring mixed-salt mineral to be synthesized with varying cation concentration from potassium and sodium sulfate. It has the chemical formula ($(K,Na)_3Na(SO_4)_2$) which occurs in a rhombohedral (trigonal) crystal system (Okada & Ossaka, 1980); (Anthony, Bideaux, Bladh, & Nichols, 2003).

The {$3Na_2SO_4 + K_2SO_4$} was mixed as 22ml {Na_2SO_4}-solution with 9ml {K_2SO_4}-solution.

The {$Na_2SO_4 + K_2SO_4$} had a mixing ratio of 4ml {Na_2SO_4}-solution to 5ml-{K_2SO_4} solution.

And the {$Na_2SO_4 + 3K_2SO_4$} was mixed from 2ml {Na_2SO_4}-solution and 7ml {K_2SO_4}-solution.

It was expected that the varying sodium contents would influence the water uptake of the mixed salts. However, the three sodium-potassium sulfate mixtures did not react with the supplied water vapor to create heat within measurable margins. Instead endothermic peaks were observed during hydration, with simultaneous weight loss, indicating the dissolving of a phase of high crystal order. This concurred with water uptakes and emissions of below 3% of the maximum sample weight. The material absorbed water only after the water supply was cut off and the partial water pressure e was low enough for the samples to re-solidify at the end of the hydration measurements.

5.1.2. {$2Na_2SO_4 + MgSO_4$}, {$7Na_2SO_4 + 4MgSO_4$}, {$2K_2SO_4 + MgSO_4$}

Mixed salts of sodium sulfate {Na_2SO_4} and magnesium sulfate {$MgSO_4$} can occur in monoclinic form as Blodite ($Na_2Mg(SO_4)_2 \cdot 4H_2O$) (Hawthorne, Refinement of the crystal structure of bloedite; structural similarities in the [VI M(IV TPhi 4) 2 Phi n) finite-cluster minerals , 1985), (Anthony, Bideaux, Bladh, & Nichols, 2003) or in trigonal form as Loweite ($Na_{12}Mg_7(SO_4)_{13} \cdot 15H_2O$) (Fang & Robinson, CRYSTAL STRUCTURES AND MINERAL CHEMISTRY OF DOUBLE-SALT HYDRATES. 2. CRYSTAL STRUCTURE OF LOEWEITE, 1970), (Anthony, Bideaux, Bladh, & Nichols, 2003). As the Loweite incorporates more water into its crystal structure than the Blodite, the heat storage capacity was expected to be higher as well. Due to using {$MgSO_4 \cdot 7H_2O$} instead of {$MgSO_4$}, the chemical composition created from the calculated mixing ratios deviated from the planned compositions.

The mixing ratio for the synthetic form of Blodite was 7ml {Na_2SO_4} solution to 6ml {$MgSO_4 \cdot 7H_2O$} solution. This created a {$2Na_2SO_4 + MgSO_4$} mixture.

The sample held about n = 7.9 {H_2O} per unit {$2Na_2SO_4 + MgSO_4$} at the start of the measurement.

Two overlapping peaks were observed during the 1st dehydration at T_{p1} = 51.5°C and T_{p2} = 68.78°C. The sample still held about n = 1.7 {H_2O} per unit {$2Na_2SO_4 + MgSO_4$} after drying at T_{max} = 100°C.

The 1st hydration began with an endothermic peak event and a correlated weight loss, where the water content of the sample is reduced to n = 1.3 {H_2O} per unit {$2Na_2SO_4 + MgSO_4$}. Two exothermic peaks were observed with $H_1 = 43.83 Jg^{-1}$ at e = 14.80mbar and $H_2 = 29.96 Jg^{-1}$ at e = 17.66mbar with an overall enthalpy of $H_{all} = 73.79 Jg^{-1}$. A water content of n = 5.3 {H_2O} per unit {$2Na_2SO_4 + MgSO_4$} was reached at the end of the 1st hydration stage, which equals about 16.3% of the observed minimum sample weight.

The material still contained n = 5.3 {H_2O} per unit {$2Na_2SO_4 + MgSO_4$} at the start of the 2nd cycle.

During the 2nd dehydration, the two peaks observed at the 1st dehydration joined together into a single peak at T_{p1} = 67.84°C. Two more peaks occurred, when the temperature reached T_{p2} = 128.85°C and T_{p3} = 195.05°C. The water content stabilized at T = 104°C with n = 2.0 {H_2O} per unit {$2Na_2SO_4$ + $MgSO_4$} and was reduced to n = 0.8 {H_2O} per unit {$2Na_2SO_4$ + $MgSO_4$} after heating to T_{max} = 200°C.

The 2nd hydration again showed first an endothermic peak event, where the water content was reduced to about n = 0.25 {H_2O} per unit {$2Na_2SO_4$ + $MgSO_4$}, followed by two exothermic peaks which were stronger though than during the 1st hydration with H_1 = 64.63Jg^{-1} at e = 14.80mbar and H_2 = 53.42Jg^{-1} at e = 17.66mbar for an overall enthalpy of H_{all} = 118.05Jg^{-1}. A water content of n = 3.0 {H_2O} per unit {$2Na_2SO_4$ + $MgSO_4$} was reached at the end of the 2nd hydration stage, which equals about 10.1% of the observed minimum sample weight.

The material contained n = 3.1 {H_2O} per unit {$2Na_2SO_4$ + $MgSO_4$} at the start of the 3rd cycle.

Like at the 2nd cycle, three peaks were observed during the 3rd dehydration, with only one peak below T = 100°C at T_{p1} = 63.96°C. However, the second peak T_{p2} = 168.74°C was at a higher temperature by ΔT = 40°C than during the 2nd dehydration measurement. The third peak was measured again at T_{p3} = 195.05°C. The water content declined first to n = 1.9 {H_2O} per unit {$2Na_2SO_4$ + $MgSO_4$} at T = 82°C, then sank to n = 0.7 {H_2O} per unit {$2Na_2SO_4$ + $MgSO_4$} after the sample was heated to T_{max} = 200°C.

The synthetic Loweite equivalent was mixed at a ratio of 1ml {Na_2SO_4} solution to 1ml {$MgSO_4 \cdot 7H_2O$} solution, which created a {$7Na_2SO_4$ + $4MgSO_4$} mixture.

The sample held a water content of n = 21.0 {H_2O} per unit {$7Na_2SO_4$ + $4MgSO_4$} at the start of the 1st measurement cycle.

The 1st dehydration curve showed two overlapping peaks at T_{p1} = 57.16°C, T_{p2} = 97.0°C. The water content was reduced to n = 11.7 {H_2O} per unit {$7Na_2SO_4 + 4MgSO_4$} after heating to T_{max} = 100°C.

The 1st hydration curve begins with an endothermic peak event with a correlated loss of weight where the water content of the sample is reduced to about n = 10.1 {H_2O} per unit {$7Na_2SO_4 + 4MgSO_4$}, followed by two exothermic peaks with H_1 = 61.70Jg^{-1} at e = 14.80mbar and H_2 = 70.23Jg^{-1} at e = 17.66mbar for an overall enthalpy of H_{all} = 131.93Jg^{-1}. A water content of n = 17.5 {H_2O} per unit {$7Na_2SO_4 + 4MgSO_4$} was reached at the end of the 1st hydration stage, which equals about 22.1% of the observed minimum sample weight.

The mixture contained a water content of n = 17.6 {H_2O} per unit {$7Na_2SO_4 + 4MgSO_4$} at the start of the 2nd measurement cycle.

At the 2nd dehydration, the two low temperature peaks seen before were merged into a single peak at T_{p1} = 73.17°C while a second peak was visible when the temperature rose above the T = 100°C threshold at T_{p2} = 132.83°C. At T =105°C the water content was about n = 12.0 {H_2O} per unit {$7Na_2SO_4 + 4MgSO_4$}, after T_{max} = 200°C the water content was reduced to n = 5.0 {H_2O} per unit {$7Na_2SO_4 + 4MgSO_4$}.

The 2nd hydration curve also begins with an endothermic peak event correlated with a loss of weight but here the water content of the sample is reduced to about n = 3.6 {H_2O} per unit {$7Na_2SO_4 + 4MgSO_4$}, followed by two exothermic peaks with H_1 = 125.23Jg^{-1} at e = 14.80mbar and H_2 = 38.81Jg^{-1} at e = 17.66mbar with an overall enthalpy of H_{all} = 164.05Jg^{-1}. A water content of n = 12.3 {H_2O} per unit {$7Na_2SO_4 + 4MgSO_4$} was reached at the end of the 2nd hydration stage, which equals about 12.2% of the observed minimum sample weight.

The mixture contained a water content of n = 12.4 {H_2O} per unit {$7Na_2SO_4 + 4MgSO_4$} at the start of the 3rd measurement cycle.

During the 3rd dehydration, there were again two overlapping peaks below T = 100°C at T_{p1} = 68.83°C and T_{p2} = 97.73°C while the third peak occurred at T_{p3} = 145.7°C. At T =106°C the water content was about n = 8.5 {H_2O} per unit {$7Na_2SO_4 + 4MgSO_4$}, after T_{max} = 200°C the water content was reduced to n = 5.4 {H_2O} per unit {$7Na_2SO_4 + 4MgSO_4$}.

The mixed salt of potassium sulfate and magnesium sulfate occurs naturally in form of Leonite ($K_2Mg(SO_4)_2 \cdot 4H_2O$) which crystallizes in a monoclinic crystal system (Weiner & Hochleitner, 1987), (Anthony, Bideaux, Bladh, & Nichols, 2003).

The chosen mixing ratio for the {$K_2SO_4 + MgSO_4$} salt was 13ml {K_2SO_4} solution to 9ml {$MgSO_4 \cdot 7H_2O$} solution which resulted in a {$2K_2SO_4 + MgSO_4$} mixture.

The sample held about n = 7.8 {H_2O} per unit {$2K_2SO_4 + MgSO_4$} at the start of the measurement.

The 1st dehydration shows only a single peak at T_{p1} = 93.88°C. After heating to T_{max} = 100°C the sample still contained about n = 2.1 {H_2O} per unit {$2K_2SO_4 + MgSO_4$}.

Aside from three endothermic peak events, two exothermic peaks were observed during the 1st hydration with $H_1 = 17.71 Jg^{-1}$ at e = 14.80mbar and $H_2 = 29.97 Jg^{-1}$ at e = 17.66mbar with an overall enthalpy of $H_{all} = 47.68 Jg^{-1}$. The water uptake was low and the sample held n = 4.2 {H_2O} per unit {$2K_2SO_4 + MgSO_4$} at the end of the hydration, which equals about 10.4% of the observed minimum sample weight. The water content remained stable until the next measurement cycle began.

At the start of the 2nd cycle the sample held still about n = 4.2 {H_2O} per unit {$2K_2SO_4 + MgSO_4$}.

During the 2nd dehydration, two peaks were measured at T_{p1} = 80.05°C and T_{p2} = 134.13°C. At T = 104°C the sample contained about n = 2.3 {H_2O} per unit {$2K_2SO_4 + MgSO_4$}, after heating to T_{max} = 200°C the water content was reduced to n = 1.6 {H_2O} per unit {$2K_2SO_4 + MgSO_4$}.

Like at the 1st hydration, three endothermic peaks were observed during the 2nd hydration, interspersed by two exothermic peaks of H_1 = 12.50Jg^{-1} at e = 14.80mbar and H_2 = 24.78Jg^{-1} at e = 17.66mbar with an overall enthalpy of H_{all} = 37.28Jg^{-1}. The sample only hydrated to a water content of n = 2.9 {H_2O} per unit {$2K_2SO_4 + MgSO_4$} which equaled 5.8% of the observed minimum sample weight and remained stable until the start of the next measurement cycle.

At the start of the 3rd cycle the sample still held about n = 2.9 {H_2O} per unit {$2K_2SO_4 + MgSO_4$}.

The endothermic peaks of the 3rd dehydration that were found at T_{p1} = 75.69°C, T_{p2} = 158.46°C were weak and showed barely any reaction of the material, which correlates with the low water content of the sample. At T = 104°C the sample contained about n = 2.0 {H_2O} per unit {$2K_2SO_4 + MgSO_4$}, after heating to T_{max} = 200°C the water content was reduced to n = 1.6 {H_2O} per unit {$2K_2SO_4 + MgSO_4$}.

5.1.3. {$7Na_2SO_4 + 4ZnSO_4$}, {$10K_2SO_4 + 7ZnSO_4$}, {$3MgSO_4 + 2ZnSO_4$}

The naturally occurring sodium-zinc sulfate mineral is the monoclinic Changoite ($Na_2Zn(SO_4)_2 \cdot 4H_2O$) (Schlüter, Klaska, & Gebhard, 1999), (Mandarino J. A., 1999), (R.A.H, 1999), (Anthony, Bideaux, Bladh, & Nichols, 2003). Due to using {$MgSO_4 \cdot 7H_2O$} and {$ZnSO_4 \cdot 7H_2O$} instead of {$MgSO_4$} or {$ZnSO_4$}, the chemical composition created from the calculated mixing ratios deviated from the wanted compositions.

The mixing ratio for the synthesis of Changoite was 7ml of {Na_2SO_4} solution to 8ml of {$ZnSO_4 \cdot 7H_2O$} solution, resulting in a {$7Na_2SO_4 + 4ZnSO_4$} mixture.

The sample held n = 26.3 {H_2O} per unit {$7Na_2SO_4 + 4ZnSO_4$} at the start of the measurement.

During the 1st dehydration, two overlapping peaks were observed at T_{p1} = 85.31°C and T_{p2} = 97.8°C. After heating the sample to T_{max} = 100°C the water content was still n = 21.6 {H_2O} per unit {$7Na_2SO_4 + 4ZnSO_4$}.

Three endothermic peaks were observed during the 1st hydration and no measurable amount of heat was released. The sample regained only a small amount of water once the water supply was cut off and the partial water pressure e was low enough for the partially dissolved sample to re-solidify, which was marked by a single exothermic peak event. The water content was about n = 23.2 {H_2O} per unit {$7Na_2SO_4 + 4ZnSO_4$} at the end of the hydration measurement, which equaled 15.8% of the observed minimum sample weight.

At the start of the 2nd cycle the sample held a water content of n = 23.3 {H_2O} per unit {$7Na_2SO_4 + 4ZnSO_4$}.

The 2nd dehydration curve showed four peaks, all of them overlapping, at T_{p1} = 84.36°C, T_{p2} = 97.7°C, T_{p3} = 111.08°C and T_{p4} = 129.45°C. The fourth peak was rather a melting- than a dehydration-peak, observed for a heating rate of $\frac{dT}{dt}$ = 5 $Kmin^{-1}$. The water content stabilizes at T = 153°C with n = 10.0 {H_2O} per unit {$7Na_2SO_4 + 4ZnSO_4$}. At the end of the 2nd dehydration it was reduced to n = 9.2 {H_2O} per unit {$7Na_2SO_4 + 4ZnSO_4$}.

The 2nd hydration curve showed two endothermic peaks interrupted by one exothermic peak at e = 14.80mbar with a hydration-enthalpy of H_{all} = 135.39Jg^{-1}. The partially dissolved sample re-solidified once the water supply was cut off in a second exothermic peak event. The water content was replenished to about n = 17.2 {H_2O} per unit {$7Na_2SO_4 + 4ZnSO_4$} after

the 2nd hydration, which equaled about 9.8% of the observed minimum sample weight.

At the start of the 3rd cycle the sample held a water content of n = 17.0 {H_2O} per unit {$7Na_2SO_4 + 4ZnSO_4$}.

During the 3rd dehydration only three peaks were observed, all of them at temperatures of T > 100 °C. The first two peaks at T_{p1} = 139.98°C, T_{p2} = 160.12°C were overlapping, with T_{p2} being a melting peak. The third peak occurred at T_{p3} = 195.26°C. At the end of the 3rd dehydration the water content was reduced to n = 9.5 {H_2O} per unit {$7Na_2SO_4 + 4ZnSO_4$}.

There is no known naturally occurring potassium-zinc sulfate equivalent to Changoite. It is therefore unknown whether the mixture {$K_2SO_4 + ZnSO_4$} forms a compound, how much water it incorporates into its structure or what class that potential crystal structure would be.

The mixing ratio was 7ml {K_2SO_4} solution to 8ml of {$ZnSO_4 \cdot 7H_2O$} solution, resulting in a {$10K_2SO_4 + 7ZnSO_4$} mixture.

The sample was holding approximately about n = 63.9 {H_2O} per unit {$10K_2SO_4 + 7ZnSO_4$} at the start of the measurement. Two overlapping peaks were observed during the 1st dehydration at T_{p1} = 85.15°C and T_{p2} = 89.42°C. After heating the sample to T_{max} = 100°C the mixture was still holding about n = 21.0 {H_2O} per unit {$10K_2SO_4 + 7ZnSO_4$}.

The 1st hydration curve showed three weak peaks, H_1 = 11.97Jg^{-1} at e = 8.65mbar, H_2 = 50.32Jg^{-1} at e = 14.80mbar and H_3 = 19.63Jg^{-1} at e = 17.66mbar, with an overall hydration-enthalpy of H_{all} = 81.91Jg^{-1}. The water content was restored to about n = 36.75 {H_2O} per unit {$10K_2SO_4 + 7ZnSO_4$}, which equaled 11.6% of the observed minimum sample weight.

The water content of the sample sunk to about n = 33.67 {H_2O} per unit {$10K_2SO_4 + 7ZnSO_4$} before the start of the 2nd cycle.

The two peaks observed at the 1st dehydration did not occur during the 2nd dehydration. Only a single melting-peak was observed at T_{p1} = 134.87°C. At T = 150°C the sample was still holding about n = 18.5 {H_2O} per unit {$10K_2SO_4 + 7ZnSO_4$}.

No measurable heat was released during the hydration stage of the 2nd cycle, as the reaction only showed three endothermic peaks. The sample only absorbed 4.78% of its observed minimum weight in water when the partial water vapor pressure was lowered after the water supply was cut off. This replenished the water content to about n = 33.4 {H_2O} per unit {$10K_2SO_4 + 7ZnSO_4$}.

Before the start of the 3rd cycle the water content of the sample sank to about n = 21.7 {H_2O} per unit {$10K_2SO_4 + 7ZnSO_4$}.

The curve of the 3rd dehydration didn't show any measurable peaks but the water content declined to n = 17.1 {H_2O} per unit {$10K_2SO_4 + 7ZnSO_4$} while the sample was heated to T_{max} = 200°C.

The material became unreactive after melting once during the dehydration of the 2nd cycle. While this could be avoided by keeping operating temperatures below T_{max} = 100°C, the heat storage as can be observed during the hydration of the 1st cycle would be low.

The naturally occurring example for a mixed magnesium-zinc sulfate is the monoclinic mineral Boyleite ($(Zn,Mg)SO_4 \cdot 4H_2O$) (Walenta, 1978), (Anthony, Bideaux, Bladh, & Nichols, 2003).

The calculated mixing ratio was 4ml {$MgSO_4 \cdot 7H_2O$} solution to 3ml {$ZnSO_4 \cdot 7H_2O$} solution, resulting in a {$3MgSO_4 + 2ZnSO_4$} mixture.

At the start of the measurement, the sample held n = 34.1 {H_2O} per unit {$3MgSO_4 + 2ZnSO_4$}.

The 1st dehydration showed two overlapping peaks at T_{p1} = 56.68°C and T_{p2} = 69.17°C. The water content was reduced to n = 9.5 {H_2O} per unit {$3MgSO_4 + 2ZnSO_4$} after heating to T_{max} = 100°C.

The 1st hydration curve starts with an endothermic peak event, followed by two exothermic peaks with H_1 = 227.00Jg^{-1} at e = 14.80mbar and H_2 = 76.03Jg^{-1} at e = 17.66mbar for a total enthalpy of H_{all} = 303.04Jg^{-1}. The water content was replenished to n = 20.2 {H_2O} per unit {$3MgSO_4 + 2ZnSO_4$} at the end of the hydration measurement, which equaled about 23.3% of the observed minimum sample weight.

At the start of the 2nd measurement cycle the sample held n = 20.33 {H_2O} per unit {$3MgSO_4 + 2ZnSO_4$}.

Four peaks were observed during the 2nd dehydration, though only one of them of significance and occurring below T = 100°C at a temperature of T_{p1} = 62.74°C. The sample was probably partially molten at T_{p1} due to the increased heating rate of $\frac{dT}{dt}$ = 5$Kmin^{-1}$ compared to the heating rate of $\frac{dT}{dt}$ = 1$Kmin^{-1}$ during the dehydration of the 1st cycle. The other peaks occurred at T_{p2} = 125.84°C, T_{p3} = 165.54°C and T_{p4} = 195.5°C. After heating to T_{max} = 200°C, the sample still held n = 10.0 {H_2O} per unit {$3MgSO_4 + 2ZnSO_4$}.

The 2nd hydration started again with an endothermic peak event, here correlated with a distinct loss of water, where the sample only held n = 9.25 {H_2O} per unit {$3MgSO_4 + 2ZnSO_4$}. The two exothermic peaks with H_1 = 134.00Jg^{-1} at e = 14.80mbar and H_2 = 41.67Jg^{-1} at e = 17.66mbar with an overall enthalpy of H_{all}= 175.67Jg^{-1} are much weaker than during the 1st dehydration, which can be attributed to the partial melting of the sample at low temperatures during the previous dehydration, caused by the too high heating rate. The water content recovered to n = 14.6 {H_2O} per unit {$3MgSO_4 + 2ZnSO_4$} at the end of the hydration measurement, which equaled about 11.3% of the observed minimum sample weight.

At the start of the 3rd cycle, the sample was still holding n = 14.6 {H_2O} per unit {$3MgSO_4 + 2ZnSO_4$}.

The 3rd dehydration curve showed only three peaks with the most significant at T_{p1} = 59.61°C which like during the 2nd dehydration was a melting peak. The peaks 2 and 3 of the 2nd dehydration unify to a single peak at T_{p2} = 158.45°C during the third measurement. The last peak occurred again at T_{p3} = 195.41°C. The sample was holding n = 9.8 {H_2O} per unit {$3MgSO_4 + 2ZnSO_4$} after heating to T_{max} = 200°C.

5.1.4. {$Na_2SO_4 + Fe^{2+}SO_4$}, {$2Na_2SO_4 + Fe^{2+}SO_4$}, {$K_2SO_4 + Fe^{2+}SO_4$}

A naturally occurring sodium-iron sulfate is the monoclinic Amarillite ($Na_2Fe^{2+}(SO_4)_2 \cdot 6H_2O$) (Jambor & Grew, New mineral names, 1992), (Anthony, Bideaux, Bladh, & Nichols, 2003). As mentioned in the section about material choice, due to the synthesis from liquid solution, it is likely that some of the Fe^{2+} reacted to Fe^{3+}, which allows for a wider range of products forming from the brine.

The chosen mixing ratio for Amarillite was 1ml {Na_2SO_4} solution to 2ml {$Fe^{2+}SO_4 \cdot 7H_2O$} solution, resulting in a {$Na_2SO_4 + Fe^{2+}SO_4$} mixture.

The sample held about n = 7.0 {H_2O} per unit {$Na_2SO_4 + Fe^{2+}SO_4$} at the start of the measurement.

The 1st dehydration showed five peaks at T_{p1} = 44.58°C, T_{p2} = 62.65°C, T_{p3} = 71.46°C, T_{p4} = 84.36°C and T_{p5} = 92.62°C, where peaks 2 and 3 as well as 4 and 5 were overlapping with each other. The lowest water content after heating the sample to T_{max} = 100°C was n = 5.2 {H_2O} per unit {$Na_2SO_4 + Fe^{2+}SO_4$} but the sample reabsorbed some water during cooldown.

Three endothermic peak events were observed during the 1st hydration, interrupted by a single exothermic peak at e = 14.80mbar with an enthalpy of H_{all} = 21.44Jg^{-1}. The water content first dropped to n = 4.9 {H_2O} per unit

{Na_2SO_4 + $Fe^{2+}SO_4$} then recovered only to n = 5.9 {H_2O} per unit {Na_2SO_4 + $Fe^{2+}SO_4$}, which equaled 16.7% of the observed minimum sample weight.

At the start of the 2nd cycle the sample was still holding about n = 5.9 {H_2O} per unit {Na_2SO_4 + $Fe^{2+}SO_4$}.

The five peaks observed earlier became a single peak at T_{p1} = 95.28°C during the 2nd dehydration. Two more peaks at T > 100°C were measured at T_{p2} = 128.83°C and T_{p3} = 164.78°C. While the mixture appears to have melted completely after the third peak, a partial melting may have already occurred at the second peak. At T = 105°C the sample was holding a water content of n = 5.1 {H_2O} per unit {Na_2SO_4 + $Fe^{2+}SO_4$}, which was reduced to n = 3.0 {H_2O} per unit {Na_2SO_4 + $Fe^{2+}SO_4$} after heating to T_{max} = 200°C.

The 2nd hydration showed three endothermic peaks, interspersed by three exothermic peaks, one at e = 14.80mbar with $H_1 = 42.27 Jg^{-1}$ and two at e = 17.66mbar with $H_2 = 15.50 Jg^{-1}$ and $H_3 = 39.11 Jg^{-1}$, for an overall enthalpy of $H_{all} = 96.88 Jg^{-1}$. The water content was first reduced to n = 2.75 {H_2O} per unit {Na_2SO_4 + $Fe^{2+}SO_4$}, then replenished to n = 4.6 {H_2O} per unit {Na_2SO_4 + $Fe^{2+}SO_4$}, which equaled about 9.5% of the observed minimum sample weight.

At the start of the 3rd cycle the sample was holding about n = 4.5 {H_2O} per unit {Na_2SO_4 + $Fe^{2+}SO_4$}.

The 3rd dehydration revealed only two peaks at T_{p1} = 51.75°C and T_{p2} = 159.32°C respectively, where the second peak was a melting peak.

The sample was holding n = 4.0 {H_2O} per unit {Na_2SO_4 + $Fe^{2+}SO_4$} at T = 105°C and the water content was reduced to n = 3.2 {H_2O} per unit {Na_2SO_4 + $Fe^{2+}SO_4$} after heating to T_{max} = 200°C.

The second sodium sulfate – iron sulfate mixing ratio of 1ml {Na_2SO_4} solution to 1ml {$Fe^{2+}SO_4 \cdot 7H_2O$} solution which equals a {$2Na_2SO_4$ + $Fe^{2+}SO_4$} mixture, has no natural occurring mineral to be based off. It is possible though, that rhombohedral

(trigonal) Ferrinatrite ($Na_3Fe^{3+}(SO_4)_3{\cdot}3H_2O$) (Neues Jahrbuch für Mineralogie, Monatshefte, 1987), (Anthony, Bideaux, Bladh, & Nichols, 2003) formed in the mixing process.

The sample held a water content of n = 6.8 {H_2O} per unit {$2Na_2SO_4$ + $Fe^{2+}SO_4$} at the start of the measurement.

Only one peak was observed during the 1st dehydration at T_{p1} = 39.03°C. The water content was reduced to n = 6.1 {H_2O} per unit {$2Na_2SO_4$ + $Fe^{2+}SO_4$} after heating to T_{max} = 100°C.

No measurable exothermic peaks were observed during the 1st hydration, instead the hydration curve showed two small endothermic peaks with a corresponding weight loss, where the water content was reduced to n = 5.7 {H_2O} per unit {$2Na_2SO_4$ + $Fe^{2+}SO_4$}. The water content recovered after the water supply was cut off where the sample absorbed the remaining water vapor until it held n = 6.5 {H_2O} per unit {$2Na_2SO_4$ + $Fe^{2+}SO_4$} which equaled about 23.3% of the observed minimum sample weight.

At the start of the 2nd cycle, the sample was still holding n = 6.5 {H_2O} per unit {$2Na_2SO_4$ + $Fe^{2+}SO_4$}.

The low temperature peak did not show during the 2nd dehydration but the sample was constantly losing water. Two melting peaks were observed at T_{p1} = 130.03°C and T_{p2} = 164.13°C. The water content evened out at T = 105°C with n = 6.0 {H_2O} per unit {$2Na_2SO_4$ + $Fe^{2+}SO_4$}, before it sank to n = 0.9 {H_2O} per unit {$2Na_2SO_4$ + $Fe^{2+}SO_4$} after heating to T_{max} = 200°C.

The 2nd hydration curve showed three endothermic events with a single weak exothermic peak at e = 14.80mbar for an enthalpy of H_{all} = 29.59Jg^{-1}. The sample first lost water until the water content was reduced to a minimum of n = 0.67 {H_2O} per unit {$2Na_2SO_4$ + $Fe^{2+}SO_4$}, before it recovered to n = 2.4 {H_2O} per unit {$2Na_2SO_4$ + $Fe^{2+}SO_4$}, still taking up water after the water supply was cut off, which equaled about 6.8% of the observed minimum sample weight.

At the start of the 3rd cycle, the sample was still holding n = 2.4 {H_2O} per unit {$2Na_2SO_4 + Fe^{2+}SO_4$}.

The 3rd dehydration curve showed two weak peaks at T_{p1} = 74.62°C and T_{p2} = 158.6°C. The sample was holding about n = 1.6 {H_2O} per unit {$2Na_2SO_4 + Fe^{2+}SO_4$} at T = 108°C, before the water content was reduced to n = 1.0 {H_2O} per unit {$2Na_2SO_4 + Fe^{2+}SO_4$} after heating to T_{max} = 200°C.

Aside from a decrease in heat yield, the {$2Na_2SO_4 + Fe^{2+}SO_4$} mixture reacted similar to the {$Na_2SO_4 + Fe^{2+}SO_4$} mixture. It is likely that either a similar compound was generated, with the excess of the starting material {Na_2SO_4} slowing the reaction down, or that only the {$Fe^{2+}SO_4$} component reacted with the water and neither mixture formed any compounds.

A naturally occurring potassium-iron sulfate is the monoclinic Mereiterite ($K_2Fe^{2+}(SO_4)_2 \cdot 4H_2O$) (Giester & Rieck, 1995), (Anthony, Bideaux, Bladh, & Nichols, 2003).

To synthesize it, 8ml of the {K_2SO_4} solution was mixed with 7ml of the {$Fe^{2+}SO_4 \cdot 7H_2O$} solution which resulted in a {$9K_2SO_4 + 5Fe^{2+}SO_4 \cdot 7H_2O$} mixture, due to using hydrated iron-sulfate in the synthesis.

The sample was holding n = 34.0 {H_2O} per unit {$9K_2SO_4 + 5Fe^{2+}SO_4$} at the start of the measurement.

The 1st dehydration showed two separate peaks at T_{p1} = 62.3°C and T_{p2} = 88.96°C. The water content was reduced to n = 21.0 {H_2O} per unit {$9K_2SO_4 + 5Fe^{2+}SO_4$} at T = 81°C and decreased further to n = 16.0 {H_2O} per unit {$9K_2SO_4 + 5Fe^{2+}SO_4$} after heating to T_{max} = 100°C.

During the 1st hydration no measurable exothermic peaks occurred, instead three endothermic peaks were observed. The water content was first reduced to n = 14.9 {H_2O} per unit {$9K_2SO_4 + 5Fe^{2+}SO_4$}, before it recovered to n = 19.0 {H_2O} per unit {$9K_2SO_4 + 5Fe^{2+}SO_4$} once the water supply was cut off in an exothermic event. The water content equaled about 11.3% of the observed minimum sample weight.

At the start of the 2nd cycle, the sample was holding n = 19.2 $\{H_2O\}$ per unit $\{9K_2SO_4 + 5Fe^{2+}SO_4\}$.

None of the low temperature peaks from the 1st dehydration measurement were observed again during the 2nd dehydration. Instead the curve showed a single melting peak at T_{p1} = 165.52°C. After heating to T_{max} = 200°C the sample held a water content of n = 4.6 $\{H_2O\}$ per unit $\{9K_2SO_4 + 5Fe^{2+}SO_4\}$.

During the 2nd hydration again only three endothermic peaks occurred. The water content of the sample was reduced to the minimum of n = 4.0 $\{H_2O\}$ per unit $\{9K_2SO_4 + 5Fe^{2+}SO_4\}$ at the start of the hydration stage, where also the minimum sample weight occurred. Then the water content recovered to n = 10.2 $\{H_2O\}$ per unit $\{9K_2SO_4 + 5Fe^{2+}SO_4\}$ once the water supply was cut off, which equaled about 4.7% of the observed minimum weight.

Neither of the two hydration curves showed exothermic peaks while the water supply was activated. Instead three endothermic peak events were observed during both measurements, correlated with a loss of weight.

At the start of the 3rd cycle, the sample was holding n = 10.4 $\{H_2O\}$ per unit $\{9K_2SO_4 + 5Fe^{2+}SO_4\}$.

Two weak peaks were measured at T_{p1} = 64.34°C and T_{p2} = 158.28°C respectively during the 3rd dehydration. The water content was reduced to n = 5.8 $\{H_2O\}$ per unit $\{9K_2SO_4 + 5Fe^{2+}SO_4\}$ at T = 105°C and sank further until it reached a value of n = 4.5 $\{H_2O\}$ per unit $\{9K_2SO_4 + 5Fe^{2+}SO_4\}$ after heating to T_{max} = 200°C.

An insoluble rust colored deposit (presumably $\{Fe^{3+}{}_2O_3\}$) settled at the bottom of the sample bottles with liquid solutions of the mixtures $\{Na_2SO_4 + Fe^{2+}SO_4\}$, $\{2Na_2SO_4 + Fe^{2+}SO_4\}$ and $\{9K_2SO_4 + 5Fe^{2+}SO_4\}$ during storage. As the observed decomposition in combination with water not only lowers the overall cycle stability but the necessary removal of the deposits from the battery system also increases the maintenance requirements, the mixtures containing $\{Fe^{3+}{}_2O_3\}$ were set aside

as ineffectual for thermochemical heat storage purposes which are using {H_2O} as the main solvent.

5.1.5. {$2Na_2SO_4 + Al_2(SO_4)_3$}

A naturally occurring sodium-aluminum sulfate is the cubic Alum-(Na) ($NaAl(SO_4)_2 \cdot 12H_2O$). For creating a synthetic variant, a mixing ratio of 7ml {Na_2SO_4} solution to 17ml {$Al_2(SO_4)_3 \cdot 18H_2O$} solution was used resulting in a {$2Na_2SO_4 + Al_2(SO_4)_3$} mixture, due to using hydrated aluminium-sulfate. As the sulfate content of the mixture is higher than that of the naturally occurring mineral, {H_2SO_4} was expected to be a side product of the reaction in the liquid solution but was not monitored.

The sample was holding approximately about n = 37.0 {H_2O} per unit {$2Na_2SO_4 + Al_2(SO_4)_3$} at the start of the measurement, indicating that the sodium-sulfate components were hydrated as well as the aluminum-sulfate.

Three peaks overlapping with each other, were observed during the 1st dehydration at T_{p1} = 43.35°C, T_{p2} =90.29 °C and T_{p3} =83.51 °C. The third, weakest peak occurred, while the sample was already being cooled back down. The sample was still holding about n = 14.7 {H_2O} per unit {$2Na_2SO_4 + Al_2(SO_4)_3$} after the three peak events.

The 1st hydration curve started off with two endothermic peak events, where the water content sank to n = 13.8 {H_2O} per unit {$2Na_2SO_4 + Al_2(SO_4)_3$}. They were followed by two exothermic peaks at e = 14.80mbar with an enthalpy of H_1 = 45.88Jg^{-1} and e = 17.66mbar and an enthalpy of H_2 = 91.15Jg^{-1} for a total of H_{all} = 137.03Jg^{-1}, where the sample reabsorbed water. The water content was restored to n = 17.8 {H_2O} per unit {$2Na_2SO_4 + Al_2(SO_4)_3$} at the end of the hydration measurement, which equaled about 17.9% of the observed minimum sample weight.

At the start of the 2nd cycle the sample held a water content of n = 18.66 {H_2O} per unit {$2Na_2SO_4 + Al_2(SO_4)_3$}.

The 2nd dehydration showed four peaks at T_{p1} = 93.6°C, T_{p2} = 133.31°C, T_{p3} = 196.25°C and T_{p4} = 172.97°C, with the first and second peak overlapping as were the third and the fourth. The fourth peak was again measured during the cooldown stage. The sample was holding about n = 16.9 {H_2O} per unit {$2Na_2SO_4 + Al_2(SO_4)_3$} after the low temperature peak at T = 98°C. After the fourth peak the water content had declined to n = 11.8 {H_2O} per unit {$2Na_2SO_4 + Al_2(SO_4)_3$}.

During the 2nd hydration only three endothermic events occurred. The water content reached the observed minimum of n = 10.5 {H_2O} per unit {$2Na_2SO_4 + Al_2(SO_4)_3$}, when the sample started to dissolve, where also the minimum weight was recorded. The water content recovered to n = 12.3 {H_2O} per unit {$2Na_2SO_4 + Al_2(SO_4)_3$}, which equaled about 3.3% of the minimum weight, after the hydration stage when the water supply was cut off. A single exothermic peak signaled that the sample re-solidified, as soon as the water pressure eased up.

At the start of the 3rd cycle the sample held a water content of n = 12.4 {H_2O} per unit {$2Na_2SO_4 + Al_2(SO_4)_3$}.

The 3rd dehydration only showed two measurable, overlapping, endothermic peaks which coincided with a loss of weight at T_{p1} = 196.23°C and T_{p2} = 172.55°C, the latter peak was again occurring during the cooldown stage. The sample held a water content of n = 11.5 {H_2O} per unit {$2Na_2SO_4 + Al_2(SO_4)_3$} at the end of the dehydration measurement.

While no melting peaks were identified, the material proved to be of low cycle stability, as it dissolved easily during hydration.

5.1.6. {$MgSO_4 + Al_2(SO_4)_3$}, {$17MgSO_4 + 3Al_2(SO_4)_3$}, {$2Fe_n(SO_4)_m + Al_2(SO_4)_3$}

Magnesium-aluminum minerals occur naturally in the form of monoclinic Pickeringite ($MgAl_2(SO_4)_4 \cdot 22H_2O$) (Hayes, 1844), (Anthony, Bideaux, Bladh, & Nichols, 2003).

The mixing ratio for a synthetic Pickeringite-like sample was chosen as 7ml {$MgSO_4 \cdot 7H_2O$} solution to 20ml {$Al_2(SO_4)_3 \cdot 18H_2O$} solution, which resulted in a {$MgSO_4 + Al_2(SO_4)_3$} mixture.

At the start of the measurement the sample was holding about n = 25.2 {H_2O} per unit {$MgSO_4 + Al_2(SO_4)_3$}.

The 1st dehydration curve shows two overlapping peaks at T_{p1} = 65.59 °C and T_{p2} = 83.6°C. After heating to T_{max} = 100°C the sample was holding about n = 6.7 {H_2O} per unit {$MgSO_4 + Al_2(SO_4)_3$}.

Two endothermic peaks were observed at the start of the 1st hydration, followed by two exothermic peaks at e = 14.80mbar with an enthalpy of H_1 = 147.80Jg^{-1} and at e = 17.66mbar with an enthalpy of H_2 = 224.85Jg^{-1} for a total of H_{all} = 372.65Jg^{-1}. During the endothermic events the water content was reduced to n = 6.5 {H_2O} per unit {$MgSO_4 + Al_2(SO_4)_3$}, before it recovered to n = 14.8 {H_2O} per unit {$MgSO_4 + Al_2(SO_4)_3$} at the end of the hydration measurement, which equaled about 40.0% of the observed minimum sample weight.

At the start of the 2nd cycle the sample was holding about n = 14.8 {H_2O} per unit {$MgSO_4 + Al_2(SO_4)_3$}.

During the 2nd dehydration the low temperature peaks were joined into a single peak at T_{p1} = 72.85 °C and a new second peak was observed at T_{p2} = 158.82°C. At T = 104°C the sample was holding about n = 8.0 {H_2O} per unit {$MgSO_4 + Al_2(SO_4)_3$}. The water content declined to n = 3.8 {H_2O} per unit {$MgSO_4 + Al_2(SO_4)_3$} after heating to T_{max} = 200°C.

Similar if weaker endothermic and exothermic peaks like at the 1st hydration were observed again during the 2nd hydration, at e = 14.80mbar with an enthalpy of H_1 = 112.18Jg^{-1} and at e = 17.66mbar with an enthalpy of H_2 = 100.44Jg^{-1} for a total of H_{all} = 212.61Jg^{-1}. The water content was reduced to its minimum of n = 3.33 {H_2O} per unit {$MgSO_4 + Al_2(SO_4)_3$}, where also the

minimum sample weight was recorded, during the endothermic events. The water content recovered to n = 7.9 {H_2O} per unit {$MgSO_4$ + $Al_2(SO_4)_3$} at the end of the hydration measurement, which equaled 16.3% of the observed minimum sample weight.

At the start of the 3rd cycle the sample was holding about n = 8.0 {H_2O} per unit {$MgSO_4$ + $Al_2(SO_4)_3$}.

The low temperature peak observed before, split up again into two overlapping peak events during the 3rd dehydration at T_{p1} = 63.09 °C and T_{p2} = 92.96°C, while the peak that was measured at T >100°C shifted by ΔT = 34.54°C to T_{p3} = 193.36 °C. At T = 106°C the sample was still holding n = 5.0 {H_2O} per unit {$MgSO_4$ + $Al_2(SO_4)_3$}. After heating to T_{max} = 200°C the water content was reduced to n = 3.7 {H_2O} per unit {$MgSO_4$ + $Al_2(SO_4)_3$}.

A second magnesium-aluminum mineral (of unknown crystal symmetry) is Aromite with a chemical composition reported as ($Mg_6Al_2(SO_4)_9 \cdot 54H_2O$) (Darapsky, Neues Jahrbuch für Mineralogie, Geologie und Paleontologie, 1890).

Its mixing ratio was calculated as 19ml {$MgSO_4 \cdot 7H_2O$} solution to a 9ml {$Al_2(SO_4)_3 \cdot 18H_2O$} solution, which resulted in a {$17MgSO_4$ + $3Al_2(SO_4)_3$} mixture, due to using hydrated educts rather than anhydrates.

At the start of the measurement the sample was holding about n = 174.1 {H_2O} per unit {$17MgSO_4$ + $3Al_2(SO_4)_3$}.

The 1st dehydration showed four overlapping peaks at T_{p1} = 43.77°C, T_{p2} = 55.73°C, T_{p3} = 77.59°C and T_{p4} = 94.63°C. After heating to T_{max} = 100°C the sample was still holding about n = 62.0 {H_2O} per unit {$17MgSO_4$ + $3Al_2(SO_4)_3$}.

The 1st hydration curve started with two endothermic peak events before the reaction turned exothermic with two more peaks at e = 14.80mbar with an enthalpy of H_1 = 181.39Jg^{-1} and e = 17.66mbar H_2 = 299.98Jg^{-1} respectively for a total of H_{all} = 481.37Jg^{-1}. The water content was reduced to n = 59.21

{H_2O} per unit {$17MgSO_4 + 3Al_2(SO_4)_3$} during the endothermic events but recovered to n = 118.2 {H_2O} per unit {$17MgSO_4 + 3Al_2(SO_4)_3$} at the end of the hydration measurement, which equaled about 41.6% of the observed minimum sample weight.

At the start of the 2nd cycle, the sample contained about n = 116.9 {H_2O} per unit {$17MgSO_4 + 3Al_2(SO_4)_3$}.

Only two peaks were observed during the 2nd dehydration at T_{p1} = 71.28°C and T_{p2} = 152.72°C. After the first peak at T = 104°C, the sample was holding n = 66.4 {H_2O} per unit {$17MgSO_4 + 3Al_2(SO_4)_3$}. The water content decreased to n = 36.9 {H_2O} per unit {$17MgSO_4 + 3Al_2(SO_4)_3$} after heating to T_{max} = 200°C.

During the 2nd hydration, two endothermic and two weaker exothermic peaks were observed as well, the exothermic peaks at e = 14.80mbar with an enthalpy of H_1 = 53.84Jg^{-1} and e = 17.66mbar H_2 = 77.23Jg^{-1} for a total of H_{all} = 131.07Jg^{-1}. The water content was reduced to its observed minimum of n = 33.33 {H_2O} per unit {$17MgSO_4 + 3Al_2(SO_4)_3$} during the endothermic peak events. It recovered to n = 61.6 {H_2O} per unit {$17MgSO_4 + 3Al_2(SO_4)_3$} at the end of the hydration measurement, which equaled 13.9% of the observed minimum sample weight.

The sample's water content at the start of the 3rd cycle was n = 62.1 {H_2O} per unit {$17MgSO_4 + 3Al_2(SO_4)_3$}.

The 3rd dehydration curve showed two peaks as well, the first of them at T_{p1} = 64.98°C. Compared to the 2nd dehydration, the temperature of the second peak was increased by ΔT = 40.54°C to T_{p2} = 193.26°C. At T = 105°C the water content was about n = 42.1 {H_2O} per unit {$17MgSO_4 + 3Al_2(SO_4)_3$} and was reduced to n = 34.1 {H_2O} per unit {$17MgSO_4 + 3Al_2(SO_4)_3$} after heating to T_{max} = 200°C.

There are two naturally occurring iron-aluminum sulfate minerals, distinguished by the degree of oxidation of the iron incorporated. The first is the monoclinic Halotrichite ($Fe^{2+}Al_2(SO_4)_4 \cdot 22H_2O$) (Zodrow & Mc Candlish, 1978), (Anthony, Bideaux, Bladh, & Nichols, 2003), the second is the trigonal Aluminocoquimbite ($Fe^{3+}Al(SO_4)_3 \cdot 9H_2O$) (Williams, Hatert, Pasero, & Mills, 2010), (Demartin, Castellano, Gramaccioli, & Campostrini, 2010), (Welch, Smith, Camara, & Gatta, 2013).

While the mixing ratio of 6ml {$Fe^{2+}SO_4 \cdot 7H_2O$} solution to 7ml {$Al_2(SO_4)_3 \cdot 18H_2O$} solution was calculated to recreate Halotrichite, a change in the oxidation level can occur within the brine, which would result in the formation of Aluminocoquimbite with an excess of {$Al_2(SO_4)_3 \cdot 18H_2O$} instead.

The chosen mixing ratio resulted in a {$2Fe^{2+}SO_4 + Al_2(SO_4)_3$} mixture (not taking a possible change of Fe^{2+} to Fe^{3+} into account), due to using the hydrated phases instead of anhydrate educts.

At the start of the measurement the water content of the sample was about n = 31.8 {H_2O} per unit {$2Fe^{2+}SO_4 + Al_2(SO_4)_3$}.

Three overlapping peaks were measured during the 1st dehydration at T_{p1} = 49.21°C, T_{p2} = 84.68°C and T_{p3} = 86.81°C. After heating to T_{max} = 100°C, the sample still held about n = 10.8 {H_2O} per unit {$2Fe^{2+}SO_4 + Al_2(SO_4)_3$}.

An endothermic peak event, followed by two exothermic peaks occurred during the 1st hydration, the exothermic events were found at e = 14.80mbar with an enthalpy of H_1 = 141.14Jg^{-1} and at e = 17.66mbar H_2 = 238.79Jg^{-1} respectively for a total of H_{all} = 379.93Jg^{-1}. The water content of the sample declined to n = 10.0 {H_2O} per unit {$2Fe^{2+}SO_4 + Al_2(SO_4)_3$} during the endothermic reaction. It recovered to n = 18.5 {H_2O} per unit {$2Fe^{2+}SO_4 + Al_2(SO_4)_3$} at the end of the hydration measurement, which equaled about 26.3% of the observed minimum sample weight.

At the start of the 2nd cycle, the sample was holding about n = 17.9 {H_2O} per unit {$2Fe^{2+}SO_4 + Al_2(SO_4)_3$}.

The 2nd dehydration showed four peaks at T_{p1} = 91.26 °C, T_{p2} = 157.41 °C, T_{p3} = 196.21°C and T_{p4} = 173.88°C with the first and second peak overlapping as well as the third and fourth. The fourth peak occurred while the measurement was already at the cooldown stage. At T = 105°C the sample was holding about n = 12.2 {H_2O} per unit {$2Fe^{2+}SO_4 + Al_2(SO_4)_3$}. The water content was reduced further to n = 8.0 {H_2O} per unit {$2Fe^{2+}SO_4 + Al_2(SO_4)_3$} after the fourth peak.

During the 2nd hydration again first two endothermic peak events, then two exothermic peaks were observed, the latter at e = 14.80mbar with an enthalpy of H_1 = 22.74Jg^{-1} and e = 17.66mbar with H_2 = 74.06Jg^{-1} for a total enthalpy of H_{all} = 96.80Jg^{-1}. The water content of the sample declined to the observed minimum of n = 7.2 {H_2O} per unit {$2Fe^{2+}SO_4 + Al_2(SO_4)_3$} during the endothermic reaction, where also the minimum sample weight was recorded. It recovered to n = 11.0 {H_2O} per unit {$2Fe^{2+}SO_4 + Al_2(SO_4)_3$} at the end of the hydration measurement, which equaled 8.9% of the observed minimum sample weight.

At the start of the 3rd cycle, the sample was holding about n = 11.0 {H_2O} per unit {$2Fe^{2+}SO_4 + Al_2(SO_4)_3$}.

The 3rd dehydration too showed four peaks similar to those, measured during the 2nd dehydration at T_{p1} = 73.51°C, T_{p2} = 157.86°C, T_{p3} = 196.18°C and T_{p4} = 174.03°C where again the first and the second peak were overlapping with each other as well as the third and fourth and the fourth peak occurred while the measurement was already at the cooldown stage. At T = 104°C the sample was holding about n = 9.0 {H_2O} per unit {$2Fe^{2+}SO_4 + Al_2(SO_4)_3$}. The water content was reduced further to n = 7.6 {H_2O} per unit {$2Fe^{2+}SO_4 + Al_2(SO_4)_3$} after the fourth peak.

Overall the performance of the 16 different tested sulfate mixtures was found lacking and as a result the measurements with sulfate-only mixtures were discontinued. The results are summarized in Table 7.

Table 7 Sulfate-samples with varying mixing ratios tested for energy storage density and water uptake in percent of the hydrated sample weight. While the Al-Sulfates show the highest initial heat storage density, they also show the lowest cycle stability of the tested samples.

Materials	Energy storage density [Jg^{-1}] T_{max} = 100°C	Water uptake wgt [%] T_{max} = 100°C	Energy storage density [Jg^{-1}] T_{max} = 200°C	Water uptake wgt [%] T_{max} = 200°C
{$3Na_2SO_4 + K_2SO_4$}	---	2.35	---	2.35
{$Na_2SO_4 + K_2SO_4$}	---	2.73	---	2.64
{$Na_2SO_4 + 3K_2SO_4$}	---	2.72	---	2.55
{$2Na_2SO_4 + MgSO_4$}	73.79	16.30	118.05	10.13
{$7Na_2SO_4 + 4MgSO_4$}	131.93	22.09	164.05	12.21
{$2K_2SO_4 + MgSO_4$}	17.71	10.41	37.28	5.78
{$7Na_2SO_4 + 4ZnSO_4$}	---	15.80	135.39	9.76
{$10K_2SO_4 + 7ZnSO_4$}	81.91	11.62	---	4.78
{$3MgSO_4 + 2ZnSO_4$}	303.04	23.28	175.67	11.25
{$Na_2SO_4 + Fe^{2+}SO_4$}	21.44	16.69	96.88	9.5
{$2Na_2SO_4 + Fe^{2+}SO_4$}	---	23.29	29.59	6.84
{$9K_2SO_4 + 5Fe^{2+}SO_4$}	---	11.28	---	4.68
{$2Fe_n(SO_4)_m + Al_2(SO_4)_3$}	379.93	26.26	96.80	8.85
{$2Na_2SO_4 + Al_2(SO_4)_3$}	137.03	17.87	---	3.32
{$17MgSO_4 + 3Al_2(SO_4)_3$}	481.37	41.60	131.07	13.87
{$MgSO_4 + Al_2(SO_4)_3$}	372.65	40.00	212.61	16.31

5.2. Chlorides

Aside from 19 different chloride mixtures, the 4 untreated starting materials were tested by TGA/DSC for comparison.

5.2.1. {$MgCl_2$}

An extra complication for the calculation of the water content of this material was the expected and observed decay of {MgCl2} at T > 117°C. As a result, the sample turned at least partially into {Mg(OH)Cl·xH2O} during the 2nd and 3rd dehydration.

Gauging that the {$MgCl_2$} sample had not split off any {HCl} yet and was still holding about n = 5 {H_2O} water per unit {$MgCl_2$} after the T_{max} = 100°C measurement, the water content at the start of the measurement was calculated as n = 7.8 {H_2O} water per unit {$MgCl_2$}.

The dehydration reaction was already ongoing a T = 25°C at the start of the 1st dehydration and two peaks were observed at T_{p1} = 42.09°C and T_{p2} = 96.18°C respectively.

The 1st hydration showed three peaks at e = 8.65mbar with an enthalpy of H_1 = 38.04Jg^{-1}, e = 14.80mbar with an enthalpy of H_2 = 58.87Jg^{-1} and e = 17.66mbar with H_3 = 151.01Jg^{-1} for a total of H_{all} = 247.92Jg^{-1}. Only the second and third peak were overlapping. The water content reached a maximum of n = 6.4 {H_2O} per unit {$MgCl_2$} during the hydration, which equaled about 172.3% of the observed minimum sample weight. The material emitted excess water as soon as the water supply was cut off in an endothermic event. The water content stabilized at about n = 6.2 {H_2O} per unit {$MgCl_2$} at T = 25°C.

The 2nd dehydration showed seven peaks at T_{p1} = 87.93 °C, T_{p2} = 117.34°C, T_{p3} = 140.36 °C, T_{p4} = 184.11 °C, T_{p5} = 195.86 °C, T_{p6} = 196.01 °C and T_{p7} = 184.84°C which were all overlapping each other and the 7th peak being observed during the cooldown stage. The peak at T_{p2} = 117.34 is likely the indicator for {HCl} being split off from the {$MgCl_2$}-hydrate and the phase change to the tetrahydrate. Partial melting may have occurred at T_{p4} = 184.11 °C and T_{p5} = 195.86 °C but the peaks are not clear indicators.

Assuming that the {$MgCl_2 \cdot xH_2O$} had undergone a reaction to {$Mg(OH)Cl \cdot (x-1)H_2O + HCl$} after heating to T_{max} = 200°C during the 2nd dehydration, the remaining water content was gauged as n = 3.5 {H_2O} per unit {Mg(OH)Cl}.

During the 2nd hydration three stronger, overlapping peaks were observed at e = 8.65mbar with an enthalpy of H_1 = 202.01Jg^{-1}, e = 14.80mbar with an enthalpy of H_2 = 268.34Jg^{-1} and e = 17.66mbar H_3 = 347.91Jg^{-1} for a total of H_{all} = 818.27Jg^{-1}. The water content reached a maximum of n = 5.9 {H_2O} per unit {Mg(OH)Cl} during the hydration, which equaled about 80.04% of the observed minimum sample weight. The material emitted excess water as soon as the water supply was cut off in an endothermic event. The water content stabilized at about n = 5.6 {H_2O} per unit {Mg(OH)Cl} at T = 25°C.

Six overlapping peaks were observed during the 3rd dehydration at T_{p1} = 91.75°C, T_{p2} = 117.9°C, T_{p3} = 138.47°C, T_{p4} = 177.34°C, T_{p5} = 196.23°C and T_{p6} = 180.95°C, the latter again measured during the cooldown stage. Like during the 2nd dehydration T_{p2} was likely the point at which {HCl} split off from the hydrate.

The remaining water content was gauged as n = 3.0 {H_2O} per unit {Mg(OH)Cl} after heating to T_{max} = 200°C.

5.2.2. {$CaCl_2$}

The sample chosen for the TGA/DSC analysis had originally a composition of {$CaCl_2 \cdot 2H_2O$} resembling Sinjarite.

The sample hydrated further before the analysis started, until it contained about n = 9.2 {H_2O} per unit {$CaCl_2$}. While cut off from the air humidity in the oven chamber of the TGA, the overhydrated sample began to emit excess water at T ~ 25°C.

The 1st dehydration curve showed two individual peaks at T_{p1} = 61.07°C and T_{p2} = 96.28°C, followed by an exothermic event during the cooldown stage. The sample contained about n = 2.8 {H_2O} per unit {$CaCl_2$} at the end of the T_{max} = 100°C measurement.

The material did not display distinct melting peaks during the 1st dehydration, this may have been caused by the slow heating rate of β = 1Kmin^{-1}, but the exothermic event points to a partial re-solidification of the sample, indicating that a (partial) melting or dissolving event had already occurred before the start of the recording.

Three overlapping peaks were observed during the 1st hydration at e = 8.65mbar with an enthalpy of H_1 = 22.17Jg^{-1}, e = 14.80mbar with an enthalpy of H_2 = 400.29Jg^{-1} and e = 17.66mbar H_3 = 207.57Jg^{-1} for a total of H_{all} = 630.03Jg^{-1}. The sample contained a maximum water content of n = 6.5 {H_2O} per unit {$CaCl_2$} during the hydration, which equaled about 89.7% of the observed minimum sample weight. The material emitted excess water once the water supply was cut off. The water content then stabilized at about n = 5.25 {H_2O} per unit {$CaCl_2$} at T = 28.67°C.

Three overlapping peaks were observed during the 2nd dehydration at T_{p1} = 47.67°C, T_{p2} = 97.28°C and T_{p3} = 151.83°C, with the first peak being a melting peak. The temperature of the peak concurs with known melting temperatures for the tetrahydrate {$CaCl_2 \cdot 4H_2O$} (IFA Institut für Arbeitsschutz Datenbank), (Ropp, 2012), the calculated water content of the sample at the melting event was about n = 5.1 {H_2O} per unit {$CaCl_2$}.

Three strong, overlapping peaks were observed during the 2nd hydration at e = 8.65mbar with an enthalpy of H_1 = 64.02Jg^{-1}, e = 14.80mbar with an enthalpy of H_2 = 308.87Jg^{-1} and e = 17.66mbar H_3 = 471.27Jg^{-1} for a total of H_{all} = 844.16Jg^{-1} despite the partially molten and then re-solidified state of the sample. The sample contained a maximum water content of n = 4.7 {H_2O} per unit {$CaCl_2$} during the hydration, which equaled about 62.9% of the observed minimum sample weight. The material emitted excess water

once the water supply was cut off. The water content stabilized at about n = 4.25 {H_2O} per unit {$CaCl_2$} at T ~ 25°C.

Three overlapping peaks similar to those which occurred during the 2nd dehydration, were observed during the 3rd dehydration at T_{p1} = 39.43°C, T_{p2} = 97.52°C and T_{p3} = 144.72°C, with the first peak being a melting peak.

The sample contained about n = 0.5 {H_2O} per unit {$CaCl_2$} at the end of the T_{max} = 200°C measurement.

5.2.3. {$ZnCl_2$}

Gauging that the {$ZnCl_2$} sample was still holding n = 1.5 {H_2O} per unit {$ZnCl_2$} at the end of the T_{max} = 200°C dehydrations, the material held n = 6.5 {H_2O} per unit {$ZnCl_2$} at the beginning of the evaluation at T = 25°C.

Only a single peak was observed during the 1st dehydration at T_{p1} = 73.9°C. At T_{max} = 100°C the sample was holding about n = 2.5 {H_2O} per unit {$ZnCl_2$}.

Three peaks were observed during the 1st hydration at e = 8.65mbar with an enthalpy of H_1 = 47.55Jg^{-1}, e = 14.80mbar with an enthalpy of H_2 = 157.73Jg^{-1} and e = 17.66mbar H_3 = 182.38Jg^{-1} for a total of H_{all} = 387.66Jg^{-1}. The sample held a maximum water content of n = 5.1 {H_2O} per unit {$ZnCl_2$} during the hydration, which equaled about 39.6% of the observed minimum sample weight.

The 2nd dehydration showed two peaks at T_{p1} = 90.61°C and T_{p2} = 148.04°C. The sample continued to lose weight during the isothermal stage where two more endothermic events occurred, which indicated a partial melting or a phase change to a higher crystal order, where water was expelled from the crystal lattice, before the water content reached approximately n = 1.5 {H_2O} per unit {$ZnCl_2$} after the cooldown stage.

Three strong exothermic peaks showed during the 2nd hydration as well at e = 8.65mbar with an enthalpy of H_1 = 142.55Jg^{-1}, e = 14.80mbar with an enthalpy

of H_2 = 240.68Jg^{-1} and e = 17.66mbar H_3 = 205.26Jg^{-1} for a total of H_{all} = 588.49Jg^{-1}. The sample held a maximum water content of n = 5.6 {H_2O} per unit {$ZnCl_2$} during the hydration, which equaled 45.4% of the observed minimum sample weight. The material emitted excess water as soon as the water supply was cut off. The water content stabilized at about n = 4.75 {H_2O} per unit {$ZnCl_2$} at T = 32.30°C

The 3rd dehydration showed similar peaks to those observed during the 2nd dehydration, at T_{p1} = 89.18°C and T_{p2} = 157.32°C. During the T = 200°C isothermal stage of the 2nd and 3rd dehydration, the sample showed some exothermic behavior but also a few sudden endothermic events, which are hinting at a phase instability.

5.2.4. {KCl}

There were no measurable endothermic reactions observed during dehydration.

And during each of both hydrations instead of exothermic events only three endothermic peak events occurred, where the sample's water content first dropped to a minimum before it recovered after the water supply was cut off, as had been observed before with some of the sulfate mixtures. With a water-uptake of about 2.5% of the minimum sample weight observed at the start of the 2nd hydration. The sample's water content was gauged to vary between a minimum value of n = 0.9 {H_2O} per unit {KCl} and a maximum value of n = 1.0 {H_2O} per unit {KCl} over the measurement cycles.

5.2.5. {$CaCl_2 + 2MgCl_2$}, {$CaCl_2 + MgCl_2$}, {$2CaCl_2 + MgCl_2$}

A natural occurring form of calcium-magnesium-chloride mineral is the rhombohedral (trigonal) Tachyhydrite ($CaMg_2Cl_6 \cdot 12H_2O$) (Anthony, Bideaux, Bladh, & Nichols, 1997). The mixing ratio was altered however to create two more

mixtures to gauge, how the heat storage capacity and cycle stability was influenced, with the deviation from the original composition. Since calcium-chloride-hydrates have a low melting point, a decrease of cycle stability correlated to the higher {$CaCl_2$} content was expected.

The {$CaCl_2$ + 2$MgCl_2$} mixture was synthesized with a mixing ratio of 7ml {$CaCl_2$} solution to 12ml {$MgCl_2$} solution.

The sample held n = 19.2 {H_2O} per unit {$CaCl_2$+ 2$MgCl_2$} at the start of the measurement. The material began already to dehydrate at T = 25°C, indicating an overhydration.

The 1st dehydration curve showed two overlapping peaks, found at T_{p1} = 25.92°C and T_{p2} = 95.86°C. The sample still held about n = 12.0 {H_2O} per unit {$CaCl_2$+ 2$MgCl_2$} after the T_{max} = 100°C measurement.

The 1st hydration curve showed three overlapping peaks at e = 8.65mbar with an enthalpy of H_1 = 31.02Jg^{-1}, e = 14.80mbar with an enthalpy of H_2 = 201.60Jg^{-1} and e = 17.66mbar with an enthalpy of H_3 = 217.53Jg^{-1}, for a total of H_{all} = 450.16Jg^{-1}. The sample held a maximum water content of n = 20.1 {H_2O} per unit {$CaCl_2$ + 2$MgCl_2$} during hydration, which equaled about 155.3% of the observed minimum sample weight. The mixture emitted excess water as soon as the water supply was cut off. The water content stabilized at n = 16.6 {H_2O} per unit {$CaCl_2$ + 2$MgCl_2$} at T = 27.23°C.

During the 2nd dehydration four overlapping peaks were observed at T_{p1} = 69.19°C, T_{p2} = 153.06°C, T_{p3} = 170.11°C, T_{p4} = 181.42°C. The second peak shows characteristics of either partial melting or {HCl} splitting off from the sample. It was assumed that the sample reacted to {$CaCl_2$ + 2Mg(OH)Cl + xH_2O} in the temperature interval from the second peak to the end of the dehydration stage. The sample held about n = 10.0 {H_2O} per unit {$CaCl_2$ + 2Mg(OH)Cl} after the 2nd dehydration (at T_{max} = 200°C).

Three strong, overlapping peaks were measured during the 2nd hydration at e = 8.65mbar with an enthalpy of H_1 = 313.25Jg^{-1}, e = 14.80mbar with an enthalpy of H_2 = 639.29Jg^{-1} and e = 17.66mbar with an enthalpy of H_3 = 601.25Jg^{-1} for H_{all} = 1553.79Jg^{-1}. The sample held a maximum water content of n = 36.1 {H_2O} per unit {$CaCl_2$ + 2Mg(OH)Cl}, which equaled 114.3% of the observed minimum sample weight. The mixture started emitting excess water as soon as the water supply was cut off. The water content did not stabilize before the 3rd dehydration stage began.

Six overlapping peaks were measured during the 3rd dehydration at T_{p1} = 59.93°C, T_{p2} = 90.72°C, T_{p3} = 97.68°C, T_{p4} = 123.31°C, T_{p5} = 156.71°C and T_{p6} = 171.77°C, none of them showed characteristics of {HCl}-emission or melting, indicating that the reaction to {$CaCl_2$ + 2Mg(OH)Cl + xH_2O} was complete before the start of the 3rd dehydration measurement.

The sample held about n = 9.0 {H_2O} per unit {$CaCl_2$ + 2Mg(OH)Cl} after the 3rd dehydration (at T_{max} = 200°C).

The mixing ratio for the {$CaCl_2$ + $MgCl_2$} sample was calculated as 7ml {$CaCl_2$} solution to 6ml {$MgCl_2$} solution.

The sample held about n = 13.4 {H_2O} per unit {$CaCl_2$ + $MgCl_2$} at the start of the measurement and was already reacting by emitting excess water at T ~ 25°C, indicating an overhydration.

During the 1st dehydration, two overlapping peaks were observed at T_{p1} = 45.74°C and T_{p2} = 95.77°C. After the 1st dehydration the sample held about n = 6.67 {H_2O} per unit {$CaCl_2$ + $MgCl_2$}.

The 1st hydration curve only showed two overlapping peaks at e = 14.80mbar with an enthalpy of H_1 = 198.40Jg^{-1} and e = 17.66mbar for an enthalpy of H_2 = 249.45Jg^{-1} and a total of H_{all} = 447.85Jg^{-1}. The sample held a maximum water content of n = 11.0 {H_2O} per unit {$CaCl_2$ + $MgCl_2$}, which equaled 156.4% of the observed minimum sample weight.

The mixture began to emit excess water as soon as the water supply was cut off. The water content balanced at n = 7.9 {H_2O} per unit {$CaCl_2$ + $MgCl_2$} and T = 27.60°C.

The 2nd dehydration curve showed five overlapping peaks at T_{p1} = 88.69°C, T_{p2} = 154.53°C, T_{p3} = 171.88°C, T_{p4} = 181.11°C and T_{p5} = 190.67°C. Where the second and third peaks have characteristics to indicate a {HCl}-emission or a partial melting of the sample. The mixture still held about n = 1.9 {H_2O} per unit {Mg(OH)Cl + $CaCl_2$} after the dehydration to T_{max} = 200°C.

The 2nd hydration curve showed three overlapping peaks at e = 8.65mbar with an enthalpy of H_1 = 217.93Jg^{-1}, e = 14.80mbar with an enthalpy of H_2 = 509.80Jg^{-1} and e = 17.66mbar with an enthalpy of H_3 = 495.99Jg^{-1} for a total of H_{all} = 1223.73Jg^{-1}. The maximum water content during dehydration was n = 12.0 {H_2O} per unit {Mg(OH)Cl + $CaCl_2$}, which equaled about 90.9% of the observed minimum sample weight. The mixture emitted excess water as soon as the water supply was cut. The water content balanced out at n = 9.9 {H_2O} per unit {Mg(OH)Cl + $CaCl_2$} at a temperature of T = 27.57°C.

Only two overlapping peaks were observed during the 3rd dehydration at T_{p1} = 94.82°C and T_{p2} = 180.8°C. There were no signs of melting or of {HCl}-emissions during this measurement, which indicates that the reaction to {Mg(OH)Cl + $CaCl_2$} was already complete at the end of the 2nd dehydration step. The sample held about n = 1.33 {H_2O} per unit {Mg(OH)Cl + $CaCl_2$} after heating to T_{max} = 200°C.

The mixing ratio for the {2$CaCl_2$ + $MgCl_2$} sample was calculated as 7ml {$CaCl_2$} solution to 3ml {$MgCl_2$} solution.

The sample held about n = 22.4 {H_2O} per unit {$MgCl_2$+2$CaCl_2$} at the start of the measurements.

During the 1st dehydration, two overlapping peaks were observed at T_{p1} = 53.22 °C and T_{p2} = 97.22°C. The reaction was already in progress before

the measurement started, indicating that the sample had been overhydrated. The sample held n = 9.0 {H_2O} per unit {$MgCl_2$+2$CaCl_2$} after the dehydration to T_{max} = 100°C.

The 1st hydration curve showed three overlapping peaks at e = 8.65mbar with an enthalpy of H_1 = 28.78Jg^{-1}, e = 14.80mbar with an enthalpy of H_2 = 245.77$Jg^{-1}$and e = 17.66mbar for an enthalpy of H_3 = 354.Jg^{-1} for a total of H_{all} = 628.80Jg^{-1}. The maximum water content during hydration was n = 16.0 {H_2O} per unit {$MgCl_2$+2$CaCl_2$}, which equaled about 232.3% of the observed minimum sample weight. The mixture emitted excess water as soon as the water supply was cut off. The water content did not stabilize at T = 25°C before the next dehydration measurement started.

The 2nd dehydration curve showed six overlapping peaks at T_{p1} = 62.5°C, T_{p2} = 97.6°C, T_{p3} = 128.7°C, T_{p4} = 154.47°C, T_{p5} = 159.8°C and T_{p6} = 181.95°C, where the fourth and fifth peak have the characteristics of a {HCl}-emission or a partial melting of the sample with the {HCl}-emission being more likely as no re-solidification peaks were observed.

The 2nd hydration curve showed three overlapping peaks at e = 8.65mbar with an enthalpy of H_1 = 178.33Jg^{-1}, e = 14.80mbar with an enthalpy of H_2 = 579.25Jg^{-1} and e = 17.66mbar with H_3 = 518.63Jg^{-1} for a total of H_{all} = 1276.22Jg^{-1}. The maximum water content during hydration was n = 17.0 {H_2O} per unit {Mg(OH)Cl + 2$CaCl_2$}, which equaled about 183.6% of the observed minimum sample weight. The mixture emitted excess water as soon as the water supply was cut off. The water content did not stabilize at T = 25°C before the next dehydration measurement started.

Four overlapping peaks were observed during the 3rd dehydration at T_{p1} = 59.02°C, T_{p2} = 95.01°C, T_{p3} = 147.68°C and T_{p4} = 192.61°C. The fourth peak again showed indicators of an {HCl}-emission (or less likely a melting as again no corresponding solidification peak was observed), indicating that the reaction to {Mg(OH)Cl+2$CaCl_2$} during the 2nd dehydration was

incomplete. The sample held about n = 1.0 {H_2O} per unit {$Mg(OH)Cl+2CaCl_2$} after heating to T = 200°C.

5.2.6. {$CaCl_2 + 2ZnCl_2$}, {$CaCl_2 + ZnCl_2$}, {$2CaCl_2 + ZnCl_2$}

As there are no known naturally occurring calcium-zinc chlorides of similar composition to a Tachyhydrite, it is unknown whether any compounds formed within the synthesized mixture or of which crystal symmetry they would be.

The {$CaCl_2 + 2ZnCl_2$} sample was mixed at a ratio of 2ml {$CaCl_2$} solution to 7ml {$ZnCl_2$} solution.

The sample was holding n = 12.7 {H_2O} per unit {$CaCl_2 + 2ZnCl_2$} at the start of the measurement. The mixture began the dehydration reaction at T ~ 25°C implying an overhydration.

Only a single peak occurred during the 1st dehydration at T_{p1} = 60.29°C but the curve showed some endothermic activity with no correlated weight changes during the cooldown stage. The sample was holding n = 6.0 {H_2O} per unit {$CaCl_2 + 2ZnCl_2$} at after heating to T_{max} = 100°C.

The 1st hydration curve displayed three overlapping peaks at e = 8.65mbar with an enthalpy of H_1 = 118.25Jg^{-1}, at e = 14.80mbar with an enthalpy of H_2 = 334.12Jg^{-1} and at e = 17.66mbar with H_3 = 298.00Jg^{-1} for a total of H_{all} = 750.37Jg^{-1}. The exothermic reaction continued for a time even after the water supply was turned off before it turned endothermic and excess water was emitted. The sample held a maximum water content of n = 19.0 {H_2O} per unit {$CaCl_2 + 2ZnCl_2$}, which equaled about 59.2% of the observed minimum sample weight. The water content did not balance out after the endothermic reaction before the next dehydration measurement started.

During the 2nd dehydration two peaks were recorded at T_{p1} = 88.52°C and T_{p2} = 143.79°C. The curve showed the endothermic reaction turning

exothermic after the 2nd peak at T ~ 190°C, then during the cooldown stage four endothermic and exothermic events occurred in close succession of each other, likely due to several instable phase changes. The sample was holding about n = 4.1 {H_2O} per unit {$CaCl_2 + 2ZnCl_2$} at the end of the 2nd dehydration.

The 2nd hydration curve displayed a similar behavior as the 1st hydration curve, with three overlapping peaks at e = 8.65mbar for an enthalpy of H_1 = 113.23Jg^{-1}, at e = 14.80mbar with an enthalpy of H_2 = 385.15Jg^{-1} and at e = 17.66mbar with H_3 = 346.43Jg^{-1} for a total of H_{all} = 844.81Jg^{-1}, as well as the continued exothermic reaction beyond the point of the water supply shutting down. The sample held a maximum water content of n = 18.25 {H_2O} per unit {$CaCl_2 + 2ZnCl_2$}, which equaled about 56.4% of the observed minimum sample weight. The water content declined after the endothermic reaction and did not balance out before the next dehydration measurement started.

The 3rd dehydration curve was developing similar to the 2nd, with two peaks at T_{p1} = 88.21°C and T_{p2} = 144.37°C with the same turn from an endothermic to an exothermic reaction after the second peak at T ~ 190°C. The sample was holding about n = 4.0 {H_2O} per unit {$CaCl_2 + 2ZnCl_2$} at the end of the 3rd dehydration.

The {$CaCl_2 + ZnCl_2$} sample was mixed at a ratio of 4ml {$CaCl_2$} solution to 7ml {$ZnCl_2$} solution.

The sample was holding about n = 11.2 {H_2O} per unit {$CaCl_2 + ZnCl_2$} at the start of the measurement. The reaction started already at T = 25°C, indicating an overhydration of the sample.

The 1st dehydration showed an endothermic peak at T_{p1} = 67.58°C directly followed by an exothermic event at T_{p2} = 100.00°C. The sample held about n = 2.66 {H_2O} per unit {$CaCl_2 + ZnCl_2$} at the end of the 1st dehydration (T = 100°C).

Three overlapping peaks were observed during the 1st hydration at e = 8.65mbar with an enthalpy of H_1 = 81.59Jg^{-1}, at e = 14.80mbar with an enthalpy of H_2 = 320.58Jg^{-1} and at e = 17.66mbar with H_3 = 337.09Jg^{-1} for a total of H_{all} = 739.25Jg^{-1}. The reaction continued for a time after the water supply was cut off, where the sample held a maximum water content of n = 10.0 {H_2O} per unit {$CaCl_2$ + $ZnCl_2$}, which equaled about 51.0% of the observed minimum sample weight. The reaction turned endothermic afterwards and the water content did not balance out before the next dehydration stage started.

The 2nd dehydration curve had three endothermic peaks at T_{p1} = 91.25°C, T_{p3} = 97.95°C and T_{p4} = 119.66°C and an exothermic peak at T_{p2} = 97.90°C. The sample held about n = 2.1 {H_2O} per unit {$CaCl_2$ + $ZnCl_2$} after heating to T_{max} = 200°C.

Three peaks were shown by the 2nd hydration curve at e = 8.65mbar with an enthalpy of H_1 = 78.61Jg^{-1}, at e = 14.80mbar with an enthalpy of H_2 = 327.62Jg^{-1} and at e = 17.66mbar with H_3 = 357.17Jg^{-1} for a total of H_{all} = 763.40Jg^{-1}. Again, there was a delay between the disconnection of the water supply and the end of the reaction. The sample held a maximum water content of n = 9.9 {H_2O} per unit {$CaCl_2$ + $ZnCl_2$}, which equaled about 50.3% of the observed minimum sample weight. The reaction turned endothermic afterwards and the water content did not balance out before the next dehydration stage started.

The 3rd dehydration curve showed three endothermic peaks similar to those of the 2nd hydration curve at T_{p1} = 91.31°C, T_{p3} = 97.88°C and at T_{p4} = 120.02°C and an equivalent exothermic peak at T_{p2} = 97.80°C. The sample held about n = 2.0 {H_2O} per unit {$CaCl_2$ + $ZnCl_2$} after heating to T_{max} = 200°C.

The mixing ratio for the {2$CaCl_2$ + $ZnCl_2$} sample was calculated as 8ml {$CaCl_2$} solution to 5ml {$ZnCl_2$} solution.

The sample held about n = 21.6 {H_2O} per unit {$2CaCl_2 + ZnCl_2$} at the start of the measurement. As the reaction already started at T ~ 25°C, the sample was overhydrated.

The 1st dehydration curve showed three overlapping peaks at T_{p1} = 61.10°C, T_{p2} = 64.82°C and T_{p3} = 79.89°C. The sample held about n = 10.1 {H_2O} per unit {$2CaCl_2 + ZnCl_2$} after heating to T_{max} = 100°C.

During the 1st hydration, three peeks were observed at e = 8.65mbar with an enthalpy of H_1 = 51.61Jg^{-1}, at e = 14.80mbar with an enthalpy of H_2 = 239.61Jg^{-1} and at e = 17.66mbar with H_3 = 359.56Jg^{-1} for a total of H_{all} = 650.78Jg^{-1}. The exothermic reaction was continuing for a while after the water supply was cut off and reached a maximum water content of n = 21.0 {H_2O} per unit {$2CaCl_2 + ZnCl_2$}, which equaled about 58.0% of the observed minimum sample weight. The water content slowly declined after that but did not balance out before the next dehydration stage started.

A total of six peaks appeared during the 2nd dehydration with a double peak at T_{p1} = 89.77°C and T_{p2} = 96.21°C followed by four overlapping peaks at T_{p3} = 129.81°C, T_{p4} = 157.97°C, T_{p5} = 192.87°C and T_{p6} = 194.8°C. The peaks five and six showed signs of partial melting events taking place. A single exothermic peak during the cooldown phase was likely caused by the re-solidification of the sample at $T_{cooldown}$ = 40°C. The sample held about n = 6.3 {H_2O} per unit {$2CaCl_2 + ZnCl_2$} after heating to T_{max} = 200°C.

Three peaks were seen in the 2nd hydration curve at e = 8.65mbar with an enthalpy of H_1 = 77.64Jg^{-1}, at e = 14.80mbar with an enthalpy of H_2 = 285.39Jg^{-1} and at e = 17.66mbar with H_3 = 355.09Jg^{-1} for a total of H_{all} = 718.12Jg^{-1}. The exothermic reaction was continuing for a while after the water supply was cut off and reached a maximum water content of n = 18.5 {H_2O} per unit {$2CaCl_2 + ZnCl_2$}, which equaled about 48.3% of the observed minimum sample weight. The water content slowly declined after that but did not balance out before the next dehydration stage started.

Eight peaks were observed during the 3rd dehydration, again starting with a double peak at T_{p1} = 79.34°C and T_{p2} = 95.08°C, followed by a group of five overlapping peaks at T_{p3} = 146.08°C, T_{p4} = 172.05°C, T_{p5} = 187.52°C, T_{p6} = 192.82°C and T_{p7} = 194.32°C. Occurring last was a single peak at T_{p8} = 196.09°C. The peaks three, six and eight showed signs of being melting events. A single exothermic peak without corresponding mass change during the cooldown stage was likely caused by the re-solidification of the sample mass at $T_{cooldown}$ = 50°C. The sample held about n = 6.0 {H_2O} per unit {$2CaCl_2 + ZnCl_2$} after heating to T_{max} = 200°C.

5.2.7. {$MgCl_2 + 2ZnCl_2$}, {$MgCl_2 + ZnCl_2$}, {$2MgCl_2 + ZnCl_2$}

There are no naturally occurring magnesium-zinc chloride minerals of similar compositions to tachyhydrite known to exist. It is unknown whether any compounds formed from the brine or which crystal structures were to expect.

The {$MgCl_2 + 2ZnCl_2$} sample was mixed at a ratio of 7ml {$MgCl_2$} solution to 20ml {$ZnCl_2$} solution.

The sample held about n = 22.0 {H_2O} per unit {$MgCl_2 + 2ZnCl_2$} at the start of the measurement. The dehydration reaction started already at T ~ 25°C indicating an overhydration.

Only a single peak occurred during the 1st dehydration at T_{p1} = 55.55°C. While the reaction was beginning before the start of the heating, a peak event at a lower temperature than T_{p1} was not observed. The sample held about n = 10.0 {H_2O} per unit {$MgCl_2 + 2ZnCl_2$} after the 1st dehydration (T_{max} = 100°C).

The 1st hydration showed three overlapping peaks at e = 8.65mbar with an enthalpy of H_1 = 87.84Jg^{-1}, at e = 14.80mbar with an enthalpy of H_2 = 247.36Jg^{-1} and at e = 17.66mbar with H_3 = 231.40Jg^{-1} for a total of H_{all} =

566.61Jg^{-1}. The sample held a maximum water content of n = 19.8 {H_2O} per unit {$MgCl_2$ + $2ZnCl_2$} during the 1st hydration, which equaled about 50.4% of the observed minimum sample weight. The exothermic reaction was continuing for a moment after the water supply was cut off, before it turned into an endothermic peak, with simultaneous emission of excess water. The water content did not balance out at T ~ 25°C before the next dehydration stage started.

The 2nd dehydration curve showed three endothermic peaks at T_{p1} = 83.73°C, with a double peak at T_{p2} = 132.78°C and T_{p3} = 149.54°C. The peaks 2 and 3 have characteristics of either a melting event or since {$MgCl_2$} is involved a possible emission of {HCl}. An exothermic peak not coupled with a mass change was observed during the cooldown stage at $T_{cooldown}$ = 108.19°C likely caused by re-solidification of the sample which points rather to a melting event. The sample held n = 6.33 {H_2O} per unit {$MgCl_2$ + $2ZnCl_2$} after the 2nd dehydration (T_{max} = 200°C).

The 2nd hydration developed similar to the 1st hydration, also with three overlapping peaks at e = 8.65mbar with an enthalpy of H_1 = 93.48Jg^{-1}, at e = 14.80mbar with an enthalpy of H_2 = 280.38Jg^{-1} and at e = 17.66mbar with H_3 = 267.16Jg^{-1} for a total of H_{all} = 641.02Jg^{-1}. The sample held a maximum water content of n = 18.7 {H_2O} per unit {$MgCl_2$ + $2ZnCl_2$} during the 1st hydration, which equaled about 46.2% of the observed minimum sample weight. The exothermic reaction was continuing for a moment after the water supply was cut off, before it turned into an endothermic peak, with simultaneous emission of excess water. The water content did not balance out at T ~ 25°C before the next dehydration stage started.

The 3rd dehydration developed similar to the 2nd dehydration with three peaks at T_{p1} = 82.60°C, T_{p2} = 132.58°C, T_{p3} = 148.93°C, where 2 and 3 were again a double peak with signs of melting or {HCl} emission followed by an exothermic peak during the cooldown stage at $T_{cooldown}$ = 106.45°C. The

sample held n = 6.5 {H_2O} per unit {$MgCl_2 + 2ZnCl_2$} after the 3rd dehydration (T_{max} = 200°C).

The {$MgCl_2 + ZnCl_2$} sample was mixed at a ratio of 7ml {$MgCl_2$} solution to 10ml {$ZnCl_2$} solution.

The sample was holding about n = 13.9 {H_2O} per unit {$MgCl_2 + ZnCl_2$} at the start of the measurement. The reaction was already starting at T ~ 25°C, indicating that the sample was overhydrated.

The 1st dehydration curve showed two peaks at T_{p1} = 42.42°C and T_{p2} = 93.98°C. The sample was holding about n = 10.1 {H_2O} per unit {$MgCl_2 + ZnCl_2$} after heating to T_{max} = 100°C.

The reaction of the material during the 1st hydration begins with an endothermic peak at e = 8.65mbar before it turns exothermic with two overlapping peaks at e = 14.80mbar with an enthalpy of $H_1 = 81.54 Jg^{-1}$ and at e = 17.66mbar with $H_2 = 95.29 Jg^{-1}$ for a total of $H_{all} = 176.82 Jg^{-1}$. The sample was holding a maximum water content of n = 12.6 {H_2O} per unit {$MgCl_2 + ZnCl_2$} during the hydration stage, which equaled about 42.8% of the minimum sample weight. The reaction turned endothermic after the water supply was cut off and the material emitted excess water. The water content balanced out at n = 12.0 {H_2O} per unit {$MgCl_2 + ZnCl_2$} at T = 27.22°C.

The 2nd dehydration showed four peaks at T_{p1} = 70.70°C, T_{p2} = 87.60°C, T_{p3} = 154.00°C and T_{p4} = 169.32°C. The first as well as the fourth peak show the signs of occurring melting events which would correspond with the observation of two exothermic peaks during the cooldown stage at $T_{cooldown1}$ = 120 °C and $T_{cooldown2}$ = 70°C indicating a phase change back to a solid. The sample was holding about n = 5.0 {H_2O} per unit {$MgCl_2 + ZnCl_2$} after heating to T_{max} = 200°C.

The reaction of the material during the 2nd hydration, too begins with an endothermic peak at e = 8.65mbar but it turns exothermic with three overlapping peaks starting already during the e = 8.65mbar stage with an enthalpy of H_1 = 18.19Jg^{-1}, at e = 14.80mbar with an enthalpy of H_2 = 167.89Jg^{-1} and at e = 17.66mbar with H_3 = 171.51Jg^{-1} for a total of H_{all} = 357.59Jg^{-1}. The sample was holding a maximum water content of n = 8.8 {H_2O} per unit {$MgCl_2$ + $ZnCl_2$} at the end of the hydration stage, which equaled 21.3% of the observed minimum sample weight. The reaction turned endothermic as soon as the water supply was cut off. The mixture emitted excess water until the water content balanced out at about n = 8.0 {H_2O} per unit {$MgCl_2$ + $ZnCl_2$}.

During the 3rd dehydration the reaction shifted to higher temperatures with four peaks at T_{p1} = 104.65°C, T_{p2} = 115.17°C, T_{p3} = 142.75°C and T_{p4} = 161.09°C. Followed by an exothermic peak observed at $T_{cooldown}$ = 75.97°C. The peaks 1, 2 and 4 appear to be partial melting events though a {HCl}-decay event can not be excluded as the cause either. The sample was holding about n = 5.4 {H_2O} per unit {$MgCl_2$ + $ZnCl_2$} after heating to T_{max} = 200°C.

The {2$MgCl_2$ + $ZnCl_2$} sample was mixed at a ratio of 7ml {$MgCl_2$} solution to 5ml {$ZnCl_2$} solution.

The sample was holding about n = 20.1 {H_2O} per unit {2$MgCl_2$ + $ZnCl_2$} at the start of the measurement. The mixture began reacting already at T ~ 25°C, indicating an overhydration.

Three peaks were observed during the 1st dehydration at T_{p1} = 51.8°C and a double peak at T_{p2} = 74.85°C and T_{p3} = 95.51°C, they were followed by an exothermic peak at $T_{cooldown}$ = 87.85°C, indicating a re-solidification, though none of the observed endothermic peaks indicated a melting event. The sample was holding n = 11.3 {H_2O} per unit {2$MgCl_2$ + $ZnCl_2$} after heating to T_{max} = 100°C.

The 1st hydration started with an endothermic peak event at e = 8.65mbar, followed by three overlapping exothermic peaks at e = 8.65mbar with an enthalpy of H_1 = 14.38Jg^{-1}, at e = 14.80mbar with an enthalpy of H_2 = 17.37Jg^{-1} and at e = 17.66mbar with H_3 = 302.73Jg^{-1} for a total of H_{all} = 334.48Jg^{-1}. The sample was holding a maximum water content of n = 17.66 {H_2O} per unit {2$MgCl_2$ + $ZnCl_2$} after the 1st hydration, which equaled about 28.8% of the observed minimum sample weight. As soon as the water supply was cut off, the reaction turned endothermic with a simultaneous water loss. The water content did not balance out at T ~ 25°C before the next dehydration stage started.

The 2nd dehydration curve showed seven endothermic peaks, starting with a double peak at T_{p1} = 59.72°C and T_{p2} = 83.63°C followed by five overlapping peaks at T_{p3} = 127.48°C, T_{p4} = 144.17°C, T_{p5} = 152.37°C, T_{p6} = 186.38°C and T_{p7} = 195.21°C. During the cooldown stage an exothermic peak occurred at $T_{cooldown}$ = 137.4°C, indicating a phase change to a solid material. Of the previously observed endothermic peaks 4, 5, 6 and 7 showed some indicators for partial melting though they were not distinctive. The sample was holding n = 6.0 {H_2O} per unit {2$MgCl_2$ + $ZnCl_2$} after heating to T_{max} = 200°C.

The 2nd hydration event showed a similar endothermic peak event at e = 8.65mbar like during the 1st hydration, followed by two overlapping exothermic peaks at e = 8.65mbar with an enthalpy of H_1 = 20.80Jg^{-1}, at e = 14.80mbar and e = 17.66mbar with an enthalpy of H_2 = 479.91Jg^{-1} for a total of H_{all} = 500.71Jg^{-1}. The sample was holding a maximum water content of n = 12.9 {H_2O} per unit {2$MgCl_2$ + $ZnCl_2$} after the 2nd hydration, which equaled about 28.8% of the observed minimum sample weight. The sample emitted excess water after the water supply was cut off. The water content balanced out at n = 12.0 {H_2O} per unit {2$MgCl_2$ + $ZnCl_2$} and T = 27.67°C.

The 3rd dehydration curve only showed four peaks, with a single peak at T_{p1} = 88.03°C, followed by a triple peak at T_{p2} = 136.51°C, T_{p3} = 151.96°C and

T_{p4} =181.34 °C. Again, an exothermic peak was observed during the cooldown stage at $T_{cooldown}$ = 139.59°C, the corresponding melting likely occurred during the third endothermic peak. The sample was holding n = 6.2 {H_2O} per unit {$2MgCl_2 + ZnCl_2$} after the 3rd dehydration (T_{max} = 200°C).

The observed events interpreted as melting and re-solidification for all three samples indicate a severe cycle instability of these materials. For that reason, the tests with magnesium-zinc chlorides were discontinued.

5.2.8. {$MgCl_2 + 2KCl$}, {$MgCl_2 + KCl$}, {$2MgCl_2 + KCl$}

The naturally occurring potassium-magnesium chloride is the orthorhombic mineral Carnallite with the composition ($KMgCl_3 \cdot 6H_2O$) (Armstrong, Dunham, Harvey, Sabine, & Waters, 1951), (Anthony, Bideaux, Bladh, & Nichols, 1997). After a first test of the synthetic Carnallite-equivalent, a new batch of samples including two more variations in composition were synthesized, to test how an excess in one of the starting materials influences the sample properties.

The mixing ratio for the {$MgCl_2 + KCl$} sample #1 was 7ml {KCl} solution to 9ml {$MgCl_2$} solution.

The sample held about n = 5.1 {H_2O} per unit {$MgCl_2 + KCl$} at the start of the measurement. The sample lost some water at T ~ 25°C and balanced out at n = 5.0 {H_2O} per unit {$MgCl_2 + KCl$}. It held this water content until a temperature of T = 59.84°C was reached and the dehydration reaction began.

The 1st dehydration showed a single endothermic peak at T_{p1} = 96.91°C overlapping with an also endothermic peak, observed during the cooldown stage at $T_{cooldown}$ = 84.53°C. The sample held a water content of n = 2.4 {H_2O} per unit {$MgCl_2 + KCl$} after heating to T_{max} = 100°C.

The 1st hydration showed two peaks at e = 8.65mbar with an enthalpy of H_1 = 167.05Jg^{-1} and at e = 14.80mbar with an enthalpy of H_2 = 268.17Jg^{-1} for a total of H_{all} = 435.22Jg^{-1}, followed by an endothermic event at e = 17.66mbar. The reaction turned exothermic again after the water supply was cut and the sample progressed to absorb the remaining water vapor, reaching a maximum water content of n = 5.1 {H_2O} per unit {$MgCl_2$ + KCl}, which equaled 39.0% of the observed minimum sample weight. The water content then balanced out at about n = 5.0 {H_2O} per unit {$MgCl_2$ + KCl}.

The 2nd dehydration curve had two peaks at T_{p1} = 97.15°C and T_{p2} = 167.02°C. The sample held a water content of n = 1.1 {H_2O} per unit {$MgCl_2$ + KCl} after heating to T_{max} = 200°C.

The 2nd hydration developed similar to the 1st hydration, with two peaks at e = 8.65mbar with an enthalpy of H_1 = 198.94Jg^{-1}, at e = 14.80mbar with an enthalpy of H_2 = 447.19Jg^{-1} for a total of H_{all} = 646.13Jg^{-1}, again followed by an endothermic event at e = 17.66mbar. The reaction turned exothermic then, after the water supply was cut and the sample progressed to absorb the remaining water vapor, reaching a maximum water content of n = 4.7 {H_2O} per unit {$MgCl_2$ + KCl}, which equaled 35.7% of the observed minimum sample weight. The water content balanced out at about n = 4.6 {H_2O} per unit {$MgCl_2$ + KCl} afterwards.

Two similar peaks as those recorded during the 2nd dehydration were observed during the 3rd dehydration at T_{p1} = 97.32°C and T_{p2} = 167.04°C. The sample held a water content of n = 1.0 {H_2O} per unit {$MgCl_2$ + KCl} after heating to T_{max} = 200°C.

The mixing ratio for the {$MgCl_2$ + 2KCl} sample was 10ml {KCl} solution to 7ml {$MgCl_2$} solution.

The sample held about n = 5.4 {H_2O} per unit {$MgCl_2$ + 2KCl} at the start of the measurement.

The 1st dehydration showed only a single peak at T_{p1} = 96.79°C. After heating to T_{max} = 100°C, the mixture held n = 2.5 {H_2O} per unit {$MgCl_2$ + 2KCl}.

The 1st hydration showed two overlapping, exothermic peaks at e = 8.65mbar with an enthalpy of $H_1 = 114.94 Jg^{-1}$ and at e = 14.80mbar with an enthalpy of $H_2 = 154.97 Jg^{-1}$ for a total of $H_{all} = 269.91 Jg^{-1}$, followed by an endothermic event at e = 17.66mbar. The reaction turned exothermic again after the water supply was cut and the sample progressed to absorb the remaining water vapor, reaching a maximum water content of n = 5.4 {H_2O} per unit {$MgCl_2$ + 2KCl}, where it balanced out. The weight of the absorbed water equaled about 30.4% of the observed minimum sample weight.

Three peaks were observed during the 2nd dehydration with a double peak at T_{p1} = 50.42°C and T_{p2} = 97.38°C followed by a single peak at T_{p3} = 169.38°C. The sample was holding about n = 1.1 {H_2O} per unit {$MgCl_2$ + 2KCl} after heating to T_{max} = 200°C.

The 2nd hydration curve showed a similar behavior to the 1st hydration with two overlapping, exothermic peaks at e = 8.65mbar with an enthalpy of $H_1 = 127.69 Jg^{-1}$ and at e = 14.80mbar with an enthalpy of $H_2 = 240.97 Jg^{-1}$ for a total of $H_{all} = 368.67 Jg^{-1}$, followed again by an endothermic event at e = 17.66mbar. The reaction then turned exothermic after the water supply was cut and the sample progressed to absorb the remaining water vapor, reaching a maximum water content of n = 5.0 {H_2O} per unit {$MgCl_2$ + 2KCl} where it balanced out. The weight of the absorbed water equaled about 27.6% of the observed minimum sample weight.

Three similar peaks to those observed during the 2nd dehydration occurred during the 3rd dehydration, again with a double peak at T_{p1} = 56.87°C and T_{p2} = 97.59°C, followed by a single peak at T_{p3} = 170.44°C. The sample was holding about n = 1.0 {H_2O} per unit {$MgCl_2$ + 2KCl} after heating to T_{max} = 200°C.

The mixing ratio for the {$MgCl_2$ + KCl} sample #2 was similar to that of sample #1 with 7ml {KCl} solution to 9ml {$MgCl_2$} solution. A similar result of the TGA/DSC analysis was expected.

The sample held about n = 6.5 {H_2O} per unit {$MgCl_2$ + KCl} at the start of the measurement.

The 1st dehydration curve shows only one endothermic peak at T_{p1} = 97.4°C, followed and overlapped by a second, also endothermic, peak during the cooldown stage at $T_{cooldown}$ = 80°C. After heating to T_{max} = 100°C, the sample held n = 3.0 {H_2O} per unit {$MgCl_2$ + KCl}.

The 1st hydration showed two overlapping, exothermic peaks at e = 8.65mbar with an enthalpy of H_1 = 106.03Jg^{-1} and at e = 14.80mbar with an enthalpy of H_2 = 219.51Jg^{-1} for a total of H_{all} = 325.54Jg^{-1}, followed by an endothermic event at e = 17.66mbar. The reaction turned exothermic again after the water supply was cut and the sample progressed to absorb the remaining water vapor, reaching a maximum water content of n = 7.7 {H_2O} per unit {$MgCl_2$ + KCl}, which equaled 55.46% of the observed minimum sample weight.

The water content then balanced out at about n = 6.4 {H_2O} per unit {$MgCl_2$ + KCl}.

The 2nd dehydration begins with a double peak at T_{p1} = 96.88°C and T_{p2} = 119.01°C, followed by a third single peak at T_{p3} = 176.13°C. After heating to T_{max} = 200°C, the sample held n = 0.9 {H_2O} per unit {$MgCl_2$ + KCl}.

The 2nd hydration developed similar to the 1st hydration, showing two overlapping, exothermic peaks at e = 8.65mbar with an enthalpy of H_1 = 75.03Jg^{-1} and at e = 14.80mbar with an enthalpy of H_2 = 270.50Jg^{-1} for a total of H_{all} = 345.53Jg^{-1}, followed by an endothermic event at e = 17.66mbar. The reaction turned exothermic again after the water supply was cut and the sample progressed to absorb the remaining water vapor, reaching a maximum water content of n = 5.75 {H_2O} per unit {$MgCl_2$ + KCl},

where it balanced out. The weight of the absorbed water equaled about 49.1% of the observed minimum sample weight.

A double peak occurs at the start of the 3rd dehydration at T_{p1} = 97.28°C and T_{p2} = 113.02°C, followed by a single peak at T_{p3} = 174.97°C. After heating to T_{max} = 200°C, the sample held n = 0.75 {H_2O} per unit {$MgCl_2$ + KCl}.

The mixing ratio for the {2$MgCl_2$ + KCl} sample was chosen as 2ml {KCl} solution to 5ml {$MgCl_2$} solution.

The sample held about n = 20.75 {H_2O} per unit {2$MgCl_2$ + KCl} at the start of the measurement. The sample losing excess water at T ~ 25°C, indicated an overhydration.

Three peaks were observed during the 1st dehydration at T_{p1} = 45.90°C, T_{p2} = 72.89°C and T_{p3} = 97.19°C. The sample held n = 9.2 {H_2O} per unit {2$MgCl_2$ + KCl} after heating to T_{max} = 100°C.

The 1st hydration showed two overlapping, exothermic peaks at e = 8.65mbar with an enthalpy of H_1 = 278.24Jg^{-1} and at e = 14.80mbar to e = 17.66mbar with an enthalpy of H_2 = 135.26Jg^{-1} for a total of H_{all} = 413.49Jg^{-1}, followed by a third exothermic peak event after the water supply had been cut off, though it wasn't counted into the enthalpy total. The sample held the maximum water content of n = 20.4 {H_2O} per unit {2$MgCl_2$ + KCl}, which equaled 103.8% of the observed minimum sample weight. The reaction turned endothermic shortly after, with a simultaneous loss of water. No balance was reached for the water content before the next dehydration stage began.

The 2nd dehydration showed four peaks, a single low temperature peak at T_{p1} = 90.60°C, a double peak at T_{p2} = 124.73°C and T_{p3} = 135.73°C, followed by another single peak at T_{p4} = 177.86°C. The sample held n = 3.0 {H_2O} per unit {2$MgCl_2$ + KCl} after heating to T_{max} = 200°C.

The 2nd hydration developed similar to the 1st hydration but the two peaks at e = 8.65mbar with an enthalpy of H_1 = 132.17Jg^{-1} and at e = 14.80mbar to e = 17.66mbar with an enthalpy of H_2 = 451.25Jg^{-1} for a total of H_{all} = 583.42Jg^{-1} were stronger. A third peak event occurred after the water supply had been cut off, but this peak wasn't counted into the enthalpy-total. The sample held a maximum water content of n = 15.5 {H_2O} per unit {2$MgCl_2$ + KCl}, which equaled about 75.4% of the observed minimum sample weight. The reaction turned endothermic shortly after with a simultaneous loss of water.

The water content balanced out at n = 14.5 {H_2O} per unit {2$MgCl_2$ + KCl} and T = 27.38 °C.

The four peaks observed during the 3rd dehydration, were similar to those of the 2nd dehydration, found at T_{p1} = 84.13°C, followed by a double peak at T_{p2} = 122.09°C and T_{p3} = 130.46°C and another single peak at T_{p4} = 177.58°C. The sample held n = 2.5 {H_2O} per unit {2$MgCl_2$ + KCl} after heating to T_{max} = 200°C.

5.2.9. {$CaCl_2$ + 2KCl}, {$CaCl_2$ + KCl}, {2$CaCl_2$ + KCl}

The naturally occurring potassium-calcium chloride mineral is the orthorhombic (pseudo cubic) Chlorocalcite ($KCaCl_3$). The mineral has no known hydrated stages. (National Bureau of Standards, Monograph, 7, 1969); (Anthony, Bideaux, Bladh, & Nichols, 1997). Two additional mixtures with a variation in composition ratios were synthesized to test, how the component-balance influences the cycle stability, heat storage density or possible water uptake.

The mixing ratio of the {$CaCl_2$ + 2KCl} sample was 3ml {$CaCl_2$} solution to 4ml {KCl} solution.

The sample was holding about n = 8.1 {H_2O} per unit {$CaCl_2$ + 2KCl} at the start of the measurement as the reaction was already ongoing, when the measurement started, the sample was likely overhydrated and partially dissolved. While there were three cations present per formula unit likely only the Ca^{++} cation of the {$CaCl_2$} component was attracting water while the two K^+ cations remained mostly passive during the reaction.

Only a single peak was observed during the 1st dehydration at T_{p1} = 44.46°C. The sample was holding about 4.6 {H_2O} per unit {$CaCl_2$ + 2KCl} after heating to T_{max} = 100°C. Another endothermic event occurred after the cooldown stage, which might be caused by a slow phase change from a crystal structure of high to a crystal structure of lower order.

The 1st hydration curve started with an endothermic event at e = 8.65mbar before it turns into an exothermic triple peak beginning still at e = 8.65mbar with an enthalpy of H_1 = 39.20Jg^{-1} and continuing at e = 14.80mbar with an enthalpy of H_2 = 197.13Jg^{-1} as well as at e = 17.66mbar with H_3 = 201.30Jg^{-1} for a total of H_{all} = 437.62Jg^{-1}. The sample was holding a maximum water content of about 10.2 {H_2O} per unit {$CaCl_2$ + 2KCl} during hydration, which equaled about 65.6% of the observed minimum sample weight. After the water supply was cut off, the curve relapses into endothermic behavior and the material released excess water.

The water content did not balance out before the next dehydration stage started.

During the 2nd dehydration two peaks were observed at T_{p1} = 62.11°C and T_{p2} = 147.18°C. The curve showed hints of exothermic behavior before and after both peaks. The second one appears to be a melting peak. The sample was holding about 0.33 {H_2O} per unit {$CaCl_2$ + 2KCl} after heating to T_{max} = 200°C. Again an endothermic peak was observed after the cooldown stage, suggesting a slow phase change to a lower crystal order for the material.

The 2nd hydration curve developed similar to the 1st hydration curve, with an endothermic event at e = 8.65mbar, followed by three exothermic peaks at e = 8.65mbar with an enthalpy of $H_1 = 48.94 Jg^{-1}$, at e = 14.80mbar with an enthalpy of $H_2 = 275.03 Jg^{-1}$ and at e = 17.66mbar with $H_3 = 315.00 Jg^{-1}$ for a total of $H_{all} = 638.97 Jg^{-1}$. The sample was holding a maximum water content of about 8.1 {H_2O} per unit {$CaCl_2$ + 2KCl} during hydration, which equaled about 53.6% of the observed minimum sample weight. After the water supply was cut off, the curve relapsed into endothermic behavior and the material released excess water. The water content did not balance out before the next dehydration stage started.

The 3rd dehydration curve had four peaks at $T_{p1} = 62.00°C$, $T_{p2} = 122.98°C$ and a double peak at $T_{p3} = 141.06°C$ and $T_{p4} = 147.29°C$. Peaks two to four appeared to be melting events. The curve showed hints of exothermic behavior before and after the peaks. The sample was holding about 0.4 {H_2O} per unit {$CaCl_2$ + 2KCl} after heating to $T_{max} = 200°C$. An endothermic phase change to lower crystal order was recorded after the cooldown stage of the 3rd dehydration as well.

The mixing ratio of the {$CaCl_2$ + KCl} sample was 3ml {$CaCl_2$} solution to 2ml {KCl} solution.

The sample held about n = 10.8 {H_2O} per unit {$CaCl_2$ + KCl} at the start of the measurement. The sample emitted excess water at T~25°C, which indicated an overhydration. While two cations were present in the mixture, likely only the Ca^{++} of the {$CaCl_2$}-component attracted the supplied water.

Only a single peak was observed during the 1st dehydration at $T_{p1} = 64.61°C$. The sample held about n = 5.2 {H_2O} per unit {$CaCl_2$ + KCl} after heating to $T_{max} = 100°C$. A very weak endothermic peak without corresponding weight change was recorded after the cooldown stage, indicating a phase change from a high to a lower crystal order.

The 1st hydration began with an endothermic event at e = 8.65mbar before three exothermic peaks occurred at e = 8.65mbar with an enthalpy of H_1 = 20.82Jg^{-1}, at e = 14.80mbar with an enthalpy of H_2 = 151.08Jg^{-1} and at e = 17.66mbar with H_3 = 187.42Jg^{-1} for a total of H_{all} = 359.32Jg^{-1}. The sample was holding a maximum water content of n = 8.4 {H_2O} per unit {$CaCl_2$ + KCl} during hydration, which equaled about 75.9% of the observed minimum sample weight. But after the water supply was cut off, the reaction turned endothermic while simultaneously emitting excess water. The water content balanced out at n = 7.4 {H_2O} per unit {$CaCl_2$ + KCl} and T = 28.02°C.

A low temperature peak was observed during the 2nd dehydration at T_{p1} = 79.83°C, followed by a double peak at T_{p2} = 141.05°C and T_{p3} = 148.65°C, which had the characteristics of a melting event. The sample held about n = 0.33 {H_2O} per unit {$CaCl_2$ + KCl} after heating to T_{max} = 200°C. Another endothermic peak without corresponding weight change was recorded after the cooldown stage, again indicating a phase change from a high to a lower crystal order.

The endothermic event at the start of the 2nd hydration is weaker than that observed during the 1st hydration. It is followed by three stronger exothermic peaks at e = 8.65mbar with an enthalpy of H_1 = 43.72Jg^{-1}, at e = 14.80mbar with an enthalpy of H_2 = 221.13Jg^{-1} and at e = 17.66mbar with H_3 = 264.36Jg^{-1} for a total of H_{all} = 529.21Jg^{-1}. The sample was holding a maximum water content of n = 5.4 {H_2O} per unit {$CaCl_2$ + KCl} during hydration, which equaled about 47.8% of the observed minimum sample weight. After the water supply was cut off, the sample emitted some excess water.

The water content balanced out at n = 5.0 {H_2O} per unit {$CaCl_2$ + KCl} and T = 29.42°C.

The two peaks observed during the 3rd dehydration showed similarities to those which occurred during the 2nd dehydration, with a low temperature peak at T_{p1} = 69.06°C but then with only a single peak following at T_{p2} =

142.44°C. The second peak appears to have been a melting event. The sample held about n = 0.4 {H_2O} per unit {$CaCl_2$ + KCl} after heating to T_{max} = 200°C. An endothermic peak without corresponding weight change occurred here after the cooldown stage as well, likely marking a phase change from a high to a lower crystal order.

The mixing ratio of the {$2CaCl_2$ + KCl} sample was 3ml {$CaCl_2$} solution to 1ml {KCl} solution.

The sample was holding about n = 16.1 {H_2O} per unit {$2CaCl_2$ + KCl} at the start of the measurement. As the sample was emitting excess water at T ~ 25°C, it was likely overhydrated.

While three cations were present per formula unit, likely only the two Ca^{++} of the {$CaCl_2$} component were attracting the water molecules.

A single peak was observed during the 1st dehydration at T_{p1} = 58.28°C. The sample was holding about n = 7.66 {H_2O} per unit {$2CaCl_2$ + KCl} after heating to T_{max} = 100°C. After the cooldown stage an endothermic event without a corresponding weight change was recorded, indicating a phase change from higher to lower crystal order.

A small endothermic event occurred at the beginning of the 1st hydration, followed by three exothermic peaks at e = 8.65mbar with an enthalpy of H_1 = 60.21Jg^{-1}, at e = 14.80mbar with an enthalpy of H_2 = 245.21Jg^{-1} and at e = 17.66mbar with H_3 = 255.70Jg^{-1} for a total of H_{all} = 561.12Jg^{-1}. The sample was holding a maximum water content of about n = 16.9 {H_2O} per unit {$2CaCl_2$ + KCl} during the hydration, which equaled about 95.0% of the observed minimum sample weight. The reaction turned endothermic after the water supply was cut and emitted excess water simultaneously.

The water content did not balance out before the next dehydration stage started.

The 2nd dehydration shows four peaks one at T_{p1} = 74.89°C, followed by a triple peak at T_{p2} = 142.79°C, T_{p3} = 169.02°C and T_{p4} = 190.19°C. The second peak indicated a melting event. The sample was holding about n = 0.7 {H_2O} per unit {2$CaCl_2$ + KCl} after heating to T_{max} = 200°C. After the cooldown stage an endothermic event was observed again, also without any corresponding weight change, indicating a phase change from high crystal order to a lower one.

Contrary to the 1st hydration, no endothermic event was observed at the beginning of the 2nd hydration. Instead there were three exothermic peaks at e = 8.65mbar with an enthalpy of H_1 = 90.01Jg^{-1}, at e = 14.80mbar with an enthalpy of H_2 = 301.72Jg^{-1} and at e = 17.66mbar with H_3 = 347.07Jg^{-1} for a total of H_{all} = 738.80Jg^{-1}. The sample was holding a maximum water content of about n = 13.6 {H_2O} per unit {2$CaCl_2$ + KCl} during the hydration, which equaled about 75.5% of the observed minimum sample weight. The reaction turned endothermic after the water supply was cut and emitted excess water simultaneously.

The water content did not balance out before the next dehydration stage started.

The 3rd dehydration curve developed similar to the 2nd, also with a low temperature peak at T_{p1} = 72.55°C and a triple peak at T_{p2} = 144.96°C, T_{p3} = 168.48°C and T_{p4} = 193.29°C where the second peak indicated a melting event as well. The sample was holding about n = 0.66 {H_2O} per unit {2$CaCl_2$ + KCl} after heating to T_{max} = 200°C. Again, an endothermic event without related weight change occurred after the cooldown stage, which was likely caused by a phase change from higher to lower crystal order.

5.2.10. {2$ZnCl_2$ + 7KCl}, {4$ZnCl_2$ + 7KCl}, {8$ZnCl_2$ + 7KCl}

A synthetic zinc-potassium chloride dihydrate compound exists in form of monoclinic ($KZnCl_3 \cdot 2H_2O$) (Suesse & Brehler, 1964).

Another synthetic form is the anhydrate potassium tetrachlorozincate (K_2ZnCl_4). The applied measurement temperatures of T = 25 to 200°C fall into the interval of T = -128 to +282°C where the (K_2ZnCl_4) compound occurs orthorhombic (Ferrrari, Roberts, Thomson, Gale, & Catlow, 2001).

The mixing ratios were supposed to mimic the two known synthetic compositions as well as a zinc-enriched variant and were calculated on the assumption that anhydrates were used for the synthesis. During calculation of the water content of the zinc-potassium chlorides it was noticed, that the values were deviating from the expected water uptake. The cause of the deviation was identified as the zinc chloride having hydrated to at least its tetrahydrate {$ZnCl_2 \cdot 4H_2O$} during storage before the synthesis, leading to three altered mixing ratios in the products.

The mixing ratio calculated for the {$ZnCl_2$ + 2KCl} sample was 11ml {$ZnCl_2$} to 12ml {KCl} solution. Due to using a tetra- or even a hexahydrate in synthesis, this resulted in a {$2ZnCl_2$ + 6KCl} to {$2ZnCl_2$ + 7KCl} mixture.

The sample held about 7.0 {H_2O} per unit {$2ZnCl_2$ + 7KCl} at the start of the measurement. The sample was emitting excess water at T ~ 25°C, indicating an overhydration.

The 1st dehydration curve showed three overlapping peaks at T_{p1} = 42.39°C, T_{p2} = 68.69°C and T_{p3} = 83,23°C. The mixture was holding n = 6.1 {H_2O} per unit {$2ZnCl_2$ + 7KCl} after heating to T_{max} = 100°C.

The 1st hydration curve began with an endothermic event at e = 8.65mbar which continues until the water supply is cut off. The water content sank to n = 5.6 {H_2O} before it rose to a maximum of n = 6.66 {H_2O} per unit {$2ZnCl_2$ + 7KCl}, when the water supply was cut off, where it balanced out. The weight of the absorbed water equaled about 3.4% of the observed minimum sample weight.

Only a minimal weight loss of 3.4% of the observed minimum sample weight was measured during the 2nd dehydration, ignoring a singular disturbance

during the weight-measurement where the TGA/DSC was likely recording a vibration from outside. The heat flow curve showed a weak exothermic peak at T_{p1} = 85.0°C, followed by an endothermic peak during the isothermal heating stage at T_{max} = 200°C. Two more endothermic peaks were observed during the cooldown stage. The sample's weight loss continued over the entire dehydration measurement and the sample was holding about n = 5.0 to 5.3 {H_2O} per unit {$2ZnCl_2$ + 7KCl} after heating to T_{max} = 200°C.

The 2nd hydration developed similar to the 1st hydration, with an endothermic event lasting over all three steps of the hydration stage. The water content rose to a maximum of n = 6.6 {H_2O} per unit {$2ZnCl_2$ + 7KCl}, when the water supply was cut off, where it balanced out. The weight of the absorbed water equaled about 3.3% of the observed minimum sample weight.

The 3rd dehydration developed similar to the 2nd, with a weight loss of 3.4% of the observed minimum sample weight, a weak endothermic peak at T = 55.0°C and observed exothermic peak behavior during the isothermal stage at T_{max} = 200°C, followed by an endothermic peak during the cooldown stage. The sample held about n = 5.66 {H_2O} per unit {$2ZnCl_2$ + 7KCl} at after heating to T_{max} = 200°C.

The mixing ratio for the {$ZnCl_2$ + KCl} sample was 11ml {$ZnCl_2$} to 6ml {KCl} solution. Due to using a tetra- to hexahydrate in synthesis, this resulted in a {$4ZnCl_2$ + 6KCl} to {$4ZnCl_2$ + 7KCl} mixture.

The sample was holding about n = 23.7 {H_2O} per unit {$4ZnCl_2$ + 7KCl} at the start of the measurement and the dehydration reaction was already ongoing at T = 25°C.

The 1st dehydration curve showed four peaks T_{p1} = 50.28°C, T_{p2} = 54,43°C, T_{p3} = 77.49°C and T_{p4} = 89.2°C. The mixture still held about n = 14.4 {H_2O} per unit {$4ZnCl_2$ + 7KCl} after heating to T_{max} = 100°C.

The 1st hydration curve began with an endothermic event at e = 8.65mbar, followed by two exothermic peaks at e = 14.80mbar with an enthalpy of H_1 = 88.00Jg^{-1} and at e = 17.66mbar with H_2 = 110.97Jg^{-1} for a total of H_{all} = 198.97Jg^{-1}. The water content sank to n = 14.0 {H_2O} before it rose to a maximum of n = 24.9 {H_2O} per unit {4$ZnCl_2$ + 7KCl}, which equaled 22.1% of the observed minimum sample weight.

The water content declined after the water supply was cut off and did not balance out before the next dehydration stage started.

The 2nd dehydration showed seven peaks, a triple peak at T_{p1} = 63.65°C, T_{p2} = 79.38°C and T_{p3} = 89.05°C, followed by four overlapping peaks at T_{p4} = 122.00°C, T_{p5} = 134.17°C, T_{p6} = 180.42°C and T_{p7} = 188.5°C, after that the curve shows exothermic behavior. The mixture held about n = 9.67 {H_2O} per unit {4$ZnCl_2$ + 7KCl} after heating to T_{max} = 200°C. But the water content rose again as soon as the temperature was reduced, apparently by reabsorbing some of the previously emitted water.

The 2nd hydration curve developed similar to the 1st hydration curve, with an endothermic event at e = 8.65mbar, followed by two overlapping peaks at e = 14.80mbar with an enthalpy of H_1 = 89.78Jg^{-1} and at e = 17.66mbar with H_2 = 146.34Jg^{-1} for a total of H_{all} = 236.12Jg^{-1}. The water content started out at n = 10.0 {H_2O} before it rose to a maximum of n = 23.0 {H_2O} per unit {4$ZnCl_2$ + 7KCl}, which equaled 19.4% of the observed minimum sample weight.

The water content declined after the water supply was cut off and did not balance out before the next dehydration stage began.

The 3rd dehydration curve is difficult to interpret, the reaction was already ongoing when the measurement started and after five to seven peaks at T_{p1} = 57.09°C, T_{p2} = 80.99°C, T_{p3} = 120.27°C, T_{p4} = 147.48°C, T_{p5} = 167.50°C, T_{p6} = 183.13°C and T_{p7} = 194.94°C, an exothermic event begins. The mixture held about n = 9.67 {H_2O} per unit {4$ZnCl_2$ + 7KCl} after heating to T_{max} = 200°C.

The mixing ratio for the {$2ZnCl_2$ + KCl} sample was 11ml {$ZnCl_2$} to 3ml {KCl} solution. Due to using a tetra- to hexahydrate in synthesis, this resulted in a {$8ZnCl_2$ + 6KCl} to {$8ZnCl_2$ + 7KCl} mixture.

The sample held n = 50.7 {H_2O} per unit {$8ZnCl_2$ + 7KCl} at the start of the measurement and was already dehydrating at T = 25°C. One endothermic peak was observed at the beginning of the 1st dehydration curve at T_{p1} = 56.19°C. It was followed by a small exothermic peak. The sample held about n = 31.8 {H_2O} per unit {$8ZnCl_2$ + 7KCl} after heating to T_{max} = 100°C.

The 1st hydration curve started with an endothermic event at e = 8.65mbar before three overlapping, exothermic peaks occurred, two at e = 14.80mbar with an enthalpy of H_1 = 101.28Jg^{-1} and H_2 = 79.80Jg^{-1} and one at e = 17.66mbar with H_3 = 77.64Jg^{-1} for a total of H_{all} = 258.72Jg^{-1}. The water content sank to n = 31.3 {H_2O} before it was rising to a maximum of n = 55.1 {H_2O} per unit {$8ZnCl_2$ + 7KCl}, which equaled about 32.7% of the observed minimum sample weight.

The reaction turned endothermic and the water content declined after the water supply was cut off and did not balance out before the next dehydration stage began.

The 2nd dehydration shows one low temperature peak at T_{p1} = 71.72°C, followed by four overlapping peaks at T_{p2} = 158.18°C, T_{p3} = 192.96°C, T_{p4} = 194.10°C and T_{p5} = 196.21°C, which were embedded into an exothermic event. The fourth peak has the characteristics of a melting event. The sample held about n = 19.5 {H_2O} per unit {$8ZnCl_2$ + 7KCl} after heating to T_{max} = 200°C.

The 2nd hydration curve shows three overlapping peaks at e = 8.65mbar with an enthalpy of H_1 = 78.14Jg^{-1}, at e = 14.80mbar with an enthalpy of H_2 = 159.65Jg^{-1} and at e = 17.66mbar with H_3 = 173.06Jg^{-1} for a total of H_{all} =

410.85Jg^{-1}. The water content stagnated at n = 22.0 {H_2O} before it rose to a maximum of n = 60.0 {H_2O} per unit {8$ZnCl_2$ + 7KCl}, which equaled about 37.1% of the observed minimum sample weight.

The water content then declined in an endothermic event, after the water supply was cut off and did not balance out before the next measurement stage began.

The 3rd dehydration curve shows one peak at T_{p1} = 73.44°C followed by exothermic behavior, before an extreme loss in measured sample weight occurs, which was likely caused by the crucible falling from its position on the mounting support. This disturbance concurred with a similar temperature (T~194°C) as measured during the melting event observed during the 2nd dehydration. It is possible that the emitted crystal water evaporated with a sudden volume expansion, while the melting sample was still of a relatively high viscosity. This may have caused a shock that dislodged the crucible from the sample holder.

Upon the first examination, the tested chloride-mixtures showed an overall higher heat storage density than the sulfates. The cycle stability appeared to have improved compared to the untreated materials but further testing with more than three TGA-cycles was necessary to verify or invalidate that first observation. The TGA/DSC results for the chlorides are summarized in Table 8.

Table 8 Chloride-samples with varying mixing ratios tested for energy storage density and water uptake in percent of the hydrated sample weight. The untreated salts were measured with the same method for comparison.

Materials	Energy storage density [Jg^{-1}] T_{max} = 100°C	Water uptake wgt [%] T_{max} = 100°C	Energy storage density Jg^{-1}] T_{max} = 200°C	Water uptake wgt [%] T_{max} = 200°C
{$MgCl_2 \cdot 6H_2O$}	247.92	172.30	818.27	80.04
{$CaCl_2 \cdot 2H_2O$}	630.03	89.71	844.16	62.90
{$ZnCl_2$}	387.66	39.57	588.49	45.40
{KCl}	---	2.49	---	2.08
{$CaCl_2 + 2MgCl_2$}	450.16	155.25	1553.79	114.29
{$CaCl_2 + MgCl_2$}	447.85	156.43	1223.73	90.91
{$2CaCl_2 + MgCl_2$}	628.80	232.25	1276.22	183.55
{$2CaCl_2 + ZnCl_2$}	650.78	58.04	718.12	48.30
{$CaCl_2 + ZnCl_2$}	739.25	51.00	763.40	50.30
{$CaCl_2 + 2ZnCl_2$}	750.37	59.16	844.80	56.38
{$2MgCl_2 + ZnCl_2$}	334.48	48.33	500.71	28.77
{$MgCl_2 + ZnCl_2$}	176.82	42.84	357.59	21.30
{$MgCl_2 + 2ZnCl_2$}	566.61	50.38	641.02	46.21
{$2MgCl_2$ + KCl}	413.49	103.77	583.42	75.38
{$MgCl_2$ + KCl} #1	435.22	38.95	646.13	35.65
{$MgCl_2$ + KCl} #2	325.54	55.46	345.53	49.10
{$MgCl_2 + 2$KCl}	269.91	30.40	368.67	27.58
{$2CaCl_2$ + KCl}	561.12	94.95	738.80	75.46
{CaCl2 + KCl}	359.32	75.94	529.21	47.79
{$CaCl_2 + 2$KCl}	437.62	65.60	638.97	52.59
{$8ZnCl_2 + 7$KCl}	258.72	32.70	410.85	37.14
{$4ZnCl_2 + 7$KCl}	198.97	22.13	236.12	19.35
{$2ZnCl_2 + 7$KCl}	---	3.39	---	3.32

5.3. Bromides

The price of {$SrBr_2$} ranges between 169€ for m = 10g of an anhydrate of 99.99% purity (MaTecK, 2017) and ~10 to 20$ for m = 1kg hexahydrate of 99% purity (Richest group, 2017), which equals a water content of ~30.6%. Not counting the energy costs for drying this would amount to an anhydrate price of ~14 to 30$. While bulk prices can be lower, this still does not allow for a cost-efficient energy storage system for household settings. With the goal to decrease the overall material cost, it was tested, whether the {$SrBr_2$} can be diluted by mixing it with other bromides, with special attention to compromise neither cycle stability nor heat storage density.

Additionally to the initial three cycles of TGA/DSC evaluation, a special measurement of combined heating to T_{max} = 110°C and hydration at e = 18.68mbar was applied, to observe up to which temperatures the materials were still able to absorb water before the reactions turn endothermic.

The materials were also heated to T_{max} = 500°C, for reducing them to (or at least close to) their anhydrates.

Since severe material changes as melting and agglomeration were to be expected when heating the samples to T_{max} = 500°C, the two new evaluations were done on a separate sample of the same batch of material like that of the standard three cycle measurements.

Due to a mistake during the calculations, the actual mixing ratios of the {$CaBr_2$ + $SrBr_2$} mixtures were deviating from the 2 to 1, 1 to 1 and 1 to 2 ratios used for the rest of the bromides. The affected measurements were later repeated with samples mixed to the corrected ratios.

5.3.1. {$SrBr_2 \cdot 6H_2O$}

For the TGA/DSC analysis the hexahydrate {$SrBr_2 \cdot 6H_2O$} was used.

Sample #1 was holding about n = 6.9 {H_2O} per unit {$SrBr_2$} at the start of the measurement.

The 1st dehydration showed a single peak at T_{p1} = 63.12°C. The sample was holding about n = 2.2 {H_2O} per unit {$SrBr_2$} after the peak at T = 79°C, the water content only marginally decreased when the sample was further heated to T_{max} =100°C.

The 1st hydration showed three overlapping peaks at e = 8.65mbar, e = 14.80mbar and e = 17.66mbar for a total of H_{all} = 798.14Jg^{-1}. The sample absorbed 45.34% of its observed minimum weight in water until the water supply was cut off, which equals a water content of about n = 6.9 {H_2O} per formula unit {$SrBr_2$}.

At the start of the 2nd cycle, the sample was holding about n = 7.5 {H_2O} per unit {$SrBr_2$}.

Two peaks occurred during the 2nd dehydration at T_{p1} = 90.02°C and T_{p2} = 188.76°C. After the first peak at T = 97°C, the water content was about n = 2.0 {H_2O} per unit {$SrBr_2$}, after heating to T_{max} = 200°C the water content had declined to n = 0.76 {H_2O} per unit {$SrBr_2$}.

The 2nd hydration curve developed similar to the 1st with three overlapping peaks at e = 8.65mbar, e = 14.80mbar and e = 17.66mbar for a total of H_{all} = 834.17Jg^{-1}. The sample absorbed 45.34% of its observed minimum weight in water until the water supply was cut off, which equals a water content of about n = 6.9 {H_2O} per formula unit {$SrBr_2$}.

At the start of the 3rd cycle, the sample was holding again about n = 7.5 {H_2O} per unit {$SrBr_2$}.

The 3rd dehydration curve developed similar to the 2nd with two peaks at T_{p1} = 90.18°C and T_{p2} = 189.08°C. After the first peak at T = 97°C, the water content was about n = 2.0 {H_2O} per unit {$SrBr_2$}, after heating to T_{max} = 200°C the water content had declined to n = 0.76 {H_2O} per unit {$SrBr_2$}.

Sample #2 was holding n = 6.0 {H_2O} per unit {$SrBr_2$} at the start of the measurement, which equals 42.9% of the anhydrate weight. It held that

water content at a water vapor pressure of e = 18.68mbar until the temperature exceeded T = 51,63°C. After heating to T = 80,31°C the water content had declined to n = 1.1 {H_2O} per unit {$SrBr_2$}. The water content did not recover when the temperature was lowered back to T = 60°C after first heating to T_{max} = 110°C and kept water content about this value until the end of this measurement section and the start of the next one.

Heating the sample to T_{max} = 500°C showed a single peak at T_{p1} = 197.8°C, after which the water content declined to n = 0.1 {H_2O} per unit {$SrBr_2$}, for a nearly anhydrous sample. A melting event was not observed.

5.3.2. {NaBr}

Sample #1 held about n = 1.16 {H_2O} per formula unit {NaBr} at the start of the measurement.

Two weak, endothermic peaks were observed during the 1st dehydration at T_{p1} = 33.33°C, T_{p2} = 98.02°C. The water content sank to about n = 1.12 {H_2O} per formula unit {NaBr} after heating to T_{max} = 100°C.

The 1st hydration showed three weak, overlapping, exothermic peaks at e = 8.65mbar, e = 14.80mbar and e = 17.66mbar for a total of H_{all} = 214.25Jg^{-1}.

The sample had reached its minimum weight at the start of the 1st hydration curve, with a water content gauged as n = 0.82 {H_2O} per unit {NaBr}. The sample absorbed 6.1% of its own minimum weight in water during hydration until the water supply was cut off, which equals about n = 1.2 {H_2O} per formula unit {NaBr}. The reaction changed to an endothermic event as soon as the water supply was cut off and the sample emitted excess water.

At the start of the 2nd cycle the sample was holding about n = 1.23 {H_2O} per formula unit {NaBr}.

The 2nd dehydration curve showed two peaks at T_{p1} = 42.26°C, T_{p2} = 196.05°C. The water content sank to about n = 1.06 {H_2O} per formula unit {NaBr} after heating to T_{max} = 200°C.

The 2nd hydration curve showed three weak, overlapping, exothermic peaks similar to those observed during the 1st hydration, at e = 8.65mbar, e = 14.80mbar and e = 17.66mbar for a total of H_{all} = 192.11Jg^{-1}. The sample absorbed 7.2% of its minimum weight in water until the water supply was cut off, which equals a water content of about n = 1.29 {H_2O} per formula unit {NaBr}. The reaction changed to an endothermic event as soon as the water supply was cut off and the sample emitted excess water.

At the start of the 3rd cycle the sample was holding about n = 1.23 {H_2O} per formula unit {NaBr}.

The peaks from the 2nd dehydration reappeared during the 3rd dehydration but with a third peak in between at T_{p1} = 37.03°C, T_{p2} = 133.98°C and T_{p3} = 196.41°C. The water content sank to about n = 1.01 {H_2O} per formula unit {NaBr} after heating to T_{max} = 200°C.

Sample #2 contained about n = 1.00 {H_2O} per formula unit {NaBr}, where also the minimum weight of the sample was observed at T ~ 25°C at the start of the T_{max} = 110°C measurement. While no peaks for water uptake occurred at e = 18.68mbar for temperatures of T = 25°C or higher, the sample steadily gained 0.50% of its observed minimum weight during the measurement in mass.

The sample did not show any peaks when heated to T_{max} = 500°C either but steadily increased in mass for a total of 1.2% of the minimum sample weight. It is possible that the sample took up some {O_2} that was remaining in the oven chamber during the heating. The melting temperature was not reached within the measurement parameters.

5.3.3. {KBr}

Sample #1 was holding about n = 1.15 {H_2O} per formula unit {KBr} at the start of the measurement.

Two weak peaks were recorded during the 1st dehydration at T_{p1} = 34.08°C and T_{p2} = 97.93°C. The water content sank to about n = 1.07 {H_2O} per formula unit {KBr} after heating to T_{max} = 100°C.

The minimum weight of the sample was observed at the start of the 1st hydration, where the water content was gauged as n = 0.77 {H_2O} per formula unit {KBr}.

The 1st hydration showed three weak, overlapping peaks at e = 8.65mbar, e = 14.80mbar and e = 17.66mbar for a total of H_{all} = 162.22Jg^{-1}. The sample absorbed 3.6% of its minimum weight in water until the water supply was cut off, which equals a water content of about n = 1.03 {H_2O} per formula unit {KBr}. The reaction turned into a weak endothermic event as soon as the water supply was cut off and the sample emitted excess water

At the start of the 2nd cycle the sample was holding about n = 1.19 {H_2O} per formula unit {KBr}. The sample appears to have re-absorbed water at some point in between measurements.

The 2nd dehydration curve showed two peaks at T_{p1} = 42.18°C and T_{p2} = 195.96°C. The water content stabilized at n = 1.00 {H_2O} per formula unit {KBr} and T = 143°C, then sank to about n = 0.95 {H_2O} per formula unit {KBr} after heating to T_{max} = 200°C.

The 2nd hydration curve showed three weak overlapping peaks similar to those observed during the 1st hydration at e = 8.65mbar, e = 14.80mbar and e = 17.66mbar for a total of H_{all} = 161.36Jg^{-1}. The sample absorbed 3.5% of its own minimum weight in water until the water supply was cut off, which equals a water content of about n = 1.03 {H_2O} per formula unit {KBr}. The reaction turned into a weak endothermic event as soon as the water supply was cut off and the sample emitted excess water.

At the start of the 3rd cycle the sample was holding about n = 1.19 {H_2O} per formula unit {KBr}.

The 3rd dehydration developed similar to the 2nd with two peaks at T_{p1} = 41.91°C and T_{p2} = 195.94°C. The water content stabilized at n = 1.00 {H_2O} per formula unit {KBr} and T = 143°C, then sank to about n = 0.95 {H_2O} per formula unit {KBr} after heating to T_{max} = 200°C.

Sample #2 was gauged to have contained about n = 1.0 {H_2O} per formula unit {KBr} at the start of the T_{max} = 110°C measurement. While no hydration peaks occurred, the sample steadily took up 0.48% of its observed minimal weight in mass at e = 18.68mbar at temperatures of T = 25°C and higher over the course of the measurement.

The sample had reached its measured minimum weight at the start of the T_{max} = 500°C measurement, where the water content was gauged as n = 1.00 {H_2O} per formula unit {KBr}. No peaks were observed, while heating the sample to T_{max} = 500°C but the sample steadily gained 0.48% mass of its observed minimum weight during the dehydration. As no water source was present, it is possible that the sample absorbed the {O_2} remaining in the oven during heating. The melting temperature was not reached within the measurement parameters.

5.3.4. {LiBr}

Sample #1 was holding about n = 8.2 {H_2O} per unit {LiBr} at the start of the measurement.

A single peak was observed during the 1st dehydration at T_{p1} = 74.41°C. The water content declined to n = 4.4 {H_2O} per unit {LiBr} after heating to T_{max} = 100°C but began to increase again during the cooldown stage.

The 1st hydration showed three overlapping peaks at e = 8.65mbar, e = 14.80mbar and e = 17.66mbar for a total of H_{all} = 900.69Jg^{-1}. The sample absorbed 106.2% of its own minimum weight in water until the water supply was cut off, which equals about n = 9.2 {H_2O} per formula unit {LiBr}. The reaction changed to an endothermic event as soon as the water supply was cut off and the sample emitted excess water.

At the start of the 2nd cycle the water content was n = 8.6 {H_2O} per unit {LiBr}.

The 2nd dehydration showed three peaks the first at T_{p1} = 44.64°C, followed by a double peak at T_{p2} = 154.86°C and T_{p3} = 200.00°C. At T = 98°C the sample held a water content of n = 4.9 {H_2O} per unit {LiBr} which declined further to about n = 2.0 {H_2O} per unit {LiBr} after heating to T_{max}= 200°C.

The 2nd hydration curve showed three overlapping peaks similar to those observed during the 1st dehydration at e = 8.65mbar, e = 14.80mbar and e = 17.66mbar for a total of H_{all} = 1,251.26Jg^{-1}. The sample absorbed 89.5% of its observed minimum weight in water until the water supply was cut off, which equals about n = 8.1 {H_2O} per formula unit {LiBr}. The reaction changed to a weak endothermic event as soon as the water supply was cut off and the sample emitted excess water.

At the start of the 3rd cycle the water content was n = 8.0 {H_2O} per unit {LiBr}.

The 3rd dehydration curve developed similar to the 2nd with three peaks, one at T_{p1} = 45.22°C but then followed by two separate peaks at T_{p2} = 154.36°C and T_{p3} = 196.23°C. At T = 169°C the sample held a water content of n = 3.0 {H_2O} per unit {LiBr} which declined further to about n = 2.0 {H_2O} per unit {LiBr} after heating to T_{max}= 200°C.

The {LiBr} sample #2 held n = 5.8 {H_2O} per unit {LiBr} at the start of the measurement. Without a water supply the material dehydrated at T = 25°C. At a water flow of e = 18.68mbar it hydrated up to a temperature of T = 43.39 °C and a water content of n = 6.0 {H_2O} per unit {LiBr}, which equaled 85.9% of

the anhydrate sample weight. After drying the sample to T_{max} = 110°C at e = 18.68mbar, the lithium bromide rehydrated at T = 60.00°C to about n = 3.7 {H_2O} per unit {LiBr} which equals 47.2% of the anhydrate weight.

Two peaks were recorded when the sample was heated to T_{max} = 500°C, T_{p1} = 155.89°C, T_{p2} = 229.39°C after which the sample was holding a minimum water amount of n = 1 {H_2O} per unit {LiBr}. The first peak shows signs of a melting event, which is about ~10K lower than the literature value for {LiBr·H_2O} (Matsuo, Oguchi, Maekawa, Takamura, & Orimo, 2007), indicating a higher hydration stage at this point. It corresponds with the perceived melting peaks during the 2nd and the 3rd dehydration to T_{max} = 200°C of sample #2.

5.3.5. {$MgBr_2$}

Sample # 1 was holding n = 19.1 {H_2O} per unit {$MgBr_2$} at the start of the measurement.

During the 1st dehydration two overlapping peaks were observed at T_{p1} = 34.46°C and T_{p2} = 96.08°C. The sample was still holding about n = 18.1 {H_2O} per unit {$MgBr_2$} after heating to T_{max} = 100°C.

The 1st hydration showed three overlapping peaks at e = 8.65mbar, e = 14.80mbar and e = 17.66mbar for a total of H_{all} = 422.13Jg^{-1}. The sample absorbed 90.8% of its own minimum weight in water until the water supply was cut off, which equals a water content of about n = 21.6 {H_2O} per formula unit {$MgBr_2$}. The reaction changed to an endothermic event as soon as the water supply was cut off and the sample emitted excess water.

The sample was holding about n = 21.5 {H_2O} per unit {$MgBr_2$} at the start of the 2nd cycle.

The 2nd dehydration showed four peaks at T_{p1} = 41.39°C, a group of three peaks with the main peak at T_{p2} = 155.71°C and the minor peaks at T_{p3} = 181.00°C, T_{p4} = 200.00°C. The second peak indicated a melting event.

The water content sank to n = 13.3 {H_2O} per unit {$MgBr_2$} at T = 171.0°C and declined further but only by a negligible amount until the end of the dehydration stage.

The 2nd hydration curve showed three overlapping peaks similar to those of the 1st curve, at e = 8.65mbar, e = 14.80mbar and e = 17.66mbar for a total of H_{all} = 788.14Jg^{-1}. The sample absorbed 67.76% of its own minimum weight in water until the water supply was cut off, which equals a water content of about n = 19.22 {H_2O} per formula unit {$MgBr_2$}. The reaction changed to an endothermic event as soon as the water supply was cut off and the sample emitted excess water.

The sample was holding about n = 19.0 {H_2O} per unit {$MgBr_2$} at the start of the 3rd cycle.

The 3rd dehydration curve developed similar to the 2nd dehydration curve, showing four peaks at T_{p1} = 41.40°C with a group of three peaks where the main peak was at T_{p3} = 178.09°C and the minor peaks at T_{p2} = 163.00°C, T_{p4} = 200.00°C. Contrary to the 2nd dehydration, here the third peak indicated a melting event instead of the second, which means the melting was delayed by about ΔT = 22°C. At T = 98°C the water content was about n = 17.9 {H_2O} per unit {$MgBr_2$}. After heating to T_{max} = 200°C, the water content reached a minimum of n = 13.0 {H_2O} per unit {$MgBr_2$}.

The {$MgBr_2 \cdot 6H_2O$} sample #2 showed marginal water uptake at e = 18.68mbar until a temperature of T = 35.15°C was reached. The exact grade of hydration of the sample could not be determined as the corresponding T_{max} = 500°C measurement of the same sample was interrupted and the sample lost before a temperature of T = 200°C was reached. Therefore, the water content was gauged as about n = 21.2 {H_2O} per unit {$MgBr_2$} at the start of the measurement and n = 20.0 {H_2O} per unit {$MgBr_2$} after heating to T_{max} = 110°C. The water content did not recover before the start of the next measurement.

The first T_{max} = 500°C dehydration curve showed a cluster of at least 6 peaks with the main peak at T = 185.6°C. The measurement continued till a temperature of T = 455.54°C was reached. The water content was gauged to be about n = 0.3 {H_2O} per unit {$MgBr_2$} when the measurement was interrupted.

A secondary T_{max} = 500°C dehydration curve was recorded since the first measurement was incomplete. Four peaks were observed at T_{p1} = 52.52°C, T_{p2} = 152.06°C, T_{p3} = 214.33°C and T_{p4} = 405.52°C. The second peak had the characteristics of a melting event. The water content was calculated as n = 33.33 {H_2O} per unit {$MgBr_2$} at the start of the measurement and n = 14.1 {H_2O} per unit {$MgBr_2$} at T = 200°C after the first peak under the assumption that the water content equaled n = 0 {H_2O} per unit {$MgBr_2$} after heating to T_{max} = 500°C. The unusual high water content indicated a severe overhydration and a likely dissolving of the sample from air humidity before the start of the measurement.

5.3.6. {$CaBr_2 \cdot 6H_2O$}

Sample #1 was holding about n = 9.0 {H_2O} per unit {$CaBr_2$} at the start of the measurement.

Two peaks were observed during the 1st dehydration. While the reaction was already ongoing when the measurement started, the first peak was observed at T_{p1} = 64.57°C, the second peak occurred at T_{p2} = 97.90°C. The sample was holding a water content of n = 5.4 {H_2O} per unit {$CaBr_2$} after the first peak at T = 81°C, which declined to n = 3.7 {H_2O} per unit {$CaBr_2$} after heating to T_{max} = 100°C.

The 1st hydration showed three overlapping peaks at e = 8.65mbar, e = 14.80mbar and e = 17.66mbar for a total of H_{all} = 946.87Jg^{-1}. The sample absorbed 75.2% of its observed minimum weight in water until the water supply was cut off, which equals a water content of about n = 10.1 {H_2O} per

formula unit {$CaBr_2$}. The reaction turned endothermic as soon as the water supply was cut off and the sample emitted excess water.

At the start of the 2nd cycle, the sample was holding about n = 9.3 {H_2O} per unit {$CaBr_2$}.

The 2nd dehydration showed two peaks at T_{p1} = 89.75°C and T_{p2} = 188.09°C. The water content sank to n = 5.1 {H_2O} per unit {$CaBr_2$} at T = 98,0°C the water content declined further to n = 1.0 {H_2O} per unit {$CaBr_2$} after heating to T_{max} = 200°C.

The 2nd hydration curve showed three overlapping peaks similar to those observed during the 1st hydration, at e = 8.65mbar, e = 14.80mbar and e = 17.66mbar for a total of H_{all} = 1078.53Jg^{-1}. The sample absorbed 63.3% of its own observed minimum weight in water until the water supply was cut off, which equals a water content of about n = 8.7 {H_2O} per formula unit {$CaBr_2$}. The reaction turned endothermic as soon as the water supply was cut off and the sample emitted excess water.

At the start of the 3rd cycle, the sample was holding about n = 8.6 {H_2O} per unit {$CaBr_2$}.

Two similar peaks were observed during the 3rd dehydration at T_{p1} = 89.53°C and T_{p2} = 190.94°C. The water content declined from n = 5.1 {H_2O} per unit {$CaBr_2$} to n = 4.3 {H_2O} per unit {$CaBr_2$} at the isothermal stage between the peaks at a temperature of T = 98°C before it reached its minimum weight and water content of n = 1.0 {H_2O} per unit {$CaBr_2$} after heating to T_{max} = 200°C.

The {$CaBr_2 \cdot xH_2O$} sample #2 held about n = 11.9 {H_2O} per unit {$CaBr_2$} at the start of the T_{max} = 110°C measurement, which equals a water content of about 98.9% of the observed minimum sample weight. As long as no water was supplied, it emitted excess water at room temperature T ~ 25°C. At a partial water vapor pressure of e = 18.68mbar, the sample rehydrated until a temperature of T = 33.73°C and a water content of n = 11.2 {H_2O} per unit

{$CaBr_2$} were reached. After heating to T_{max} = 110°C and dehydrating to n = 4.7 {H_2O} per unit {$CaBr_2$}, the sample rehydrated to n = 6.6 {H_2O} per unit {$CaBr_2$} at T = 60.38°C, which equals a water content of 52.9% of the observed minimum sample mass.

At the start of the T_{max} = 500°C measurement the calcium bromide was holding n = 5.06 {H_2O} per unit {$CaBr_2$}.

Heating the sample to T_{max} = 500°C showed two peaks at T_{p1} = 201.54°C and T_{p2} = 450.27°C. A melting event without a corresponding weight change was observed at T = 65°C. The water content declined to n = 1.0 {H_2O} per unit {$CaBr_2$} after the first peak at T = 290°C, then to a minimum of n = 0.5 {H_2O} per unit {$CaBr_2$} after heating to T_{max} = 500°C.

5.3.7. {2NaBr + SrBr2·6H2O}, {NaBr + $SrBr_2$·6H_2O}, {NaBr + 2$SrBr_2$·6H_2O}

The {2NaBr + $SrBr_2$·6H_2O} sample was mixed at a ratio of 5g {NaBr} to 6g {$SrBr_2$·6H_2O}.

Sample #1 was holding about n = 5.4 {H_2O} per unit {2NaBr + $SrBr_2$} at the start of the measurement.

The 1st dehydration showed a single peak at T_{p1} = 59.66°C. The water content declined to n = 1.0 {H_2O} per unit {2NaBr + $SrBr_2$} after the peak.

The 1st hydration showed three overlapping peaks at e = 8.65mbar, e = 14.80mbar and e = 17.66mbar for a total of H_{all} = 540.29Jg^{-1}, with the water uptake declining after the sample absorbed 26.6% of its own observed minimum weight in water, which equals a water content of about n = 6.7 {H_2O} per formula unit {2NaBr + $SrBr_2$}. The reaction turned endothermic as soon as the water supply was cut off and the sample emitted excess water.

At the start of the 2nd cycle, the sample was holding n = 5.9 {H_2O} per unit {2NaBr + $SrBr_2$}.

The low temperature peak observed during the 1st dehydration was shifted to a higher temperature at T_{p1} = 80.08°C during the 2nd dehydration and joined by a second peak at T_{p2} = 186.25°C. The water content declined to n = 1.2 {H_2O} per unit {2NaBr + $SrBr_2$} after the peak at T = 94°C and sank further to about n = 0.0 {H_2O} per unit {2NaBr + $SrBr_2$} after heating to T_{max} = 200°C, where the sample's minimum weight was measured.

The 2nd hydration curve showed three overlapping peaks similar to those observed during the 1st hydration at e = 8.65mbar, e = 14.80mbar and e = 17.66mbar for a total of H_{all} = 470.70Jg^{-1}. The water uptake also declined after the sample absorbed about 25.5% of its own observed minimum weight in water, which equals a water content of about n = 6.4 {H_2O} per unit {2NaBr + $SrBr_2$}. The reaction turned endothermic as soon as the water supply was cut off and the sample emitted excess water.

At the start of the 3rd cycle, the sample was holding n = 5.8 {H_2O} per unit {2NaBr + $SrBr_2$}.

The 3rd dehydration developed similar to the 2nd with two peaks at T_{p1} = 80.11°C and T_{p2} = 184.76°C. The water content declined to n = 1.1 {H_2O} per unit {2NaBr + $SrBr_2$} after the peak at T = 98°C and sank further to n = 0.03 {H_2O} per unit {2NaBr + $SrBr_2$} after heating to T_{max} = 200°C.

Sample #2 held n = 5.5 {H_2O} per unit {2NaBr + $SrBr_2$} at the start of the measurement. It did not take up water at e = 18.68mbar and temperatures of T > 25°C. After heating to T_{max} = 110°C, the water content was reduced to n = 1.0 {H_2O} per unit {2NaBr + $SrBr_2$}.

Heating the sample to T_{max} = 500°C showed one endothermic peak at T_{p1} = 189.57°C. The water content declined to n = 0.05 {H_2O} per unit {2NaBr + $SrBr_2$} after the peak. A melting event was observed at T = 480.10°C. The water content declined to its observed minimum water content of n = 0.05 {H_2O} per unit {2NaBr + $SrBr_2$} after the peak. It is possible that the sample

took up some {O_2} during the heating stage as the weight slightly increased after the dehydration peak.

The {$NaBr + SrBr_2 \cdot 6H_2O$} sample was mixed at a ratio of 5g {NaBr} to 12g {$SrBr_2 \cdot 6H_2O$}.

Sample #1 held about n = 3.8 {H_2O} per unit {$NaBr + SrBr_2$} at the start of the measurement.

The 1st dehydration showed a single peak at T_{p1} = 57.31°C after which the water content was reduced to n = 1.0 {H_2O} per unit {$NaBr + SrBr_2$} at T = 68°C.

The 1st hydration showed three overlapping peaks at e = 8.65mbar, e = 14.80mbar and e = 17.66mbar for a total of H_{all} = 434.33Jg^{-1}, with the water uptake declining after the sample absorbed 20.8% of its own minimum weight in water, which equals a water content of about n = 4.5 {H_2O} per unit {$NaBr + SrBr_2$}. The reaction turned endothermic as soon as the water supply was cut off and the sample emitted excess water.

At the start of the 2nd cycle the sample held a water content of about n = 4.1 {H_2O} per unit {$NaBr + SrBr_2$}.

During the 2nd dehydration the single peak observed at the 1st dehydration shifted to a higher temperature of T_{p1} = 76.31°C, followed by a second peak at T_{p2} = 187.31°C. The water content was reduced to n = 1.1 {H_2O} per unit {$NaBr + SrBr_2$} at T = 98°C after the first peak and declined further to n = 0.4 {H_2O} per unit {$NaBr + SrBr_2$} after the second peak and heating to T_{max} = 200°C, where the observed minimum weight and water content were reached.

The 2nd hydration curve showed three overlapping peaks similar to those of the 1st curve at e = 8.65mbar, e = 14.80mbar and e = 17.66mbar for a total

of H_{all} = 450.67Jg^{-1}, also with the water uptake declining after the sample absorbed about 20.3% of its own minimum weight in water, which equals about n = 4.4 {H_2O} per unit {NaBr + $SrBr_2$}. The reaction turned endothermic as soon as the water supply was cut off and the sample emitted excess water.

At the start of the 3rd cycle the sample held a water content of about n = 4.1 {H_2O} per unit {NaBr + $SrBr_2$}.

The 3rd dehydration developed similar to the 2nd dehydration, with two peaks at T_{p1} = 76.95°C and T_{p2} = 184.54°C. The water content was reduced to n = 1.1 {H_2O} per unit {NaBr + $SrBr_2$} at T = 94°C after the first peak and declined further to n = 0.4 {H_2O} per unit {NaBr + $SrBr_2$} after the second peak and heating to T_{max} = 200°C.

Sample #2 held n = 4.2 {H_2O} per unit {NaBr + $SrBr_2$} at the start of the measurement. It did not take up water at e = 18.68mbar and temperatures of T > 25°C. After heating to T_{max} = 110°C the water content was reduced to n = 1.0 {H_2O} per unit {NaBr + $SrBr_2$}.

Heating the mixture to T_{max} = 500°C showed two peaks, an endothermic one at T_{p1} = 192.52°C and a melting peak at T_{p2} = 479.84 °C. After the first peak at T = 229°C the sample was still holding about n = 0.4 {H_2O} per unit {NaBr + $SrBr_2$}. The minimum water content was reached after the melting peak with n = 0.2 {H_2O} per unit {NaBr + $SrBr_2$}.

The {NaBr + $2SrBr_2 \cdot 6H_2O$} sample was mixed at a ratio of 5g {NaBr} to 24g {$SrBr_2 \cdot 6H_2O$}.

Sample #1 was holding about n = 10.7 {H_2O} per unit {NaBr + $2SrBr_2$} at the start of the measurement.

The 1st dehydration showed a single peak at T_{p1} = 63.28°C. After the peak at T = 68°C, the sample was holding about n = 2.0 {H_2O} per unit {NaBr + 2$SrBr_2$} which slightly declined to n = 1.9 {H_2O} per unit {NaBr + 2$SrBr_2$} after heating to T_{max} = 100°C.

The 1st hydration showed three overlapping peaks at e = 8.65mbar, e = 14.80mbar and e = 17.66mbar for a total of H_{all} = 675.23Jg^{-1}, with the water uptake declining after the sample absorbed 36.6% of its observed minimum weight in water. That equals a water content of about n = 12.2 {H_2O} per formula unit {NaBr + 2$SrBr_2$}. The reaction turned endothermic as soon as the water supply was cut off and the sample emitted excess water.

At the start of the 2nd cycle, the sample was holding n = 11.3 {H_2O} per unit {NaBr + 2$SrBr_2$}.

The low temperature peak observed during the 1st dehydration shifted to a higher temperature at the 2nd dehydration, which shows the peak at T_{p1} = 85.26°C, joined by a second peak at T_{p2} = 188.38°C. The water content declined to n = 2.2 {H_2O} per unit {NaBr + 2$SrBr_2$} at T = 97°C and further to n = 0,1 {H_2O} per unit {NaBr + 2$SrBr_2$} after heating to T_{max} = 200°C.

The 2nd hydration curve showed three overlapping peaks similar to those observed during the 1st hydration, at e = 8.65mbar, e = 14.80mbar and e = 17.66mbar for a total of H_{all} = 650.77Jg^{-1}, also with the water uptake declining after the sample absorbed about 36.9% of its observed minimum weight in water, which equals a water content of about n = 12.3 {H_2O} per unit {NaBr + 2$SrBr_2$}. The reaction turned endothermic as soon as the water supply was cut off and the sample emitted excess water.

At the start of the 3rd cycle, the sample was holding n = 11.3 {H_2O} per unit {NaBr + 2$SrBr_2$} as well.

The 3rd dehydration developed similar to the 2nd dehydration, with two peaks at T_{p1} = 85.48°C and T_{p2} = 188.37°C. The water content declined to n = 2.2 {H_2O} per unit {NaBr + 2$SrBr_2$} at T = 93°C and further to n = 0,0 {H_2O} per

unit {NaBr + 2$SrBr_2$} after heating to T_{max} = 200°C, where the sample's minimum weight was observed.

Sample #2 of the mixture was holding n = 11.3 {H_2O} to 11.4 {H_2O} per unit {NaBr + 2$SrBr_2$} at the start of the measurement, which equals 33.6% of the observed minimum weight. It did not take up water at e = 18.68mbar and temperatures of T > 25°C. After heating to T_{max} = 110°C the sample was still holding about n = 2.0 {H_2O} per unit {NaBr + 2$SrBr_2$}.

Heating the mixture to T_{max} = 500°C showed one endothermic peak at T_{p1} = 196.97°C and a melting event at T = 479.56°C without any corresponding weight change. The sample's observed minimum weight was measured after the first peak at T = 248°C, where the water content had declined to about n = 0.15 {H_2O} per unit {NaBr + 2$SrBr_2$}.

5.3.8. {2KBr + $SrBr_2 \cdot 6H_2O$}, {KBr + $SrBr_2 \cdot 6H_2O$}, {KBr + $2SrBr_2 \cdot 6H_2O$}

The mixing ratio for the {2KBr + $SrBr_2 \cdot 6H_2O$} sample was 1g {KBr} to1g {$SrBr_2 \cdot 6H_2O$}.

Sample #1 was holding about n = 8.0 {H_2O} per unit {2KBr + $SrBr_2$} at the start of the measurement.

The 1st dehydration showed a single peak at T_{p1} = 64.28°C. After the peak at T = 68°C the water content had declined to n = 1.7 {H_2O} per unit {2KBr + $SrBr_2$}, it sank further to n = 1.6 {H_2O} per unit {2KBr + $SrBr_2$} after heating to T_{max} = 100°C.

The 1st hydration showed three overlapping peaks at e = 8.65mbar, e = 14.80mbar and e = 17.66mbar for a total of H_{all} = 599.68Jg^{-1}, with the water uptake declining after the sample absorbed 31.3% of its observed minimum weight in water, which equals a water content of about n = 8.6 {H_2O} per

formula unit {2KBr + $SrBr_2$}. The reaction turned endothermic as soon as the water supply was cut off and the sample emitted excess water.

At the start of the 2nd cycle the sample was holding n = 8.5 {H_2O} per unit {2KBr + $SrBr_2$}.

Two peaks were observed during the 2nd dehydration at T_{p1} = 85.08°C and T_{p2} = 188.00°C. The curve showed some exothermic behavior before both peaks. After the first peak at T = 93°C the water content had declined to n = 1.8 {H_2O} per unit {2KBr + $SrBr_2$}. After heating to T_{max} = 200°C the sample's minimum weight was observed, while the water content sank to n = 0.15 {H_2O} per unit {2KBr + $SrBr_2$}.

The 2nd hydration curve showed three overlapping peaks similar to the 1st at e = 8.65mbar, e = 14.80mbar and e = 17.66mbar for a total of H_{all} = 599.94Jg^{-1}, also with the water uptake declining after the sample absorbed about 31.2% of its observed minimum weight in water, which equals about n = 8.6 {H_2O} per unit {2KBr + $SrBr_2$}. The reaction turned endothermic as soon as the water supply was cut off and the sample emitted excess water.

At the start of the 3rd cycle the sample was holding n = 8.5 {H_2O} per unit {2KBr + $SrBr_2$} as well.

The 3rd dehydration curve developed similar to the 2nd dehydration curve, with two peaks at T_{p1} = 84.99°C and T_{p2} = 186.55°C. Again, the curve showed some exothermic behavior before both peaks. After the first peak at T = 93°C the water content had declined to n = 1.8 {H_2O} per unit {2KBr + $SrBr_2$} the water content sank further to n = 0.2 {H_2O} per unit {2KBr + $SrBr_2$} after heating to T_{max} = 200°C.

Sample #2 of the mixture was holding about n = 8.0 {H_2O} per unit {2KBr + $SrBr_2$} at the start of the measurement, which equaled 29.7% of the sample's observed minimum weight. It only took up minimal amounts of water at e = 18.68mbar until it reached a temperature of T = 51.05°C and a water content

of n = 8.1 {H_2O} per unit {2KBr + $SrBr_2$}. The water content kept declining after that and didn't recover. After heating to T_{max} = 110°C the water content was about n = 1.6 {H_2O} per unit {2KBr + $SrBr_2$}.

Heating the mixture to T_{max} = 500°C, showed a single peak at T_{p1} = 196.96°C. A sudden weight loss was observed at T = 380.09 °C and while a melting event taking place was a possibility, no corresponding melting peak occurred. The water content of the sample declined to n = 0.3 {H_2O} per unit {2KBr + $SrBr_2$} after the first peak at T = 231°C and was reduced further to n = 0.0 {H_2O} per unit {2KBr + $SrBr_2$} at T = 380°C after the sudden weight loss event and the sample was considered an anhydrate for the rest of the dehydration measurement.

The mixing ratio for the {KBr + $SrBr_2 \cdot 6H_2O$} sample was 1g {KBr} to 2g {$SrBr_2 \cdot 6H_2O$}.

Sample #1 contained about n = 7.0 {H_2O} per unit {KBr + $SrBr_2$} at the start of the measurement.

The 1st dehydration curve showed a single peak at T_{p1} = 64.33°C. After the peak and heating to T_{max} = 100°C the sample was still holding about n = 2.0 {H_2O} per unit {KBr + $SrBr_2$}.

The 1st hydration showed three overlapping peaks at e = 8.65mbar, e = 14.80mbar and e = 17.66mbar for a total of H_{all} = 605.32Jg^{-1}, the water uptake was declining after the sample absorbed 30.8% of its own observed minimum weight in water, which equals a water content of about n = 7.5 {H_2O} per formula unit {KBr + $SrBr_2$}. The reaction turned into a weak endothermic event as soon as the water supply was cut off and the sample emitted excess water.

At the start of the 2nd cycle the sample was holding n = 7.4 {H_2O} per unit {KBr + $SrBr_2$}.

During the 2nd dehydration two peaks were observed at T_{p1} = 86.56°C and T_{p2} = 188.58°C. The water content sank to n = 2.2 {H_2O} per unit {KBr + $SrBr_2$} after the first peak at T = 94°C, before it further declined to n = 0.9 {H_2O} per unit {KBr + $SrBr_2$} after the second peak and heating to T_{max} = 200°C, which was where the minimum sample weight was observed.

The 2nd hydration curve showed three overlapping peaks similar to those observed during the 1st hydration, at e = 8.65mbar, e = 14.80mbar and e = 17.66mbar for a total of H_{all} = 610.19Jg^{-1}, also with the water uptake declining after the sample absorbed about 31.0% of its own observed minimum weight in water, which equals a water content of about n = 7.5 {H_2O} per unit {KBr + $SrBr_2$}. The reaction turned into a weak endothermic event as soon as the water supply was cut off and the sample emitted excess water.

At the start of the 3rd cycle the sample was holding n = 7.4 {H_2O} per unit {KBr + $SrBr_2$} as well.

The 3rd dehydration curve developed similar to the 2nd curve, with two peaks at T_{p1} = 85.92°C and T_{p2} = 188.38°C. The water content sank to n = 2.1 {H_2O} per unit {KBr + $SrBr_2$} after the first peak at T = 94°C, before it further declined to n = 0.9 {H_2O} per unit {KBr + $SrBr_2$} after the second peak and heating to T_{max} = 200°C.

Sample #2 of the mixture was holding n = 6.9 {H_2O} per unit {KBr + $SrBr_2$} at the start of the measurement, which equals 34.1% of the sample's observed minimum weight. It only took up a small amount of water at e = 18.68mbar until a water content of n = 7.0 {H_2O} per unit {KBr + $SrBr_2$} and a temperature of T = 51°C were reached. After heating to T_{max} = 110°C the water content had declined to n = 1.2 {H_2O} per unit {KBr + $SrBr_2$} and did not recover during the measurement.

Heating the mixture to T_{max} = 500°C showed a single peak at T_{p1} = 197.53°C, after which the sample was considered anhydrous with n = 0.0 {H_2O} per unit {KBr + $SrBr_2$}. A melting event was not observed.

The {KBr + $2SrBr_2 \cdot 6H_2O$} sample was mixed at a ratio of 1g {KBr} to 4g {$SrBr_2 \cdot 6H_2O$}.

Sample #1 was holding about n = 12.9 {H_2O} per unit {KBr + $2SrBr_2$} at the start of the measurement.

The 1st dehydration showed a single peak at T_{p1} = 61.30°C. The water content declined to n = 4.3 {H_2O} per unit {KBr + $2SrBr_2$} after heating to T_{max} = 100°C.

The 1st hydration showed three overlapping peaks at e = 8.65mbar, e = 14.80mbar and e = 17.66mbar for a total of H_{all} = 597.34Jg^{-1}. The water uptake was declining after the sample absorbed 31.2% of its observed minimum weight in water, which equals a water content of about n = 13.8 {H_2O} per formula unit {KBr + $2SrBr_2$}. The reaction turned into a weak endothermic event as soon as the water supply was cut off and the sample emitted excess water.

At the start of the 2nd cycle, the sample was holding about n = 13.6 {H_2O} per unit {KBr + $2SrBr_2$}.

Two peaks were observed during the 2nd dehydration at T_{p1} = 86.19°C and T_{p2} = 188.74°C. The water content first declined to n = 4.5 {H_2O} per unit {KBr + $2SrBr_2$} after the first peak at T = 94°C, then to n = 2.4 {H_2O} per unit {KBr + $2SrBr_2$} after heating to T_{max} = 200°C.

The 2nd hydration curve showed three overlapping peaks similar to those observed during the 1st hydration, at e = 8.65mbar, e = 14.80mbar and e = 17.66mbar for a total of H_{all} = 614.43Jg^{-1}, also with the water uptake

declining after the sample absorbed about 31.2% of its own observed minimum weight in water, which equals a water content of about n = 13.8 {H_2O} per unit {$KBr + 2SrBr_2$}. The reaction turned into a weak endothermic event as soon as the water supply was cut off and the sample emitted excess water.

At the start of the 3rd cycle, the sample was holding about n = 13.6 {H_2O} per unit {$KBr + 2SrBr_2$}.

The 3rd dehydration curve developed similar to the 2nd curve, with two peaks at T_{p1} = 86.85°C and T_{p2} = 188.40°C. The water content first declined to n = 4.5 {H_2O} per unit {$KBr + 2SrBr_2$} after the first peak at T = 95°C, then to n = 2.4 {H_2O} per unit {$KBr + 2SrBr_2$} after heating to T_{max} = 200°C.

Sample #2 of the mixture was holding about n = 12.8 {H_2O} per unit {$KBr + 2SrBr_2$} at the start of the measurement, which equals about 29.1% of the observed minimum sample weight. At e = 18.68mbar it took up only minimal additional water until a water content of n = 12.9 {H_2O} per unit {$KBr + 2SrBr_2$} and a temperature of T = 74.76°C were reached. After heating to T_{max} = 110°C the water content declined to n = 4.1 {H_2O} per unit {$KBr + 2SrBr_2$} and did not recover during the measurement.

Heating the mixture to T_{max} = 500°C showed one peak at T_{p1} = 198.72°C, after which the sample was still holding about n = 2.3 {H_2O} per unit {$KBr + 2SrBr_2$}. A very weak but sudden weight loss occurred at T ~ 350°C but no corresponding endothermic peak was observed.

5.3.9. {$2LiBr + SrBr_2·6H_2O$}, {$LiBr + SrBr_2·6H_2O$}, {$LiBr + 2SrBr_2·6H_2O$}

The mixing ratio for the {$2LiBr + SrBr_2·6H_2O$} sample was 7g {LiBr} to 10g {$SrBr_2·6H_2O$}.

An error occurred in the weight recording during all measurements after the first dehydration of sample #1. While the values were corrected, this may have affected the calculated water contents and enthalpies.

Sample #1 was holding about n = 15.3 {H_2O} per unit {2LiBr + $SrBr_2 \cdot 6H_2O$} at the start of the measurement.

The 1st dehydration showed two main, overlapping peaks at T_{p1} = 27.45°C, T_{p2} = 55.91°C connected to an extended endothermic event with a likely peak at T_{p3} = 97.97°C. The water content sank to about n = 7.3 {H_2O} per unit {2LiBr + $SrBr_2 \cdot 6H_2O$} after the two peaks at T = 72°C and declined further to n = 4.4 {H_2O} per unit {2LiBr + $SrBr_2 \cdot 6H_2O$} after heating to T_{max} = 100°C.

The 1st hydration showed three overlapping peaks at e = 8.65mbar, e = 14.80mbar and e = 17.66mbar for a total of H_{all} = 1,233.65Jg^{-1}. The sample absorbed 73.5% of its calculated minimum weight in water until the water supply was cut off, which equals a water content of about n = 21.0 {H_2O} per formula unit {2LiBr + $SrBr_2$}. The reaction changed to an endothermic event as soon as the water supply was cut off and the sample emitted excess water.

At the start of the 2nd cycle the sample was holding about n = 16.9 {H_2O} per unit {2LiBr + $SrBr_2 \cdot 6H_2O$}.

During the 2nd dehydration three peaks were observed, a single peak at T_{p1} = 66.77°C, followed by a double peak at T_{p2} = 150.36°C and T_{p3} = 200.00°C. The water content declined to n = 7.0 {H_2O} per unit {2LiBr + $SrBr_2 \cdot 6H_2O$} after the first peak at T = 98°C, then sank further to n = 3.1 {H_2O} per unit {2LiBr + $SrBr_2 \cdot 6H_2O$} after the double peak and heating to T_{max} = 200°C.

The 2nd hydration curve showed three overlapping peaks similar to those measured during the 1st hydration, at e = 8.65mbar, e = 14.80mbar and e = 17.66mbar for a total of H_{all} = 1079.06Jg^{-1}, also with the water uptake declining after the sample absorbed about 74.1% of its own weight (at T=

200°C) in water, which equals about n = 21.2 {H_2O} per unit {2LiBr + $SrBr_2$}. The reaction turned into a weak endothermic event as soon as the water supply was cut off and the sample emitted excess water.

At the start of the 3rd cycle the sample was holding about n = 17.1 {H_2O} per unit {2LiBr + $SrBr_2 \cdot 6H_2O$}.

The 3rd dehydration curve developed similar to the 2nd curve, with three peaks at T_{p1} = 66.43°C and a double peak at T_{p2} = 139.22°C and T_{p3} = 200.00°C. The water content declined to n = 6.7 {H_2O} per unit {2LiBr + $SrBr_2 \cdot 6H_2O$} after the first peak at T = 98°C, then sank further to n = 2.2 {H_2O} per unit {2LiBr + $SrBr_2 \cdot 6H_2O$} after the double peak and heating to T_{max} = 200°C.

Sample #2 of the mixture carried about n = 16.9 {H_2O} per unit {2LiBr + $SrBr_2 \cdot 6H_2O$} at the start of the measurement. As long as no water source was present, the material dehydrated already at T = 25°C. With water supplied at e = 18.68mbar, it reacted until a temperature of T = 39.82°C and a water content of n = 18.0 {H_2O} per unit {2LiBr + $SrBr_2 \cdot 6H_2O$} were reached, which equals a water uptake of 62.4% compared to the observed minimum sample weight. After drying the sample to T_{max} = 110°C, where the water content had declined to n = 5.5 {H_2O} per unit {2LiBr + $SrBr_2 \cdot 6H_2O$}, the material was able to take up water at e = 18.68mbar and T = 62.70°C, to n = 9.3 {H_2O} per unit {2LiBr + $SrBr_2 \cdot 6H_2O$}.

The water content declined again and sank to n = 7.6 {H_2O} per unit {2LiBr + $SrBr_2 \cdot 6H_2O$} before the next dehydration started.

Three peaks were observed when heating the mixture to T_{max} = 500°C at T_{p1} = 144.55°C, T_{p2} = 203.51°C and T_{p3} = 230.53°C. A melting event without corresponding weight change occurred at T = 443.34°C. A solidification event, also without a corresponding weight change, was recorded during the cooldown stage at T = 383,42°C. After the first peak at T = 171°C, the

sample was still holding about n = 3.4 {H_2O} per unit {2LiBr + $SrBr_2 \cdot 6H_2O$}, after heating to Tmax = 500°C the water content had declined to n = 2.1 {H_2O} per unit {2LiBr + $SrBr_2 \cdot 6H_2O$}, with the minimum sample weight being recorded at T = 380°C.

The mixing ratio for the {LiBr + $SrBr_2 \cdot 6H_2O$} sample was 7g {LiBr} to 20g {$SrBr_2 \cdot 6H_2O$}.

As with the previous mixture, an error occurred in the weight recording during all measurements after the first dehydration of sample #1. While the values were corrected, this may have affected the calculated water contents and enthalpies.

Sample #1 was holding about n = 13.2 {H_2O} per unit {LiBr + $SrBr_2$} at the start of the measurement.

Only a single peak was observed during the 1st dehydration at T_{p1} = 60.26°C. After the peak at T = 71°C the water content had declined to n = 6.1 {H_2O} per unit {LiBr + $SrBr_2$}. After heating to T_{max} = 100°C the water content was further reduced to n = 4.5 {H_2O} per unit {LiBr + $SrBr_2$}.

The 1st hydration showed three overlapping peaks at e = 8.65mbar, e = 14.80mbar and e = 17.66mbar for a total of H_{all} = 1008.84Jg^{-1}. The sample absorbed 69.3% of its calculated minimum weight in water until the water supply was cut off, which equaled a water content of about n = 16.2 {H_2O} per formula unit {LiBr + $SrBr_2$}. The reaction changed to an endothermic event as soon as the water supply was cut off and the sample emitted excess water.

At the start of the 2nd cycle, the sample was holding about n = 13.0 {H_2O} per unit {LiBr + $SrBr_2$}.

Two peaks occurred during the 2nd dehydration at T_{p1} = 73.66°C and T_{p2} = 151.77°C, with the second peak indicating a partial melting event. After the first peak at T = 98°C the sample was holding about n = 6.0 {H_2O} per unit {LiBr + $SrBr_2$}. The water content declined further to n = 2.3 {H_2O} per unit {LiBr + $SrBr_2$} after heating to T_{max} = 200°C.

The 2nd hydration curve showed three overlapping peaks similar to those observed during the 1st hydration, at e = 8.65mbar, e = 14.80mbar and e = 17.66mbar for a total of H_{all} = 1197.00Jg^{-1}, also with the water uptake declining after the sample absorbed about 69.5% of its calculated minimum weight in water, which equals a water content of about n = 16.2 {H_2O} per unit {LiBr + $SrBr_2$}. The reaction turned into a weak endothermic event as soon as the water supply was cut off and the sample emitted excess water.

At the start of the 3rd cycle, the sample was holding about n = 13.2 {H_2O} per unit {LiBr + $SrBr_2$}.

The 3rd dehydration showed two peaks at T_{p1} = 72.48°C and T_{p2} = 188.97°C. The partial melting event observed during the 2nd dehydration occurred again but weaker during the 3rd dehydration at T = 152.5°C. After the first peak at T = 98°C the sample was holding about n = 5.7 {H_2O} per unit {LiBr + $SrBr_2$}. The water content declined further to n = 2.3 {H_2O} per unit {LiBr + $SrBr_2$} after heating to T_{max} = 200°C.

Sample #2 of the mixture held about n = 11.5 {H_2O} per unit {LiBr + $SrBr_2$} at the start of the measurement, which equaled about 57.1% of the observed minimum sample weight. As long as no water source was present, the material already emitted excess water at T= 25°C. With water supplied at e = 18.68mbar, it reacted until a temperature of T = 39,54°C and a water content of n = 12.0 {H_2O} per unit {LiBr + $SrBr_2$} were reached, which equals 57.1% of the observed minimum sample weight. At T = 86°C the water content had declined to n = 4.1 {H_2O} per unit {LiBr + $SrBr_2$}, At T = 105°C the water content was reduced to n = 3.3 {H_2O} per unit {LiBr + $SrBr_2$}.

The recording of the measurement was interrupted before the maximum temperature of T_{max} = 110°C was reached or the cooldown stage for rehydration was initialized but the sample recovered to a water content of n = 11.0 {H_2O} per unit {LiBr + $SrBr_2$} before the next dehydration stage started.

Heating the mixture to T_{max} = 500°C showed three endothermic peaks at T_{p1} = 76.01°C, T_{p2} = 154.35°C and T_{p3} = 232.86°C. The peaks two and three were also partial melting events. At T = 110°C the mixture still held a water content of about n = 7.5 {H_2O} per unit {LiBr + $SrBr_2$}, at T = 223°C it contained n = 2.1 {H_2O} per unit {LiBr + $SrBr_2$}. A third melting event occurred at T = 443.49°C, after which the water content was reduced to n = 0.9 {H_2O} per unit {LiBr + $SrBr_2$}. A solidification event was observed during the cooldown stage at T = 394,50°C.

Due to the low temperature melting events observed for the hydrated phases of the mixture, cycle instability is to be expected, if the material used at a larger scale than m = 10mg.

The {LiBr + $2SrBr_2 \cdot 6H_2O$} sample was mixed at a ratio of 7g {LiBr} to 40g {$SrBr_2 \cdot 6H_2O$}.

Sample #1 was holding about n = 18.3 {H_2O} per unit {LiBr + $2SrBr_2$} at the start of the measurement.

The 1st dehydration shows a single peak at T_{p1} = 57.86°C. Directly after the peak at T = 70°C the sample was still holding about n = 6.6 {H_2O} per unit {LiBr + $2SrBr_2$}, after heating to Tmax = 100°C the water content was further reduced to n = 3.6 {H_2O} per unit {LiBr + $2SrBr_2$}.

The 1st hydration showed three overlapping peaks at e = 8.65mbar, e = 14.80mbar and e = 17.66mbar for a total of H_{all} = 703.46Jg^{-1}. The sample absorbed 66.6% of its observed minimum weight in water until the water supply was cut off, which equaled a water content of about n = 22.4 {H_2O} per formula unit {LiBr + 2$SrBr_2$}. The reaction changed to an endothermic event as soon as the water supply was cut off and the sample emitted excess water.

At the start of the 2nd cycle the sample was holding n = 18.0 {H_2O} per unit {LiBr + 2$SrBr_2$}.

Two peaks were observed during the 2nd dehydration at T_{p1} = 74.82°C and T_{p2} = 152.67°C. The second peak indicated a partial melting event. The water content was reduced to n = 8.4 {H_2O} per unit {LiBr + 2$SrBr_2$} after the first peak at T = 98°C and declined further to n = 0.5 {H_2O} per unit {LiBr + 2$SrBr_2$} after heating to T_{max} = 200°C, where also the minimum sample weight was observed.

The 2nd hydration curve showed three overlapping peaks similar to those observed during the 1st hydration at e = 8.65mbar, e = 14.80mbar and e = 17.66mbar for a total of H_{all} = 771.64Jg^{-1}, also with the water uptake declining after the sample absorbed about 66.3% of its observed minimum weight in water, which equaled about n = 22.3 {H_2O} per unit {LiBr + 2$SrBr_2$}. The reaction turned into a weak endothermic event as soon as the water supply was cut off and the sample emitted excess water.

At the start of the 3rd cycle the sample was holding n = 18.0 {H_2O} per unit {LiBr + 2$SrBr_2$} again.

The 3rd dehydration curve developed similar to the 2nd with two peaks at T_{p1} = 74.57°C and T_{p2} = 154.14°C. However, a melting event was not identified. The water content was reduced to n = 8.1 {H_2O} per unit {LiBr + 2$SrBr_2$} after the first peak at T = 98°C and declined further to n = 0.74 {H_2O} per unit {LiBr + 2$SrBr_2$} after heating to T_{max} = 200°C.

Sample #2 held a water content of n = 17.1 {H_2O} per unit {LiBr + 2$SrBr_2$} at the start of the measurement, which equaled 54.02% of the observed minimum sample weight. As long as no water source was introduced, the material dehydrated at T = 25°C. With water supplied at e = 18.68mbar, it reacted until a temperature of T = 39,12°C was reached where the water content amounted to n = 17.4 {H_2O} per unit {LiBr + 2$SrBr_2$} which equaled a weight of 54.0% of the observed minimum sample mass. After heating the mixture to T_{max} = 110°C the water content was reduced to n = 3.8 {H_2O} per unit {LiBr + 2$SrBr_2$}, the sample took up water at T = 60.37°C and e = 18.68mbar until an amount of n = 6.1 {H_2O} per unit {LiBr + 2$SrBr_2$} was reached. Without a water source the sample emitted excess water until the water content reached n = 5.0 {H_2O} per unit {LiBr + 2$SrBr_2$}.

Heating the mixture to T_{max} = 500°C showed three peaks at T_{p1} = 151.86°C, T_{p2} = 205.72°C and T_{p3} = 232.01°C. The water content had declined to n = 1.0 {H_2O} per unit {LiBr + 2$SrBr_2$} at T = 225°C after the second peak, then it sank further to n = 0.05 {H_2O} per unit {LiBr + 2$SrBr_2$} at T = 307°C. A melting event without corresponding weight change was observed at T = 444.81°C, followed by a solidification event at T = 408,75°C during the cooldown stage, the sample was considered anhydrous afterwards.

5.3.10. {2$MgBr_2$ + $SrBr_2$·6H_2O}, {$MgBr_2$ + $SrBr_2$·6H_2O}, {$MgBr_2$ + 2$SrBr_2$·6H_2O}

The mixing ratio for the {2$MgBr_2$·6H_2O + $SrBr_2$·6H_2O} sample was 3g {$MgBr_2$·6H_2O} to 2g {$SrBr_2$·6H_2O}.

Sample #1 held about n = 52.6 {H_2O} per unit {2$MgBr_2$ + $SrBr_2$} at the start of the measurement.

The 1st dehydration showed two peaks at T_{p1} = 57.52°C and T_{p2} = 97.91°C. After the first peak at T = 75°C the water content had declined to n = 46.2 {H_2O} per unit {2$MgBr_2$ + $SrBr_2$}, after heating to T_{max} = 100°C it was reduced to n = 40.6 {H_2O} per unit {2$MgBr_2$ + $SrBr_2$}.

The 1st hydration showed three overlapping peaks at e = 8.65mbar, e = 14.80mbar and e = 17.66mbar for a total of H_{all} = 655.14Jg^{-1}. The sample absorbed 142.9% of its observed minimum weight in water until the water supply was cut off, which equaled a water content of about n = 80.5 {H_2O} per formula unit {2$MgBr_2$ + $SrBr_2$}.

At the start of the 2nd cycle, the sample held a water content of n = 81.0 {H_2O} per unit {2$MgBr_2$ + $SrBr_2$}.

Three peaks were observed during the 2nd dehydration at T_{p1} = 79.19°C, followed by a double peak at T_{p2} = 155.00°C and T_{p3} = 175.24°C. All three peaks show signs of occurring melting events. At T = 98°C after the first peak, the water content was about n = 56.3 {H_2O} per unit {2$MgBr_2$ + $SrBr_2$}. It declined further to n = 21.1 {H_2O} per unit {2$MgBr_2$ + $SrBr_2$} after heating to T_{max} = 200°C.

The 2nd hydration curve showed three overlapping peaks similar to the 1st curve, at e = 8.65mbar, e = 14.80mbar and e = 17.66mbar for a total of H_{all} = 703.75Jg^{-1}. The water uptake was 100.2% of its observed minimum weight in water, which equaled a water content of about n = 60.3 {H_2O} per unit {2$MgBr_2$ + $SrBr_2$}. Unlike during the 1st hydration, the reaction turned into a weak endothermic event as soon as the water supply was cut off and the sample emitted excess water.

At the start of the 3rd cycle, the sample held a water content of n = 57.7 {H_2O} per unit {2$MgBr_2$ + $SrBr_2$}.

The 3rd dehydration developed similar to the 2nd dehydration, with a peak at T_{p1} = 79.04°C, followed by a double peak at T_{p2} = 160.00°C and T_{p3} = 175.57°C, again the peaks show signs of occurring melting events. At T =

98°C after the first peak, the water content was about n = 43.8 {H_2O} per unit {$2MgBr_2 + SrBr_2$}. It declined further to its minimum water content of n = 13.3 {H_2O} per unit {$2MgBr_2 + SrBr_2$} after heating to T_{max} = 200°C, where also the minimum sample weight was observed.

Sample #2 of the mixture was holding n = 53.0 {H_2O} per unit {$2MgBr_2 + SrBr_2$} at the start of the measurement, which equals 155.1% of the sample's observed minimum weight. No peaks occurred but the mixture dehydrated steadily within the temperature interval T = 25°C to T_{max} = 110°C. It did not take up water at e = 18.68mbar while the temperature was raised. At the end of the dehydration measurement the water content had declined to n = 36.2 {H_2O} per unit {$2MgBr_2 + SrBr_2$}.

Heating the mixture to T_{max} = 500°C, shows a cluster of at least eight overlapping small peaks with the main peak at T_{p1} = 197.76°C, followed by a second peak at T_{p2} = 405.60°C. A partial melting event occurred at T = 65.00°C, several of the other peaks in the cluster were likely partial melting events as well. The water content sank to n = 12.5 {H_2O} per unit {$2MgBr_2 + SrBr_2$} after the peak cluster, which equals 36.44% of the observed minimum weight. After heating to T = 496°C the water content had declined to n = 0.45 {H_2O} per unit {$2MgBr_2 + SrBr_2$}. The water content kept declining until the sample reached an anhydrate state.

The {$MgBr_2 \cdot 6H_2O + SrBr_2 \cdot 6H_2O$} sample was mixed at a ratio of 3g {$MgBr_2 \cdot 6H_2O$} to 4g {$SrBr_2 \cdot 6H_2O$}.

Sample #1 held about n = 43.9 {H_2O} per unit {$MgBr_2 + SrBr_2$} at the start of the measurement.

Two peaks were observed during the 1st dehydration at T_{p1} = 53.79°C and T_{p2} = 90.21 °C. After the first peak at T = 68°C the water content was

reduced to n = 38.5 {H_2O} per unit {$MgBr_2$ + $SrBr_2$}, it declined further to n = 35.1 {H_2O} per unit {$MgBr_2$ + $SrBr_2$} after heating to T_{max} = 100°C.

The 1st hydration showed three overlapping peaks at e = 8.65mbar, e = 14.80mbar and e = 17.66mbar for a total of H_{all} = 473.68Jg^{-1}. The sample absorbed 105.5% of its observed minimum weight in water until the water supply was cut off, which equals a water content of about n = 54.5 {H_2O} per formula unit {$MgBr_2$ + $SrBr_2$}. The reaction turned into a strong endothermic event as soon as the water supply was cut off and the sample emitted excess water.

At the start of the 2nd cycle, the sample was holding about n = 51.5 {H_2O} per unit {$MgBr_2$ + $SrBr_2$}.

The 2nd dehydration showed thee peaks, the first at T_{p1} = 78.53°C followed by a double peak at T_{p2} = 165.00°C and T_{p3} = 175.22°C. The peaks two and three appear to be partial melting events. After the first peak at T = 98°C the water content was reduced to n = 47.6 {H_2O} per unit {$MgBr_2$ + $SrBr_2$}, it further declined to n = 18.2 {H_2O} per unit {$MgBr_2$ + $SrBr_2$} after heating to T_{max} = 200°C.

The 2nd hydration curve showed three overlapping peaks similar to those observed during the 1st hydration, at e = 8.65mbar, e = 14.80mbar and e = 17.66mbar for a total of H_{all} = 707.67Jg^{-1}. The sample absorbed about 77.3% of its observed minimum weight in water, which equals a water content of about n = 43.8 {H_2O} per unit {$MgBr_2$ + $SrBr_2$}. The reaction turned into a strong endothermic event as soon as the water supply was cut off and the sample emitted excess water.

At the start of the 3rd cycle, the sample was holding about n = 40.0 {H_2O} per unit {$MgBr_2$ + $SrBr_2$}.

The 3rd dehydration curve developed similar to the 2nd curve and showed three peaks, starting with a single peak at T_{p1} = 78.32°C then followed by a double peak at T_{p2} = 164.69°C and T_{p3} = 175.00°C during this dehydration

stage all three peaks indicate partial melting events. After the first peak at T = 98°C the water content was reduced to n = 36.2 {H_2O} per unit {$MgBr_2$ + $SrBr_2$}, it further declined to n = 14.3 {H_2O} per unit {$MgBr_2$ + $SrBr_2$} after heating to T_{max} = 200°C, where the sample's minimum weight was observed.

Sample #2 was holding n = 44.1 {H_2O} per unit {$MgBr_2$ + $SrBr_2$} at the start of the measurement, which equals 176.7% of the observed minimum sample weight. Without a water supply, the mixture dehydrated slightly at T = 25°C. The sample took up water at e = 18.68mbar until a temperature of T= 34.40°C was reached and it held about n = 43.7 {H_2O} per unit {$MgBr_2$ + $SrBr_2$} again. After heating the mixture to T_{max} = 110°C the sample held n = 35.4 {H_2O} per unit {$MgBr_2$ + $SrBr_2$} which equals 141.3% of its observed minimum weight. The water content did not recover until the next dehydration stage begun

Heating the mixture to T_{max} = 500°C, showed a cluster of seven small overlapping peaks with the main peak at T_{p1} = 159.59°C, followed by another peak at T_{p2} = 405.44°C. Two peaks of the cluster at T = 90°C and T = 159.59°C were identified as partial melting events. At T = 330°C after the peak cluster, the sample was still holding about n = 12.0 {H_2O} per unit {$MgBr_2$ + $SrBr_2$}. The water content sank to n = 0.9 {H_2O} per unit {$MgBr_2$ + $SrBr_2$} directly after the second peak at T = 429.39°C and reached a minimum of n = 0.66 {H_2O} per unit {$MgBr_2$ + $SrBr_2$} after heating to T_{max} = 500°C.

The {$MgBr_2 \cdot 6H_2O$ + $2SrBr_2 \cdot 6H_2O$} sample was mixed at a ratio of 3g {$MgBr_2 \cdot 6H_2O$} to 8g {$SrBr_2 \cdot 6H_2O$}.

Sample #1 was holding about n = 26.7 {H_2O} per unit {$MgBr_2$ + $2SrBr_2$} at the start of the measurement.

The 1st dehydration showed two peaks at Tp_1 = 66.50°C and Tp_2 = 97.91°C. The water content declined to n = 13.9 {H_2O} per unit {$MgBr_2$ + 2$SrBr_2$} after the first peak at T = 76°C and sank to n = 12.1 {H_2O} per unit {$MgBr_2$ + 2$SrBr_2$} after heating to T_{max} = 100°C.

The 1st hydration showed three overlapping peaks at e = 8.65mbar, e = 14.80mbar and e = 17.66mbar for a total of H_{all} = 687.90Jg^{-1}. The sample absorbed 77.0% of its observed minimum weight in water until the water supply was cut off, which equals a water content of about n = 32.3 {H_2O} per formula unit {$MgBr_2$ + 2$SrBr_2$}. The reaction turned into a strong endothermic event as soon as the water supply was cut off and the sample emitted excess water.

At the start of the 2nd cycle the mixture held a water content of n = 30.0 {H_2O} per unit {$MgBr_2$ + 2$SrBr_2$}.

During the 2nd dehydration four peaks were observed with a double peak at T_{p1} = 65.00°C and T_{p2} = 84.34°C and a second double peak at T_{p3} = 152.21°C and T_{p4} = 185.00°C. The second and the third peak indicated partial melting events. At T = 98°C after the first double peak, the sample was still holding about n = 22.0 {H_2O} per unit {$MgBr_2$ + 2$SrBr_2$}. After heating to T_{max} = 200°C it had declined to n = 6.4 {H_2O} per unit {$MgBr_2$ + 2$SrBr_2$}.

The 2nd hydration curve showed three overlapping peaks similar to those observed during the 1st hydration, at e = 8.65mbar, e = 14.80mbar and e = 17.66mbar for a total of H_{all} = 651.74Jg^{-1}. The sample absorbed about 69.9% of its observed minimum weight in water, which equals a water content of about n = 29.5 {H_2O} per unit {$MgBr_2$ + 2$SrBr_2$}. The reaction turned into a strong endothermic event as soon as the water supply was cut off and the sample emitted excess water.

At the start of the 3rd cycle the mixture held a water content of n = 24.1 {H_2O} per unit {$MgBr_2$ + 2$SrBr_2$}.

Only three peaks were observed during the 3rd dehydration at T_{p1} = 80.88°C, T_{p2} = 138.62°C and T_{p3} = 188.45°C. And only the first peak showed signs of a melting event taking place. At T = 98°C after the first peak, the sample was still holding about n = 10.7 {H_2O} per unit {$MgBr_2$ + 2$SrBr_2$}, after the second peak at T = 155°C the water content was reduced to n = 7.2 {H_2O} per unit {$MgBr_2$ + 2$SrBr_2$} and after heating to T_{max} = 200°C it had declined to n = 1.85 {H_2O} per unit {$MgBr_2$ + 2$SrBr_2$}, where the minimum sample weight was observed.

Sample #2 was holding n = 24.0 {H_2O} per unit {$MgBr_2$ + 2$SrBr_2$} at the start of the measurement. This equals 58.4% of the sample's observed minimum weight. The mixture only took up marginal amounts of water at e = 18.68mbar until a temperature of T = 34.70°C and a water content of n = 24.2 {H_2O} per unit {$MgBr_2$ + 2$SrBr_2$} were reached. No water uptake was observed during the T = 60°C stage after dehydration to T_{max} = 110°C, after which the sample was holding about n = 10.0 {H_2O} per unit {$MgBr_2$ + 2$SrBr_2$}.

Heating the mixture to T_{max} = 500°C showed two peaks at T_{p1} = 195.70°C, T_{p2} = 405.89°C, neither was identified as a melting event. After the first peak at T = 330°C the sample was still holding about n = 3.6 {H_2O} per unit {$MgBr_2$ + 2$SrBr_2$}. The water content sank to n = 1.4 {H_2O} per unit {$MgBr_2$ + 2$SrBr_2$} after the second peak at T = 496°C and declined further till the end of the measurement, where the sample reached its observed minimum weight and a water content of n = 1.27 {H_2O} per unit {$MgBr_2$ + 2$SrBr_2$}.

The low temperature melting events observed for the hydrated phases of the three magnesium-strontium bromide mixtures indicate that a low cycle stability is to be expected, if the materials are used at a larger scale than m = 10mg.

5.3.11. {5CaBr$_2$·xH$_2$O + 4SrBr$_2$·6H$_2$O}, {5CaBr$_2$·xH$_2$O + 8SrBr$_2$·6H$_2$O}, {5CaBr$_2$·xH$_2$O + 16SrBr$_2$·6H$_2$O}

The {5CaBr$_2$·xH$_2$O + 4SrBr$_2$·6H$_2$O} sample was mixed at a ratio of 1g {CaBr$_2$·xH$_2$O} to 1g {SrBr$_2$·6H$_2$O}.

Sample #1 was holding about n = 63.0 {H$_2$O} per unit {5CaBr$_2$ + 4SrBr$_2$} at the start of the measurement.

The 1st dehydration showed three peaks, first a double peak at T_{p1} = 35.00°C and T_{p2} = 63.28°C, followed by a single peak at T_{p3} = 97.96°C. After the double peak at T = 83°C the water content had declined to n = 29.4 {H$_2$O} per unit {5CaBr$_2$ + 4SrBr$_2$}, it sank further to n = 18.3 {H$_2$O} per unit {5CaBr$_2$ + 4SrBr$_2$} after heating to T_{max} = 100°C.

The 1st hydration showed three overlapping peaks at e = 8.65mbar, e = 14.80mbar and e = 17.66mbar for a total of H_{all} = 755.89Jg^{-1}. The sample absorbed 66.1% of its observed minimum weight in water until the water supply was cut off, which equals about n = 78.0 {H$_2$O} per formula unit {5CaBr$_2$ + 4SrBr$_2$}. The reaction turned into a strong endothermic event as soon as the water supply was cut off and the sample emitted excess water.

At the start of the 2nd cycle the sample was holding about n = 68.7 {H$_2$O} per unit {5CaBr$_2$ + 4SrBr$_2$}.

During the 2nd dehydration three peaks were observed at T_{p1} = 74.72°C, with a double peak at T_{p2} = 172.14°C and T_{p3} = 195.00°C. The water content at T = 98°C after the first peak was n = 20.8 {H$_2$O} per unit {5CaBr$_2$ + 4SrBr$_2$}, it was further reduced to n = 3.0 {H$_2$O} per unit {5CaBr$_2$ + 4SrBr$_2$} after heating to T_{max} = 200°C, where also the minimum sample weight was observed.

The 2nd hydration curve showed three overlapping peaks similar to those observed during the 1st hydration, at e = 8.65mbar, e = 14.80mbar and e = 17.66mbar for a total of H_{all} = 912.85Jg^{-1}. The sample absorbed about 61.8%

of its observed minimum weight in water, which equals about n = 73.1 {H_2O} per unit {$5CaBr_2 + 4SrBr_2$}. The reaction turned into a strong endothermic event as soon as the water supply was cut off and the sample emitted excess water.

At the start of the 3rd cycle the sample was holding about n = 66.4{H_2O} per unit {$5CaBr_2 + 4SrBr_2$}.

The 3rd dehydration showed three peaks at T_{p1} = 73.43°C, with the double peak at T_{p2} = 192.22°C and T_{p3} = 196.22°C. At T = 98°C after the first peak the water content had declined to n = 26.1 {H_2O} per unit {$5CaBr_2 + 4SrBr_2$}, after heating to T_{max} = 200°C the water content sank to n = 3.2 {H_2O} per unit {$5CaBr_2 + 4SrBr_2$}.

Sample #2 of the mixture held n = 63.0 {H_2O} per unit {$5CaBr_2 + 4SrBr_2$} at the start of the measurement. As long as no water source was supplied, the mixture dehydrated at T = 25°C. With a water flow of e = 18.68mbar, the sample took up water until T = 42.66°C and n = 69.3 {H_2O} per unit {$5CaBr_2 + 4SrBr_2$} were reached, which equaled 62.4% of the observed minimum sample weight. After heating to T_{max} = 110°C at e = 18.68mbar the water content declined to n = 26.6 {H_2O} per unit {$5CaBr_2 + 4SrBr_2$}, the sample rehydrated at T = 60.59°C to n = 38.0 {H_2O} per unit {$5CaBr_2 + 4SrBr_2$}.

Heating the mixture to T_{max} = 500°C showed two peaks at T_{p1} = 211.79°C and T_{p2} = 496.27°C. An event observed at T = 60.00°C indicated a partial melting. At T = 279°C after the first peak the water content declined to n = 4.7 {H_2O} per unit {$5CaBr_2 + 4SrBr_2$}. After heating to T_{max} = 500°C the water content sank further to about n = 0.3 {H_2O} per unit {$5CaBr_2 + 4SrBr_2$}, which was also where the minimum sample weight was observed.

The {$5CaBr_2 \cdot xH_2O + 8SrBr_2 \cdot 6H_2O$} sample was mixed at a ratio of 1g {$CaBr_2 \cdot xH_2O$} to 2g {$SrBr_2 \cdot 6H_2O$}.

Sample #1 was holding about n = 91.0 {H_2O} per unit {$5CaBr_2 + 8SrBr_2$} at the start of the measurement.

The 1st dehydration showed two peaks at T_{p1} = 58.1°C and T_{p2} = 95.86°C. At T = 71°C after the first peak the water content had declined to n = 36.6 {H_2O} per unit {$5CaBr_2 + 8SrBr_2$}, it sank further to n = 22.2 {H_2O} per unit {$5CaBr_2 + 8SrBr_2$} after heating to T_{max} = 100°C.

The 1st hydration showed three overlapping peaks at e = 8.65mbar, e = 14.80mbar and e = 17.66mbar for a total of H_{all} = 909.99Jg^{-1}. The sample absorbed 65.3% of its observed minimum weight in water until the water supply was cut off, which equals about n = 115.1 {H_2O} per formula unit {$5CaBr_2 + 8SrBr_2$}. The reaction turned into a strong endothermic event as soon as the water supply was cut off and the sample emitted excess water. At the start of the 2nd cycle the sample was holding about n = 95.4 {H_2O} per unit {$5CaBr_2 + 8SrBr_2$}.

During the 2nd dehydration two endothermic peaks were observed at T_{p1} = 77.97°C and T_{p2} = 194.32°C, a minor peak indicating a partial melting event occurred at T = 181.80°C. After the first peak at T = 98°C the water content was reduced to n = 31.5 {H_2O} per unit {$5CaBr_2 + 8SrBr_2$}, the sample's minimum weight was observed after heating to T_{max} = 200°C where the water content had declined to n = 4.3 {H_2O} per unit {$5CaBr_2 + 8SrBr_2$}.

The 2nd hydration curve showed three overlapping peaks similar to those observed during the 1st hydration at e = 8.65mbar, e = 14.80mbar and e = 17.66mbar but was interrupted before the 3rd hydration stage was complete. Until then the sample absorbed about 50.5% of its observed minimum weight in water, which equals a water content of about n = 89.8 {H_2O} per unit {$5CaBr_2 + 8SrBr_2$}.

Since the sample was lost during the 2nd hydration, no data of a 3rd dehydration was available.

Sample #2 of the mixture held n = 82.4 {H_2O} per unit {$5CaBr_2 + 8SrBr_2$} at the beginning of the measurement. Without a water supply the sample emitted marginal amounts of water at T = 25°C. With a water flow of e = 18.68mbar, the sample hydrated up to a temperature of T = 39,58 °C where it held n = 93.1 {H_2O} per unit {$5CaBr_2 + 8SrBr_2$} which equals 54.6% of the observed minimum sample weight. After heating to T_{max} = 110°C, the water content declined to n = 26.0 {H_2O} per unit {$5CaBr_2 + 8SrBr_2$}. The sample rehydrated at T = 60.61°C to n = 37.0 {H_2O} per unit {$5CaBr_2 + 8SrBr_2$} which equals 21.0% of the observed minimum sample weight.

Heating the mixture to T_{max} = 500°C showed a cluster of five peaks with two partial melting events at T_{m1} = 35.00°C and T_{m2} = 60.00°C followed by three endothermic peaks at T_{p1} = 135°C, T_{p2} = 175.00°C and T_{p3} = 212.41°C. After the peak cluster at T = 312°C the sample's water content was reduced to n = 3.5 {H_2O} per unit {$5CaBr_2 + 8SrBr_2$} and sank further to n = 1.85 {H_2O} per unit {$5CaBr_2 + 8SrBr_2$} after heating to T_{max} = 500°C, where also the minimum sample weight was observed.

The mixing ratio for the {$5CaBr_2 \cdot xH_2O + 16SrBr_2 \cdot 6H_2O$} sample was 1g {$CaBr_2 \cdot xH_2O$} to 4g {$SrBr_2 \cdot 6H_2O$}.

Sample #1 was holding about n = 157.9 {H_2O} per unit {$5CaBr_2 + 16SrBr_2$} at the start of the measurement.

The 1st dehydration showed a single peak at T_{p1} = 61.95°C. The water content declined to n = 45.0 {H_2O} per unit {$5CaBr_2 + 16SrBr_2$} after heating to T_{max} = 100°C.

The sample started into the 1st hydration with a water content of only n = 30.9 {H_2O} per unit {$5CaBr_2 + 16SrBr_2$}, showing that without a water supply the sample dehydrated further at T = 25°C.

The 1st hydration had three overlapping peaks at e = 8.65mbar, e = 14.80mbar and e = 17.66mbar for a total of H_{all} = 913.70Jg^{-1}. The sample absorbed 56.9% of its observed minimum weight in water, until the water supply was cut off, which equals about n = 170.2 {H_2O} per formula unit {5$CaBr_2$ + 16$SrBr_2$}. The reaction turned into a strong endothermic event as soon as the water supply was cut off and the sample emitted excess water. The water content then balanced out at about n = 151.1 {H_2O} per unit {5$CaBr_2$ + 16$SrBr_2$}.

At the start of the 2nd cycle the sample was holding about n = 163.5 {H_2O} per unit {5$CaBr_2$ + 16$SrBr_2$}.

The peak observed during the 1st dehydration shifted to a higher temperature during the 2nd dehydration and was found at T_{p1} = 87.66°C, followed by two more peaks at T_{p2} = 136.85°C and T_{p3} = 189.41°C. After the first peak at T = 98°C the sample was holding about n = 39.5 {H_2O} per unit {5$CaBr_2$ + 16$SrBr_2$}, at T = 149°C after the second peak it had declined to n = 35.0 {H_2O} per unit {5$CaBr_2$ + 16$SrBr_2$} and it sank to n = 12.8 {H_2O} per unit {5$CaBr_2$ + 16$SrBr_2$} after heating to T_{max} = 200°C.

The minimum weight of the sample was observed at the start of the 2nd hydration curve, it equaled a water content of n = 8.7 {H_2O} per unit {5$CaBr_2$ + 16$SrBr_2$}. The curved showed an instantly starting hydration, followed by three overlapping peaks similar to those observed during the 1st hydration, at e = 8.65mbar, e = 14.80mbar and e = 17.66mbar for a total of H_{all} = 1014.74Jg^{-1}. The sample also absorbed about 56.9% of its observed minimum weight in water, which equals about n = 170.2 {H_2O} per unit {5$CaBr_2$ + 16$SrBr_2$}. The reaction turned into a strong endothermic event as soon as the water supply was cut off and the sample emitted excess water.

At the start of the 3rd cycle the sample was holding about n = 163.8 {H_2O} per unit {5$CaBr_2$ + 16$SrBr_2$}.

The 3rd dehydration developed similar to the 2nd dehydration, with three peaks at T_{p1} = 87.87°C, T_{p2} = 142.16°C and T_{p3} = 191.50°C. After the first

peak at T = 98°C the sample was holding about n = 39.5 {H_2O} per unit {$5CaBr_2 + 16SrBr_2$}, at T = 164°C after the second peak it had declined to n = 35.0 {H_2O} per unit {$5CaBr_2 + 16SrBr_2$} and it sank to about n = 12.8 {H_2O} per unit {$5CaBr_2 + 16SrBr_2$} after heating to T_{max} = 200°C.

Sample #2 of the mixture held n = 135.9 {H_2O} per unit {$5CaBr_2 + 16SrBr_2$} at the beginning of the measurement. Without a water supply the sample emitted marginal amounts of water at T = 25°C. With a water flow of e = 18.68mbar, the sample hydrated up to T = 37.50 ° C where it held n = 147.0 {H_2O} per unit {$5CaBr_2 + 16SrBr_2$} which equals 53.3% of the observed minimum sample weight. After drying to T_{max} = 110°C the water content declined to n = 37.1 {H_2O} per unit {$5CaBr_2 + 16SrBr_2$}, the sample rehydrated at T = 60.61°C to n = 52.5 {H_2O} per unit {$5CaBr_2 + 16SrBr_2$} which equals 19.0% of the observed minimum weight.

The sample rapidly absorbed water when the temperature was further reduced to T = 25°C, which indicates that the water supply was not shut off at the end of the measurement as intended.

The sample started with a water content of n = 96.9 {H_2O} per unit {$5CaBr_2 + 16SrBr_2$} into the next dehydration stage and absorbed more water until a temperature of T = 38°C and a water content of n = 113.3 {H_2O} per unit {$5CaBr_2 + 16SrBr_2$} were reached.

Heating the hydrated mixture to T_{max} = 500°C showed two overlapping peaks at T_{p1} = 83.32°C, T_{p2} = 230°C. No melting events were observed. After the first peak at T = 262°C the water content had declined to n = 7.2 {H_2O} per unit {$5CaBr_2 + 16SrBr_2$}. After heating to T_{max} = 500°C, the minimum water content of the sample was observed, while the water content reached a minimum of n = 0.15 {H_2O} per unit {$5CaBr_2 + 16SrBr_2$}.

5.3.12. {2CaBr$_2$·xH$_2$O + SrBr$_2$·6H$_2$O}, {CaBr$_2$·xH$_2$O + SrBr$_2$·6H$_2$O}, {CaBr$_2$·xH$_2$O + 2SrBr$_2$·6H$_2$O}

Since the mixing ratio of the first three calcium-strontium bromide samples was miscalculated, but the materials had good cycle stability and heat storage capacity readings on the TGA/DSC analysis, a second batch with corrected mixing ratios was mixed up for further tests. The mixing ratios were calculated, on the assumption that the calcium bromide as a drying agent continued to hydrate during prolonged storage to {CaBr$_2$·6H$_2$O}. As this was an extra measurement, only one sample of each mixing ratio was analyzed, starting with the T_{max} = 100°C and T_{max} = 200°C measurements with two hydrations in between, followed by the Tmax = 110°C at e = 18.68mbar rehydration-test. A 3rd hydration stage was implemented before the T_{max} = 500°C dehydration recording.

The {2CaBr$_2$·xH$_2$O + SrBr$_2$·6H$_2$O} sample was mixed at a ratio of 7g {CaBr$_2$·6H$_2$O} to 4g {SrBr$_2$·6H$_2$O}.

The sample was holding n = 18.4 {H$_2$O} per unit {2CaBr$_2$ + SrBr$_2$} at the start of the measurement.

The 1st dehydration showed two peaks at T_{p1} = 60.39°C and T_{p2} = 95.55°C. The reaction was already ongoing before the measurement started. At T = 80°C after the first peak the sample still held about n = 4.8 {H$_2$O} per unit {2CaBr$_2$ + SrBr$_2$}. The water content declined further to n = 3.0 {H$_2$O} per unit {2CaBr$_2$ + SrBr$_2$}, after the second peak and heating to T_{max} = 100°C.

The 1st hydration curve showed three overlapping peaks at e = 8.65mbar with an enthalpy of H_1 = 88.49Jg^{-1}, at e = 14.80mbar with an enthalpy of H_2 = 277.01Jg^{-1} and at e = 17.66mbar with H_3 = 282.71Jg^{-1} for a total of H_{all} = 648.21Jg^{-1}. The water content was replenished to n = 18.4 {H$_2$O} per unit {2CaBr$_2$ + SrBr$_2$} which equals about 49.2% of the observed minimum sample weight. As soon as the water supply was cut off, the mixture emitted

excess water. The water content balanced out at n = 16.0 {H_2O} per unit {$2CaBr_2 + SrBr_2$}.

Before the start of the 2nd cycle the sample had taken up water again and was holding about n = 18.0 {H_2O} per unit {$2CaBr_2 + SrBr_2$}.

Three peaks were occurring during the 2nd dehydration at T_{p1} = 81.62°C and a double peak at T_{p2} = 152.28°C and T_{p3} = 187.45°C. The water content was reduced to n = 4.1 {H_2O} per unit {$2CaBr_2 + SrBr_2$} at T = 98°C after the first peak and sank further to n = 2.8 {H_2O} per unit {$2CaBr_2 + SrBr_2$} after the second peak at T = 163°C. After heating to T_{max} = 200°C, the sample reached a water content of n = 0.9 {H_2O} per unit {$2CaBr_2 + SrBr_2$}.

The minimum weight of the sample was observed at the start of the 2nd hydration with a corresponding water content of about n = 0.5 {H_2O} per unit {$2CaBr_2 + SrBr_2$}.

Three overlapping peaks were observed during the 2nd hydration, similar to those recorded during the 1st hydration, at e = 8.65mbar with an enthalpy of $H_1 = 132.85Jg^{-1}$, at e = 14.80mbar with an enthalpy of $H_2 = 290.39Jg^{-1}$ and at e = 17.66mbar with $H_3 = 350.12Jg^{-1}$ for a total of $H_{all} = 773.36Jg^{-1}$. The mixture took up 44.4% of the observed minimum sample weight in water, which equaled n = 16.6 {H_2O} per unit {$2CaBr_2 + SrBr_2$}. The sample emitted excess water after the water supply was shut off, but the water content did not balance out before the next measurement started.

At the start of the 3rd cycle the sample was holding about n = 17.6 {H_2O} per unit {$2CaBr_2 + SrBr_2$}.

The 3rd dehydration showed three similar peaks at T_{p1} = 80.64°C, T_{p2} = 149.49°C and T_{p3} = 187.29°C. The water content was reduced to n = 4.0 {H_2O} per unit {$2CaBr_2 + SrBr_2$} at T = 98°C after the first peak and sank further to n = 2.7 {H_2O} per unit {$2CaBr_2 + SrBr_2$} after the second peak at T = 162°C. Then after heating to T_{max} = 200°C, the sample reached a water content of n = 1.0 {H_2O} per unit {$2CaBr_2 + SrBr_2$}.

No melting events were observed during the three dehydration measurements.

The measurement for the maximum water uptake temperature and the T_{max} = 500°C dehydration measurement did not return valid readings.

The {$CaBr_2 \cdot xH_2O$ + $SrBr_2 \cdot 6H_2O$} sample was mixed at a ratio of 7g {$CaBr_2 \cdot 6H_2O$} to 8g {$SrBr_2 \cdot 6H_2O$}.

The sample was holding n = 15.8 {H_2O} per unit {$CaBr_2$ + $SrBr_2$} at the start of the measurement.

The 1st dehydration showed four peaks at T_{p1} = 26.95°C, T_{p2} = 57.3°C, T_{p3} = 68.73°C and T_{p4} = 96.13°C. The dehydration reaction was already ongoing, when the measurement started. The peaks one to three were overlapping. At T = 80°C after the first three peaks, the sample was still holding a water content of about n = 6.4 {H_2O} per unit {$CaBr_2$ + $SrBr_2$}. The water content declined further to n = 4.9 {H_2O} per unit {$CaBr_2$ + $SrBr_2$} after heating to T_{max} = 100°C.

The 1st hydration had three overlapping peaks at e = 8.65mbar with an enthalpy of H_1 = 71.36Jg^{-1}, at e = 14.80mbar with an enthalpy of H_2 = 189.53Jg^{-1} and at e = 17.66mbar with H_3 = 318.61Jg^{-1} for a total of H_{all} = 579.50Jg^{-1}. The sample absorbed about 67.9% of its observed minimum weight in water, which equals about n = 17.0 {H_2O} per unit {$CaBr_2$ + $SrBr_2$}. The reaction turned into a strong endothermic event as soon as the water supply was cut off and the sample emitted excess water.

At the start of the 2nd cycle the sample was holding n = 17.2 {H_2O} per unit {$CaBr_2$ + $SrBr_2$}.

The 2nd dehydration curve showed three separate peaks at T_{p1} = 78.60°C, T_{p2} = 146.83°C and T_{p3} = 184.36°C. At T = 98°C after the low temperature

peak the sample held a water content of about n = 6.3 {H_2O} per unit {$CaBr_2$ + $SrBr_2$}. The water content declined further to n = 5.2 {H_2O} per unit {$CaBr_2$ + $SrBr_2$} at T = 161°C after the second peak and to n = 3.8 {H_2O} per unit {$CaBr_2$ + $SrBr_2$} after heating to T_{max} = 200°C.

The 2nd hydration showed three similar, overlapping peaks to the 1st hydration at e = 8.65mbar with an enthalpy of H_1 = 107.48Jg^{-1}, at e = 14.80mbar with an enthalpy of H_2 = 252.04Jg^{-1} and at e = 17.66mbar with H_3 = 264.90Jg^{-1} for a total of H_{all} = 624.43Jg^{-1}. The sample absorbed about 68.1% of its observed minimum weight in water, which equals about n = 17.1 {H_2O} per unit {$CaBr_2$ + $SrBr_2$}. The reaction turned into a strong endothermic event as soon as the water supply was cut off and the sample began to emit excess water. The water content recovered before the next measurement.

At the start of the 3rd cycle the sample was holding n = 17.2 {H_2O} per unit {$CaBr_2$ + $SrBr_2$}.

During the 3rd dehydration the first peak observed during the 2nd dehydration became a double peak at T_{p1} = 79.17°C and T_{p2} = 97.91°C followed by two peaks similar to those measured during the 2nd dehydration at T_{p3} = 147.63°C and T_{p4} = 184.09°C. At T = 98°C after the two low-temperature peaks the sample held a water content of about n = 6.4 {H_2O} per unit {$CaBr_2$ + $SrBr_2$}. The water content declined further to n = 5.2 {H_2O} per unit {$CaBr_2$ + $SrBr_2$} at T = 158°C after the second peak and to n = 3.9 {H_2O} per unit {$CaBr_2$ + $SrBr_2$} after heating to T_{max} = 200°C.

The mixture contained n = 4.1 {H_2O} per unit {$CaBr_2$ + $SrBr_2$} at the start of the T_{max} = 110°C measurement at T = 25°C. When heated, the sample took up water at e = 18.68mbar until a temperature of T = 56.19°C and a water content of n = 8.8 {H_2O} per unit {$CaBr_2$ + $SrBr_2$} were reached. This water content was equal to 34.7% of the observed minimum sample mass. After heating the sample to T_{max} = 110°C at e = 18.68mbar, it was still holding

about n = 6.0 {H_2O} per unit {$CaBr_2$ + $SrBr_2$}. The sample rehydrated at T = 60.91°C until a water content of n = 8.9 {H_2O} per unit {$CaBr_2$ + $SrBr_2$} was reached, which equaled 35.2% of the observed minimum sample mass.

The 3rd hydration curve was showing four peaks at e = 8.65mbar with an enthalpy of H_1 = 5.40Jg^{-1} and H_2 = 118.47Jg^{-1} at e = 14.80mbar with an enthalpy of H_3 = 252.80Jg^{-1} and at e = 17.66mbar with H_4 = 241.89Jg^{-1} for a total of H_{all} = 376.67Jg^{-1}, with peaks two to four overlapping with each other. The sample reached a water content of n = 19.1 {H_2O} per unit {$CaBr_2$ + $SrBr_2$}, which equals 76.2% of the observed minimum sample weight.

Without a water source, the sample emitted excess water and started into the T_{max} = 500°C measurement with a water content of n = 15.1 {H_2O} per unit {$CaBr_2$ + $SrBr_2$}.

Three overlapping peaks were observed, when the sample was heated up to T_{max} = 500°C at T_{p1} = 83.71°C, T_{p2} = 132.06°C and T_{p3} = 203.98°C. A melting event was not recorded. At T = 243°C after the peaks, the sample was still holding n = 1.3 {H_2O} per unit {$CaBr_2$ + $SrBr_2$}. The water content declined further to n = 0.1 {H_2O} per unit {$CaBr_2$ + $SrBr_2$} after heating to T_{max} = 500°C, where also the minimum sample weight was observed.

The {$CaBr_2 \cdot xH_2O$ + $2SrBr_2 \cdot 6H_2O$} sample was mixed at a ratio of 7g {$CaBr_2 \cdot 6H_2O$} to 16g {$SrBr_2 \cdot 6H_2O$}.

At the start of the measurement, the sample was holding a water content of about n = 23.1 {H_2O} per unit {$CaBr_2$ + $2SrBr_2$}.

The 1st dehydration curve showed two overlapping peaks at T_{p1} = 62.24°C and T_{p2} = 93.25°C. At T = 78°C the water content had declined to n = 9.1 {H_2O} per unit {$CaBr_2$ + $2SrBr_2$}, it sank further to n = 8.0 {H_2O} per unit {$CaBr_2$ + $2SrBr_2$} after heating to T_{max} = 100°C.

The 1st hydration showed three overlapping peaks at e = 8.65mbar with an enthalpy of H_1 = 62.40Jg^{-1}, at e = 14.80mbar with an enthalpy of H_2 =

190.77Jg^{-1} and at e = 17.66mbar with H_3 = 336.91Jg^{-1} for a total of H_{all} = 590.09Jg^{-1}. The sample absorbed about 60.0% of its observed minimum weight in water, which equaled a water content of about n = 23.1 {H_2O} per unit {$CaBr_2$ + 2$SrBr_2$}. The reaction turned into a strong endothermic event as soon as the water supply was cut off and the sample emitted excess water.

At the start of the 2nd cycle the sample was holding about n = 25.0 {H_2O} per unit {$CaBr_2$ + 2$SrBr_2$}.

During the 2nd dehydration three peaks were observed at T_{p1} = 82.37°C, T_{p2} = 143.1°C and T_{p3} = 187.51°C. The water content declined to n = 9.8 {H_2O} per unit {$CaBr_2$ + 2$SrBr_2$} at T = 98°C after the first peak, then sank to n = 8.5 {H_2O} per unit {$CaBr_2$ + 2$SrBr_2$} at T = 156°C after the second peak and to n = 5.8 {H_2O} per unit {$CaBr_2$ + 2$SrBr_2$} after heating to T_{max} = 200°C.

Three overlapping peaks were observed during the 2nd hydration, similar to those seen during the 1st hydration, at e = 8.65mbar with an enthalpy of H_1 = 90.64Jg^{-1}, at e = 14.80mbar with an enthalpy of H_2 = 247.16Jg^{-1} and at e = 17.66mbar with H_3 = 336.89Jg^{-1} for a total of H_{all} = 674.69Jg^{-1}. The sample absorbed about 61.8% of its observed minimum weight in water, which equaled about n = 23.8 {H_2O} per unit {$CaBr_2$ + 2$SrBr_2$}. The reaction turned into a strong endothermic event as soon as the water supply was cut off and the sample emitted excess water.

At the start of the 3rd cycle the sample was holding about n = 25.5 {H_2O} per unit {$CaBr_2$ + 2$SrBr_2$}.

The first peak observed during the 2nd dehydration, turned into a double peak during the 3rd dehydration at T_{p1} = 83.99°C and T_{p2} = 97.22°C followed by another two peaks similar to those that occurred during the 2nd dehydration at T_{p3} = 143.15°C and T_{p4} = 189.09°C. The water content declined to n = 9.8 {H_2O} per unit {$CaBr_2$ + 2$SrBr_2$} at T = 98°C after the first two peaks, then sank to n = 8.6 {H_2O} per unit {$CaBr_2$ + 2$SrBr_2$} at T = 152°C

after the third peak and to n = 5.9 {H_2O} per unit {$CaBr_2$ + 2$SrBr_2$} after heating to T_{max} = 200°C.

The sample was holding about n = 6.0 {H_2O} per unit {$CaBr_2$ + 2$SrBr_2$} at the start of the T_{max} = 110°C measurement.

It took up water at e = 18.68mbar until a temperature of T = 49.02°C and a water content of n = 11.3 {H_2O} per unit {$CaBr_2$ + 2$SrBr_2$} were reached, which equaled 29.3% of the observed minimum sample mass. After heating to T_{max} = 85.15°C at e = 18.68mbar the water content had declined to n = 8.3 {H_2O} per unit {$CaBr_2$ + 2$SrBr_2$} but recovered to n = 8.6 {H_2O} per unit {$CaBr_2$ + 2$SrBr_2$} while heating to T_{max} = 110°C. The sample rehydrated to n = 11.1 {H_2O} per unit {$CaBr_2$ + 2$SrBr_2$} at T = 60.83°C, which equaled 28.7% of the observed minimum sample mass.

The 3rd hydration curve was showing three overlapping peaks at e = 8.65mbar with an enthalpy of H_1 = 129.97Jg^{-1}, at e = 14.80mbar with an enthalpy of H_2 = 295.68Jg^{-1} and at e = 17.66mbar with H_3 = 215.56Jg^{-1} for a total of H_{all} = 641.21Jg^{-1}. The sample absorbed about 70.6% of its own weight in water, which equals about n = 27.2 {H_2O} per unit {$CaBr_2$ + 2$SrBr_2$}. The reaction turned into a strong endothermic event as soon as the water supply was cut off and the sample emitted excess water.

When heated to T_{max} = 500°C four peaks occurred at T_{p1} = 91.80°C, T_{p2} = 130.27°C, T_{p3} = °C and T_{p4} = 206.83°C. No melting event was observed. At T = 232°C after the peaks, the water content had declined to n = 2.0 {H_2O} per unit {$CaBr_2$ + 2$SrBr_2$}. The water content declined further and at T_{max} = 500°C where the sample's minimum weight was observed, the mixture was considered to be anhydrous.

A compilation of the results of the bromides' TGA/DSC evaluation can be found in Table 9.

Table 9 Energy storage density and water uptake of the tested bromide-mixture samples and their starting materials for dehydration temperatures T_{max} =100°C, T_{max} = 200°C and T_{max} = 500°C.

Materials	Energy storage density [Jg^{-1}] T_{max} = 100°C	Water uptake wgt [%] T_{max} = 100°C	Energy storage density [Jg^{-1}] T_{max} = 200°C	Water uptake wgt [%] T_{max} = 200°C	Water loss wgt [%] T_{max} = 500°C
{$SrBr_2 \cdot 6H_2O$}	798.14	45.34	834.17	45.34	43.21
{NaBr}	214.25	6.11	192.11	7.22	0.50
{KBr}	162.22	3.57	161.36	3.47	0.48
{LiBr}	900.69	106.19	1251.26	89.52	85.87
{$MgBr_2 \cdot 6H_2O$}	422.13	90.83	788.14	67.76	---
{$CaBr_2 \cdot xH_2O$}	946.87	75.18	1078.53	63.29	98.90
{2NaBr + $SrBr_2$}	540.29	26.56	470.70	25.48	21.87
{NaBr + $SrBr_2$}	434.33	20.84	450.67	20.26	20.67
{NaBr + 2$SrBr_2$}	675.23	36.63	650.77	36.93	33.64
{2KBr + $SrBr_2$}	599.68	31.34	599.94	31.21	29.93
{KBr + $SrBr_2$}	605.32	30.83	610.19	30.96	34.38
{KBr + 2$SrBr_2$}	597.34	31.15	614.43	31.15	29.13
{2LiBr + $SrBr_2$}	1233.65	73.52	1079.06	74.13	62.37
{LiBr + $SrBr_2$}	1008.84	69.31	1197.00	69.46	57.10
{LiBr + 2$SrBr_2$}	703.46	66.57	771.64	66.27	54.02
{2$MgBr_2$ + $SrBr_2$}	655.14	142.86	703.75	100.19	155.11
{$MgBr_2$ + $SrBr_2$}	473.68	105.45	707.67	77.34	176.71
{$MgBr_2$ + 2$SrBr_2$}	687.90	76.99	651.74	69.92	58.84
{2$CaBr_2$ + $SrBr_2$}	648.21	49.21	773.36	44.37	---
{$CaBr_2$ + $SrBr_2$}	579.50	67.90	624.43	68.05	35.18
{$CaBr_2$ + 2$SrBr_2$}	590.09	59.97	674.69	61.81	29.29
{5$CaBr_2$ + 4$SrBr_2$}	755.89	66.13	912.85	61.77	62.37
{5$CaBr_2$ + 8$SrBr_2$}	909.99	65.33	---	~50.45	54.56
{5$CaBr_2$ + 16$SrBr_2$}	913.70	56.87	1014.74	56.87	53.31

5.4. Other salt mixtures

5.4.1. Mixtures of three to four basic materials

Since depending on the exact mixing ratio, the melting points of mixtures are always lower than those of at least one or more of their educts, adding more than two materials to a synthesis was not expected to improve the results of the cycle

stability analysis. But {KCl} has a melting point of T = 773°C (Merck & Co., Inc., 2006), adding it to a salt-mixture with an expected melting point of T_{melt} < 100°C, at a high enough mixing ratio, might raise the melting temperature by a few degrees and improve their cycle stability.

The mixed salts with multiple educts do not occur naturally in this form and the XRPD-results for the salt mixtures were overall inconclusive. For that reason, it is unknown whether or which compounds formed or which crystal structures were to be expected.

The brine solutions of the starting materials were combined in the mixing ratios in Table 10. The {$MgCl_2$+$CaCl_2$+$ZnCl_2$} sample's mixing ratio encourages the formation of a crystal lattice similar to Tachyhydrite ($Mg_2CaCl_6 \cdot 12H_2O$), while the {KCl} containing mixtures were aimed to develop a structure comparable to that of Carnallite ($KMgCl_3 \cdot 6H_2O$).

The {KCl} was then added to a {$MgCl_2$+$CaCl_2$+$ZnCl_2$} mixture to compare the material properties.

Mixture	{$MgCl_2$} [ml]	{$CaCl_2$} [ml]	{$ZnCl_2$} [ml]	{KCl} [ml]
{$MgCl_2$ + $CaCl_2$ + $ZnCl_2$}	11	13	16	---
{$MgCl_2$ + $CaCl_2$ + 2KCl}	5	6	---	8
{$MgCl_2$ + $ZnCl_2$ + 2KCl}	7	---	10	11
{$CaCl_2$ + $ZnCl_2$ + 2KCl}	---	9	11	12
{$MgCl_2$ + $CaCl_2$ +$ZnCl_2$ +3KCl}	4	5	6	10

Table 10 The mixtures with more than two different starting materials with corresponding mixing ratios of the salt solutions (1 [g ml^{-1}]).

a) {$MgCl_2$ + $CaCl_2$ + $ZnCl_2$}

The water content at the start of the measurement was gauged as n = 21.0 {H_2O} water per unit {$MgCl_2$+$CaCl_2$+$ZnCl_2$}.

Two overlapping peaks were observed during the 1st dehydration, the main peak at T_{p1} = 63.19°C and a smaller one T_{p2} = 68.42°C. The second peak shows signs of being a partial melting event. The water content sank to n = 12.0 {H_2O} per unit {$MgCl_2$+$CaCl_2$+$ZnCl_2$} after the two peaks and heating to T_{max} = 100°C.

The 1st hydration started with a small endothermic event, followed by three overlapping exothermic peaks at e = 8.65mbar with an enthalpy of H_1 = 44.24Jg^{-1}, e = 14.80mbar with an enthalpy of H_2 = 190.14Jg^{-1} and e = 17.66mbar H_3 = 237.32Jg^{-1} for a total of H_{all} = 471,70Jg^{-1}. The water content reached a maximum of n = 19.9 {H_2O} per unit {$MgCl_2$+$CaCl_2$+$ZnCl_2$} during the hydration, which equals about 55.7% of the observed minimum sample weight, but the sample emitted excess water as soon as the water supply was cut off in an endothermic event. The water content didn't stabilize before the next measurement cycle began.

At the start of the 2nd cycle, the sample was holding about n = 18.0 {H_2O} per unit {$MgCl_2$+$CaCl_2$+$ZnCl_2$}.

The 2nd dehydration showed seven peaks, with a single low temperature peak at T_{p1} = 88.62°C, followed by a cluster of six peaks at T_{p2} = 167.15°C, T_{p3} = 178.96°C, T_{p4} = 182.14°C, T_{p5} = 184.07°C, T_{p6} = 186.02°C and T_{p7} = 190.42°C. Aside of T_{p2}, all the peaks in the cluster showed characteristics of being either partial melting or {HCl}-emission events. The change in water content for this sample was calculated, ignoring possible {HCl}-emissions. The water content declined to n = 11.7 {H_2O} per unit {$MgCl_2$+$CaCl_2$+$ZnCl_2$} after the first peak at T = 98°C and sank further to n = 6.6 {H_2O} per unit {$MgCl_2$+$CaCl_2$+$ZnCl_2$} after the peak cluster and heating to T_{max} = 200°C.

The 2nd hydration showed a similar endothermic event at the beginning, also followed by three overlapping exothermic peaks at e = 8.65mbar with an enthalpy of H_1 = 65.42Jg^{-1}, e = 14.80mbar with an enthalpy of H_2 = 279.34Jg^{-1} and e = 17.66mbar H_3 = 324.05Jg^{-1} for a total of H_{all} = 668.81Jg^{-1}. The water content reached a maximum of n = 17.2 {H_2O} per unit {$MgCl_2$+$CaCl_2$+$ZnCl_2$} during the hydration, which equals 44.59% of the observed minimum sample

weight, but the mixture emitted excess water as soon as the water supply was cut off. The water content did not stabilize out before the next measurement cycle began.

At the start of the 3rd cycle, the sample was holding about n = 16.4 {H_2O} per unit {$MgCl_2$+$CaCl_2$+$ZnCl_2$}.

Six peaks were identified during the 3rd dehydration, with a low temperature peak at T_{p1} = 87.77°C, followed again by a peak cluster of at least five peaks at T_{p2} = 174.58°C, T_{p3} = 181.11°C, T_{p4} = 184.85°C, T_{p5} = 192.82°C and T_{p6} = 194.39°C. Contrary to the peaks observed during the 2nd dehydration, the melting or {HCl}-emission events were not as distinct. At T = 99°C after the first peak, the water content sank to n = 11.6 {H_2O} per unit {$MgCl_2$+$CaCl_2$+$ZnCl_2$}, after heating to T_{max} = 200°C the remaining water content was gauged as n = 6.0 {H_2O} per unit {$MgCl_2$+$CaCl_2$+$ZnCl_2$}.

b) {$MgCl_2$ + $CaCl_2$ + 2KCl}

The water content at the start of the measurement was gauged as n = 16.2 {H_2O} per unit {$MgCl_2$ + $CaCl_2$ + 2KCl}. The sample was already emitting water at T = 25°C before the measurement began.

Two peaks were observed during the 1st dehydration at T_{p1} = 49.61°C and T_{p2} = 96.24°C. After the first peak at T = 59°C the water content had declined to n = 9.9 {H_2O} per unit {$MgCl_2$ + $CaCl_2$ + 2KCl}, after the second peak and heating to T_{max} = 100°C the water content sank further to n = 7.0 {H_2O} per unit {$MgCl_2$ + $CaCl_2$ + 2KCl}.

The 1st hydration began with a weak endothermic event, followed by three exothermic peaks at e = 8.65mbar with an enthalpy of H_1 = 54.20Jg^{-1}, e = 14.80mbar with an enthalpy of H_2 = 245.33Jg^{-1} and e = 17.66mbar H_3 = 226.48Jg^{-1} for a total of H_{all} = 526.02Jg^{-1}. The water content reached a maximum of n = 14.2 {H_2O} per unit {$MgCl_2$ + $CaCl_2$ + 2KCl} during the hydration, which equals about 64.7% of the observed minimum sample weight,

but the mixture emitted excess water as soon as the water supply was cut off in an endothermic event. The water content did not stabilize before the next cycle began.

At the start of the 2nd cycle, the sample was holding about n = 12.0 {H_2O} per unit {$MgCl_2 + CaCl_2 + 2KCl$}.

The 2nd dehydration showed seven peaks, two low temperature peaks at T_{p1} = 60.95°C and T_{p2} = 91.12°C, followed by a cluster of five overlapping peaks at T_{p3} = 120.92°C, T_{p4} = 135.39°C, T_{p5} = 149.68°C, T_{p6} = 166.48°C and T_{p7} = 189.33°C. Of the peak cluster at least peak 6 and 7 showed indicators for partial melting or {HCl}-emission events. The change in water content for this sample was calculated, ignoring possible {HCl}-emissions. The water content declined to n = 10.1 {H_2O} per unit {$MgCl_2 + CaCl_2 + 2KCl$} after the first peak at T = 73°C, sank further to n = 9.6 {H_2O} per unit {$MgCl_2 + CaCl_2 + 2KCl$} at T = 99°C after the second peak and then to n = 1.0 {H_2O} per unit {$MgCl_2 + CaCl_2 + 2KCl$} after the peak cluster and heating to T_{max} = 200°C.

The 2nd hydration like the 1st began with a weak endothermic event, followed by three overlapping peaks, observed at e = 8.65mbar with an enthalpy of H_1 = 49.54Jg^{-1}, e = 14.80mbar with an enthalpy of H_2 = 362.14Jg^{-1} and e = 17.66mbar H_3 = 423.99Jg^{-1} for a total of H_{all} = 835.66Jg^{-1}. The water content reached a maximum of n = 10.1 {H_2O} per unit {$MgCl_2 + CaCl_2 + 2KCl$} during the hydration, which equals 44.58% of the observed minimum sample weight. The sample emitted a small amount of excess water as soon as the water supply was cut off, which caused another endothermic peak event, likely by a phase change to a higher crystal order or a re-solidification. The water content did not balance out before the next measurement cycle began.

At the start of the 3rd cycle, the sample was holding about n = 12.0 {H_2O} per unit {$MgCl_2 + CaCl_2 + 2KCl$}.

Eight peaks were observed during the 3rd dehydration, two overlapping low temperature peaks at T_{p1} = 34.38°C and T_{p2} = 93.86°C, followed by a cluster of six peaks at T_{p3} = 120.49°C, T_{p4} = 135.40°C, T_{p5} = 140.51°C, T_{p6} = 149.49°C,

T_{p7} = 164.53°C and T_{p8} = 191.20°C. Aside from the peaks 2 and 3 all show characteristics of partial melting or {HCl}-emission events. At T = 73°C after the first peak the water content had declined to n = 10.1 {H_2O} per unit {$MgCl_2$ + $CaCl_2$ + 2KCl}, and sank further to n = 9.6 {H_2O} per unit {$MgCl_2$ + $CaCl_2$ + 2KCl} after the second peak at T = 99°C. The remaining water content was gauged as n = 0.9 {H_2O} per unit {$MgCl_2$ + $CaCl_2$ + 2KCl} after the peak cluster and heating to T_{max} = 200°C.

c) {$MgCl_2$ + $ZnCl_2$ + 2KCl}

The water content at the start of the measurement was gauged as n = 13.3 {H_2O} water per unit {$MgCl_2$ + $ZnCl_2$ + 2KCl}. The sample already emitted water at T = 25°C before the dehydration stage began.

A single peak was observed during the 1st dehydration at T_{p1} = 94.73°C. The water content had declined to n = 11.7 {H_2O} water per unit {$MgCl_2$ + $ZnCl_2$ + 2KCl} at T = 72°C before the peak, after the peak and heating to T_{max} = 100°C it sank further to n = 9.4 {H_2O} water per unit {$MgCl_2$ + $ZnCl_2$ + 2KCl}.

The 1st hydration started with a weak endothermic event, followed by three peaks at e = 8.65mbar with an enthalpy of H_1 = 13.05Jg^{-1}, e = 14.80mbar with an enthalpy of H_2 = 148.64Jg^{-1} and e = 17.66mbar H_3 =6.15Jg^{-1} for a total of H_{all} = 167.83Jg^{-1}. Only the second and third peak were overlapping. The water content reached a maximum of n = 13.6 {H_2O} per unit {$MgCl_2$ + $ZnCl_2$ + 2KCl} during the hydration, which equals about 30.5% of the observed minimum sample weight, but the mixture emitted excess water as soon as the water supply was cut off in an endothermic event. The water content stabilized at about n = 12.0 {H_2O} per unit {$MgCl_2$ + $ZnCl_2$ + 2KCl}.

At the start of the 2nd cycle, the sample was holding about n = 12.2 {H_2O} per unit {$MgCl_2$ + $ZnCl_2$ + 2KCl}.

The 2nd dehydration showed five peaks, a low temperature peak at T_{p1} = 95.82°C, followed by a cluster of four peaks at T_{p2} = 112.22°C, T_{p3} = 135.22°C,

T_{p4} = 162.33°C and T_{p5} = 195.50°C, with the third peak indicating a partial melting or {HCl}-emission event. The change in water content for this sample was calculated, ignoring possible {HCl}-emissions. The water content declined to n = 9.9 {H_2O} per unit {$MgCl_2$ + $ZnCl_2$ + 2KCl} at T = 99°C after the low temperature peak, it sank further to n = 5.9 {H_2O} per unit {$MgCl_2$ + $ZnCl_2$ + 2KCl} after the peak cluster and heating to T_{max} = 200°C.

No endothermic event occurred at the start of the 2nd hydration, three exothermic, overlapping peaks were observed at e = 8.65mbar with an enthalpy of H_1 = 97.38Jg^{-1}, e = 14.80mbar with an enthalpy of H_2 = 162.23Jg^{-1} with a weak peak at e = 17.66mbar H_3 = 9.88Jg^{-1} for a total of H_{all} = 269.48Jg^{-1}. The water content reached a maximum of n = 12.3 {H_2O} per unit {$MgCl_2$ + $ZnCl_2$ + 2KCl} during the hydration, which equals 25.6% of the observed minimum sample weight. An exothermic event occurred when the water supply was cut off, indicating a sudden phase change, then the reaction turned endothermic and the sample emitted excess. The water content stabilized at about n = 10.7 {H_2O} per unit {$MgCl_2$ + $ZnCl_2$ + 2KCl}.

At the start of the 3rd cycle, the sample was holding about n = 10.9 {H_2O} per unit {$MgCl_2$ + $ZnCl_2$ + 2KCl}.

Six peaks were observed during the 3rd dehydration, two low temperature peaks at T_{p1} = 49.82°C and T_{p2} = 97.61°C, followed by four overlapping peaks at T_{p3} = 120.6°C, T_{p4} = 127.05°C, T_{p5} = 162.25°C and T_{p6} = 193.57°C. Peak four indicated a melting or {HCl}-emission event. The water content was reduced to n = 10.6 {H_2O} per unit {$MgCl_2$ + $ZnCl_2$ + 2KCl} after the first peak at T = 62°C, at T = 99°C it had declined to n = 8.0 {H_2O} per unit {$MgCl_2$ + $ZnCl_2$ + 2KCl} and sank further to n = 5.8 {H_2O} per unit {$MgCl_2$ + $ZnCl_2$ + 2KCl} after heating to T = 180°C after the fifth peak. The remaining water content after heating to T_{max} = 200°C was gauged as n = 5.5 {H_2O} per unit {$MgCl_2$ + $ZnCl_2$ + 2KCl}.

d) {$CaCl_2 + ZnCl_2 + 2KCl$}

The water content at the start of the measurement was gauged as n = 14.0 {H_2O} per unit {$CaCl_2 + ZnCl_2 + 2KCl$}.

A single peak was observed during the 1st dehydration at T_{p1} = 59.33°C. The water content sank to n = 8.4 {H_2O} per unit {$CaCl_2 + ZnCl_2 + 2KCl$} at T = 63°C directly after the peak and declined further to n = 7.8 {H_2O} per unit {$CaCl_2 + ZnCl_2 + 2KCl$} after heating to T_{max} = 100°C.

The 1st hydration began with a small endothermic event, followed by three exothermic peaks at e = 8.65mbar with an enthalpy of H_1 = 34.72Jg^{-1}, e = 14.80mbar with an enthalpy of H_2 = 155.17Jg^{-1} and e = 17.66mbar H_3 = 186.32Jg^{-1} for a total of H_{all} = 376.21Jg^{-1}. The water content reached a maximum of n = 13.4 {H_2O} per unit {$CaCl_2 + ZnCl_2 + 2KCl$} during the hydration, which equals 40.4% of the observed minimum sample weight. Another short exothermic event occurred, when the water supply was cut off, indicating a sudden change of phase. The reaction turned endothermic afterwards as the sample emitted excess water. The water content did not stabilize before the next measurement cycle began.

At the start of the 2nd cycle, the sample was holding about n = 11.3 {H_2O} per unit {$CaCl_2 + ZnCl_2 + 2KCl$}.

The 2nd dehydration showed five peaks, a low temperature peak at T_{p1} = 77.12°C, followed by four overlapping peaks at T_{p2} = 148.14°C, T_{p3} = 165.92°C, T_{p4} = 174.93°C and T_{p5} = 193.48°C. The second peak indicated a melting event. The water content sank to n = 7.9 {H_2O} per unit {$CaCl_2 + ZnCl_2 + 2KCl$} at T = 93°C directly after the first peak and declined further to a minimum of about n = 3.25 {H_2O} per unit {$CaCl_2 + ZnCl_2 + 2KCl$} after the group of four peaks and heating to T_{max} = 200°C, where also the minimum sample weight was observed.

During the 2nd hydration three overlapping peaks were observed at e = 8.65mbar with an enthalpy of H_1 = 58.59Jg^{-1}, e = 14.80mbar with an enthalpy of H_2 = 261.71Jg^{-1} and e = 17.66mbar H_3 = 277.21Jg^{-1} for a total of H_{all} =

597.51Jg^{-1}. The water content reached a maximum of n = 11.3 {H_2O} per unit {$CaCl_2 + ZnCl_2 + 2KCl$} during the hydration which equals 32.0% of the observed minimum sample weight. Another exothermic event occurred when the water supply was cut off, likely a sudden phase change though no corresponding endothermic event was observed, before the sample emitted excess water in an endothermic reaction. The water content did not stabilize before the next cycle began.

At the start of the 3rd cycle, the sample was holding about n = 10.0 {H_2O} per unit {$CaCl_2 + ZnCl_2 + 2KCl$}.

Five peaks were observed during the 3rd dehydration, again a low temperature peak at T_{p1} = 77.63°C, followed by a group of four peaks at T_{p2} = 155.13°C, T_{p3} = 158.27°C, T_{p4} = 180.92°C and T_{p5} = 193.07°C. The peaks two, three and four indicated partial melting events. The water content sank to n = 6.5 {H_2O} per unit {$CaCl_2 + ZnCl_2 + 2KCl$} at T = 96°C. After heating to T_{max} = 200°C, where again the minimum sample weight was reached, the remaining water content had declined to n = 3.25 {H_2O} per unit {$CaCl_2 + ZnCl_2 + 2KCl$}.

e) {$MgCl_2 + CaCl_2 + ZnCl_2 + 3KCl$}

The water content at the start of the measurement was gauged as n = 28.4 {H_2O} per unit {$MgCl_2 + CaCl_2 + ZnCl_2 + 3KCl$}. The sample was likely overhydrated, as it already emitted water at T = 25°C.

A single peak was observed during the 1st dehydration at T_{p1} = 60.12 °C. The water content declined to n = 16.5 {H_2O} per unit {$MgCl_2 + CaCl_2 + ZnCl_2 + 3KCl$} at T = 72°C directly after the peak, after heating to T_{max} = 100°C it sank further to n = 15.7 {H_2O} per unit {$MgCl_2 + CaCl_2 + ZnCl_2 + 3KCl$}.

The 1st hydration started with a weak endothermic event, followed by three exothermic peaks at e = 8.65mbar with an enthalpy of H_1 = 34.63Jg^{-1}, e = 14.80mbar with an enthalpy of H_2 = 144.27Jg^{-1} and e = 17.66mbar H_3 = 162.73Jg^{-1} for a total of H_{all} = 341.61Jg^{-1}. The water content reached a

maximum of n = 24.3 {H_2O} per unit {$MgCl_2$ + $CaCl_2$ + $ZnCl_2$ + 3KCl} during the hydration, which equals about 56.8% of the observed minimum sample weight. When the water supply was cut off, an exothermic event occurred, indicating a phase change, then the sample emitted excess water in an endothermic event. The water content did not stabilize before the next measurement cycle began.

At the start of the 2nd cycle, the sample was holding about n = 21.6 {H_2O} per unit {$MgCl_2$ + $CaCl_2$ + $ZnCl_2$ + 3KCl}.

The 2nd dehydration showed two peaks at T_{p1} = 84.56°C and T_{p2} = 154.12°C. The second peak shows the characteristics of either a melting or a {HCl}-emission event. Since there was no corresponding exothermic peak to signal a solidification during the cooldown stage, a {HCl}-emission is more likely. However, an endothermic event without corresponding weight change was observed during the cooldown stage. The change in water content for this sample was calculated, ignoring possible {HCl}-emissions. The water content declined to about n = 16.0 {H_2O} per unit {$MgCl_2$ + $CaCl_2$ + $ZnCl_2$ + 3KCl} after the first peak at T = 97°C and sank further to about n = 4.7 {H_2O} per unit {$MgCl_2$ + $CaCl_2$ + $ZnCl_2$ + 3KCl} after the second peak and heating to T_{max} = 200°C.

During the 2nd hydration three overlapping exothermic peaks were observed at e = 8.65mbar with an enthalpy of H_1 = 72.11Jg^{-1}, e = 14.80mbar with an enthalpy of H_2 = 263.73Jg^{-1} and e = 17.66mbar H_3 = 285.79Jg^{-1} for a total of H_{all} = 621.64Jg^{-1}. The water content reached a maximum of n = 18.1 {H_2O} per unit {$MgCl_2$ + $CaCl_2$ + $ZnCl_2$ + 3KCl} during the hydration, which equals 39.4% of the observed minimum sample weight. A small exothermic event occurred, when the water supply was cut off and the sample emitted a small amount of excess water. The water content did not stabilize before the next measurement cycle began.

At the start of the 3rd cycle, the sample was holding about n = 17.6 {H_2O} per unit {$MgCl_2$ + $CaCl_2$ + $ZnCl_2$ + 3KCl}.

Six peaks were observed during the 3rd dehydration, a low temperature peak at T_{p1} = 82.44°C, followed by a group of five overlapping peaks at T_{p2} = 117.59°C,

T_{p3} = 151.14°C, T_{p4} = 172.00°C, T_{p5} = 177.07°C and T_{p6} = 180.62°C. Peaks 4 to 6 indicated either {HCl}-emission or partial melting events taking place. An endothermic event without corresponding weight change occurred during the cooldown stage. After the first peak at T = 99°C the water content had declined to n = 11.9 {H_2O} per unit {$MgCl_2$ + $CaCl_2$ + $ZnCl_2$ + 3KCl}. After the group of five peaks and heating to T_{max} = 200°C, the remaining water content was gauged as n = 4.1 {H_2O} per unit {$MgCl_2$ + $CaCl_2$ + $ZnCl_2$ + 3KCl}.

A compilation of the TGA/DSC evaluation results of the chloride multi-mixtures can be found in Table 11.

Table 11 Energy storage density and water uptake for chloride-mixtures with more than two educts. Energy storage density was calculated by the sample's minimum weight during the hydration stage. The water uptake was calculated by the total observed minimum sample weight.

Materials and mixing ratios	Energy storage density [Jg^{-1}] T_{max} = 100°C	Water uptake wgt [%] T_{max} = 100°C	Energy storage density Jg^{-1}] T_{max} = 200°C	Water uptake wgt [%] T_{max} = 200°C
{$MgCl_2$ + $CaCl_2$ + $ZnCl_2$}	471.70	55.72	668.81	44.59
{$MgCl_2$ + $CaCl_2$ + 2KCl}	526.02	64.69	835.66	44.58
{$MgCl_2$ + $ZnCl_2$ + 2KCl}	167.83	30.53	269.48	25.59
{$CaCl_2$ + $ZnCl_2$ + 2KCl}	376.21	40.35	597.51	31.98
{$MgCl_2$ + $CaCl_2$ + $ZnCl_2$ + 3KCl}	341.63	56.82	621.64	39.35

5.4.2. Sulfate, chloride and bromide inter-mixtures

Contrary to the procedures described in the material synthesis section above, most samples listed in this section were prepared by dry mixing within a mortar only, as the forming of compounds was not necessarily expected by the intermixing of salts with different anions. Instead the goal for this test series was to find out whether two different heat storage materials working in tandem would keep the unwanted properties of the untreated salts from arising.

Despite heating the materials to T_{max} = 500°C the anhydrate state was not realized in most cases. Therefore, the water contents listed for the different stages of hydration were calculated based on estimates of residue water in the driest observed states of the individual samples.

The exceptions concerning the synthesis procedure are the {$ZnSO_4$ + 5$ZnCl_2$} and the {$MgSO_4$ + KCl} mixtures which were based on the naturally occurring minerals Guarinoite ($(Zn,Co,Ni)_6(SO_4)(OH,Cl)_{10}\cdot 5H_2O$) (Sarp, 1993), (Mandarino, 1997), (Anthony, Bideaux, Bladh, & Nichols, 2003) and Kainite ($MgSO_4\cdot KCl\cdot 3H_2O$) (Robinson, Fang, & Ohya, 1972), (Anthony, Bideaux, Bladh, & Nichols, 2003). They were crystallized from a brine solution at room temperature within a desiccator with silica gel {SiO_2} as a drying agent (Podder, Gao, Evitts, Besant, & Matthews, 2014).

a) {$ZnSO_4$ + 36$ZnCl_2$}

Based on the hexagonal chloride sulfate mineral Guarinoite ($(Zn,Co,Ni)_6(SO_4)(OH,Cl)_{10}\cdot 5H_2O$) (Sarp, 1993), (Anthony, Bideaux, Bladh, & Nichols, 2003), a simplified mixed salt {$ZnSO_4$ + 5$ZnCl_2$} was to be prepared with a mixing ratio of 9ml {$ZnCl_2$}-solution to 40ml {$ZnSO_4$}-solution. However due to using {$ZnSO_4\cdot 7H_2O$} rather than the anhydrate sulfate in the synthesis process, the created mixture deviated from the expected composition. The sample showed a behavior close to untreated {$ZnCl_2$} during measurement and the water content was calculated as such.

The sample held about n = 8.3 {H_2O} per unit {$ZnCl_2$} at the start of the measurement.

The 1st dehydration curve showed a single peak at T_{p1} = 63.98°C and the sample was still holding n = 4.0 {H_2O} per unit {$ZnCl_2$} at the end of the measurement after heating it to T_{max} = 100°C.

During the 1st hydration, three overlapping peaks were observed at e = 8.65mbar with an enthalpy of H_1 = 150.15Jg^{-1}, e = 14.80mbar with an enthalpy of H_2 = 394.73Jg^{-1}, and e = 17.66mbar for H_3 = 311.72Jg^{-1}, for a total of H_{all} = 856.60Jg^{-1}. The sample absorbed 43.3% of its observed

minimum weight in water until it reached a water content of n = 8.1 {H_2O} per unit {$ZnCl_2$} and was slightly overhydrated. It emitted Δn = 1.1 {H_2O} per unit {$ZnCl_2$} once the water supply was cut off before the next cycle started.

The water content of the 2nd cycle started at n = 7.0 {H_2O} per unit {$ZnCl_2$}.

During the 2nd dehydration the low temperature peak shifted to T_{p1} = 90.4°C. Two additional, smaller peaks were observed at T_{p2} = 134.77°C and T_{p3} = 193.17°C. After the first peak at a temperature of T = 105°C the sample again held about n = 4.0 {H_2O} per unit {$ZnCl_2$}. After heating to T_{max} = 200°C the sample had its lowest water content of n = 3.33 H_2O per unit {$ZnCl_2$}, which also marked where the lowest sample weight was observed.

The 2nd hydration curve showed three similar, overlapping peaks at e = 8.65mbar with an enthalpy of H_1 = 173.19Jg^{-1}, e = 14.80mbar with an enthalpy of H_2 = 448.42Jg^{-1}, and e = 17.66mbar for an enthalpy of H_3 = 362.18Jg^{-1}, and a total of H_{all} = 983.79Jg^{-1}. The sample absorbed 41.1% of its observed minimum weight in water which equals a water content of n = 7.8 {H_2O} per unit {$ZnCl_2$} and was slightly overhydrated. It emitted Δn = 0.9 {H_2O} per unit {$ZnCl_2$} when the water supply was cut off, before the next cycle started.

The water content of the 3rd cycle started at n = 7.0 {H_2O} per unit {$ZnCl_2$}.

Three similar peaks, as seen during the 2nd dehydration, were observed again during the 3rd dehydration at T_{p1} = 90.4°C, T_{p2} = 140.16°C and T_{p3} = 194.9°C respectively. After heating to T_{max} = 200°C the sample still held about n = 3.4 {H_2O} per unit {$ZnCl_2$}.

b) {3MgSO₄ + 16KCl}

The mixed salt synthesized from {KCl} and {$MgSO_4$} was based on the monoclinic mineral Kainite ($MgSO_4 \cdot KCl \cdot 3H_2O$) (Robinson, Fang, & Ohya, The crystal structure of kainite, 1972), (Anthony, Bideaux, Bladh, & Nichols, 2003).

The mixing ratio was calculated as 13ml {KCl} solution to 21ml {$MgSO_4$} solution. Due to using {$MgSO_4 \cdot 7H_2O$} instead of the anhydrate sulfate, the actual composition of the sample was {3MgSO4 + 16KCl} rather than that of the wanted Kainite.

The sample was holding about n = 27.0 {H_2O} per unit {$3MgSO_4$ + 16KCl} at the start of the measurement.

Three overlapping peaks were observed during the 1st dehydration at T_{p1} = 57.06°C, T_{p2} = 90.01°C and T_{p3} = 83.87°C. The third peak occurred, while the sample was already at the cooldown stage, and no corresponding weight change was measured. After the third peak of the T_{max} = 100°C dehydration the sample was still holding about n = 8.2 {H_2O} per unit {$3MgSO_4$ + 16KCl}.

The 1st hydration curve showed four peaks at e = 8.65mbar with an enthalpy of H_1 = 92.52Jg^{-1}, e = 14.80mbar with an enthalpy of H_2 = 72.22Jg^{-1}, e = 17.66mbar H_3 = 68.91Jg^{-1}, the fourth peak was observed, when the water supply had already been cut off. A corresponding weight change to the irregular peak was observed and the measured enthalpy was H_4 = 85,58Jg^{-1}. Not counting the fourth peak as it was likely caused by a technical problem in the water supply of the TGA/DSC apparatus, the total enthalpy was H_{all} = 233.64Jg^{-1}. A maximum water content of about n = 21.1 {H_2O} per unit {$3MgSO_4$ + 16KCl} was reached, which equals 23.4% of the observed minimum sample weight.

The mixture started into the 2nd cycle with a water content of n = 20.7 {H_2O} per unit {$3MgSO_4$ + 16KCl} at T = 28°C.

The 2nd dehydration curve showed six peaks at T_{p1} = 70.04°C, T_{p2} = 96.24°C, T_{p3} = 150.11°C, T_{p4} = 180.71°C, T_{p5} = 196.23°C and T_{p6} = 174.09°C, where the first four peaks were overlapping with each other. The fifth and sixth peak were overlapping each other as well, but the sixth peak was observed during the sample's cooldown stage. At T = 104°C the sample held still n = 8.3 {H_2O} per unit {$3MgSO_4$ + 16KCl}. The water content then stabilized at

n = 1.2 {H_2O} per unit {$3MgSO_4$ + 16KCl} at T = 196°C, where the minimum sample weight was observed.

The 2nd hydration curve showed four peaks as well at e = 8.65mbar with an enthalpy of H_1 = 151.03Jg^{-1}, e = 14.80mbar with an enthalpy of H_2 = 197.42Jg^{-1}, e = 17.66mbar for H_3 = 156.56Jg^{-1} and with the fourth peak again being observed after the water supply was cut off with an enthalpy of H_4 = 79.11Jg^{-1}. The first three peaks had a total enthalpy of H_{all} = 505.01Jg^{-1}. And a maximum water content of about n = 21.1 {H_2O} per unit {$3MgSO_4$ + 16KCl} was reached, which again equaled 23.4% of the observed minimum sample weight.

Like before the mixture started the 3rd cycle also with a water content of n = 20.7 {H_2O} per unit {$3MgSO_4$ + 16KCl} at T = 28°C.

The 3rd dehydration showed six peaks, however the reaction started at T_{p1} = 56.23°C. The other peaks showed at T_{p2} = 70.85°C, T_{p3} = 96.27°C, T_{p4} = 151.88°C, T_{p5} = 196.23°C and T_{p6} = 172.57°C, with peaks one to four overlapping each other, peak five and six overlapping and the sixth peak again being measured during the cooldown stage. At T = 104°C the water content was reduced to n = 6.0 {H_2O} per unit {$3MgSO_4$ + 16KCl} but it stabilized again at n = 1.2 {H_2O} per unit {$3MgSO_4$ + 16KCl} at T = 196°C.

While the TGA/DSC analysis showed an improved cycle stability of the mixture, compared to untreated {$MgSO_4$}, the energy storage density was below the performance of that of most tested chlorides, as the chemical composition contained an excess of low reactive {KCl}.

Table 12 Energy storage density and water uptake of both tested chloride-sulfate mixtures with the TGA/DSC results for an untreated {ZnCl2} sample for comparison.

Materials and mixing ratios	Energy storage density [J/g] T_{max} = 100°C	Water uptake wgt [%] T_{max} = 100°C	Energy storage density [J/g] T_{max} = 200°C	Water uptake wgt [%] T_{max} = 200°C
{16KCl + 3$MgSO_4$}	205.29	23.44	409.12	23.44
{$ZnSO_4$ + 36$ZnCl_2$}	632.49	43.30	697.95	41.08
{$ZnCl_2$}	387.66	39.57	588.49	45.40

c) {$SrBr_2$ + $MgSO_4$}

Despite no naturally occurring compounds of strontium-bromide-sulfate mixtures being known, {$MgSO_4$} was chosen as the second educt for the mix, since it loses cycle stability when overhydrated and it was to be evaluated, whether the performance would improve by a material like {$SrBr_2$} absorbing excess water during hydration.

The salts {$SrBr_2 \cdot 6H_2O$} and {$MgSO_4 \cdot 7H_2O$} were dry-mixed at three different ratios.

While no additional water was provided during the three mixing processes, the substances liquefied and reacted with each other within the mortar. The reaction taking place was likely:

$$SrBr_2 \cdot 6H_2O + MgSO_4 \cdot 7H_2O \rightarrow SrSO_4\downarrow + MgBr_2 + 13H_2O$$

Where the sparingly soluble {$SrSO_4$} crystallized from the solution while the {$MgBr_2$} and the excess starting materials (depending on the respective mixing ratio) remained completely dissolved.

The first mixing ratio was 2g {$SrBr_2 \cdot 6H_2O$} to 1g {$MgSO_4 \cdot 7H_2O$} which equals {4$SrBr_2$ + 3$MgSO_4$}.

Sample #1 was holding about n = 98.4 {H_2O} per formula unit {$4SrBr_2 + 3MgSO_4$} at the start of the measurement. The material was already reacting at T = 25°C before the initialization of the dehydration stage.

The 1st dehydration curve showed three peaks at T_{p1} = 34.94°C, T_{p2} = 61.57°C and T_{p3} = 99.43°C. While no melting peak was identified, an exothermic peak event, indicating a solidification, occurred during the cooldown stage. After the first peak at T = 36°C, the sample was still holding about n = 84.0 {H_2O} per formula unit {$4SrBr_2 + 3MgSO_4$}. After heating to T_{max} = 100°C the water content had declined to n = 63.0 {H_2O} per formula unit {$4SrBr_2 + 3MgSO_4$}.

During the 1st hydration, four overlapping peaks were observed at e = 8.65mbar with an enthalpy of $H_1 = 13.22 Jg^{-1}$, e = 14.80mbar with an enthalpy of $H_2 = 109.61 Jg^{-1}$ and two at e = 17.66mbar with an enthalpy of $H_3 = 13.55 Jg^{-1}$ and $H_4 = 112.64 Jg^{-1}$, for a total of $H_{all} = 249.02 Jg^{-1}$. At the end of the hydration stage, the sample was holding about n = 93.4 {H_2O} per unit {$4SrBr_2 + 3MgSO_4$} which equals 73.3% of the observed minimum sample weight. When the water supply was cut off, the sample released excess water in two separate endothermic events until the water content stabilized at about n = 78.7 {H_2O} per unit {$4SrBr_2 + 3MgSO_4$}.

The sample started into the 2nd cycle with a water content of about n = 79.4 {H_2O} per unit {$4SrBr_2 + 3MgSO_4$}.

The first peak observed during the 1st dehydration was absent during the 2nd dehydration as the sample was not as overhydrated. The second and the third peak unified into one at T_{p1} = 78.96°C, followed by a double peak of T_2 and T_3 with the main peak at T_{p2} = 197.16°C. The water content declined to n = 67.3 {H_2O} per unit {$4SrBr_2 + 3MgSO_4$} at T = 103°C after the first peak, then sank further to n = 29.8 {H_2O} per unit {$4SrBr_2 + 3MgSO_4$} after the double peak and heating to T_{max} = 200°C.

The 2nd hydration showed four overlapping peaks similar to those observed during the 1st hydration, at e = 8.65mbar with an enthalpy of H_1 = 126.37Jg^{-1}, e = 14.80mbar with an enthalpy of H_2 = 139.63Jg^{-1} and again two at e = 17.66mbar H_3 = 15.11Jg^{-1}, H_4 = 89.72Jg^{-1}, for a total of H_{all} = 370.83Jg^{-1}. At the end of the hydration stage, the sample was holding about n = 76.6 {H_2O} per unit {4$SrBr_2$ + 3$MgSO_4$} which equals 56.0% of the observed minimum sample weight. When the water supply was cut off, the sample also released excess water in two separate endothermic events until the water content stabilized at about n = 56.7 {H_2O} per unit {4$SrBr_2$ + 3$MgSO_4$}.

At the start of the 3rd cycle, the sample was still holding about n = 56.7 {H_2O} per unit {4$SrBr_2$ + 3$MgSO_4$}.

The 3rd dehydration curve showed five not easily distinguishable peaks. First a double peak of T_{p1} and T_{p2} with the main peak at T_{p1} = 78.29°C followed by a triple peak of T_{p3}, T_{p4} and T_{p5}, with the main peak at T_{p3} = 145.16°C. T_{p1} was a partial melting event. The minimum sample weight was observed during the cooldown stage after heating to T_{max} = 200°C. At T = 105°C after the first double peak, the water content had declined to n = 41.9 {H_2O} per unit {4$SrBr_2$ + 3$MgSO_4$}, it further declined to n = 27.2 {H_2O} per unit {4$SrBr_2$ + 3$MgSO_4$} at T = 197°C directly after the triple peak and reached a minimum of n = 22.2 {H_2O} per unit {4$SrBr_2$ + 3$MgSO_4$} during the cooldown stage.

Sample #2 was holding about n = 28.4 {H_2O} per unit {4$SrBr_2$ + 3$MgSO_4$} at the beginning of the measurement and was taking up water at e = 18.68mbar until a temperature of T = 51.05°C and a water content of n = 42.4 {H_2O} per unit {4$SrBr_2$ + 3$MgSO_4$} were reached, which equals 56.6% of the observed minimum sample weight. After heating to T_{max} = 110°C, the water content had declined to n = 34.9 {H_2O} per unit {4$SrBr_2$ + 3$MgSO_4$} and recovered to n = 35.5 {H_2O} per unit {4$SrBr_2$ + 3$MgSO_4$} when the temperature decreased to T = 60°C.

At the start of the T_{max} = 500°C measurement, the material held n = 36.2 {H_2O} per unit {$4SrBr_2 + 3MgSO_4$} and six peaks were observed when the material was dehydrated.

First was a double peak at T_{p1} = 102.82°C and T_{p2} = 121.62°C, then a triple peak of T_{p3}, T_{p4} and T_{p5} with the main peak T_{p5} = 213.82°C. Last was a single peak at T_{p6} = 312.17°C. A melting point was not observed.

After the first double peak at T = 135°C the water content had declined to n = 27.7 {H_2O} per unit {$4SrBr_2 + 3MgSO_4$}, it sank further to n = 19.5 {H_2O} per unit {$4SrBr_2 + 3MgSO_4$} at T = 242°C after the triple peak. The full anhydrate phase was likely not realized, since the material was still reacting when the heating stage of the measurement ended at T_{max} = 500°C.

The second mixing ratio was 1g {$SrBr_2 \cdot 6H_2O$} to 1g {$MgSO_4 \cdot 7H_2O$}, which equals {$2SrBr_2 + 3MgSO_4$}.

Sample #1 was gauged to be holding about n = 41.5 {H_2O} per unit {$2SrBr_2+3MgSO_4$} at the start of the measurement. The mixture already emitted excess water at T = 25°C before the dehydration stage started.

Three peaks were observed in the 1st dehydration curve with T_{max} = 100°C at T_{p1} = 32.01°C, T_{p2} = 87.15°C and T_{p3} = 97.96°C. All three peaks had a weak, positive enthalpy output, indicating an exothermic reaction taking place during the 1st dehydration. An endothermic event only occurred during the cooldown stage. The mixture constantly lost water until it reached a water content of n = 28.8 {H_2O} per unit {$2SrBr_2+3MgSO_4$} during the cooldown stage, after heating to T_{max} = 100°C.

Three exothermic peaks were observed during the 1st hydration at e = 8.65mbar with an enthalpy of H_1 = 29.31Jg^{-1}, peaks two and three overlapping at e = 14.80mbar and e = 17.66mbar with an enthalpy of H_{2+3} = 201.06Jg^{-1} for a total of H_{all} = 230.37Jg^{-1}. The sample emitted excess water

in an endothermic event, as soon as the water supply was cut off. The sample held a maximum water content of n = 44.3 {H_2O} per unit {$2SrBr_2 + 3MgSO_4$}, which equals 52.6% of the observed minimum sample weight. To the end of the 1st hydration measurement the water content had declined to n = 40.2 {H_2O} per unit {$2SrBr_2 + 3MgSO_4$}.

The sample started into the 2nd cycle with a water content of about n = 40.7 {H_2O} per unit {$2SrBr_2 + 3MgSO_4$}, which had sunken again to n = 40.1 {H_2O} at T = 44°C before the first peak.

The 2nd dehydration curve started with an exothermic event at T = 43.55°C, an endothermic triple-peak at $T_{p1.1}$ = 67°C, $T_{p1.2}$ = 86.52°C and $T_{p1.3}$ = 99.90°C, with the main peak at $T_{p1.2}$ and $T_{p1.3}$ occurring during the isothermal stage. The triple peak was followed by another exothermic event still occurring during the isothermal stage at T = 99.90°C. Next was an endothermic double-peak at $T_{p2.1}$ = 151.03°C and $T_{p2.2}$ = 171°C with the main peak event at $T_{p2.1}$. Another strong endothermic event but without a significant corresponding weight change occurred during the cooldown stage. The peaks at $T_{p1.2}$ = 86.52°C, $T_{p2.1}$ = 151.03°C and $T_{p2.2}$ = 171°C indicate partial melting events. The water content declined to n = 31.0 {H_2O} per unit {$2SrBr_2 + 3MgSO_4$} at the exothermic event at T = 99.90°C. After the double peak and heating to T_{max} = 200°C the water content declined to n = 14.8 {H_2O} per unit {$2SrBr_2 + 3MgSO_4$} during the cooldown stage.

Three overlapping peaks were observed during the 2nd hydration at e = 8.65mbar, e = 14.80mbar and e = 17.66mbar, for a total of H_{all} = 329.36Jg^{-1}. When the water supply was cut off, the mixture emitted excess water in two endothermic events, separated by a single endothermic event. The sample held a maximum water content of n = 37.9 {H_2O} per unit {$2SrBr_2 + 3MgSO_4$}, which equals 42.0% of the observed minimum sample weight but it had declined to n = 28.3 {H_2O} per unit {$2SrBr_2 + 3MgSO_4$} at the end of the 2nd hydration measurement.

The sample started into the 3rd cycle with a water content of n = 28.7 {H_2O} per unit {$2SrBr_2 + 3MgSO_4$}.

The 3rd dehydration curve showed a total of nine peaks, five of them exothermic at T_{p1} = 36.24°C, T_{p3} = 78.30°C, T_{p5} = 103,70°C, T_{p7} = 149.26°C and T_{p9} = 182,83°C and four endothermic events at T_{p2} = 64.54°C, T_{p4} = 98.87°C, T_{p6} = 138.51°C and T_{p8} = 181.35°C. Another endothermic event took place during the cooldown stage, where also the minimum sample weight was observed. The water content had declined to n = 25.6 {H_2O} per unit {$2SrBr_2 + 3MgSO_4$} when the exothermic event at T_{p3} = 78.30°C occurred, it sank further to n = 21.0 {H_2O} per unit {$2SrBr_2 + 3MgSO_4$} at T = 104°C after the fourth peak and reached its minimum of approximately n = 12.1 {H_2O} per unit {$2SrBr_2 + 3MgSO_4$} after heating to T_{max} = 200°C during the cooldown stage.

Sample #2 held n = 15.8 {H_2O} per unit {$2SrBr_2 + 3MgSO_4$} at the start of the measurement, which equals 26.8% of the observed minimum sample weight. The mixture was taking up water at e = 18.68mbar until it reached a temperature of T = 53.80°C and the sample held a water content of n = 22.4 {H_2O} per unit {$2SrBr_2 + 3MgSO_4$}, which equals 40.7% of the observed minimum sample weight. The water content balanced out at T = 65.87°C at n = 21.1 {H_2O} per unit {$2SrBr_2 + 3MgSO_4$} before the temperature was further increased and the water content continued to decline to n = 19.5 {H_2O} per unit {$2SrBr_2 + 3MgSO_4$} after drying to T = 110°C. The water content recovered at T = 64.11°C to n = 20.0 {H_2O} per unit {$2SrBr_2 + 3MgSO_4$}, which equals 35.6% of the observed minimum sample weight. An endothermic peak without corresponding weight change was observed occurring during the T = 110 to 60°C cooldown stage which hints to a phase change from a form of high crystal order like cubic or hexagonal to a form of lower order.

At the start of the T_{max} = 500°C dehydration measurement, sample held a water content of about n = 20.2 {H_2O} per unit {$2SrBr_2 + 3MgSO_4$}. The curve showed four peaks at T_{p1} = 98.27°C, T_{p2} = 116.15°C, T_{p3} = 153.72°C and T_{p4} = 348.05°C. A melting event was not observed. At T = 227°C after the third peak, the sample still held about n = 13.0 {H_2O} per unit {$2SrBr_2 + 3MgSO_4$}. Directly after the fourth peak at T = 443°C the water content had declined to n = 5.0 {H_2O} per unit {$2SrBr_2 + 3MgSO_4$}. A completely anhydrate sample was not achieved, as the mixture still held about n = 3.1 {H_2O} per unit {$2SrBr_2 + 3MgSO_4$} after heating to T_{max} = 500°C.

The third mixing ratio was 1g {$SrBr_2 \cdot 6H_2O$} to 2g {$MgSO_4 \cdot 7H_2O$} which equals {$SrBr_2 + 3MgSO_4$}.

Sample #1 of the mixture was holding approximately n = 32.4 {H_2O} per unit {$SrBr_2 + 3MgSO_4$} at the start of the measurement. The sample began emitting excess water at T = 25°C until it stabilized at a water content of n = 32.0 {H_2O} per unit {$SrBr_2 + 3MgSO_4$}.

The 1st dehydration showed two overlapping peaks at T_{p1} = 80.27°C and T_{p2} = 99.35°C. The water content had declined to n = 23.0 {H_2O} per unit {$SrBr_2 + 3MgSO_4$} after heating to T_{max} = 100°C.

Five overlapping exothermic peaks were observed during the 1st hydration. Two occurred at e = 8.65mbar with an enthalpy of H_{1+2} =21.26 Jg^{-1}, e = 14.80mbar with an enthalpy of H_3 = 127.64Jg^{-1} and two more at e = 17.66mbar with an enthalpy of H_{4+5} = 140.20Jg^{-1} for a total of H_{all} = 289.10Jg^{-1}. The first and the fourth peak indicate solidification events. Since there was no observed melting during the dehydration or deliquescence at the start of the hydration, a phase change to a higher crystal order such as cubic or hexagonal is more likely than a solidification, though. The sample held a maximum water content of n = 39.6 {H_2O} per unit {$SrBr_2 + 3MgSO_4$},

which equals 56.6% of the observed minimum sample weight during the hydration stage. When the water supply was cut off, the sample emitted excess water, first in one short endothermic event, which was immediately followed by a brief exothermic peak Indicating two rapid phase changes. They were followed by another endothermic event. The water content sank to n = 31.8 $\{H_2O\}$ per unit $\{SrBr_2 + 3MgSO_4\}$.

The sample started into the 2nd cycle with a water content of about n = 32.0 $\{H_2O\}$ per unit $\{SrBr_2 + 3MgSO_4\}$.

During the 2nd dehydration nine peaks were observed. Three of those peaks were exothermic events without significant weight changes at T_{p1} = 38.11 °C, T_{p5} = 100.87°C, T_{p8} = 197.28°C. The other six were endothermic events at T_{p2} = 54°C, T_{p3} = 79.90°C, T_{p4} = 98.78 °C, T_{p6} = 147.96°C T_{p7} = 180°C and T_{p9} = 197.28°C, with the peaks two and three overlapping and indicating partial melting events, peaks six and seven overlapping each other and peak nine occurring during the isothermal stage. The water content had declined to n = 23.4 $\{H_2O\}$ per unit $\{SrBr_2 + 3MgSO_4\}$, when the exothermic event at T_{p5} = 100.87°C occurred. After heating to T_{max} = 200°C, the water content sank further to n = 14.3 $\{H_2O\}$ per unit $\{SrBr_2 + 3MgSO_4\}$ during the cooldown stage. Another endothermic event occurred during cooldown, during which the water content increased marginally.

The 2nd hydration showed only four overlapping exothermic peaks at e = 8.65mbar with an enthalpy of $H_1 = 56.22Jg^{-1}$, e = 14.80mbar with an enthalpy of $H_2 = 105.83Jg^{-1}$ and e = 17.66mbar with an enthalpy of $H_{3+4} = 56.05Jg^{-1}$ for a total of $H_{all} = 218.11Jg^{-1}$. The sample held a maximum water content of n = 29.9 $\{H_2O\}$ per unit $\{SrBr_2 + 3MgSO_4\}$ during hydration, which equals 36.1% of the observed minimum sample weight. When the water supply was cut off, the sample emitted excess water in a brief endothermic event, followed by an also brief exothermic event upon which another endothermic event followed until the water content stabilized at about n = 21.6 $\{H_2O\}$ per unit $\{SrBr_2 + 3MgSO_4\}$.

At the start of the 3rd cycle, the sample was holding n = 21.9 {H_2O} per unit {$SrBr_2 + 3MgSO_4$}.

Nine peaks were observed during the 3rd dehydration. Five events were again exothermic at T_{p1} = 30.40°C, T_{p3} = 74.49°C, T_{p5} = 109.25°C, with a double peak at T_{p7} = 154.54°C and T_{p9} = 189.48°C and four endothermic at T_{p2} = 62.86°C, T_{p4} = 99.11°C, T_{p6} = 134.62°C and T_{p8} = 164.46°C. The water content declined steadily, first to n = 17.7 {H_2O} per unit {$SrBr_2 + 3MgSO_4$} at T_{p5} = 109.25°C then to n = 12.9 {H_2O} per unit {$SrBr_2 + 3MgSO_4$} after heating to T_{max} = 200°C, where also the minimum sample weight was observed.

Sample #2 held approximately n = 18.3 {H_2O} per unit {$SrBr_2 + 3MgSO_4$} at the start of the measurement and was taking up water at e = 18.68mbar, until it reached a temperature of T = 41.11°C and a water content of n = 21.3 {H_2O} per unit {$SrBr_2 + 3MgSO_4$}, which equals 35.9% of the observed minimum sample weight. The exothermic peak at T = 30.47°C shows some characteristics of a solidification or fast phase change event to a higher crystal order. At T = 62.45°C the water content stabilized for a moment with n = 21.0 {H_2O} per unit {$SrBr_2 + 3MgSO_4$} before it continued to decrease steadily with increasing temperature until it reached n = 20.0 {H_2O} per unit {$SrBr_2 + 3MgSO_4$} at the end of the heating stage.

An endothermic peak was occurred during the T = 110 to 60°C cooldown stage. The event hinted to a change of phase from higher to lower order. The water content increased only marginally during and after the cooldown stage and remained at about n = 20.0 {H_2O} per unit {$SrBr_2 + 3MgSO_4$}. Apparently, the sample absorbed residue water after the water supply was cut off and recovered to n = 20.4 {H_2O} per unit {$SrBr_2 + 3MgSO_4$} at T = 64.10°C.

The sample held about n = 20.5 {H_2O} per unit {$SrBr_2 + 3MgSO_4$} at the start of the T_{max} = 500°C measurement.

Upon dehydration, only four weak peaks were observed at T_{p1+2} = 100,42°C, T_{p3} = 314.69°C, T_{p4} = 370.34°C aside from the difference in mass change it was not possible to differentiate between the overlapping peaks 1 and 2. No melting event was observed. After the double peak at T = 121°C, the sample was holding approximately n = 18.4 {H_2O} per unit {$SrBr_2$ + 3$MgSO_4$}, without measurable peak events, the water content declined further until it reached n = 14.9 {H_2O} per unit {$SrBr_2$ + 3$MgSO_4$} before the third peak at T = 290°C, sank to n = 12.4 {H_2O} per unit {$SrBr_2$ + 3$MgSO_4$} at T = 331°C after the third peak and to n = 9.5 {H_2O} per unit {$SrBr_2$ + 3$MgSO_4$} at T = 386°C directly after the fourth peak. The sample had likely not dried completely at T_{max} = 500°C as an ongoing loss of weight was still recorded at that point. The remaining water content was gauged as n = 6.75 {H_2O} per unit {$SrBr_2$ + 3$MgSO_4$}.

d) {$SrBr_2 \cdot 6H_2O$ + KCl}

While {KCl} is not a very reactive heat storage material on its own and rather shows endothermic reactions than exothermic events upon hydration due to dissolving of its cubic crystal structure, the TGA/DSC of the mixed chloride salts had indicated a stabilizing influence over the measurement cycles.

While the three {$SrBr_2 \cdot 6H_2O$ + KCl} mixtures remained dry even after extended storage periods, the samples appear to have drawn water, when exposed to air, while waiting on the TGA's sample-tray for the measurement.

During the measurements apparently a malfunction occurred, which prevented the isolation of the water supply from the oven chamber and enabled the sample to take up additional water during the supposed dry stages.

The first mixing ratio was 2g {$SrBr_2 \cdot 6H_2O$} to 1g {KCl}, which equals a {2$SrBr_2$ + 5KCl} mixture.

Sample #1 was holding approximately about n = 21.2 {H_2O} per unit {$2SrBr_2$ + 5KCl} at the start of the measurement. The sample was already emitting excess water at T = 25°C.

Only a single peak was observed during the 1st dehydration at T_{p1} = 64.41°C. Directly after the peak at T = 74°C, the water content had declined to n = 8.8 {H_2O} per unit {$2SrBr_2$ + 5KCl}, it sank further to n = 8.3 {H_2O} per unit {$2SrBr_2$ + 5KCl} after heating to T_{max} = 100°C and the cooldown stage.

The 1st hydration started with a short endothermic event, followed by three overlapping exothermic peaks at e = 8.65mbar with an enthalpy of H_1 = 111.40Jg^{-1}, at e = 14.80mbar with an enthalpy of H_2 = 166.33Jg^{-1} and at e = 17.66mbar with H_3 = 58.33Jg^{-1} for a total of H_{all} = 385.93Jg^{-1}. The material continued to react after the water supply had been shut off in a fourth exothermic peak event. This excess heat was not counted into the total, as the corresponding continued weight gain was likely a result of a malfunction in the water supply. The sample held a maximum water content of n = 18.5 {H_2O} per unit {$2SrBr_2$ + 5KCl} at the end of the measurement, which equaled about 22.7% of the observed minimum sample weight.

The sample started into the 2nd cycle with a water content of n = 18.6 {H_2O} per unit {$2SrBr_2$ + 5KCl}.

The 2nd dehydration showed two peaks at T_{p1} = 83.88°C and T_{p2} = 178.40°C. At T = 92°C after the first peak, the water content had declined to n = 8.9 {H_2O} per unit {$2SrBr_2$ + 5KCl} at T = 197°C after the second peak, the water content sank further to n = 6.5 {H_2O} per unit {$2SrBr_2$ + 5KCl}.

No endothermic peak occurred at the start of the 2nd hydration, it began with three exothermic peaks at e = 8.65mbar with an enthalpy of H_1 = 112.72Jg^{-1}, at e = 14.80mbar with an enthalpy of H_2 = 179.41Jg^{-1} and at e = 17.66mbar with H_3 = 41.17Jg^{-1} for a total of H_{all} = 371.34Jg^{-1}. Again, the reaction did not stop immediately after the water supply was cut and the measured excess

heat was not included in the total. The sample held about n = 20.7 {H_2O} per unit {2$SrBr_2$ + 5KCl} at the end of the hydration, which equaled 26.6% of the observed minimum sample weight.

The sample started into the 3rd cycle with about the same water content as at the end of the 2nd hydration at n = 20.7 {H_2O} per unit {2$SrBr_2$ + 5KCl}.

Again, two peaks were observed during the 3rd dehydration, at T_{p1} = 86.10°C, T_{p2} = 179.47°C. An exothermic event occurred at the start of the cooldown stage. At T = 96°C after the first peak, the water content had declined to n = 9.0 {H_2O} per unit {2$SrBr_2$ + 5KCl} at T = 197°C after the second peak, the water content sank further to n = 6.5 {H_2O} per unit {2$SrBr_2$ + 5KCl}. After the exothermic event, the minimum sample weight was reached as well as a water content of n = 6.2 {H_2O} per unit {2$SrBr_2$ + 5KCl}.

Sample #2 held approximately n = 7.9 {H_2O} per unit {2$SrBr_2$ + 5KCl} at the start of the measurement. It reacted with water at e = 18.68mbar until it reached a water content of n = 14.9 {H_2O} per unit {2$SrBr_2$ + 5KCl} which equals 15.8% of the observed minimum sample weight and a temperature of T = 53.59°C. When the temperature reached T = 67.89°C and a water content of n = 9.7 {H_2O} per unit {2$SrBr_2$ + 5KCl}, the dehydration reaction stopped and the water content began to recover despite increasing temperatures to about n = 10.1 {H_2O} per unit {2$SrBr_2$ + 5KCl} at T_{max} = 110°C. An endothermic peak occurred during the cooldown stage from T = 110 to 60°C which corresponded with a shift in water content to n = 9.7 {H_2O} per unit {2$SrBr_2$ + 5KCl}. As soon as the water supply was cut off this reversed in a short exothermic peak event where the water content of the sample was raised back to 9.9 {H_2O} per unit {2$SrBr_2$ + 5KCl}. This may have been caused by the afore mentioned malfunction in the water supply.

The sample held approximately n = 10.1 {H_2O} per unit {2$SrBr_2$ + 5KCl} at the beginning of the dehydration to T_{max} = 500°C but the measurement failed due to an outdated baseline being applied. The curve nevertheless showed

a peak at T ~200°C. A remaining water content of 6.33 {H_2O} per unit {2$SrBr_2$ + 5KCl} was estimated from the recorded weight change at this point.

The second mixing ratio was 1g {$SrBr_2 \cdot 6H_2O$} to 1g {KCl}, which equals a {$SrBr_2$ + 5KCl} mixture.

It was estimated that sample #1 was holding about n = 5.0 {H_2O} per unit {$SrBr_2$ + 5KCl} at the start of the measurement.

Only a single peak was observed during the 1st dehydration at T_{p1} = 58.64°C. Before and after the peak, the curve showed signs of exothermic activity but no significant, corresponding mass changes were recorded. Another endothermic peak event occurred during the cooldown stage. At T = 66°C directly after the main peak the water content had declined to n = 1.7 {H_2O} per unit {$SrBr_2$ + 5KCl} after the peak at cooldown it sank further to n = 1.5 {H_2O} per unit {$SrBr_2$ + 5KCl}.

The 1st hydration curve showed only two overlapping peaks at e = 8.65mbar with an enthalpy of H_1 = 117.08Jg^{-1} and at e = 14.80mbar with an enthalpy of H_2 = 79.22Jg^{-1} for a total of H_{all} = 196.31Jg^{-1}. As soon as the water supply was shut off, the material appeared to react again. It is possible that aside from a malfunction in the water supply, a phase change to a crystal structure of higher order caused the additional exothermic peak, which was not counted into the enthalpy total. The sample held a maximum water content of n = 6.3 {H_2O} per unit {$SrBr_2$ + 5KCl} during the additional peak, which equaled 14.4% of the sample's observed minimum weight, it declined afterwards and balanced out again at n = 5.7 {H_2O} per unit {$SrBr_2$ + 5KCl}.

The sample held that water content and started into the 2nd cycle with n = 5.7 {H_2O} per unit {$SrBr_2$ + 5KCl}.

The 2nd dehydration curve had two peaks at T_{p1} = 78.21°C and T_{p2} = 172.75°C. Before and after either of the peaks exothermic activity without

mass change was observed as well. Another endothermic peak event occurred during the cooldown stage. At T = 92°C after the first peak the water content sank to n = 2.1 {H_2O} per unit {$SrBr_2$ + 5KCl}, it declined further to n = 1.3 {H_2O} per unit {$SrBr_2$ + 5KCl} at T = 191°C after the second peak and to n = 1.2 {H_2O} per unit {$SrBr_2$ + 5KCl} after the peak event during cooldown.

The 2nd hydration curve showed similarities to the 1st, with two peaks at e = 8.65mbar with an enthalpy of H_1 = 121.91Jg^{-1} and at e = 14.80mbar with an enthalpy of H_2 = 74.17Jg^{-1} for a total of H_{all} = 196.08Jg^{-1}. An endothermic event occurred during the e = 17.66mbar hydration stage, where the water content temporarily declined. It was followed by a short exothermic reaction period after the water supply was cut off. The enthalpy from the last exothermic event was not counted into the total, as again likely a malfunction in the water supply was the cause. The sample held a maximum water content of n = 5.7 {H_2O} per unit {$SrBr_2$ + 5KCl}, which was equal to 12.9% of the observed minimum sample weight, declined to n = 5.3 {H_2O} per unit {$SrBr_2$ + 5KCl} during the endothermic event and recovered to about n = 5.7 {H_2O} per unit {$SrBr_2$ + 5KCl} afterwards.

The sample started into the 3rd cycle with a water content of about n = 5.7 {H_2O} per unit {$SrBr_2$ + 5KCl} as well.

The 3rd dehydration curve showed similarities to the 2nd, with two peaks at T_{p1} = 77.81°C, T_{p2} = 173.06°C, exothermic activity before and after both peaks, followed by another endothermic peak event during cooldown. At T = 91°C after the first peak, the sample still held a water content of n = 2.1 {H_2O} per unit {$SrBr_2$ + 5KCl}, it sank to n = 1.3 {H_2O} per unit {$SrBr_2$ + 5KCl} at T = 189°C after the second peak and to n = 1.2 {H_2O} per unit {$SrBr_2$ + 5KCl} after the peak which occurred during the cooldown stage. The sample's minimum weight was observed after the cooldown peak as well.

Sample #2 held a water content of about n = 2.8 {H_2O} per unit {$SrBr_2$ + 5KCl} at the start of the measurement but began immediately absorbing water.

At e = 18.68mbar the mixture reacted, until it reached a water content of n = 6.2 {H_2O} per unit {$SrBr_2$ + 5KCl}, which equals 9.1% of the starting sample mass, at a temperature of T = 53.12°C. From there the water content declined until n = 3.5 {H_2O} per unit {$SrBr_2$ + 5KCl} were reached at T 70.08°C from there it recovered to n = 3.7 {H_2O} per unit {$SrBr_2$ + 5KCl}, where it balanced out at T_{max} = 110°C.

An endothermic peak occurred during the cooldown stage from T = 110 to 60°C which corresponded with a shift in water content from to n = 3.3 {H_2O} per unit {$SrBr_2$ + 5KCl}. As soon as the water supply was cut off this reversed in a short exothermic peak event where the water content of the sample was raised back to 3.5 {H_2O} per unit {$SrBr_2$ + 5KCl}. This may be an indicator for the material partially dissolving and recrystallizing once the water pressure is reduced but was likely caused by a malfunction in the water supply.

The T_{max} = 500°C measurement failed and provided no data.

The third mixing ratio was 1g {$SrBr_2 \cdot 6H_2O$} to 2g {KCl}, which equals a {$SrBr_2$ + 10KCl} mixture.

Sample #1 was holding about n = 2.6 {H_2O} per unit {$SrBr_2$ + 10KCl} at the start of the measurement.

Only a single endothermic peak was observed during the 1st dehydration atT_{p1} = 45.92°C. An exothermic event occurred during the cooldown stage. At T = 54°C directly after the peak, the water content had declined to n = 0.7

{H_2O} per unit {$SrBr_2$ + 10KCl} it recovered to n = 0.9 {H_2O} per unit {$SrBr_2$ + 10KCl} despite the temperature rising to T_{max} = 100°C. after the exothermic peak the water content had declined again until it reached n = 0.4 {H_2O} per unit {$SrBr_2$ + 10KCl}.

The minimum sample weight was observed at the start of the 1st hydration measurement with an estimated water content of n = 0.33 {H_2O} per unit {$SrBr_2$ + 10KCl}.

The 1st hydration curve began with a weak endothermic event, followed directly by a strong exothermic peak at e = 8.65mbar with an enthalpy of H_1 = 66.66Jg^{-1}, the reaction turned endothermic again right afterwards. A small exothermic peak was observed at e = 14.80mbar with an enthalpy of H_2 = 1.43Jg^{-1} also followed directly by an endothermic event this pattern is repeated with another small exothermic peak at e = 17.66mbar with H_3 = 4.63Jg^{-1} for a total of H_{all} = 72.72Jg^{-1} and another endothermic event at the end of the hydration stage. An additional exothermic reaction occurred after the water supply was cut off but wasn't counted into the enthalpy total as it was likely a result of a malfunction in the water supply. The sample was holding n = 2.6 {H_2O} per unit {$SrBr_2$ + 10KCl} at the end of the hydration stage but increased further to a maximum of n = 3.1 {H_2O} per unit {$SrBr_2$ + 10KCl} where it balanced out, this equaled about 5.0% of the observed minimum sample weight.

The water content of n = 3.1 {H_2O} per unit {$SrBr_2$ + 10KCl} was still stable at the start of the 2nd cycle.

Two endothermic peaks occurred during the 2nd dehydration at T_{p1} = 68.81°C and T_{p2} = 168.50°C. An exothermic event was observed during the cooldown stage, which concurs with a minimal loss of mass.

The water content declined to n = 0.9 {H_2O} per unit {$SrBr_2$ + 10KCl} at T = 77°C after the first peak, sank further to n = 0,5 {H_2O} per unit {$SrBr_2$ + 10KCl} at T = 197°C and reached n = 0.4 {H_2O} per unit {$SrBr_2$ + 10KCl} during cooldown.

The 2nd hydration curve starts with an exothermic peak at e = 8.65mbar with an enthalpy of $H_1 = 71.31Jg^{-1}$, directly followed by an endothermic event. At e = 14.80mbar a second but weaker exothermic event occurred with an enthalpy of $H_2 = 2.15Jg^{-1}$ also followed directly by an endothermic event. The enthalpy total of the exothermic peaks was $H_{all} = 73.46Jg^{-1}$. The second exothermic peak was correlated to a sudden gain and drop in sample mass. The additional exothermic reaction that occurred after the water supply was cut off, was not counted into the enthalpy total as again it was likely caused by a malfunction in the water supply, though it showed as well as the second exothermic peak event during hydration, signs of a sudden shift in phase. It was followed by a weak endothermic event. The sample was holding a maximum content of n = 4.2 {H_2O} per unit {$SrBr_2$ + 10KCl}, which equals about 7.0% of the observed minimum sample weight. The mixture emitted excess water after the third exothermic event until the water content evened out at n = 3.3 {H_2O} per unit {$SrBr_2$ + 10KCl}.

The sample started into the 3rd cycle with the water content still at n = 3.3 {H_2O} per unit {$SrBr_2$ + 10KCl}.

The 3rd dehydration shows a low temperature peak at T_{p1} = 71.02°C, followed by a double peak at T_{p2} = 130.00°C and T_{p3} = 167.33°C, the curve shows an exothermic peak event with a corresponding minimal mass loss during the cooldown stage. The water content sank to n = 1.0 {H_2O} per unit {$SrBr_2$ + 10KCl} at T = 82°C after the first peak, then declined further to n = 0.6 {H_2O} per unit {$SrBr_2$ + 10KCl} at T = 197°C after the double peak, then during the cooldown stage it reached n = 0.4 {H_2O} per unit {$SrBr_2$ + 10KCl}.

Sample #2 held about n = 2.7 {H_2O} per unit {$SrBr_2$ + 10KCl} at the start of the measurement. The mixture reacted with water at e = 18.68mbar until a temperature of T = 51.38°C and a water content of n = 4.4 {H_2O} per unit {$SrBr_2$ + 10KCl} were reached, which equals 3.0% of the observed minimum sample weight. The water content declined to n = 3.2 {H_2O} per unit {$SrBr_2$

+ 10KCl} at T = 68.60°C before it recovered again to n = 3.5 {H_2O} per unit {$SrBr_2$ + 10KCl} while the temperature was raised to T_{max} = 110°C.

An exothermic peak occurred during the cooldown stage from T = 110 to 60°C which corresponded with a decline in water content to n = 3.0 {H_2O} per unit {$SrBr_2$ + 10KCl}. As soon as the water supply was cut off this reversed in another short exothermic peak event where the water content of the sample was recovered back to n = 3.2 {H_2O} per unit {$SrBr_2$ + 10KCl}. This may be an indicator for the material partially dissolving and recrystallizing once the water pressure was reduced or correlated to a malfunction in the water supply.

The dehydration measurement to T_{max} = 500°C failed.

e) {$SrBr_2$ + $CaCl_2$}

Strontium bromide hexahydrate {$SrBr_2 \cdot 6H_2O$} and calcium chloride hexahydrate {$CaCl_2 \cdot 6H_2O$} were mixed at three different ratios to evaluate whether the varying calcium chloride content was improving the heat output during reactions or a high percentage of strontium bromide content was shifting the melting points of the hydrated states of the mixture to higher temperatures than those of untreated {$CaCl_2 \cdot 6H_2O$}.

Since the material proved to be deliquescent and liquefied during storage, it was dried in the oven at T_{max} = 110°C and p_{min} = 800mbar previous to the TGA/DSC-analysis.

The first mixing ratio was 2g {$SrBr_2 \cdot 6H_2O$} to1g {$CaCl_2 \cdot 6H_2O$}, which equals a {5$SrBr_2$ + 4$CaCl_2$} mixture.

Sample #1 was holding about n = 32.4 {H_2O} per unit {$5SrBr_2 + 4CaCl_2$} at the start of the measurement. The mixture already emitted excess water at T = 25°C.

Two peaks were observed at the 1st dehydration at T_{p1} = 49.41°C and T_{p2} = 94.73°C. the water content declined to n = 28.2 {H_2O} per unit {$5SrBr_2 + 4CaCl_2$} at T = 57°C after the first peak and sank further to n = 27.8 {H_2O} per unit {$5SrBr_2 + 4CaCl_2$} at T = 76°C before the second peak. After heating to T_{max} = 100°C the water content was reduced to n = 18.8 {H_2O} per unit {$5SrBr_2 + 4CaCl_2$}.

Three overlapping peaks were observed during the 1st hydration at e = 8.65mbar with an enthalpy of H_1 = 109.59Jg^{-1}, at e = 14.80mbar with an enthalpy of H_2 = 298.31Jg^{-1} and at e = 17.66mbar with H_3 = 313.69Jg^{-1} for a total of H_{all} = 721.59Jg^{-1}. The sample was holding a maximum water content of n = 60.0 {H_2O} per unit {$5SrBr_2 + 4CaCl_2$} during the hydration, which equals 50.8% of the observed minimum sample weight but the mixture emitted excess water, when the water supply was cut off. The water content did not balance out before the next measurement stage began.

The sample started into the 2nd cycle with a water content of n = 52.8 {H_2O} per unit {$5SrBr_2 + 4CaCl_2$} and kept emitting excess water at T = 25°C.

The low temperature endothermic peak from the 1st dehydration did not reappear during the 2nd dehydration. Instead two endothermic peaks were observed at T_{p1} = 89.76°C and T_{p2} = 165.26°C, additionally a small exothermic event occurred during the cooldown stage. At T = 98°C after the first peak, the water content was reduced to n = 28.4 {H_2O} per unit {$5SrBr_2 + 4CaCl_2$} and it sank further during the isothermal stage to n = 20.4 {H_2O} per unit {$5SrBr_2 + 4CaCl_2$} at T = 100.1°C directly before the second peak. The minimum sample weight was observed after heating to T_{max} = 200°C at the end of the cooldown stage, where the water content was reduced to n = 8.3 {H_2O} per unit {$5SrBr_2 + 4CaCl_2$}.

The 2nd hydration showed three overlapping peaks at e = 8.65mbar with an enthalpy of H_1 = 114.40Jg^{-1}, at e = 14.80mbar with an enthalpy of H_2 = 338.14Jg^{-1} and at e = 17.66mbar with H_3 = 339.45Jg^{-1} for a total of H_{all} = 791.98Jg^{-1}. The sample was holding a maximum water content of n = 60.1 {H_2O} per unit {5$SrBr_2$ + 4$CaCl_2$} during the hydration, which equals 50.9% of the observed minimum sample weight, however the sample emitted excess water as soon as the water supply was cut off. The water content did not balance out before the next measurement stage.

The sample started into the 3rd cycle with a water content of n = 54.1 {H_2O} per unit {5$SrBr_2$ + 4$CaCl_2$}.

Two endothermic peaks occurred during the 3rd dehydration at T_{p1} = 89.70°C and T_{p2} = 161.95°C, followed by a small exothermic event during the cooldown stage. At T = 99°C after the first peak, the water content was reduced to n = 26.1 {H_2O} per unit {5$SrBr_2$ + 4$CaCl_2$} and it sank further during the isothermal stage to n = 18.3 {H_2O} per unit {5$SrBr_2$ + 4$CaCl_2$} at T = 119°C directly before the second peak. At T = 185°C directly after the second peak, the water content was about n = 8.6 {H_2O} per unit {5$SrBr_2$ + 4$CaCl_2$}.

Sample #2 was holding n = 10.2 {H_2O} per unit {5$SrBr_2$ + 4$CaCl_2$} at the start of the measurement. The mixture was taking up water at e = 18.68mbar until it reached a temperature of T = 66.69°C and a water content of n = 31.4 {H_2O} per unit {5$SrBr_2$ + 4$CaCl_2$} which equals 23.1% of the observed minimum sample weight. The water content then declined until a temperature of T = 97.08°C was reached, where it balanced out at n = 23.4 {H_2O} per unit {5$SrBr_2$ + 4$CaCl_2$} until the cooldown stage began.

The sample re-hydrated at T = 63.14°C, where the water content recovered to n = 36.0 {H_2O} per unit {5$SrBr_2$ + 4$CaCl_2$} which equals 27.7% of the observed minimum sample weight.

The sample started into the next measurement stage with a water content of n = 24.7 {H_2O} per unit {$5SrBr_2 + 4CaCl_2$}.

The dehydration to T_{max} = 500°C showed three overlapping, endothermic peaks at T_{p1} = 80.87°C, T_{p2} = 135.97°C, T_{p3} = 172.71°C, an additional exothermic event was observed during the cooldown stage. No melting event occurred. At T = 202.5°C after the three peaks the water content had declined to n = 8.5 {H_2O} per unit {$5SrBr_2 + 4CaCl_2$}, after the cooldown stage the water content was reduced to about n = 8.0 {H_2O} per unit {$5SrBr_2 + 4CaCl_2$}.

The second mixing ratio was 1g {$SrBr_2 \cdot 6H_2O$} to 1g {$CaCl_2 \cdot 6H_2O$}, which equals a {$5SrBr_2 + 8CaCl_2$} mixture.

Sample #1 was holding about n = 66.8 {H_2O} per unit {$5SrBr_2 + 8CaCl_2$} at the start of the measurement. The sample was already emitting excess water at T = 25°C.

The 1st dehydration curve showed two endothermic peaks at T_{p1} = 66.9°C and T_{p2} = 97.67°C. A short exothermic event without corresponding weight change occurred after the cooldown stage. The water content declined first to n = 36.3 {H_2O} per unit {$5SrBr_2 + 8CaCl_2$} at T = 72°C after the first peak but sank to n = 34.1 {H_2O} per unit {$5SrBr_2 + 8CaCl_2$} at T = 85°C right before the second peak and reached n = 22.5 {H_2O} per unit {$5SrBr_2 + 8CaCl_2$} after heating to T_{max} = 100°C.

Three overlapping peaks occurred during the 1st hydration at e = 8.65mbar with an enthalpy of H_1 = 132.30Jg^{-1}, at e = 14.80mbar and at e = 17.66mbar with an enthalpy of H_2 = 457.17Jg^{-1}. The third peak with H_3 = 122.07Jg^{-1} occurred only after the water supply had been cut off and is likely a result of a malfunction in the water supply. Not counting the third peak this makes for a total of H_{all} = 589.46Jg^{-1}. The sample was holding a maximum water

content of about n = 102.0 {H_2O} per unit {$5SrBr_2 + 8CaCl_2$} which equals 83.4% of the observed minimum sample weight but emitted excess water after the third peak in an endothermic event. The water content did not balance out before the next measurement stage began.

The sample started into the 2nd cycle with a water content of n = 97.1 {H_2O} per unit {$5SrBr_2 + 8CaCl_2$}.

The 2nd dehydration showed two peaks at T_{p1} = 92.57°C and at T_{p2} = 169.14°C. The water content declined to n = 33.8 {H_2O} per unit {$5SrBr_2 + 8CaCl_2$} at T = 99°C directly after the first peak and continued to sink during the isothermal stage until it reached n = 27.2 {H_2O} per unit {$5SrBr_2 + 8CaCl_2$} before the second peak. After heating to T_{max} = 200°C, the water content was reduced to n = 2.8 {H_2O} per unit {$5SrBr_2 + 8CaCl_2$} during the cooldown stage.

Three overlapping, exothermic peaks were observed during the 2nd hydration at e = 8.65mbar with an enthalpy of H_1 = 109.53Jg^{-1}, at e = 14.80mbar with an enthalpy of H_2 = 291.99Jg^{-1} and at e = 17.66mbar with H_3 = 290.12Jg^{-1} for a total of H_{all} = 691.64Jg^{-1}. The sample was holding a maximum water content of about n = 67.4 {H_2O} per unit {$5SrBr_2 + 8CaCl_2$} which equals 54.5% of the observed minimum sample weight but the mixture started emitting excess water as soon as the water supply was cut off. The water content did not balance out before the next measurement stage began.

The sample started into the 3rd cycle with a water content of n = 64.3 {H_2O} per unit {$5SrBr_2 + 8CaCl_2$}.

During the 3rd dehydration the low temperature peak appeared at T_{p1} = 85.30°C followed by the second peak at T_{p2} = 166.87°C.

The water content sank to n = 32.5 {H_2O} per unit {$5SrBr_2 + 8CaCl_2$} at T = 99°C directly after the first peak, it declined steadily to n = 23.6 {H_2O} per unit {$5SrBr_2 + 8CaCl_2$} during the isothermal stage before the second peak.

At T = 183°C after the second peak the water content had reached n = 2.4 {H_2O} per unit {$5SrBr_2 + 8CaCl_2$} but the minimum sample weight was observed during the cooldown stage, where the water content was further reduced to n = 2.0 {H_2O} per unit {$5SrBr_2 + 8CaCl_2$}.

Sample #2 was holding about n = 3.9 {H_2O} per unit {$5SrBr_2 + 8CaCl_2$} at the start of the measurement. The mixture was taking up water at e = 18.68mbar until it reached a temperature of T = 65.40°C and a water content of n = 25.1 {H_2O} per unit {$5SrBr_2 + 8CaCl_2$}, which equals 21.3% of the observed minimum sample weight. At higher temperatures the water content declined until it reached n = 18.5 {H_2O} per unit {$5SrBr_2 + 8CaCl_2$} after heating to T_{max} = 110°C and the following cooldown stage. The sample re-absorbed water at T = 63.52°C until it reached a water content of n = 35.8 {H_2O} per unit {$5SrBr_2 + 8CaCl_2$}, which equaled 30.3% of the observed minimum sample weight.

The sample started into the next measurement with a water content of n = 27.9 {H_2O} per unit {$5SrBr_2 + 8CaCl_2$}.

Heating the sample to T_{max} = 500°C showed three endothermic peaks, two of them overlapping at T_{p1} = 69.33°C and T_{p2} = 168.94°C, followed directly by the third at T_{p3} = 258.41°C. The second peak shows some signs of a melting event. The sample still held n = 2.0 {H_2O} per unit {$5SrBr_2 + 8CaCl_2$} at T = 212°C after the second peak. At T = 295°C after the third peak it had declined to n = 0.7 {H_2O} per unit {$5SrBr_2 + 8CaCl_2$}. The minimum sample weight was observed after the cooldown stage, where the sample was considered dry.

The third mixing ratio was 1g {$SrBr_2 \cdot 6H_2O$} to 2g {$CaCl_2 \cdot 6H_2O$}, which equals a {$5SrBr_2 + 16CaCl_2$} mixture.

Sample #1 was holding about n = 110.0 {H_2O} per unit {$5SrBr_2 + 16CaCl_2$} at the start of the measurement. The water content began to decline already at T = 25°C.

The 1st dehydration showed four peaks, with a double peak at T_{p1} = 52.00°C and T_{p2} = 53.67°C, followed by another double peak at T_{p3} = 79.42°C and T_{p4} = 98.19°C. The water content stabilized at T = 57°C between the second and the third peak at n = 84.4 {H_2O} per unit {$5SrBr_2 + 16CaCl_2$}, before it sank further to n = 32.5 {H_2O} per unit {$5SrBr_2 + 16CaCl_2$} during the cooldown stage after heating to T_{max} = 100°C.

Three overlapping peaks were observed for the 1st hydration at e = 8.65mbar with an enthalpy of H_1 = 101.87Jg^{-1}, e = 14.80mbar with an enthalpy of H_2 = 385.36Jg^{-1} and e = 17.66mbar with H_3 = 221.85Jg^{-1} for a total of H_{all} = 709.08Jg^{-1}. The sample was holding a maximum water content of n = 162.2 {H_2O} per unit {$5SrBr_2 + 16CaCl_2$} during the hydration, this equals 82.5% of the observed minimum sample weight. The reaction still carried on after the water supply was cut but soon after reversed to an endothermic reaction coupled with a loss of mass, as the sample released excess water. The water content did not balance out before the next measurement stage began.

The sample started into the 2nd cycle with a water content of n = 139.6 {H_2O} per unit {$5SrBr_2 + 16CaCl_2$}.

During the 2nd dehydration four overlapping peaks were observed at T_{p1} = 89.45°C, T_{p2} = 99.31°C occurred during the isothermal stage, T_{p3} = 130.0°C and T_{p4} = 160.47°C. The water content declined to n = 76.7 {H_2O} per unit {$5SrBr_2 + 16CaCl_2$} after the first peak, sank to n = 45.4 {H_2O} per unit {$5SrBr_2 + 16CaCl_2$} during the isothermal stage and reached n = 14.0 {H_2O} per unit {$5SrBr_2 + 16CaCl_2$} after heating to T_{max} = 200°C during the cooldown stage.

The 2nd hydration curve was similar to the 1st hydration curve with three overlapping peaks at e = 8.65mbar with an enthalpy of H_1 = 83.74Jg^{-1}, e = 14.80mbar with an enthalpy of H_2 = 373.04Jg^{-1} and e = 17.66mbar with H_3 = 288.43Jg^{-1} for a total of Hall = 745.22Jg^{-1}. The sample was holding a maximum water content of n = 139.1 {H_2O} per unit {5$SrBr_2$ + 16$CaCl_2$} during the hydration, which equals 69.7% of the observed minimum sample weight. There was a carry-over of reaction after the water supply was cut followed by a reverse into an endothermic reaction and release of excess water. The water content did not balance out before the next measurement stage began.

The sample started into the 3rd cycle with a water content of n = 126.5 {H_2O} per unit {5$SrBr_2$ + 16$CaCl_2$}.

Again, four overlapping peaks occurred during the 3rd dehydration at T_{p1} = 87.87°C, T_{p2} = 99.09°C during the isothermal stage, T_{p3} = 128.81°C and T_{p4} = 159.98°C. After the first peak at T = 97°C, the water content declined to n = 71.0 {H_2O} per unit {5$SrBr_2$ + 16$CaCl_2$} during the isothermal stage it was reduced to n = 41.9 {H_2O} per unit {5$SrBr_2$ + 16$CaCl_2$} and sank to n = 14.0 {H_2O} per unit {5$SrBr_2$ + 16$CaCl_2$} at T = 175°C directly after the fourth peak. The minimum sample weight was observed during the cooldown stage, where the water content was estimated as n = 13.3 {H_2O} per unit {5$SrBr_2$ + 16$CaCl_2$}.

Sample #2 was holding n = 15.0 {H_2O} per unit {5$SrBr_2$ + 16$CaCl_2$} at the start of the measurement. The sample was taking up water at e = 18.68mbar until it reached a temperature of T = 59.48°C and a water content of n = 43.7 {H_2O} per unit {5$SrBr_2$ + 16$CaCl_2$} which equals 21.3% of the observed minimum sample weight. Upon further heating the sample only dehydrated to a water content of n = 42.0 {H_2O} per unit {5$SrBr_2$ + 16$CaCl_2$}, which equals 20.3% of the observed minimum sample weight, where it remained stable until a temperature of T = 99.28°C was reached. After heating to T_{max}

= 110°C during the cooldown stage, the water content continued to decline to n = 23.5 {H_2O} per unit {$5SrBr_2 + 16CaCl_2$} before it started to recover to n = 47.8 {H_2O} per unit {$5SrBr_2 + 16CaCl_2$} at T = 62.98°C. When the water supply was cut off, the water content stabilized at n = 44.5 {H_2O} per unit {$5SrBr_2 + 16CaCl_2$} at T = 64.11°C.

Heating the sample to T_{max} = 500°C showed four peaks at T_{p1} = 68.04°C, T_{p2} = 148.89°C, T_{p3} = 162.81°C and T_{p4} = 224.51°C. Peaks one to three were overlapping and the third peak showed characteristics of a melting event. An exothermic event, which was likely caused by a solidification of the sample, was observed during the cooldown stage. The water content sank to n = 43.5 {H_2O} per unit {$5SrBr_2 + 16CaCl_2$} at T = 93°C after the first peak and to about n = 7.1 {H_2O} per unit {$5SrBr_2 + 16CaCl_2$} at T = 188°C after the third peak. The sample did not dehydrate completely and was still carrying an estimated amount of n = 6.7 {H_2O} per unit {$5SrBr_2 + 16CaCl_2$} at T = 500°C.

Table 13 TGA/DSC results for the bromide-sulfate and bromide-chloride inter-mixtures. Energy storage density was normalized by the maximum mass of the hydrated samples. Water uptake and water loss were calculated by the observed minimum sample weight.

Materials	Energy storage density [Jg^{-1}] T_{max} = 100°C	Water uptake wgt [%] T_{max} = 100°C	Energy storage density [Jg^{-1}] T_{max} = 200°C	Water uptake wgt [%] T_{max} = 200°C	Water loss wgt [%] T_{max} = 500°C
{4$SrBr_2$+ 3$MgSO_4$}	249.02	73.27	370.83	56.00	48.29
{2$SrBr_2$+ 3$MgSO_4$}	230.37	52.62	329.36	41.98	88.00
{$SrBr_2$ + 3$MgSO_4$}	289.10	56.64	218.11	36.06	33.88
{2$SrBr_2$ + 5KCl}	385.93	22.69	371.34	26.61	---
{$SrBr_2$ + 5KCl}	196.31	14.41	196.08	12.90	---
{$SrBr_2$ + 10KCl}	72.72	4.95	73.46	7.00	---
{5$SrBr_2$ + 4$CaCl_2$}	721.59	50.83	791.98	50.92	16.99
{5$SrBr_2$ + 8$CaCl_2$}	589.46	83.36	691.64	54.49	24.10
{5$SrBr_2$ + 16$CaCl_2$}	709.08	82.46	745.22	69.67	23.39

5.5. Calculated $c_p(T)$ trends from TGA/DSC results

Schematics showing the values calculated from the spot samples and the c_p trends fitted to them for each of the chosen materials are found in the appendix 5.1.

The trends used for calculation of $\Delta\phi$ and ΔH are found in Table 14.

Table 14 calculated temperature dependent c_p trends for different materials which were evaluated during the laboratory scale stage. Only the trends gauged from TGA/DSC spot samples were used for calculating heat $\Delta\Phi$ and enthalpy ΔH. In cases where not enough valid TGA/DSC data was available, the T = 25°C value from literature was added to calculate the corresponding trend.

Material	$c_p(T)$ [kJ(kgK)$^{-1}$], (T [°C])	Sources
{$CaCl_2 \cdot xH_2O$} [1]	$c_p(T) = 2.57 \cdot 10^{-07} \cdot T^3 + 18.63 \cdot 10^{-07} \cdot T^2 - 135.50 \cdot 10^{-04} \cdot T + 1.40$	TGA/DSC, (Georgia State University, 2017) (Warren, 2017)
{KCl}	$c_p(T) = 0.0003 \cdot T + 0.6774$	(Kolesov, Paukov, & Skuratov, 1962)
{KCl}	$c_p(T) = 0.0137 \cdot \ln(T) + 0.6852$	(Barskii & Egorov, 1993)
{KCl}	$c_p(T) = 0.0092 \cdot \ln(T) + 0.6504$	(Burns & Verall, 1974)
{KCl}	$c_p(T) = 3.07 \cdot 10^{-11} \cdot T^5 - 714.12 \cdot 10^{-11} \cdot T^4 - 151.85 \cdot 10^{-08} \cdot T^3 + 563.12 \cdot 10^{-06} \cdot T^2 - 441.22 \cdot 10^{-04} \cdot T + 1.43$	TGA/DSC
{$MgCl_2$}	$c_p(T) = -5 \cdot 10^{-06} \cdot T^2 + 0.0013 \cdot T + 0.6974$	(Biermann, et al., 1989)
{$MgCl_2 \cdot xH_2O$}	$c_p(T) = -1.19 \cdot 10^{-07} \cdot T^3 - 121.69 \cdot 10^{-07} \cdot T^2 + 920.48 \cdot 10^{-05} \cdot T + 1.00$	TGA/DSC

[1] Since the dehydration curve of the {$CaCl_2$} sample shows three overlapping peak events spanning the entire temperature interval from T = 25 to 200°C, the calculated trend leans on the T = 25°C values for different hydrates by (Warren, 2017).

{$Mg(OH)Cl \cdot xH_2O$} [2]		
{$SrBr_2 \cdot xH_2O$}	$c_p(T) = 4.85 \cdot 10^{-08} \cdot T^3 + 176.469 \cdot 10^{-07} \cdot T^2 + 210.89 \cdot 10^{-05} \cdot T + 0.25$	TGA/DSC, (MatWeb, LLC, 2017)
{$ZnCl_2$}	$c_p(T) = 0.0018 \cdot T + 0.4793$	(Hargittai, Tremmel, & Hargittai, 1986)
{$ZnCl_2 \cdot xH_2O$}	$c_p(T) = -6.73 \cdot 10^{-06} \cdot T^2 + 875.70 \cdot 10^{-06} \cdot T + 0.725$	TGA/DSC
{$2MgCl_2 + CaCl_2 + xH_2O$} {$2Mg(OH)Cl + CaCl_2 + xH_2O$} [3]	$c_p(T) = -3.89 \cdot 10^{-07} \cdot T^3 - 569.05 \cdot 10^{-07} \cdot T^2 + 200.13 \cdot 10^{-04} \cdot T + 1.78$	TGA/DSC
{$MgCl_2 + KCl + xH_2O$}	$c_p(T) = -4 \cdot 10^{-06} \cdot T^2 + 0.0014 \cdot T + 0.7075$	(Biermann, et al., 1989)
{$2MgCl_2 + KCl + xH_2O$}	$c_p(T) = -2.60 \cdot 10^{-05} \cdot T^2 + 156.42 \cdot 10^{-5} \cdot T + 2.37$	TGA/DSC
{$5SrBr_2 + 8CaCl_2 + xH_2O$}	$c_p(T) = 2.41 \cdot 10^{-07} \cdot T^3 - 253.44 \cdot 10^{-07} \cdot T^2 - 158.98 \cdot 10^{-04} \cdot T + 2.46$	TGA/DSC
{$2ZnCl_2 + CaCl_2 + xH_2O$} [4]	$c_p(T) = -5.95 \cdot 10^{-08} \cdot T^2 + 108.24 \cdot 10^{-05} \cdot T + 0.30$	TGA/DSC

[2] The {$MgCl_2$} underwent a reaction to {Mg(OH)Cl}, while the hydrated sample was emitting {HCl} in the temperature interval between T = 110 to 200°C of its 2nd dehydration.

[3] The {$MgCl_2$}-component of the mixture underwent a reaction to {Mg(OH)Cl}, while the hydrated sample was emitting {HCl} in the temperature interval between T = 110 to 200°C of the 2nd dehydration.

[4] The dehydration curves of the {$2ZnCl_2 + CaCl_2$} mixture show constant phase changes only interrupted during the stage of constant temperature at T = 100°C for a time interval of Δt = 11min, where reliable spot samples to calculate the c_p values were taken. However, the 2nd and 3rd dehydration curve show a distinct difference in heat flow within this time interval, though the calculated water content of the sample does not differ. It is possible that, while no melting peaks have been identified, the sample was partially molten and that the percentage of molten content varied between the two measurements.

5.6. Multi-cycle measurements

A measurement over three cycles can serve to sort out materials of low heat storage density or those which are prone to melting or dissolving easily and those which won't dehydrate at low temperatures or those that bind water into their crystal lattice in irreversible reactions. Such materials may show their undesired properties early on but to verify an improved cycle stability for a material, a series of dehydration-hydration cycles needs to be recorded. Three materials were selected for a test series, as they displayed both stability and high heat storage capacities during the previous 3-cycles TGA/DSC analysis.

5.6.1. {$MgCl_2$ + $CaCl_2$}

An m = 10mg {$2MgClr_2$ + $CaCl_2$} sample was evaluated in a 25 cycles TGA/DSC measurement. The cycles started with a dehydration at T_{max} = 120°C with a heating rate β = 1Kmin^{-1}, followed by a hydration in three stages with a partial water vapor pressure of e = 8.65 to 17.66mbar.

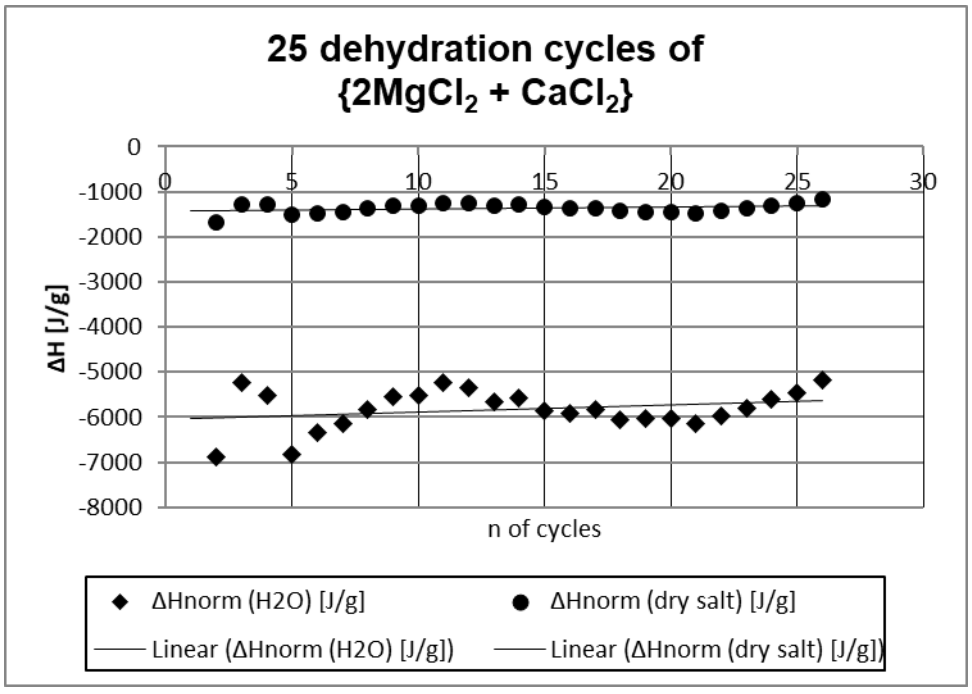

Figure 14 Total reaction enthalpy ΔH of an m = 10mg sample of {$2MgCl_2$+$CaCl_2$} over dehydrations at T_{max} = 120°C from 25 cycles. $\Delta H_{norm\ (H2O)}$ was normalized over the total mass change during dehydration Δm, while $\Delta H_{norm\ (dry\ salt)}$ was normalized over the minimum sample weight m_{min} measured for all 25 cycles.

Figure 14 shows the total dehydration enthalpy ΔH for the 25 dehydrations of the sample, normalized over the minimum mass m_{min} measured during all 25 cycles, which however does not equal the anhydrate mass, and the total dehydration enthalpy normalized over the measured mass change $\Delta m_{(H2O)}$. While $\Delta H_{(dry\ salt)}$ remains stable during the measurements, the $\Delta H_{(H2O)}$ shows a slight upwards trend, indicating that releasing the water requires less energy with every cycle.

Figure 15 shows the total hydration enthalpy ΔH for the 25 hydrations of the sample, normalized over the minimum mass m_{min} measured during all 25 cycles and the total hydration enthalpy normalized over the measured mass change $\Delta m_{(H2O)}$. Both $\Delta H_{(dry\ salt)}$ and $\Delta H_{(H2O)}$ show an upwards trend, indicating that both the sample and the water release more energy with every cycle and the heat storage density improves.

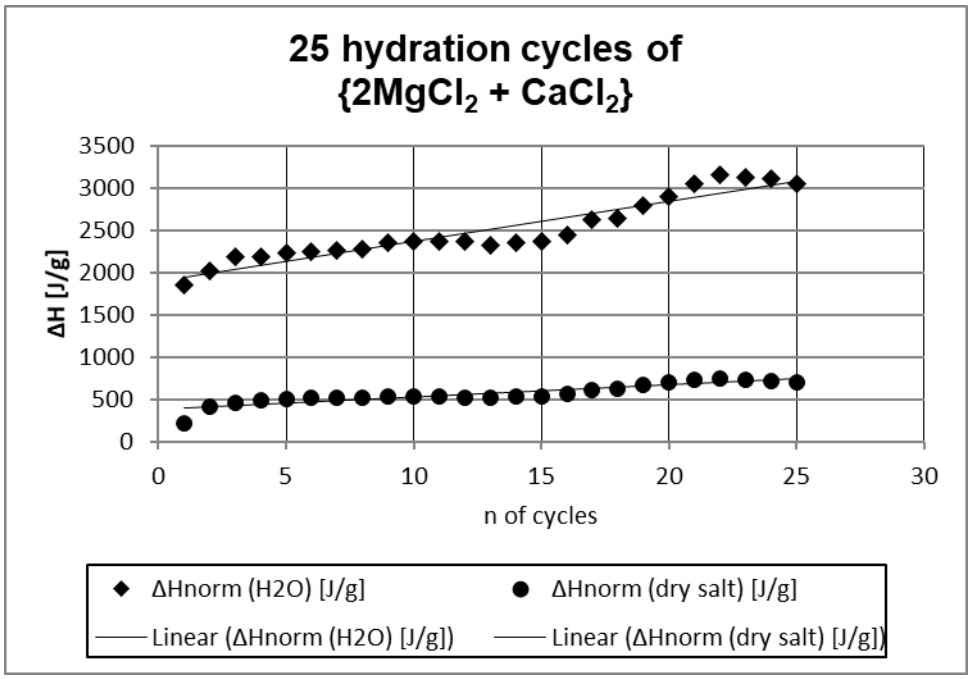

Figure 15 Total reaction enthalpy ΔH of an m = 10mg sample of {2MgCl₂+CaCl₂} over hydrations from 25 cycles. $\Delta H_{norm\ (H2O)}$ was normalized over the total mass change during dehydration Δm, while $\Delta H_{norm\ (dry\ salt)}$ was normalized over the minimum sample weight m_{min} measured for all 25 cycles.

5.6.2. {$MgCl_2$ + KCl}

An m = 10mg {$2MgClr_2$ + KCl} sample was evaluated in a 25 cycles TGA/DSC measurement. The cycles started with a dehydration at T_{max} = 120°C with a heating rate β = 1Kmin^{-1}, followed by a hydration in three stages with a partial water vapor pressure of e = 8.65 to 17.66mbar.

Figure 16 shows the total dehydration enthalpy ΔH for the 25 dehydrations of the sample, normalized over the minimum mass m_{min} measured during all 25 cycles and the total dehydration enthalpy normalized over the measured mass change $\Delta m_{(H2O)}$. Both $\Delta H_{(dry\ salt)}$ and $\Delta H_{(H2O)}$ show a slight upwards trend, indicating that releasing the water requires less energy with every cycle.

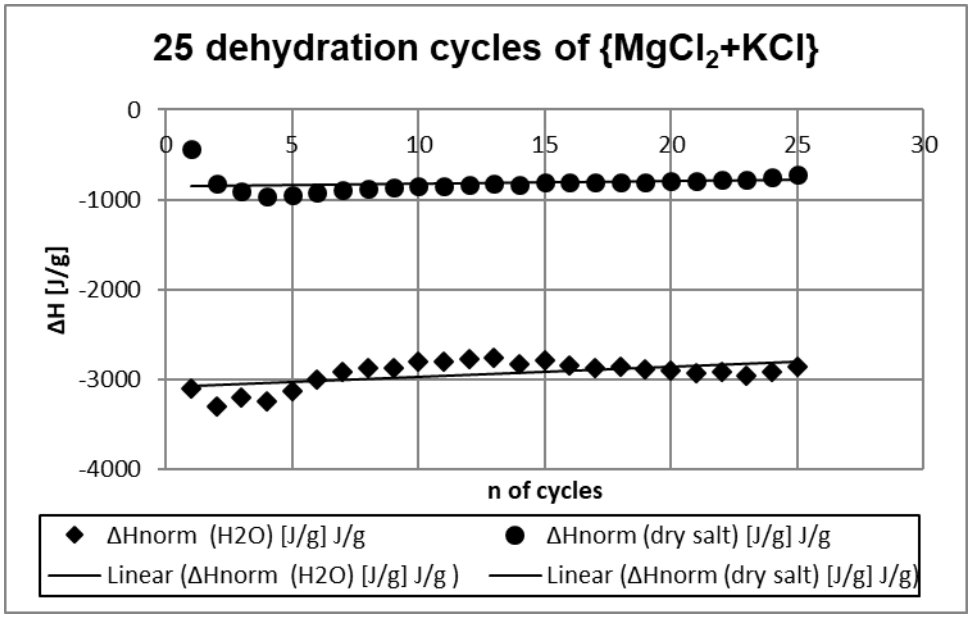

Figure 16 Total reaction enthalpy ΔH of an m = 10mg sample of {$2MgCl_2$+KCl} over dehydrations at T_{max} = 120°C from 25 cycles. $\Delta H_{norm\ (H2O)}$ was normalized over the total mass change during dehydration Δm, while $\Delta H_{norm\ (dry\ salt)}$ was normalized over the minimum sample weight m_{min} measured for all 25 cycles.

Figure 17 shows the total hydration enthalpy ΔH for the 25 hydrations of the sample, normalized over the minimum mass m_{min} measured during all 25 cycles and the total hydration enthalpy normalized over the measured mass change $\Delta m_{(H2O)}$. While $\Delta H_{(water)}$ shows an upward trend, $\Delta H_{(dry\ salt)}$ remains relatively stable

over the cycles, indicating that the water absorbed in the reaction releases more heat with every cycle.

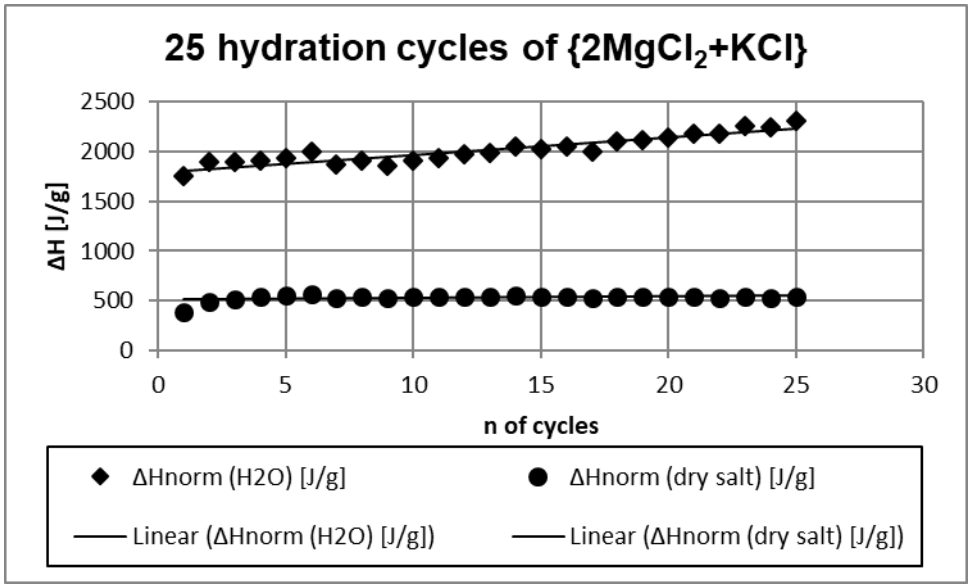

Figure 17 Total reaction enthalpy ΔH of an m = 10mg sample of {$2MgCl_2$+KCl} over hydrations from 25 cycles. $\Delta H_{norm\ (H2O)}$ was normalized over the total mass change during dehydration Δm, while $\Delta H_{norm\ (dry\ salt)}$ was normalized over the minimum sample weight m_{min} measured for all 25 cycles.

5.6.3. {$SrBr_2$ + $CaCl_2$}

An m = 10mg {$5SrBr_2$ + $8CaCl_2$} sample was evaluated in a 10 cycles TGA/DSC measurement. The cycles started with a dehydration at T_{max} = 100°C with a heating rate β = 1Kmin^{-1}, followed by a hydration in three stages with a partial water vapor pressure of e = 8.65 to 17.66mbar.

Figure 18 shows the total dehydration enthalpy ΔH for the 10 dehydrations of the sample, normalized over the minimum mass m_{min} measured during all 10 cycles and the total dehydration enthalpy normalized over the measured mass change $\Delta m_{(H2O)}$. Both $\Delta H_{(dry\ salt)}$ and $\Delta H_{(H2O)}$ remain relatively stable from the 3rd dehydration onward.

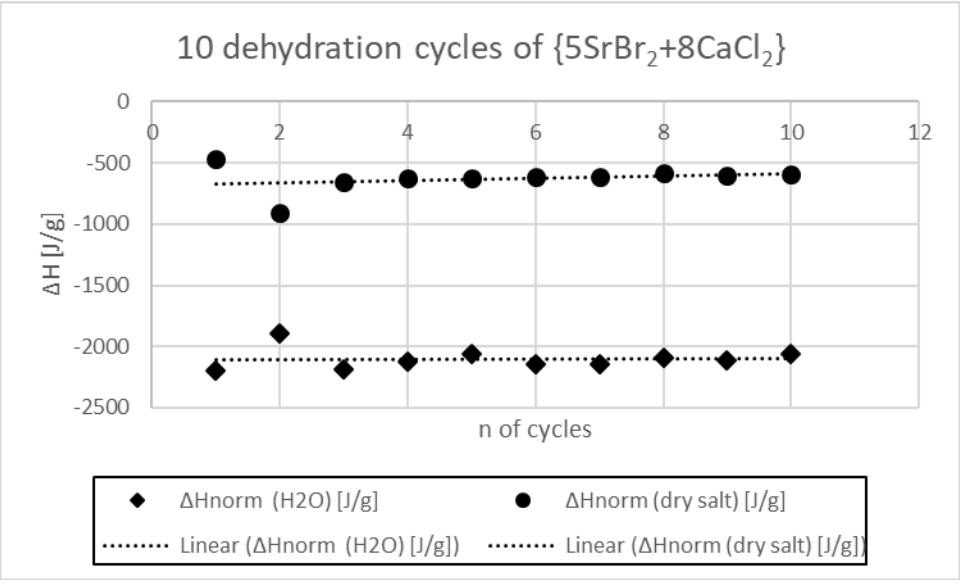

Figure 18 Total reaction enthalpy ΔH of an m = 10mg sample of {$5SrBr_2$+$8CaCl_2$} over dehydrations at T_{max} = 100°C from 10 cycles. $\Delta H_{norm\ (H2O)}$ was normalized over the total mass change during dehydration Δm, while $\Delta H_{norm\ (dry\ salt)}$ was normalized over the minimum sample weight m_{min} measured for all 10 cycles.

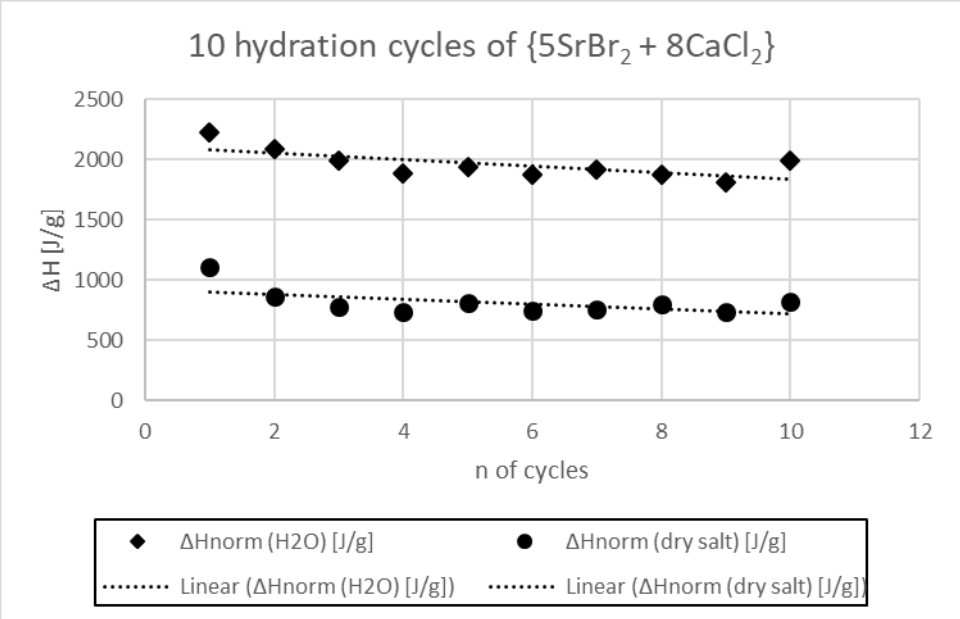

Figure 19 Total reaction enthalpy ΔH of an m = 10mg sample of {$5SrBr_2$+$8CaCl_2$} over hydrations from 10 cycles. $\Delta H_{norm\ (H2O)}$ was normalized over the total mass change during dehydration Δm, while $\Delta H_{norm\ (dry\ salt)}$ was normalized over the minimum sample weight m_{min} measured for all 10 cycles.

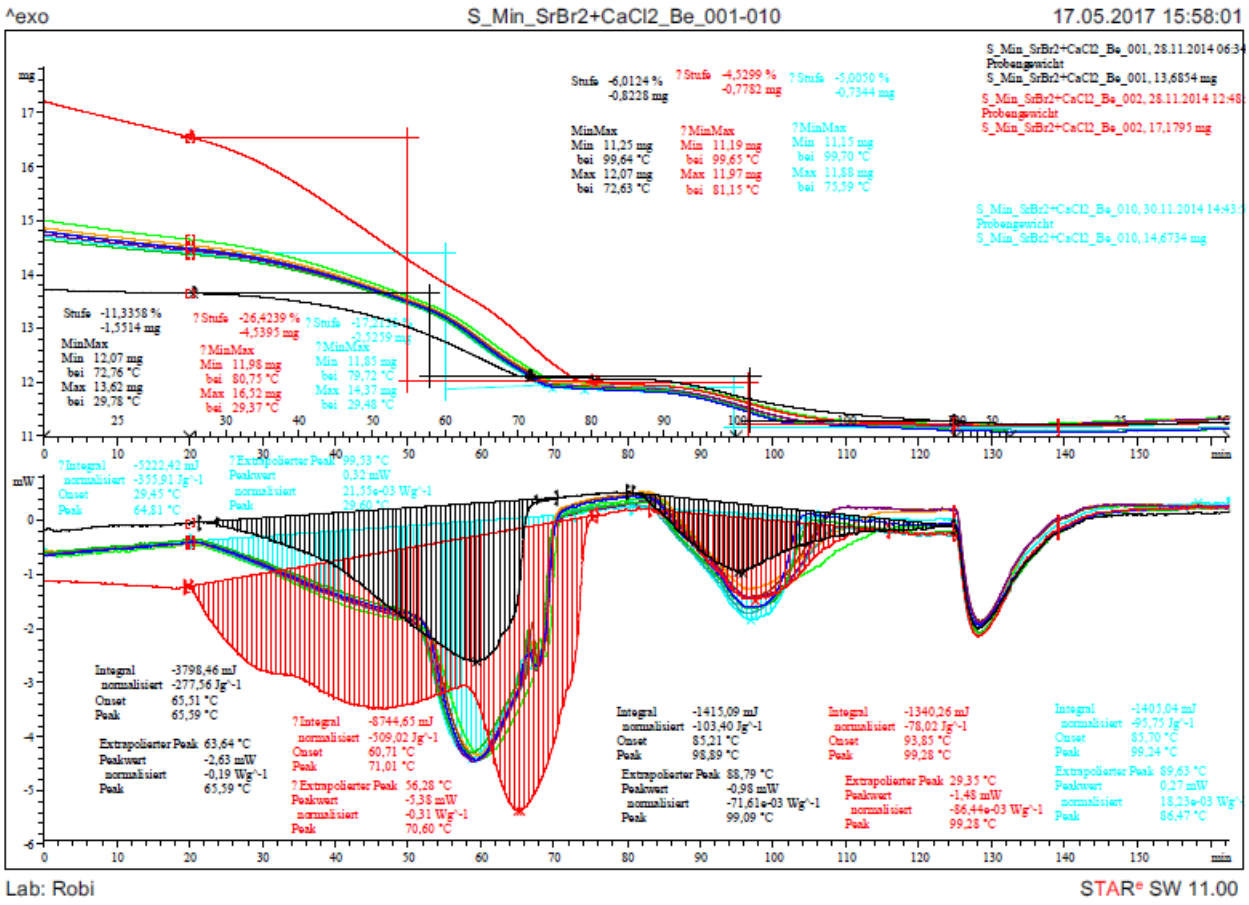

Figure 20 Dehydrations 01-10 of a {5$SrBr_2 \cdot 6H_2O$+ 8$CaCl_2 \cdot 6H_2O$} mixture. During the 1st dehydration (black curve) the material lost mass and absorbed energy below average, while during the 2nd dehydration (cyan curve), the mass loss and energy absorption were higher than average. From 3rd dehydration on, the material remains stable for all following dehydrations with only minor shifts in sample mass between dehydration curves.

Figure 19 shows the total hydration enthalpy ΔH for the 10 hydrations of the sample, normalized over the minimum mass m_{min} measured during all 10 cycles and the total hydration enthalpy normalized over the measured mass change $\Delta m_{(H2O)}$. While $\Delta H_{(water)}$ and $\Delta H_{(dry\ salt)}$ both show a downward trend, indicating the sample releases less heat during hydration with every cycle, it also shows that both trends are mostly influenced by the first three cycles after which the material stabilizes over the following cycles.

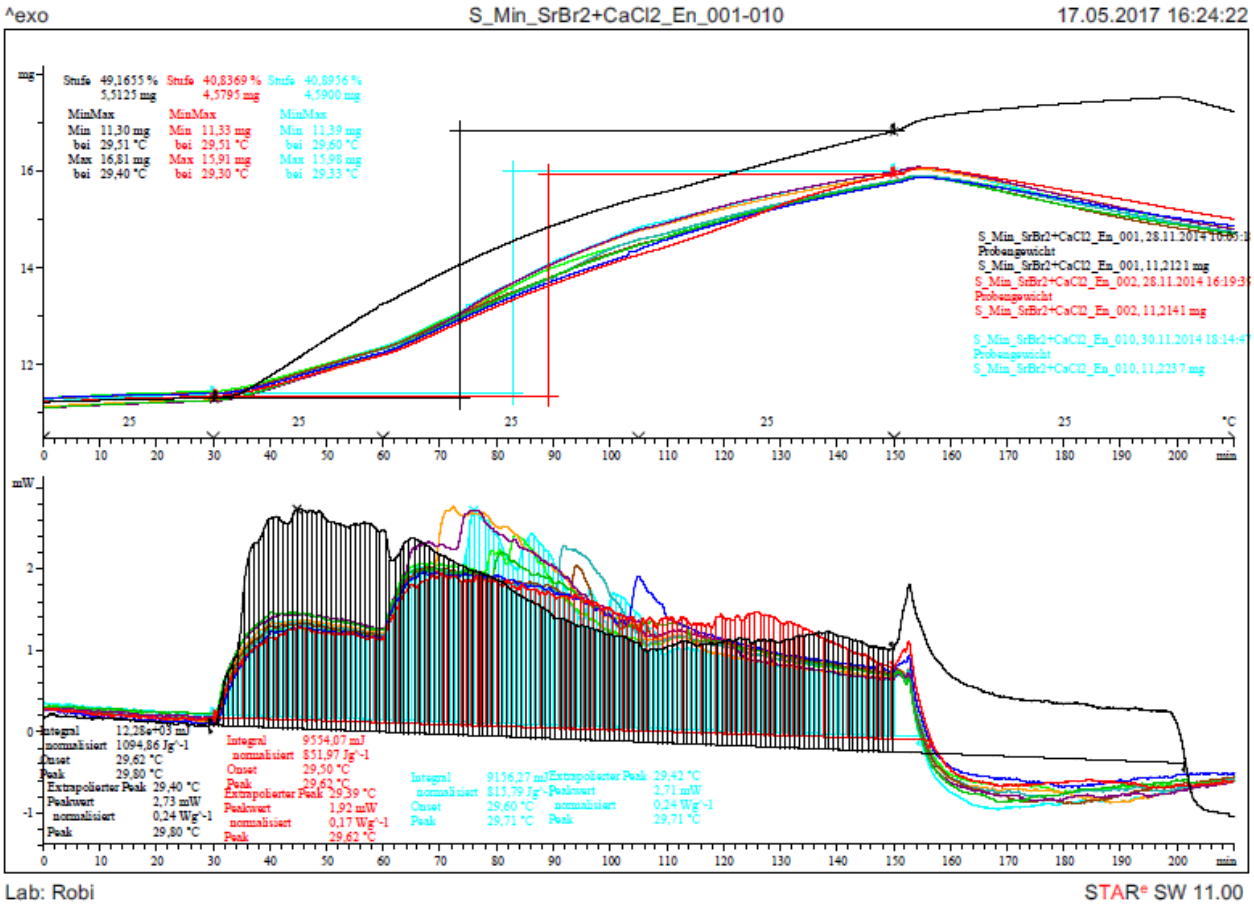

Figure 21 Hydration 01-10 of a {5SrBr₂·6H₂O + 8CaCl₂·6H₂O} mixture. During the 1st hydration (black curve) the sample absorbs water and releases energy above average. From 2nd hydration onward the curves remained mostly stable with some irregular peaks at $\dot{V}(N_2)$ = 75 [ml min^{-1}] which equals a water vapor pressure of e = 14.80mbar. The material gets over-hydrated at $\dot{V}(N_2)$ = 125 [ml min^{-1}] which equals a water vapor pressure of e = 17.66mbar and will expel the excess water as soon as the supply is shut off, in an exothermic reaction turning endothermic.

The stabilizing over the cycles can be observed in the TGA/DSC hydration and dehydration curves as well, where the curves #1 and #2 of the dehydration show a strong shift in weight loss and heat flow until the curves stabilize from #3 to #10 as seen in Figure 20.

Figure 21 shows the settling of the 10 hydrations curves after the unusual high mass gain during the 1st hydration. As the mass was still increasing after the water supply should have been cut off, it is possible that a malfunction in the water flow regulation caused the irregular result

6. Measurement results for upscaled sample size

6.1. Results for laboratory scale evaluations by setup #01 with liquid water supply

As the first testing material, a {$2MgCl_2 + CaCl_2$} sample was chosen. While an increase in temperature in the dissolved sample and the air in the sample bottle was measured and recorded for analysis during hydration, it was observed that the water vapor was not easily leaving the sample bottle during the dehydration steps. The water vapor only reached the cooling trap once a temperature of T = 150°C was surpassed and it took temperatures of up to T_{max} = 188.5°C to dry the sample within the bottle completely. Until that threshold was reached the water re-liquefied still within the sample bottle and joined back with the sample. The results of the measurement can be seen in Table 15. The corresponding measured temperature curves can be found in the appendix 6.1. The litmus paper color indicator showed the vapor in the sample bottle turning acidic during the dehydration, likely caused by {HCl} emissions. The experiment was upgraded to setup #2 after this measurement to improve the flow of the water vapor.

Table 15 Dehydration times and temperatures for experimental setup #01 with liquid water supply.

Setup #1 liquid water	Dehydration time [min]	Dehydration $T_{max\ sample}$ [°C] {$2MgCl_2 + CaCl_2$}	Dehydration $T_{max\ air}$ [°C]	pH $_{min}$	Hydration $T_{max\ sample}$ [°C] {$2MgCl_2 + CaCl_2$}	Hydration $T_{max\ air}$ [°C]
Cycle_01	159	188.5	159.0	1	39	32
Cycle_02	82	241.0	167.0	---	55	38

6.2. Results for laboratory evaluations by scale setup #02 with liquid water supply

The cycle measurement of a {$2MgCl_2 + CaCl_2$} sample was repeated with the experimental setup #2. The evaluation results can be seen in Table 16. The temperature curves for this measurement can be found in the appendix 6.2.

Table 16 Dehydration times and temperatures for experimental setup #02 with liquid water supply.

Setup #2 liquid water	time [min]	Dehydration $T_{max\ sample}$ [°C] {$2MgCl_2 + CaCl_2$}	pH_{min}	Water collected [ml]	Hydration $T_{max\ sample}$ [°C] {$2MgCl_2 + CaCl_2$}
Cycle_01	124	188.5	1	Marginal amount	77
Cycle_02	54	241.0	Not measured	13	62

While the applied vacuum pump brought an improvement by aiding the water vapor flow out of the sample bottle, the sample still needed high temperatures before the water vapor escaped the sample bottle during dehydration.

It was also observed, that the sample did not solidify at the bottom of the flask during dehydration but formed a ring around the inner flask surface at the level of the brine solution's surface during hydration. During the next hydration, only a part of the sample was in contact with the water. This hampered the measurement as more water had to be added while the reaction had already started, to cover the entire sample. Introducing a second volume of cold water to the system, altered the recorded temperature curve. As a result, the setup was changed to operate with water vapor instead of liquid water after this measurement.

6.3. Results for laboratory scale evaluations by setup #01 with water vapor

First tests with mixed salts that did well in the TGA/DSC measurements as well as with the untreated educts showed a variety of material behavior. A schematic with the temperature curves measured with this setup can be found in the appendix.

The maximum temperatures of {$CaCl_2$}, {$MgCl_2$}, {$2MgCl_2$+$CaCl_2$} and {$2MgCl_2$+KCl} which were reached during hydration can be seen in Table 17, with the maximum temperatures of the two tested types of mixed salts during the second measurement exceeding the maximum temperatures during the first measurement of the same material by ΔT = 25 to 31°C.

Material	T_{max} [°C]
{$MgCl_2$}	84.8
{$CaCl_2$}	92.6
{2$MgCl_2$ + $CaCl_2$} #01	48.9
{2$MgCl_2$ + $CaCl_2$} #02	73.9
{2$MgCl_2$ + KCl} #01	53.9
{2$MgCl_2$ + KCl} #02	85.0

Table 17 Measured maximum temperatures for m = 20g samples of different materials at dehydration in experimental setup #1 (with water vapor). The materials were oven dried at T_{max} = 120°C before and between measurements.

The temperature curves for {$MgCl_2$}, {2$MgCl_2$+$CaCl_2$} #01, {2$MgCl_2$+$CaCl_2$} #02 and {2$MgCl_2$+KCl} #01 showed sudden drops, which were likely caused by a breach in the vacuum sealing of the apparatus, which brought the production and flow of water vapor to a halt. While all the tested materials are drying-agents and can draw humidity from a water supply by themselves, the process is too slow to cause a measurable reaction.

6.4. Results for laboratory scale evaluations by setup #02 with water vapor

The heat during dehydration proved to be instable and varied between T_{max} = 140 to 180°C. As a countermeasure the tinfoil insulation wrapped around the sample bottle was removed after the first measurements, to keep the maximum temperature at T_{max} ~125°C. As keeping the temperature within the sample holder too high during hydration can slow down the reaction, since several materials proved not to take up water beyond T = 60°C during the TGA/DSC measurements. As recording the immediate material reaction was deemed more important than prolonging the cooldown process, the sample bottle was no longer insulated during the hydration stage either. For which of the measurements the tinfoil wrapping was still used is noted for the individual samples.

The $c_p(T)$ trends estimated from the TGA/DSC measurements were used for calculating the heat flow $\Delta\varphi$ and enthalpy ΔH for the laboratory scale temperature measurements. Changes in mass of the samples were disregarded in calculation during this stage.

All figures with temperature curves recorded and their chosen baselines, specific heat capacity trends and calculated heat flow curves from this stage of the measurements can be found in the appendix 6.3.

6.4.1. Köstrolith

To find the optimal drying durations and determine, whether the setup itself influences the cycle stability of the materials, first tests were made with the adhesion based drying agent Köstrolith (CWK Chemiewerk Bad Köstritz GmbH, 2017) rather than with a chemically reacting sample. With material alterations caused by chemical reactions excluded as a cause, any changes in the material's behavior had to happen due to either changes in the testing parameters or the setup of the apparatus. The test results can be seen in Table 18 and Figure 52.

Table 18 Five cycle measurements of a 20g Köstrolith sample in laboratory setup #2 with varying drying times and temperatures. Tinfoil insulation was used during dehydration.

Setup #2 Water vapor Köstrolith Cycle (with tinfoil)	Drying time t [min]	Drying temperature T[°C]	Maximum heating rate β_{max} [Kmin^{-1}]	Maximum hydration temperature T_{max} [°C]
#1 (factory dried)	357	123.5	8.5	145.7
#2	159	127.3	3.9	73.7
#3 (recording failure at dehydration)	~360	~127.0	---	62.8
#4 (oven dried)	360	120.0	---	87.2
#5	230	137.5	4.2	102.9

While a decline in the heat yield was to be expected between the first two cycles as the material was factory dried at an unknown temperature, a further decline was observed during the 3rd cycle. An extended drying period of t_3 = 360 min over t_2 = 160 min did not stop the decline in the heat yield. Only after being removed from

the sample holder and dried separately in the oven at T_4 = 120°C at the 4th cycle and being exposed to an increased drying temperature of T_5 = 137°C by applying a tinfoil insulation at the 5th cycle, the material recovered.

6.4.2. Silicagel

Like Köstrolith, Silicagel is an adhesion based drying agent. The sample (Roth, 2017) was laced with a color indicator, to indicate its state of dryness. As this indicator destabilizes at temperatures T > 140°C and the specification sheet recommends a drying time of t_{rec} = 240 min at T_{rec} = 130°C, this was assumed to be the factory dried state before the start of the first measurement.

Table 19 Maximum drying and hydration temperatures for an m = 20g factory dried Silicagel sample as measured with the experimental setup #2 (with water vapor supply) for three cycles where the sample was dried two times in-situ and a 4th cycle, where the sample was oven dried beforehand.

Setup #2 Water vapor Silicagel Cycle	Drying time t [min]	Drying temperature T[°C]	Maximum heating rate β_{max} [Kmin^{-1}]	Maximum hydration temperature T_{max} [°C]
#1 (factory dried)	~240	~130.0	---	75.1
#2 (recording error during dehydration)	~240	~111.4	0.6	53.5
#3	262	125.1	0.8	63.1
#4 (oven dried)	240	120.0	---	66.8

During the dehydration stage of the 2nd cycle, the measurement equipment failed to record, so the exact drying time and maximum temperature are not known. However, the difference of maximum temperatures reached during the hydration stage between the 1st and the 2nd cycle of ΔT = 21.6°C indicate that either one or both remained below the recommendation. The material recovered during the 3rd cycle and showed similar temperature yield after being oven dried during the heating stage of the 4th cycle. The results can be seen in Table 19 and Figure 53.

While the test of setup #2 with silica gel showed a recovery of the material after a few cycles, the tests with Köstrolith indicated an incomplete dehydration which can lead to the buildup of layers of differently hydrated phases within the sample holder. It was observed, that like in previous setups, water was not leaving the sample holder easily during dehydration.

6.4.3. {$CaCl_2 \cdot 6H_2O$}

Instead of a factory dried {$CaCl_2$} sample, the hydrated phase {$CaCl_2 \cdot 6H_2O$} was chosen for the evaluation to allow for a better comparability with the mixed salts synthesized from liquid solution.

The maximum hydration temperatures measured over three cycles can be seen in Table 20.

Table 20 Experimental setup #2, hydration measurement for a 20g {$CaCl_2 \cdot 6H_2O$} sample after dehydration with varying drying times. The sample was dried in the oven before the 1st hydration measurement in the apparatus.

Setup #2 Water vapor {$CaCl_2$} Cycle	Drying time t [min]	Drying temperature T [°C]	Maximum heating rate β_{max} [$Kmin^{-1}$]	Maximum hydration temperature T_{max} [°C]
#1 (oven dried)	~ 240	~120.0	---	57.7
#2	226	129.8	7.3	75.6
#3	235	121.6	6.8	61.7

n of cycles	T_{peak} [°C]	ΔH [Jg^{-1}]
#1	25.5 57.7	-1.60 172.21
#2	75.6	244.52
#3	25.3 61.7	-0.27 194.82

Table 21 Hydration peaks and enthalpy for hydrations 1 to 3 of a 20g {$CaCl_2$} sample over an interval of Δt = 30min, where the vacuum pump was activated. The two endothermic peaks observed are likely to be artifacts from applying the baselines. Changes in material weight were neglected.

The hydration curves show a flux in temperature yield for the 2nd hydration, where the drying

temperature during dehydration had been slightly elevated by about ΔT ~ 8°C compared to the 1st and the 3rd dehydration.

The enthalpy for the sample was calculated for this evaluation, since the equivalent measurement with setup #3 failed later the results are listed in Table 21.

6.4.4. {KCl}

The KCl sample showed temperature curves during hydration, which were similar to those of the calculated corresponding baselines. Only a low rise in temperature was observed as can be seen in Table 22, which was likely caused by the water vapor streaming through the sample being marginally heated by the water bath used to keep the temperature of the water supply at T = 25°C for easier evaporation.

Table 22 Hydration measurements for a 20g {KCl} sample after dehydration with varying drying times and temperatures. Only marginal changes in temperature were observed.

Setup #2 Water vapor {KCl} Cycle	Drying time t [min]	Drying temperature T [°C]	Maximum heating rate β_{max} [$Kmin^{-1}$]	Maximum hydration temperature T_{max} [°C]
#1 oven dried	~240	~120.0	---	27.5
#2	165	112.8	9.6	25,6

n of cycles	T_{peak} [°C]	ΔH [Jg^{-1}]
#1	21.0	-0.70
	21.6	1.29
	21.0	-0.85
	27.5	3.18
#2	16.9	-2.37
	25.6	15.71

Table 23 Hydration peaks and enthalpy for hydrations 1 and 2 of a 20g {KCl} sample over an interval of Δt = 30min, where the vacuum pump was activated. The endothermic peaks observed are indicators for a partial dissolving of the cubic {KCl}. Changes in material weight were neglected.

The baselines to the temperature curves of the {KCl} hydrations were not calculated linear in this case. The temperature difference at the end of the measurements between those curves were caused mainly by an abrupt rise in

water temperature when the vacuum was turned off during both hydration measurements.

The heat flow was calculated under the assumption, that the sample mass didn't change during measurements.

6.4.5. {$MgCl_2 \cdot 6H_2O$}

Instead of factory dried magnesium chloride {$MgCl_2$}, a magnesium chloride hexahydrate sample {$MgCl_2 \cdot 6H_2O$} was chosen for the measurement and oven dried before being placed in the sample holder for the 1st hydration for better comparison with the samples synthesized from brine solutions. The varying drying times and temperatures for each cycle as well as the temperature yield are displayed in Table 24.

Table 24 Hydration measurement for a 20g {$MgCl_2 \cdot 6H_2O$} sample. The sample was dried in the oven before the 1st hydration measurement in the apparatus. The in-situ drying times increased up to t = 4h.

Setup #2 Water vapor {$MgCl_2$} Cycle	Drying time t [min]	Drying temperature T [°C]	Maximum heating rate β_{max} [$Kmin^{-1}$]	Maximum hydration temperature T_{max} [°C]
#1 (oven dried)	~240	~ 120.0	---	57.6
#2	204	128.7	4.9	103.4
#3	235	129.6	10.2	64.3
#4	236	121.4	6.5	45.2

The material improved its temperature yield between the 1st and the 2nd hydration. This was likely caused by the {HCl} emissions expected at T > 110°C turning the {$MgCl_2$} into {$Mg(OH,Cl)_2$}. With every progressing cycle after the 2nd, a decline in temperature yield was observed, indicating an ongoing change inside the material. This change turned out to be a strong agglomeration of the material which was completely cemented at the end of the cycle-measurements. This reduced the permeability of the sample for the water vapor, resulting in a reduced heat yield.

n of cycles	T_{peak} [°C]	ΔH [Jg^{-1}]
#1	27.1 30.3	-8.58 328.79
#2	103.4	1217.94
#3	64.3	480.39
#4	22.8 42.9	4.67 259.13

Table 25 Hydration peaks and enthalpy for hydrations 1 to 4 of a 20g {$MgCl_2$} sample over an interval of Δt = 30min, where the vacuum pump was activated. Changes in material weight were neglected.

6.4.6. {$SrBr_2 \cdot 6H_2O$}

Strontium bromide hexahydrate was chosen over anhydrate strontium bromide and oven dried before the 1st hydration measurement. The maximum temperatures reached during hydration are shown in Table 26.

Table 26 Experimental setup #2, hydration measurements for a m=20g {$SrBr_2 \cdot 6H_2O$} for three cycles with different drying temperatures. A tinfoil insulation was used during dehydration.

Setup #2 Water vapor {$SrBr_2 \cdot 6H_2O$} Cycle (with tinfoil)	Drying time t [min]	Drying temperature T [°C]	Maximum heating rate β_{max} [$Kmin^{-1}$]	Maximum hydration temperature T_{max} [°C]
#1 (oven dried)	~240	~120.0	---	56.4
#2	242	136.8	8.6	60.0
#3	239	140.0	12.1	57.9

The temperature yield of the sample remained relatively stable over the three measured cycles, despite the maximum drying temperature within the sample holder being increased to T_{max} = 140°C by an insolation wrapping of tinfoil during the two in-situ dehydrations.

n of cycles	T_{peak} [°C]	ΔH [Jg^{-1}]
#1	28.0	0.48
	27.9	-1.37
	56.4	94.25
#2	24.8	-0.66
	58.6	140.65
#3	26.4	-0.21
	57.9	57.40

Table 27 Hydration peaks and enthalpy for hydrations 1 to 3 of a 20g {$SrBr_2$} sample over an interval of Δt = 30min, where the vacuum pump was activated. The weak endothermic peaks indicate either a dissolving process or a phase change at the start of the measurement. Changes in material weight were neglected during calculation.

6.4.7. {$2MgCl_2 + CaCl_2$}

The {$2MgCl_2 + CaCl_2$} sample was sent through four evaluation cycles. The 1st dehydration was done in the oven at T_{max} = 120°C and had the highest temperature yield. The output decreased rapidly at the 2nd hydration but only marginally over the next two cycles, even after the drying time was cut short by an hour. The results can be seen in Table 28.

Table 28 Hydration measurements for a 20g {$2MgCl_2 + CaCl_2$} sample after dehydration with varying drying times and temperatures.

Setup #2 Water vapor {$2MgCl_2 + CaCl_2$} Cycle	Drying time t [min]	Drying temperature T [°C]	Maximum heating rate β_{max} [$Kmin^{-1}$]	Maximum hydration temperature T_{max} [°C]
#1 oven dried	~240	~120.0	---	82.9
#2	239	122.0	6.7	56.5
#3	259	118.3	8.0	53.6
#4	177	119.0	6.7	49.2

n of cycles	T_{peak} [°C]	ΔH [Jg^{-1}]
#1	82.9	1020.42
#2	56.5	593.70
#3	53.6	846.11
#4	49.2	890.79

Table 29 Hydration peaks and enthalpy for hydrations 1 to 4 of a 20g {$2MgCl_2$ +$CaCl_2$} sample over an interval of Δt = 30min. The vacuum pump was activated at the start of the measurements but was deactivated early after 20 to 25 minutes. Changes in material weight were neglected.

6.4.8. {$2MgCl_2$ + KCl}

Three measurement cycles were taken of the {$2MgCl_2$ + KCl} sample. All dehydrations were done in-situ but at different drying times. The recording of the temperature curve of the 1st hydration failed but the maximum temperature was observed as T_{max} ~70°C. The recorded values can be found in Table 30.

Table 30 Hydration measurements for a 20g {$2MgCl_2$ + KCl} sample after dehydration with varying drying times and temperatures.

Setup #2 Water vapor {$2MgCl_2$ + KCl} Cycle	Drying time t [min]	Drying temperature T [°C]	Maximum heating rate β_{max} [$Kmin^{-1}$]	Maximum hydration temperature T_{max} [°C]
#1	215	127.5		~70.0
#2	205	124.3		57.3
#3	121	128.2		51.7

The temperature yield declined after the 1st cycle. The decline between the 2nd and 3rd cycle may have been caused by the drying time being cut short by Δt ~ 85min.

n of cycles	T_{peak} [°C]	ΔH [Jg^{-1}]
#1	~70.0	---
#2	57.3	106.48
#3	51.7	312.63

Table 31 Hydration peaks and enthalpy for hydrations 1 to 3 of a 20g {$2MgCl_2$ + KCl} sample over an interval of Δt = 30min, while the vacuum pump was activated. Changes in material weight were neglected.

6.4.9. {2$ZnCl_2$ + $CaCl_2$}

The {2$ZnCl_2$ + $CaCl_2$} mixture remained solid for the 1st dehydration at T_{max1} = 127.5°C but the sample dissolved partially during the 1st hydration and the liquid escaped the sample holder by leaking through the mesh wire. During the 2nd dehydration an isolation wrapping of tinfoil was applied to the sample holder, which increased the maximum temperature within to T_{max2} = 177.4°C at the start of the 2nd cycle as a result the remaining sample melted and the molten mass escaped the sample holder as well. The drying times and temperatures can be found in Table 32.

Table 32 Hydration measurement for a 20g {2$ZnCl_2$ + $CaCl_2$} sample after dehydration with varying drying times and temperatures. The sample melted completely during the 2nd dehydration and was lost.

Setup #2 Water vapor {2$ZnCl_2$ + $CaCl_2$} Cycle	Drying time t [min]	Drying temperature T [°C]	Maximum heating rate β_{max} [$Kmin^{-1}$]	Maximum hydration temperature T_{max} [°C]
#1	344	127.5	6.6	111.3
#2	242	177.4	10.2	---

While the initial temperature was high it declined fast and, the peak showed only a low heat output, which was likely caused by the sample dissolving and loosing mass. As a result, the remaining sample exchanged heat with its surrounding faster.

The measurements with {2$ZnCl_2$+$CaCl_2$} mixtures were discontinued due to their strong deliquescent behavior.

n of cycles	T_{peak} [°C]	ΔH [Jg^{-1}]
#1	21.1 111.3	-1.96 150.07

Table 33 Hydration peaks and enthalpy for the 1st hydration of a 20g {2$ZnCl_2$ + $CaCl_2$} sample over an interval of Δt = 30min, where the vacuum pump was activated. The first endothermic peak is likely to be an artifact from applying the baseline. Changes in material weight were neglected.

6.5. Results for laboratory scale evaluations by setup #03 with water vapor

The calculation results for the heat capacity C_a as can be seen in Table 34, vary not only between different reference materials but also during repeated measurements with the same material and for the same material heated by a different heating coil. As the strength of either the voltage U or the current I can change during measurement with the resistance of the material dependent on the temperature, it was attempted to calculate the setup's heat capacity C_a by integrating over the changing variable. However, this did not improve the accuracy of the results of the calculation. Without knowing the heat capacity of the setup C_a, the heat capacity c_p of the mixed samples could not be calculated, which impeded the calculation of the heat storage capacity for the labscale-measurement results.

Table 34 Calculated heat capacity C_a of experimental setup #3 using glass and KCl as references with known heat capacities (Kopp Glass; Galbraith, J., 2016), (Biermann, et al., 1989).

material	U [V]	I [A]	Δt [s]	m [g]	c_p [$Jkg^{-1}K^{-1}$]	ΔT [K]	C_a [JK^{-1}]
Glass $_{powder}$	10.5	1.75	1125	20	800.0	84.6	242
Glass $_{powder}$	9.0	1.75	688	20	800.0	40.2	253
KCl	10.0	1.75	1300	20	691.0	79.0	274
KCl	10.0	1.75	841	20	691.0	64.0	216
KCl new coil	14.5	1.75	605	20	691.0	96.5	145
KCl new coil	9.0	1.75	320	20	691.0	48.1	91

The $c_p(T)$ trends estimated from the TGA/DSC measurements were used for calculating the heat flow Δϕ and enthalpy ΔH for the laboratory scale temperature measurements instead.

All figures with temperature curves recorded and their chosen baselines, specific heat capacity trends and calculated heat flow curves from this stage of the measurements can be found in the appendix 6.5.

6.5.1. Köstrolith

To test whether the new sample holder with a diameter of (Ø = 25.9mm) improved the measurements, the same Köstrolith sample which was used in setup #02 to test the efficiency of the setup's dehydration function, was reused in setup #03. This had the additional advantage that contrary to an unused factory dried material, the applied drying conditions were known.

The discharged Köstrolith sample was dehydrated in-situ within the sample holder during the 1st cycle measurement. The results can be seen in Table 35 and Figure 68.

Table 35 Cycle measurements of an m = 20g Köstrolith sample measured within experimental setup #3 with a supply of water vapor. A minor but steady increase in temperature yield during the first 3 hydrations was recorded. The sample was oven dried before the 4th hydration which resulted in an increase of temperature yield of ΔT = 34°C compared to the 3rd measurement.

Setup #3 Water vapor Köstrolith Cycle	Drying time t [min]	Drying temperature T [°C]	Maximum heating rate β_{max} [$Kmin^{-1}$]	Maximum Hydration temperature T_{max} [°C]
#1	~180	~120	5.2	64.3
#2	~180	~124	5.7	66.0
#3	179	124	4.5	74.6
#4 oven dried	~190	~125	---	108.6

After the 1st hydration cycle only a small decline in temperature output of the Köstrolith sample was observed and the temperature curves stabilized with the next two cycles. Drying the sample in the oven before the 4th hydration, increased the temperature output beyond that of the 1st hydration.

While oven drying is more efficient in dehydrating the samples, the Köstrolith measurement indicates that the water flow through and out of the sample has indeed improved with the increased diameter of the sample holder.

6.5.2. {$CaCl_2 \cdot 6H_2O$}

Instead of using the factory dried anhydrate {$CaCl_2$}, a sample of the hexahydrate {$CaCl_2 \cdot 6H_2O$} was dried within the apparatus for better comparability of the different cycles at a maximum temperature of T_{max} = 106°C as can be seen in

Table 36. However, at that 1st dehydration the sample melted/liquefied almost completely at temperatures of T < 60°C. Of the starting mass of m_1= 20.12g only m_2 = 3.55g remained within the sample holder which is a loss of 82.36% of the sample material. The molten mass accumulated above the closed valve to the water reservoir and recrystallized there in form of fibrous crystals before the end of the measurement. The dehydration was stopped at t = 174min. Without enough of the sample remaining, the measurement of the 1st hydration and further cycles were not possible.

Table 36 Measurement of a 20g {$CaCl_2 \cdot 6H_2O$} sample. The material melted during the 1st dehydration stage and was lost before a hydration stage could be initialized.

Setup #3 Water vapor {$CaCl_2 \cdot 6H_2O$} Cycle	Drying time t [min]	Drying temperature T [°C]	Maximum heating rate β_{max} [$Kmin^{-1}$]	Maximum hydration temperature T_{max} [°C]
#1	174	106.0	3.7	Material lost

6.5.3. {KCl}

Two cycles were measured for the {KCl} sample. The temperature dropped by ΔT = 9°C during the 2nd hydration cycle, after the vacuum pump was activated. This was either caused by water molecules evaporating from the mineral surfaces, absorbing heat from the sample in the process or the supplied water broke up the cubic crystal lattice of the anhydrate

and the phase change caused an endothermic reaction. Since the sample had been dried for t = 240 min at T_{max} = 122°C as can be seen in Table 37, the possibility that surface water was the cause can be eliminated as unlikely.

Table 37 Cycle measurements of an m = 20g {KCl} sample measured within experimental setup #3 with a supply of water vapor. Only a minimal increase of temperature was recorded during discharge.

Setup #3 Water vapor {KCl} Cycle	Drying time t [min]	Drying temperature T [°C]	Maximum heating rate β_{max} [$Kmin^{-1}$]	Maximum hydration temperature T_{max} [°C]
#1	184	118.5	9.8	27.4
#2	240	121.7	11.9	26.3

n of cycles	T_{peak} [°C]	ΔH [Jg^{-1}]
#1	20.3	-1.03
	25.9	6.47
	25.0	-0.21
	27.0	1.75
#2	10.1	-78.01

Table 38 Hydration peaks and enthalpies of an m= 20g {KCl} sample for two cycles. The peaks are both endothermic.

The endothermic peaks during the hydration as seen in Table 38 indicate a partial phase change from a crystal structure of higher order to one of lower order that absorbs activation energy in form of heat from the surrounding. As {KCl} has a cubic crystal structure in anhydrate form but no hydrated stages, it is likely that the sample partially dissolved during hydration.

6.5.4. {$MgCl_2$}

The sample agglomerated completely after the 2nd dehydration step.

During the 3rd dehydration, fissures within the sample holder were observed. Possible causes of the fissures are pressure caused by volume change of the material during hydration or by the attempt to re-insert the thermo-element into the cemented sample mass. The fissures prevented the proper establishment of a vacuum in the experimental setup during the 3rd hydration and the re-sealing attempts failed. The sample holder was replaced before the measurement of the

next samples. While no conclusive result was reached for the heat storage capacity of the {$MgCl_2$} sample, the strong agglomeration and possible expanse in volume indicated by the fissures in the sample holder are unwanted traits for heat storage materials.

Table 39 Cycle measurements of an m = 20g {$MgCl_2$} sample measured within experimental setup #3 with a supply of water vapor. Due to strong agglomeration, the thermo-element could not be inserted completely during the 3rd hydration. Also fissures in the sample holder caused a breach in vacuum, which led to an incomplete hydration during the same cycle.

Setup #3 Water vapor {$MgCl_2$} Cycle	Drying time t [min]	Drying temperature T [°C]	Maximum heating rate β_{max} [$Kmin^{-1}$]	Maximum hydration temperature T_{max} [°C]
#1	177	123.4	8.4	120.4
#2	189	117.5	6.0	65.2
#3 breach in vacuum	181	120.5	5.9	26.6

n of cycles	T_{peak} [°C]	ΔH [Jg^{-1}]
#1	20.0 120.4	-3.83 1612.13
#2	23.3 65.2	5.66 458.52
#3	21.9	-70.01

Table 40 Hydration peaks and enthalpy for hydrations 1 to 3 of a 20g {$MgCl_2$} sample over an interval of Δt = 30min, where the vacuum pump was activated. The small endothermic peak and the small exothermic peak which were observed at the start of the 1st and 2nd hydration, are likely to be artifacts from applying the baselines. The endothermic peak of the 3rd dehydration is a result of the vacuum breach.

The calculated hydration enthalpy shows a strong decline in output between the 1st and the 2nd hydration, which was caused by the halting reaction due to increasing cementation of the sample. The endothermic peak during the 3rd dehydration was a result of the breach in vacuum caused by the fissure in the sample holder. Without the vacuum forcing water vapor through the sample, the cemented sample blocking off the water supply and relatively dry air from outside being drawn into the sample holder through the fissures, the sample rather dehydrated than hydrated.

6.5.5. {$SrBr_2 \cdot 6H_2O$}

The strontium bromide hexahydrate sample was dried in the apparatus over five cycles. While the material's temperature yield improved with the progressing cycles as can be seen in Table 41, the sample recovered from the sample holder at the end of the measurement was a densely agglomerated mass of significantly decreased volume. Despite that, the sample only lost about 13.8% of its total mass over the course of the five cycles and no melting was observed or liquid residue collected, though a minor loss of sample material due to liquefication during hydration is likely, as the sample was lighter by $\Delta m = -0.45g$ after the 5th hydration than after the previous dehydration of the same cycle. As {$SrBr_2 \cdot 6H_2O$} is made up of 30.4 wgt% H_2O, the sample likely still contained about 2.6 units of {H_2O} per unit {$SrBr_2$} at the end of the 5th dehydration.

Table 41 In-situ dehydration times and maximum temperatures of a m = 20g {$SrBr_2$} sample for experimental setup #3 over five cycles.

Setup #3 Water vapor {$SrBr_2 \cdot 6H_2O$} Cycle	Drying time t [min]	Drying temperature T [°C]	Maximum heating rate β_{max} [$Kmin^{-1}$]	Maximum hydration temperature T_{max} [°C]
#1	182	106.1	4.2	36.6
#2	288	106.0	8.2	44.2
#3	238	110.0	5.3	48.7
#4	189	99.8	7.4	50.6
#5	179	91.7	5.5	46.6

Over the course of the measurements did not only the maximum temperature increased but also the duration of the reaction time, observed during the 4th and 5th hydration. Reduced drying time appears not to influence the reaction time negatively.

n of cycles	T_{peak} [°C]	ΔH [Jg^{-1}]
#1	19.3	-1.33
	21.7	1.06
	22.3	-1.98
	36.6	8.90
#2	18.6	-1.75
	19.7	0.65
	19.8	-1.73
	44.2	17.15
#3	18.7	-0.70
	19.1	0.42
	19.7	-3.05
	48.7	8.19
#4	18.7	-1.58
	19.4	0.48
	19.4	-2.31
	50.6	25.06
#5	20.9	-1.12
	22	0.32
	22.1	-2.33
	46.3	33.94

Table 42 Hydration peaks and enthalpy for five hydrations of an m_{start} = 20g {$SrBr_2$} sample over an interval of Δt = 30min, where the vacuum pump was activated. First two endothermic and exothermic peaks at the start of each of the hydration curves are likely caused by a partial dissolving of the sample at the beginning of the measurement.

The calculated heat output and the enthalpy of the sample were low for all five hydrations. While the endothermic peaks at low temperature can be interpreted as artifacts from application of the baseline they can also be interpreted as genuine phase changing events which are slowing the reaction down. This can either be caused by partial dissolving during hydration or a change between hydration phases of a higher to a lower order.

6.5.6. {$ZnCl_2$}

While the sample of {$ZnCl_2$} was factory-dried, it was still heated to T_{max} = 114.2°C before the 1st hydration step, to make sure it had drawn no water during prolonged storage. That no water vapor escaped the sample holder during the 1st dehydration, however, indicated the sample was already dry, so the dehydration step was cut short at t = 103min as can be seen in Table 43. The material dissolved partially during the 1st hydration and of the original sample of m_1 = 20.00g only m_2 = 8.76g remained within the sample holder which accounts for a material loss of 56.2%.

For the 2nd cycle, the sample was then dehydrated again for t = 167min at T_{max} = 120.7°C and remained stable during the heating process.

During the 2nd hydration, the remaining sample liquefied and was lost. The loss of mass rather than incomplete charging was the reason for the decline in temperature output, as the water vapor had less mass to react with and there was not enough material to keep the heat within the sample holder.

Table 43 In-situ dehydration times and maximum temperatures of a m_{start} = 20g {$ZnCl_2$} sample for experimental setup #3.

Setup #3 Water vapor {$ZnCl_2$} Cycle	Drying time t [min]	Drying temperature T [°C]	Maximum heating rate β_{max} [$Kmin^{-1}$]	Maximum hydration temperature T_{max} [°C]
#1	103	114.2	6.8	83.3
#2	167	120.7	9.5	77.1

n of cycles	T_{peak} [°C]	ΔH [Jg^{-1}]
#1	19.6 83.3	-6.33 412.27
#2	18.7 77.1	-14.60 332.86

Table 44 Hydration peaks and enthalpy for two hydrations of an m_{start} = 20g {$ZnCl_2$} sample over an interval of Δt = 30min, where the vacuum pump was activated. The endothermic peaks at the start of both hydration curves indicate a partial phase change from a crystal class of high order to one of lower order or a dissolving event.

The weight loss during hydration was taken into account when calculating Δϕ and ΔH by applying a linear decline to the sample mass from start to end of the hydration. As can be seen in Table 44, two endothermic peaks were observed at the start of the hydration measurements, which indicate a partial phase change from a crystal class of high order to a lower one. As in this case the material proved deliquescent, the endothermic reaction was likely the sample partially dissolving.

6.5.7. {2MgCl$_2$ + CaCl$_2$}

Partial melting of the {2MgCl$_2$+CaCl$_2$} sample during the dehydration steps was observed like for the untreated {CaCl$_2$·6H$_2$O}. However, the process occurred slower, leaving enough material within the sample holder for ongoing measurements over five cycles. Mass losses were also measured after the 2nd and the 5th dehydration, where more material was dissolved than weight of water gained by absorption. Aside from melting, the mass losses were likely also caused partially by {HCl}-emissions, as observed during the TGA/DCS measurements though the drying temperature was kept below T = 120°C to limit the mixture's reaction to {2Mg(OH,Cl)$_2$ + CaCl$_2$}.

Despite the continuous material loss, the temperature measured remained stable for all five recorded hydration stages, as can be seen in Table 45. The maximum temperature did not exceed T_{max} = 47.4°C.

Table 45 In-situ dehydration times and maximum temperatures of a m = 20g {2MgCl$_2$ + CaCl$_2$} sample for experimental setup #3. Due to expected partial melting caused by the {CaCl2} content of the sample, the measurements started with a hydration instead of a dehydration.

Setup #3 Water vapor {2MgCl$_2$ + CaCl$_2$} Cycle	Drying time t [min]	Drying temperature T [°C]	Maximum heating rate β_{max} [Kmin^{-1}]	Maximum hydration temperature T_{max} [°C]
#1	---	---	---	47.4
#2	178	113.1	5.3	44.7
#3	243	116.0	5.1	46.9
#4	190	111.9	5.6	45.7
#5	145	104.1	4.6	45.8

The mass loss caused by the partial melting was taken into account during the calculation of $\Delta\phi$ and ΔH by adjusting the starting mass at the beginning of the hydration to the material loss weighed after dehydration and applying linear weight changes for the difference in mass before and after the hydrations.

n of cycles	T_{peak} [°C]	ΔH [Jg^{-1}]
#1	45.3	548.44
#2	17.5	-13.49
	44.2	528.07
#3	21.8	-1.44
	44.9	515.61
#4	19.5	-4.83
	44.5	563.88
#5	20.1	-5.27
	45.8	556.72

Table 46 Hydration peaks and enthalpy for five hydrations of an m_{start} = 20g {$2MgCl_2$+$CaCl_2$} sample over an interval of Δt = 30min, where the vacuum pump was activated. After the 1st, all following hydrations show an endothermic peak at the start of the measurement.

Since weight loss was recorded for two of the four hydration cycles with endothermic peaks at the start of the hydration cycle, it is likely that they were caused by the sample partially dissolving. Like the temperature yield, the heat output remained relatively stable over the course of the measurements, as can be seen in Table 46.

6.5.8. {$2MgCl_2$ + KCl}

Unlike the untreated {$MgCl_2$} the observed agglomeration of the {$2MgCl_2$ + KCl} mixture during the cycles was less severe as the material remained friable compared to the full cementation of the {$MgCl_2$}.

Table 47 In-situ dehydration times and maximum temperatures of a m = 20g {$2MgCl_2$ + KCl} sample for experimental setup #3 over five cycles.

Setup #3 Water vapor {$2MgCl_2$ + KCl} Cycle	Drying time t [min]	Drying temperature T [°C]	Maximum heating rate β_{max} [$Kmin^{-1}$]	Maximum hydration temperature T_{max} [°C]
#1	190	122.3	5.9	90.3
#2	180	127.1	8.7	64.4
#3	186	119.2	6.4	45.0
#4	205	115.7	7.1	39.4
#5	211	99.7	13.3	39.2

As can be seen in Table 47, the initial hydration reached a maximum temperature of T_{max_01} = 90.3°C. The temperature yield declined with each following cycle until it stablized at the 4th hydration, with only a maximum temperature of T_{max_04} =

39.2°C being reached during the 5th hydration. For this sample a continuous mass gain was recorded between hydration cycles, indicating incomplete dehydrations.

n of cycles	T_{peak} [°C]	ΔH [Jg^{-1}]
#1	18.2 90.3	0.37 1603.45
#2	17.9 64.4	-2.50 903.45
#3	45.0	569.58
#4	18.5 39.4	-8.92 472.13
#5	22.0 39.2	-1.42 392.88

Table 48 Hydration peaks and enthalpy for five hydrations of an m_{start} = 20g {2$MgCl_2$+KCl} sample over an interval of Δt = 30min, where the vacuum pump was activated. A strong decline in heat output can be observed over the cycles.

The mass gain was taken into account when calculating Δϕ and ΔH by adding a linear mass correction to the initial sample mass over the course of the hydration measurements. Table 48 shows the calculation results, with the {2$MgCl_2$ + KCl} displaying the strongest initial heat output of all the samples evaluated with experimental setup #3 but also the strongest decline over the ongoing cycles.

The sample showed no melting or dissolving behavior. The endothermic peaks recorded for the 2nd and 3rd cycle can be interpreted as artifacts from application of the baseline. The endothermic peak at the 4th cycle is likely a genuine phase change event. Since the sample contains {KCl} which occurs in a cubic crystal structure, a partial segregation of the material during dehydration may have been the cause.

6.5.9. {8$CaCl_2$ + 5$SrBr_2$}

The material proved to melt partially during heating. Of the original sample of m_1 = 20.16g, only m_3 = 14.55g material remained after two cycles which means a material loss of 27.83%. The molten mass was accumulating above the closed valve to the water reservoir and re-crystalized within a day in a desiccator. During the next hydration, the remaining sample gained m_{H2O} = 1.42g of weight. The dehydration times and temperatures can be seen in Table 49.

Table 49 In-situ dehydration times and maximum temperatures of an m_{start} = 20g {5$SrBr_2$ + 8$CaCl_2$} sample for experimental setup #3 over two cycles.

Setup #3 Water vapor {$SrBr_2$+$CaCl_2$} Cycle	Drying time t [min]	Drying temperature T [°C]	Maximum heating rate β_{max} [$Kmin^{-1}$]	Maximum hydration temperature T_{max} [°C]
#1	142	116.0	5.0	44.7
#2	170	113.4	5.8	49.2

n of cycles	T_{peak} [°C]	ΔH [Jg^{-1}]
#1	44.7	429.85
#2	19.3	-7.87
	49.2	564.74

Table 50 Hydration peaks and enthalpy for two hydrations of an m_{start} = 20g {5$SrBr_2$ + 8$CaCl_2$} sample over an interval of Δt = 30min, where the vacuum pump was activated. A strong incline in heat output can be observed between the cycles.

Calculating the hydration enthalpies, showed endothermic events at the beginning of each hydration stage as seen in Table 50. This can either be interpreted as a phase change from a phase of higher crystal symmetry order to a lower order, or a partial dissolving of the sample during hydration. Since a mass loss was observed either is possible. A table with all the peak temperatures and enthalpies of the materials evaluated with setups #2 and #3 can be found in the appendix.

7. Discussion

7.1. Sources of errors

7.1.1. TGA/DSC measurements

Among the most common technical problems during the automatic TGA/DSC measurements that have a direct impact on the measurements are sample losses during a multi-cycle measurement. Instead of simply continuing the measurement with a new sample, an entire new evaluation must be started for said new sample, to take the different starting mass and the sample's state of deterioration (or improvement) over the cycles into account.

While blank-curves measured with empty crucibles are subtracted automatically from the measurement curves of heat flow during a TGA/DSC evaluation, the blank curves need to be updated periodically, as an outdated blank can falsify the results up to the point of rendering the curves unreadable.

The inbuilt scale of the TGA/DSC needs to be recalibrated periodically as well. While adding a constant over- or underestimation value to the sample mass has no huge effect on the results of the calculations, an accidentally added weight trend can give the false impression of a deteriorating or recovering sample especially if not identified as such during multi-cycle measurements.

It was observed that some of the samples were absorbing water during measurement stages where the water supply was supposed to be cut off, which indicated a malfunction in the TGA/DSC setup.

In regards of user induced errors, the choice and fitting of a proper baseline for the calculation of the reaction enthalpy, identification of melting events and identification of an emission of reaction byproducts like {HCl} require experience. A misplaced baseline will give a wrong picture of a material's heat storage density and in some cases cycle stability.

An exact water content for the materials at any stage of the measurement can only be calculated for a sample, that has been dehydrated to the anhydrate. This was

not accomplished for several of the samples during the T_{max} = 500°C evaluations. The different heating rates of the chosen dehydration programs can accelerate or delay reactions, which can also introduce an error in calculating the water content when comparing different samples to the results of the T_{max} = 500°C dehydration, however running the cycle measurements with the same sample as the T_{max} = 500°C leads to changes in the testing material influencing the results.

The calculation of the specific heat capacity for various materials would have benefitted from the trends being calculated from more spot samples, ideally the entire dehydration curve and exact identification of the hydration stages. With a lack of reliable data, the fitting of the trends to the c_p-values for different temperatures calculated from the spot samples was open for interpretation.

7.1.2. XRPD

Drying the powder crushed salt crystals in a desiccator and shrink wrapping them airtight before sending them out for analysis would have prevented the materials from hydrating and dissolving before the XRPD evaluation, which would have reduced the amorphous content of the samples and allowed for easier interpretation of the powder patterns.

7.1.3. Laboratory scale evaluations

During the measurements with setup #2, no note was taken of material mass changes between measurements or cycles, which influenced the results of the later enthalpy calculations.

Other causes for aberrations during measurements with the setups #2 and #3 were variations in the applied maximum operation time of the vacuum-pump during hydrations and no recording of the changes in the surrounding temperature, which made the correct fitting of the baseline a more complex task.

The interpretation of the heat output curve, which was calculated from the temperature curve and the baseline includes deciding whether the weaker endothermic and exothermic peaks which are common at the start of the hydration stages are caused by an unfitted baseline or a relevant phase change.

During at least one of the measurements with setup #3, an intrusion of liquid water into the sample holder was observed, when the vacuum was initiated. That could have caused the partial dissolving of samples during the hydration stages.

7.2. Melting- and thermal decay- events of untreated compared to mixed salts

Whether the combination of two or more educts was beneficial to the overall cycle stability can be valued by the changes caused in the temperature stability. In part 5.4.1, the TGA/DSC measurement results of different chloride-mixtures, treated with the additional educt {KCl} were described. The thermal stability of the materials changed as follows:

7.2.1. {$MgCl_2$}

As untreated {$MgCl_2 \cdot xH_2O$} reacts to {$Mg(OH,Cl) \cdot (x-1)H_2O + HCl$}, there are {HCl}-emission peaks among the melting peaks. The temperature range for {HCl}-emissions of untreated {$MgCl_2 \cdot nH_2O$} ranges from $T_{\{HCl\}}$ = 110°C (Institut für Arbeitsschutz der Deutschen Gesetzlichen Unfallversicherung, 2017) to $T_{\{HCl\}}$ > 167°C (Qiong-Zhu Huang, Gui-Min Lu, Jin Wang, & Jian-Guo Yu, 2010). During the measurements they occurred from T = 117°C onward. The {$Mg(OH,Cl)_2 + xH_2O$} showed possible melting behavior, only from temperatures of T = 184°C and higher.

Compared to the untreated salt, the {$MgCl_2+ZnCl_2+2KCl$} mixture showed a likely {HCl}-emission peak at a slightly lower temperature of T = 112°C, which is still within the temperature range set by literature.

The mixtures {$MgCl_2 + CaCl_2 + 2KCl$}, {$MgCl_2 + ZnCl_2$} and {$MgCl_2 + CaCl_2 + ZnCl_2$} displayed melting behavior at temperatures below T = 75°C, while {HCl}-emissions

occurred at increased temperatures: From T = 135°C onward for {$MgCl_2$ + $CaCl_2$ + 2KCl}, from T =154°C for {$MgCl_2$ + $ZnCl_2$} and from T = 179°C and higher for {$MgCl_2$ + $CaCl_2$ + $ZnCl_2$}.

The mixtures {$MgCl_2$ + $CaCl_2$} and {$MgCl_2$ + $CaCl_2$ + $ZnCl_2$ + 3KCl} showed likely {HCl}-emission peaks or possible melting behavior only at temperatures above T = 154°C. After the {HCl} was emitted during the 2nd dehydration, the {$MgCl_2$ + $CaCl_2$} mixture appeared more stable during the 3rd dehydration, where neither melting nor {HCl}-emission events were recorded.

No melting or {HCl}-emission behavior was identified for the {$MgCl_2$ + KCl} mixture, which also displayed the most stable peak distribution of the tested {$MgCl_2$}-mixtures.

7.2.2. {$CaCl_2$}

The melting temperature for {$CaCl_2 \cdot 6H_2O$} lies at T = 30°C (Ropp, 2012), the lowest observed melting temperature for untreated {$CaCl_2 \cdot xH_2O$} was at T = 38°C during the TGA/DSC measurements, which would be within the temperature range for melting of {$CaCl_2 \cdot 4H_2O$} (IFA Institut für Arbeitsschutz Datenbank), (Ropp, 2012). The sample showed no further melting events within the measured temperature range of T = 50 to 200°C.

Compared to untreated {$CaCl_2 \cdot xH_2O$}, the mixture {$MgCl_2$ + $CaCl_2$ + 2KCl} displayed a melting peak at a slightly lower temperature of T = 34°C, and due to the {$MgCl_2$}-content, several {HCl}-emission or melting events were recorded at T > 125°C. The {$MgCl_2$ + $CaCl_2$ + $ZnCl_2$} showed a delay of the low temperature melting event to T = 68°C.

For the materials {$CaCl_2$ + KCl}, {$CaCl_2$ + $ZnCl_2$ + 2KCl} and {$MgCl_2$ + $CaCl_2$ + $ZnCl_2$ + 3KCl}, the melting events were delayed into the temperature range beyond T = 140°C, however below T = 100°C the {$CaCl_2$ + KCl} mixture only dehydrated to a water content of about n = 5 {H_2O} per unit and {$CaCl_2$ + $ZnCl_2$ + 2KCl} to n = 6.5

{H_2O} per unit, and nothing but the melting peaks were observed at higher temperatures, leading to an inefficient recharge.

The {$CaCl_2$ + $ZnCl_2$} mixture showed no melting events, a lowered reaction temperature and a stable peak distribution.

7.2.3. {$ZnCl_2$}

Untreated {$ZnCl_2 \cdot xH_2O$} displayed neither low melting points nor {HCl}-emissions and mixing it with other materials generally resulted in a product with an overall lower stability. The only exception was the already mentioned {$CaCl_2$+$ZnCl_2$} mixture, which showed a more stable peak distribution and lower reaction temperatures than those of either of the two untreated materials.

A full comparison of the material behavior, concerning peak temperature distribution, melting events and {HCl}-emissions for the chloride samples can be found in the diagrams Figure 36 to Figure 38 in the Appendix part 4.

7.3. Material Properties in multi cycle TGA/DSC analysis

The chloride materials chosen for the multi cycle TGA/DSC analysis were {$2MgCl_2$+$CaCl_2$} based on the mineral Tachyhydrite, and {$2MgCl_2$+KCl} a high magnesium variation of the mineral Carnallite.

The 25-cycle analysis showed a high cycle stability for both materials, where the {$2MgCl_2$+KCl} required three cycles to stabilize its reaction enthalpy during hydration and dehydration and then showed a trend of slight improvement. The {$2MgCl_2$+$CaCl_2$} remained stable over all cycles but also showed a slight improving trend with ongoing cycles.

Both materials and {$2ZnCl_2$+$CaCl_2$} a zinc variation of the mineral Tachyhydrite were synthesized in larger amounts for a series of laboratory scale evaluations, where the

two Tachyhydrite variations displayed melting behavior {$2MgCl_2$+$CaCl_2$} and high deliquescence {$2ZnCl_2$+$CaCl_2$} respectively which both led to massive material loss during the measurements. The {$2MgCl_2$+KCl} sample displayed low hydration temperatures and a decline in heat output over the measured cycles which was caused by incomplete material recovery during dehydration but displayed neither melting nor deliquescent behavior.

7.4. Material Properties comparison of TGA/DSC with the laboratory scale results

The evaluations at laboratory scale made it easier to observe mass losses and identify their cause as either melting, dissolving or the expected emission of {H_2O} (or {HCl}) while the TGA analysis served to determine the exact melting temperatures and can be used to calculate the hydration stages.

Of all the materials chosen for the evaluation at laboratory scale, melting within the T = 25 to 100°C range had only been observed beforehand, during the TGA/DSC analysis for a {$CaCl_2$} sample in hydrated state.

Melting was observed during the laboratory scale analysis as expected for the {$CaCl_2$} sample but also for the {$2MgCl_2$ + $CaCl_2$} and {$5SrBr_2$ + $8CaCl_2$} samples.

Partial deliquescence was displayed by several of the discontinued sulfate mixtures and for chloride samples containing {KCl}, as endothermic peaks occurred during the hydration stages of the TGA/DSC measurements. However, the deliquescent behavior could be observed for most of the chloride samples over extended storage periods or while they were mechanically crushed in a mortar during preparation.

The magnitude of the deliquescent behavior became obvious during hydration of the m = 20mg samples of {$ZnCl_2$}, {$2MgCl_2$ + $CaCl_2$} and {$2ZnCl_2$ + $CaCl_2$}, where it was the cause for massive material loss, which was next to material loss caused by melting one of the main reasons for interrupted measurement cycles.

Another newly observed material behavior for the m = 20g samples, that was not obvious during the TGA/DSC analysis was the strong agglomeration of the {$MgCl_2$}

and {$SrBr_2$} samples and the moderate agglomeration of the {$2MgCl_2 + KCl$} mixture. In case of the {$SrBr_2$} sample, the agglomeration caused by a phase change from {$SrBr_2 \cdot 6H_2O$} to approximately {$SrBr_2 \cdot 2.6H_2O$} concurred with an observed decrease of about $\frac{2}{3}$ of the sample's volume.

With an added strip of litmus indicator, changes in pH values can be recorded for the laboratory scale measurements but it does not allow for identifying an exact emission temperature or a statement about the quantity of emitted acid. An emission peak in a dehydration curve is difficult to tell from a melting peak during the TGA/DSC analysis but the temperature of the peak occurrence can be measured exactly.

Differences in the calculated heat output between the TGA/DSC and the laboratory scale evaluations for the different samples were likely caused by the imprecision of the individually calculated specific heat capacities.

The heat output for the {$MgCl_2$}, {$ZnCl_2$} and {$2MgCl_2+CaCl_2$} were about comparable for both methods of measurement.

The {$2MgCl_2 + KCl$} readings for the m = 20g sample exceeded the expectations at the beginning before the heat output was reduced over the observed five cycles.

The endothermic reaction of the {KCl} partially dissolving its cubic crystal structure was enhanced by the increased sample mass of m = 20g.

The reaction enthalpies of the m = 20g {$CaCl_2$}, {$5SrBr_2 + 8CaCl_2$} and {$2ZnCl_2 + CaCl_2$} samples but especially of the {$SrBr_2$} sample remained below the expectations.

All differences in observation are listed in Table 51.

The TGA/DSC and the laboratory scale evaluations complemented each other concerning the observations of the material behavior but the heat output calculations of the laboratory scale measurement were unreliable and require refining.

Table 51 Comparison of hydration enthalpies and material behaviors between the TGA/DSC T_{max} = 100° cycle and the observations and results from the laboratory scale evaluations. With the exception of the m = 20g {KCl} sample, only exothermic peaks were taken into account.

Material	ΔH [Jg^{-1}] Hydration TGA/DSC dehyd-temp T_{max} = 100°C	$\Delta H_{1\ to\ 3}$ [Jg^{-1}] e = 8.65 14.80 17.66 mbar	Material - behavior TGA/DSC	ΔH [Jg^{-1}] Hydration Laboratory scale setup #2 dehyd-temp T_{max} ~120°C	ΔH [Jg^{-1}] Hydration Laboratory scale setup #3 dehyd-temp T_{max}~120°C	Material-behavior Laboratory scale setup #2 & #3
{$CaCl_2$}	630.03	22.17 400.29 207.57	Melting observed at T = 47.67°C	172.21 244.52 194.82	--- --- ---	Melting observed at T < 60°C
{KCl}	---	---	weak endothermic reactions during hydration reactions observed.	3.18 15.71	8.22 (-78.01)	Strong endothermic reaction
{$MgCl_2$}	247.92	38.04 58.87 151.01	{HCl} emission-peak at T = 117°C	328.79 1217.94 480.39 263.80	1612.13 504.18 --- ---	Strong agglomeration and decline in heat output
{$SrBr_2$}	798.14	No individual peaks calculated	The material did not take up water at T ≥ 60°C	94.25 140.65 57.40 --- ---	8.90 17.15 8.19 25.06 33.94	Very low heat output, no observed reaction temperatures T ≥ 60°C agglomeration was observed

{$ZnCl_2$}	387.66	47.55 157.73 182.38	No melting was observed.	--- ---	412.27 332.86	No melting was observed but material was lost due to strong deliquescence
{$2MgCl_2$ + $CaCl_2$}	450.16	31.02 201.60 217.53	No melting was observed.	1020.42 593.70 846.11 890.79 ---	548.44 528.07 515.61 563.88 556.72	Material loss by melting and deliquescence
{$2MgCl_2$ + KCl}	413.49	--- 278.24 135.26	The material did not hydrate easily at low water vapor pressure	--- 106.48 312.63 --- ---	1603.45 903.45 569.58 472.13 392.88	The material did hydrate easily but did dehydrate incompletely
{$5SrBr_2$ + $8CaCl_2$}	589.46	132.30 457.17 ---	The material absorbed water at T = 60°C	--- ---	429.85 564.74	The material showed melting behavior but deliquescence was not a cause of mass loss. no hydration reactions at T ≥ 60°C were observed

{2$ZnCl_2$ + $CaCl_2$}	750.37	118.25 334.12 298.00	No melting was observed.	150.07	---	Strong deliquescence observed

8. Conclusions

8.1. Sulfates

The results of the TGA/DSC analysis of the sulfate mixtures were unsatisfactory regarding cycle stability and heat storage density. The samples {$3Na_2SO_4 + K_2SO_4$}, {$Na_2SO_4 + K_2SO_4$}, {$Na_2SO_4 + 3K_2SO_4$} and {$K_2SO_4 + Fe^{2+}SO_4$} showed only endothermic behavior during the hydration stages of the testing cycles. This indicated that the material crystallized in a structure of high order such as cubic, hexagonal or orthorhombic. Introducing water vapor to these mixtures caused partial or complete dissolving of the salt crystals and breaking up the dense crystal structures drained energy in form of heat from the surroundings.

The samples {$2Na_2SO_4 + MgSO_4$}, {$7Na_2SO_4 + 4MgSO_4$}, {$2K_2SO_4 + MgSO_4$}, {$7Na_2SO_4 + 4ZnSO_4$}, {$10K_2SO_4 + 7ZnSO_4$}, {$3MgSO_4 + 2ZnSO_4$}, {$Na_2SO_4 + Fe^{2+}SO_4$}, {$2Na_2SO_4 + Fe^{2+}SO_4$}, {$2Na_2SO_4 + Al_2(SO_4)_3$}, {$MgSO_4 + Al_2(SO_4)_3$}, {$17MgSO_4 + 3Al_2(SO_4)_3$} and {$2Fe_n(SO_4)_m + Al_2(SO_4)_3$} showed both endothermic as well as exothermic behavior during hydration, indicating that phases of low as well as of high crystal order were present in the mixtures. All of these tested sulfate mixtures displayed cycle instability, as the samples did not take up enough water during the hydration stage.

While the sulfate mixtures may not be suited as heat storage materials, the Na-K sulfates could find their usage in cold storage systems. Determining the possible applications would require a new, independent testing series.

8.2. Chlorides

The tested chloride mixtures displayed a high heat storage density but with few exceptions a low cycle stability during the TGA/DSC analysis. They showed a tendency to overhydrate, when exposed to air humidity over any extended time-period or at a partial water vapor pressure of e = 17.66mbar.

8.2.1. {$MgCl_2$}

During the measurements, the untreated {$MgCl_2$}-hydrate was observed to react to {$Mg(OH,Cl)_2$}-hydrate while emitting {HCl} at T_{HCl} = 117 to 118°C. This decay temperature corresponded with the expected phase change from monoclinic ($C\ 1\ \frac{2}{m}\ 1$) hexahydrate {$MgCl_2 \cdot 6H_2O$} to the monoclinic ($P\ 1\ \frac{2_1}{c}\ 1$) tetrahydrate {$MgCl_2 \cdot 4H_2O$} at T ~ 110°C (Kipouros & Sadoway, 2001). The observed decay temperature aligned with the IFA data from literature which described a first onset of {HCl} emissions at temperatures of T > 110°C (Institut für Arbeitsschutz der Deutschen Gesetzlichen Unfallversicherung, 2017). The delayed decay peak of the untreated material at a temperature value of T > 167°C observed by (Qiong-Zhu Huang, Gui-Min Lu, Jin Wang, & Jian-Guo Yu, 2010) may have been caused by different measurement conditions (for example the heating rate) or by using pre-dried tetrahydrate instead of the hexahydrate as the starting material, as the with the latter, the material would not undergo a phase transformation at T = 110°C.

8.2.2. {$CaCl_2 + 2MgCl_2$}, {$CaCl_2 + MgCl_2$}, {$2CaCl_2 + MgCl_2$}

Compared to the results for the untreated material, the thermal decay of the {$MgCl_2$}-hydrate components from the {$CaCl_2 + 2MgCl_2 + nH_2O$}, {$CaCl_2 + MgCl_2 + nH_2O$} and {$2CaCl_2 + MgCl_2 + nH_2O$} mixture samples, occurred with a distinct delay.

In case of the hydrated synthetic tachyhydrite {$2MgCl_2 + CaCl_2 + nH_2O$}, the sample's water content declined until it formed the trigonal ($R\ \bar{3}$) dodecahydrate {$2MgCaCl_6 \cdot 12H_2O$} at about T ~ 100°C and remained in that phase till the water content had sunk further by Δn = 1.1 {H_2O} per formula unit at T = 153°C, where the {HCl}-decay peak was recorded.

Since the other two tested calcium-magnesium chloride mixtures held a lower percentage of {$MgCl_2$} compared to the {$2MgCl_2 + CaCl_2$} sample and their decay processes were recorded within the temperature interval of T = 153 to 155°C as well, it can be assumed, that the trigonal magnesium-calcium chloride

dodecahydrate Tachyhydrite formed in all three samples despite the presence of excess {$CaCl_2$} in two cases, which caused the observed delay of the thermal decay. This is backed up by the results of the XRPD evaluations where Tachyhydrite ($2MgCaCl_6 \cdot 12H_2O$) was identified in all three mixtures (see Appendix 3, Figure 31 to Figure 33).

According to (Clark, Evans, & Erd, 1980), the Tachyhydrite structure is composed of $Mg(OH)_6$ and $CaCl_6$ octahedra, where the structure is held together over hydrogen bonds, which likely causes the higher stability regarding {HCl}-emissions.

8.2.3. {$MgCl_2 + 2ZnCl_2$}, {$MgCl_2 + ZnCl_2$}, {$2MgCl_2 + ZnCl_2$}

Distinct {HCl}-emission events couldn't be identified for the three magnesium-zinc-chloride mixtures {$MgCl_2 + 2ZnCl_2$}, {$MgCl_2 + ZnCl_2$} or {$2MgCl_2 + ZnCl_2$}.

While conspicuous peak events were recorded for the {$MgCl_2 + 2ZnCl_2$}, {$MgCl_2 + ZnCl_2$} and {$2MgCl_2 + ZnCl_2$} samples, they appear to have been correlated to re-solidification events during the respective cooldown stages of the samples, which indicates (partial) melting rather than {HCl}-decay. As the magnesium-zinc chloride mixtures have no naturally occurring counterparts, neither crystal systems nor spacegroups are known. An XRPD evaluation of {$2MgCl_2 + ZnCl_2 + nH_2O$} showed only amorphous material with no identify-able educts or products in the dried sample (see Appendix 3, Figure 35).

For the {$MgCl_2 + 2ZnCl_2$} the peaks in question occurred at T ~ 133°C and T ~ 150°C during both T_{max} = 200°C dehydrations and were of comparable strength, which also indicates that no {HCl} was emitted during either dehydration.

As the conspicuous peaks of the {$MgCl_2 + ZnCl_2$} sample's 2nd dehydration were recorded at T ~ 71°C and T ~ 169°C with two corresponding exothermic events during cooldown at T ~ 120 °C and T ~ 70°C, which does imply (partial) melting over {HCl}-emission. But during the 2nd dehydration the peaks in question were recorded at T ~ 105°C, T ~ 115°C and T ~ 161°C, so it is possible that the material

underwent a {HCl} emission at T ~ 115°C and T ~ 161 to 169°C, due to the higher percentage of {$MgCl_2$} in the mixture.

For the {$2MgCl_2 + ZnCl_2$} sample it was noted that an exothermic event occurred already during the cooldown stage of the 1st hydration at T ~ 88°C, though none of the endothermic peaks were identifiable as melting events. During the 2nd dehydration, (partial) melting or {HCl}-emissions occurred likely at the temperatures T ~ 144°C, T ~ 152°C, T ~ 186°C and T ~ 195°C, with only a single re-solidification event during cooldown at T ~ 137°C. As during the 3rd dehydration only a single conspicuous peak occurred at T ~ 152°C, complemented by an exothermic event at T ~ 140°C during the cooldown stage, the peaks from the previous measurement at T ~ 144°C, T ~ 186°C and T ~ 195°C were likely rather {HCl}-emissions, with the melting event reoccurring at T ~ 152°C.

8.2.4. {$MgCl_2 + 2KCl$}, {$MgCl_2 + KCl$} #1, {$MgCl_2 + KCl$} #2 and {$2MgCl_2 + KCl$}

During the TGA/DSC analysis neither melting events nor {HCl}-dissociation reactions were observed for the four magnesium-potassium mixtures {$MgCl_2 + 2KCl$}, {$MgCl_2 + KCl$} #1, {$MgCl_2 + KCl$} #2 or {$2MgCl_2 + KCl$}, within the temperature interval of T = 25 to 200°C.

With K^+ ions incorporated into the chemical composition, the relative maximum {H_2O} content per cation in the formula unit is lowered, which was the likely cause for the increased melting temperature.

The reason why the mixtures show also an increased stability concerning {HCl}-decay might be based on the unusual crystal structure of Carnallite ($Mg(H_2O)_6KCl_3$), which has been analyzed in detail by Schlemper, Sen Gupta and Zoltai (Schlemper, Sen Gupta, & Zoltai, 1985). They showed, that the Mg^{++} ions do not interact directly with the Cl^- ions, as the Carnallite structure consists of KCl_6 and $Mg(H_2O)_6$ octahedra, where two third of the KCl_6 octahedra share surfaces with each other while the $Mg(H_2O)_6$ octahedra occupy the free space in between (see Figure 22). According to the third rule of Pauling (Pauling, 1960) the sharing of

surfaces displayed by the KCl_6 octahedra is a destabilizing influence on the structure. However, this influence is mitigated by the charge of the water molecules, which balances out the negative ion charge of the chlorides. But going by the calculated water content of the three tested samples {$MgCl_2$ + 2KCl}, {$MgCl_2$ + KCl} #1, {$MgCl_2$ + KCl} #2, where no excess {$MgCl_2$} was present in the mixture, this balance is disturbed during dehydration already at temperatures below T = 100°C with the main dehydration peak at T = 97 to 98°C, where the water content sinks to 2.5 to 3.0 {H_2O} per formula unit, though the dehydration reaction itself can set in earlier at T = 50 to 60°C depending on sample composition. It is unknown which crystal structure the material forms in dehydrated stage, but if the Cl^- ion stay aligned to the K^+ ions, this may be the factor that prevents the {HCl}-emission.

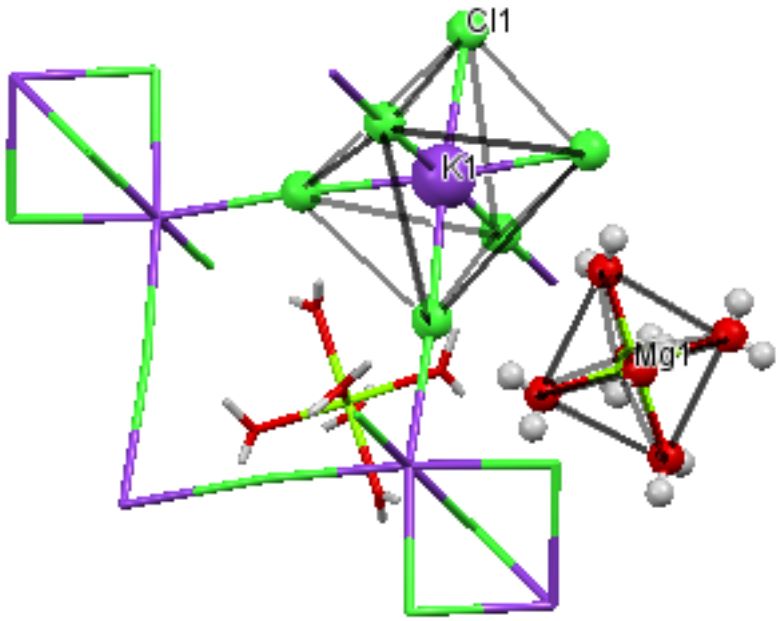

Figure 22 Examples for KCl_6 and $Mg(H2O)_6$ octahedra found within the crystal structure of Carnallite ($Mg(H_2O)_6KCl_3$) (Schlemper, Sen Gupta, & Zoltai, 1985), (Created with Mercury 3.1, 2015)

The respective peaks of Carnallite ($KMgCl_3 \cdot 6H_2O$) $P\,b\,n\,n$ (Fischer, 1973), (Cambridge Crystallographic Data Centre (CCDC), 2016) and $P\,n\,n\,a$ (Schlemper,

Sen Gupta, & Zoltai, 1985), (Cambridge Crystallographic Data Centre (CCDC), 2016) as well as one of the educts Sylvite (KCl) ($F\ m\ \bar{3}\ m$) (Heinrich Heine Universität Düsseldorf , 2013) were identified in the powder pattern of the {$MgCl_2$ + KCl} #1 sample, indicating, that an excess of {KCl} was present in the mixture. The related powder pattern can be found in Appendix 3, Figure 26.

Comparing the calculated maximum water contents of the two samples {$MgCl_2$ + KCl} #1, {$MgCl_2$ + KCl} #2, which range from n = 5.1 to 7.7 {H_2O} per formula unit, a deviation from the ideal n= 6 {H_2O} per formula unit occurs for both mixtures. It is possible that the difference in water content was caused by the excess of {KCl} in sample #1 and by an excess of {$MgCl_2$} in sample #2.

8.2.5. {$CaCl_2$}

The melting of the untreated {$CaCl_2$}-hydrate sample occurred at T = 39 to 48°C during the 2nd and the 3rd dehydration. The melting event of the 2nd dehydration lies within, the event of the third slightly above the range of melting temperatures T_{melt} = 35 to 45.5°C for the tetrahydrate ($CaCl_2 \cdot 4H_2O$) (IFA Institut für Arbeitsschutz Datenbank), (Ropp, 2012), but the water content of the sample during the melting event was calculated as n = 5.1 {H_2O} per unit {$CaCl_2$}. It is likely that the minimum water content of the sample was overestimated during the calculation. That no melting was observed during the 1st dehydration, where the sample was calculated to contain n = 9.2 {H_20} per formula unit, can be either related to the slower heating rate during that dehydration stage or mean that the sample was overhydrated to a point that it had already partially dissolved before the measurement started, though the latter is more likely as an exothermic event after the cooldown stage indicated a re-solidification of at least a part of the material.

8.2.6. {$CaCl_2$ + 2KCl}, {$CaCl_2$ + KCl} and {2$CaCl_2$ + KCl}

Combining {KCl} and {$CaCl_2$} to {$CaCl_2$ + 2KCl}, {$CaCl_2$ + KCl} and {2$CaCl_2$ + KCl} mixtures resulted in an increase of the recorded melting temperatures. This might be correlated to the formation of the orthorhombic (pseudo cubic) mineral Chlorocalcite ($KCaCl_3$) (National Bureau of Standards, Monograph, 7, 1969); (Anthony, Bideaux, Bladh, & Nichols, 1997) and an excess of the cubic educt {KCl} (Mineralogical Magazine 29, 1951); (Anthony, Bideaux, Bladh, & Nichols, 1997) as an orthorhombic or cubic crystal structure would require a higher thermal energy to melt than that of rhombohedral (trigonal) Antarcticite ($CaCl_2 \cdot 6H_2O$) (Torii & Ossaka, 1965), (Anthony, Bideaux, Bladh, & Nichols, 1997). There is no information about the crystal structures of possible hydrated stages of Chlorocalcite ($KCaCl_3$) available and there seems to be no calcium-chloride equivalent with a similar structure to Carnallite ($KMgCl_3 \cdot 6H_2O$). The latter is likely caused by the larger ion radius of Ca^{++} (r_{Ca} = 99 pm) (Hoppe, 2018) compared to Mg^{++} (r_{Mg} = 65 pm) (Hoppe, 2018). While a larger ion radius of the cation ensures that, according to the 1st rule of Pauling (Pauling, 1960), a $Ca(H_2O)_6$ octahedron can form, the octahedron's volume may not fit into the available space between the KCl_6 octahedra within the crystal structure like a $Mg(H_2O)_6$ octahedron. This leads to the question whether any compounds were able to form at all within the hydrated samples or whether the material crystallized at least partially to Chlorocalcite ($KCaCl_3$) after dehydration.

The reactions during dehydration of the {$CaCl_2$ + 2KCl} sample were irregular over the initial TGA/DSC measurement cycles. The sample took up a varying maximum water content between n = 8.1 to 10.2 {H_2O} per formula unit and partial melting events can occur at T_1 ~ 123°C, T_2 ~ 141°C and T_3 ~ 147°C. While no melting event was recorded at T < 100°C, it is possible that with a starting water content of about n = 8.1 {H_2O} per formula unit the sample was liquefied at least partially from the start.

The calculated maximum water content of the {$CaCl_2$ + KCl} sample declined with every cycle from n = 10.8 to 5.4 {H_2O} per formula unit and partial melting can occur at T_1 ~ 141 to 142°C and T_2 ~ 149°C.

The water content of the {$2CaCl_2$ + KCl} mixture varied between n = 13.6 and 16.9 {H_2O} per formula unit. Partial melting can occur between T ~ 143 to 145°C.

All of those the three samples showed endothermic behavior after cooldown, while no weight changes took place, which indicated the materials were shifting their phase from a higher crystal order like cubic, hexagonal or orthorhombic to a crystal order of lower symmetry. This points to a high order mineral phase existing only at an increased temperature of T > 44°C, going by the single low temperature peak recorded during the 1st hydration of the {$CaCl_2$+ 2KCl} sample. It is possible that a compound similar to orthorhombic Carnallite ($KMgCl_3 \cdot 6H_2O$) with shared planes of KCl_6 octahedra and $Ca(H_2O)_n$ within the gaps in the crystal lattice can form as the volume of the structure is increased by thermal expansion, which segregates back into the educts {$CaCl_2 \cdot nH_2O$} and {KCl} as the volume is reduced again by cooldown. A powder pattern analysis of a heated sample would be necessary to validate the existence of such a temporary stable phase.

8.2.7. {$CaCl_2$ + 2$ZnCl_2$}, {$CaCl_2$ + $ZnCl_2$} and {2$CaCl_2$ + $ZnCl_2$}

The powder pattern analysis of a {$CaCl_2$ + 2$ZnCl_2$} was inconclusive as the material showed overall readings of an amorphous mass. The few recorded refraction peaks could not be matched to the mixture's educts as can be seen in Appendix 3, Figure 34.

While of the three {$CaCl_2$} and {$ZnCl_2$} mixtures only the {2$CaCl_2$ + $ZnCl_2$} showed partial melting events at temperatures of T_1 ~ 146°C, T_2 ~ 193°C or T_3 ~ 195 to 196°C, all of the samples took up water easily and as observed later in the laboratory scale testing series, tended to dissolve (Table 51).

The reason there are no known natural occurring calcium-zinc chloride minerals may be due to the strong deliquescence of the material, which would require a

completely arid environment for a note-able deposit to form. If the water supply can be strictly regulated, the {$CaCl_2$ + $ZnCl_2$} mixture with its good thermal stability, low reaction temperature and stable peak distribution may still be considered as useable storage material.

8.2.8. {$ZnCl_2$}

Of the different hydrated stages of zinc chloride, the crystal structures of {$ZnCl_2 \cdot 2.5H_2O$} monoclinic ($P\ 1\ \frac{2_1}{n}\ 1$) (Hennings, Schmidt, & Voigt, 2014), {$ZnCl_2 \cdot 3H_2O$} triclinic ($P\ \bar{1}$) (Hennings, Schmidt, & Voigt, 2014), (Wilcox, et al., 2015) and {$ZnCl_2 \cdot 4.5H_2O$} orthorhombic ($P\ 2_1\ 2_1\ 2_1$) (Hennings, Schmidt, & Voigt, 2014) are known.

According to (Hennings, Schmidt, & Voigt, 2014) {$ZnCl_2 \cdot 4.5H_2O$} and {$ZnCl_2 \cdot 3H_2O$} can be treated as low temperature phases, stable at T = -50°C and T = -10°C respectively. Though {$ZnCl_2 \cdot 4H_2O$} will crystallize from solution at room temperature (Lohninger, 2013).

Due to its deliquescence the sample had drawn additional water from the atmosphere during the idle time on the sample holder of the TGA/DSC the water content had increased to n = 6.5 {H_2O} per formula unit and was likely liquefied before the start of the measurement.

Drying the sample to the full anhydrate state was not realized within the applied temperature interval. The sample was still holding about n = 2.5 {H_2O} per formula unit at T_{max} = 100°C and n = 1.5 {H_2O} per formula unit at T_{max} = 200°C respectively.

The {$ZnCl_2 \cdot 4.5H_2O$} occurs as {$2ZnCl_2 \cdot 9H_2O$} where one of the Zn^{2+} cations form a tetrahedron with all four Cl^-, and the second Zn^{2+} cation forms an octahedron with six of the {H_2O}-molecules. The remaining three {H_2O}-molecules are situated in the free spaces between the tetrahedra and octahedra.

The {$ZnCl_2 \cdot 3H_2O$} also occurs as {$2ZnCl_2 \cdot 6H_2O$}, consisting of a ($ZnCl_4$)-tetrahedron and a ($Zn(H_2O)_6$)-octahedron. While the three unbonded {H_2O}-

molecules have escaped the crystal structure, which led to the phase shift from orthorhombic to triclinic.

This continues with the {$ZnCl_2 \cdot 2.5H_2O$} where the {$2ZnCl_2 \cdot 5H_2O$} consist of a ($ZnCl(H_2O)_5$)-octahedron and a ($ZnCl_4$)-tetrahedron which share one of the Cl^- anions.

The development during dehydration can be seen in Figure 23.

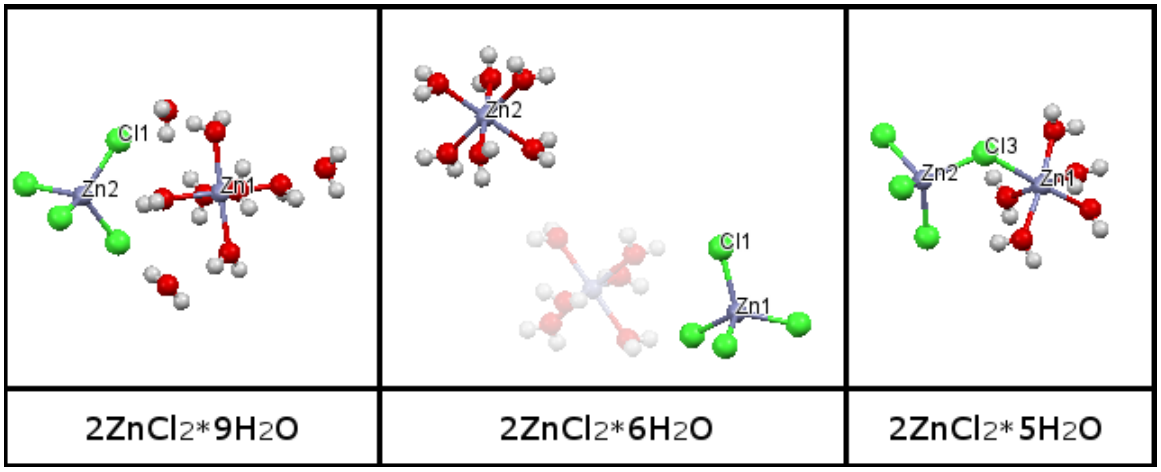

Figure 23 Changes in the crystal structure of zinc chloride hydrates during dehydration. (Hennings, Schmidt, & Voigt, 2014), (Wilcox, et al., 2015), (Created with Mercury 3.1, 2015)

While the crystal structure has not yet been confirmed, it is possible that the {$ZnCl_2 \cdot 1.5H_2O$} (Holleman & Wiberg, 2001) occurs as {$2ZnCl_2 \cdot 3H_2O$} where both Zn^{2+} cations share three of the Cl^- anions in a way that the octahedron and the tetrahedron share a face. This however would decrease the stability of the crystal structure according to the 3rd rule of Pauling (Pauling, 1960). Therefore, it is more likely that the octahedra begin to share corners with more than one tetrahedron as the {H_2O} molecules are removed, until at complete dehydration only linked ($ZnCl_4$)-tetrahedrons are left. This goes conform with the monoclinic ($P\ 1\ \frac{2_1}{n}\ 1$) (Winkler & Brehler, 1959), the tetragonal ($I\ \bar{4}\ 2\ d$) (Oswald & Jaggi, 1960) and the orthorhombic ($P\ n\ a\ 2_1$) (Brynestad & Yakel, 1978) where the crystal is arranged in

interconnected ($ZnCl_4$)-tetrahedrons but not with the trigonal crystal lattice ($R\ \bar{3}\ m$) (Wyckoff R. W., 1931) where the chlorides are stacked in layers.

8.2.9. {$ZnCl_2$ + 2KCl}, {$ZnCl_2$ + KCl}, {2$ZnCl_2$ + 2KCl}

While there are no naturally occurring potassium-zinc chloride minerals, anhydrate potassium tetrachlorozincate (K_2ZnCl_4) exists in synthetical form and can occur monoclinic ($C\ 1\ c\ 1$) at T < 145K (Mashiyama, 1993), orthorhombic ($P\ n\ a\ 2_1$) and orthorhombic ($P\ n\ a\ m$), with the latter forming at T > 555K (Ferrrari, Roberts, Thomson, Gale, & Catlow, 2001). Within the given temperature interval of T = 25 to 200°C used during the TGA/DSC analysis, only a compound with the orthorhombic ($P\ n\ a\ 2_1$) lattice would have been stable. A single unit cell contains three formula units (K_2ZnCl_4) for a total of (K_6Zn3Cl_{12}) which are aligned in three asymmetrical $ZnCl_4$-tetrahedra, three asymmetrical KCl_6-octahedra and three asymmetrical KCl_8-hexahedra. In absence of {H_2O} all connections are by the Cl^- anions. The tetrahedra, octahedra and hexahedra are all interconnected and share corners as well as edges. The three KCl_8-hexahedra are sharing planes with each other, which results in an instability in the crystal lattice according to the 3rd rule of Pauling (Pauling, 1960).

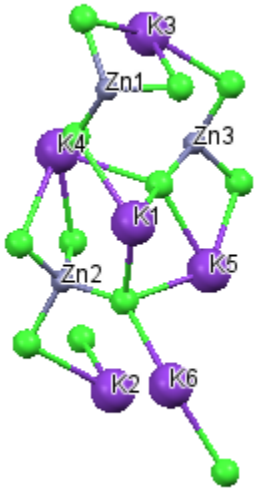

Figure 24 Orthorhombic ($P\ n\ a\ 2_1$) crystal lattice of potassium tetrachlorozincate (K_6Zn3Cl_{12}) (Ferrrari, Roberts, Thomson, Gale, & Catlow, 2001), (Created with Mercury 3.1, 2015)

A hydrated compound with a different mixing ratio was described by (Suesse & Brehler, 1964) in the form of monoclinic ($P\ 1\ \frac{2_1}{a}\ 1$) ($KZnCl_3{\cdot}2H_2O$). They described a crystal structure consisting of $ZnCl_3(H_2O)$-tetrahedra and asymmetrical $KCl_7(H_2O)$-hexahedra, where K^+ cations are surrounded by seven Cl^- anions and a single (H_2O) molecule. This (H_2O) molecule is shared with

the $ZnCl_3(H_2O)$-tetrahedra, though the asymmetrical hexahedra and the tetrahedra share an edge over the chlorides as well. This is interesting as opposite to the crystal lattice of $\{2ZnCl_2 \cdot 5H_2O\}$ the linkup is not exclusively achieved over a shared Cl^- anion. The remaining (H_2O) molecule is not connected to the tetrahedra or hexahedra and is situated in the free space of the crystal lattice as can be seen in Figure 25.

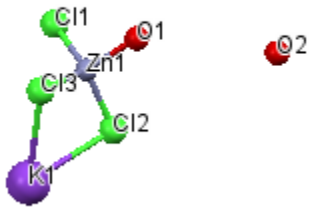

Figure 25 Crystal lattice of monoclinic ($P\ 1\ \frac{2_1}{a}\ 1$) ($KZnCl_3 \cdot 2H_2O$) (Suesse & Brehler, 1964) (hydrogens not depicted), (Created with Mercury 3.1, 2015)

As the {KCl} total in the mixtures was higher than calculated, the reaction enthalpies of possible compounds or unaltered $\{CaCl_2 \cdot nH_2O\}$ were muted compared to those of the excess {KCl}. The {KCl} influence was visible as an endothermic peak at the start of hydration, where heat was consumed for breaking up its cubic crystal structure.

The $\{2ZnCl_2 + 7KCl\}$ mixture started out with n = 3.5 $\{H_2O\}$ per Zn^{2+} cation, and still held n = 3.0 $\{H_2O\}$ at T_{max} = 100°C and n = 2.5 to 2.8 $\{H_2O\}$ per Zn^{2+} cation at T_{max} = 200°C respectively. Compared to the untreated $\{ZnCl_2 \cdot nH_2O\}$ sample this is an increased water content per Zn^{2+} cation, indicating that a compound may have formed.

The calculated water content of the $\{4ZnCl_2 + 7KCl\}$ mixture was n = 5.9 $\{H_2O\}$ per Zn^{2+} cation at the start of the measurement, with three to four peaks below T_{max} = 100°C, the hydration stages in between were likely n = 5.0, 4.5, 4.0 and 3.5 per Zn^{2+} cation, which indicates that like for the untreated $\{ZnCl_2 \cdot nH_2O\}$ sample, at least two zinc cations were required to form a unit cell. However, the dehydration curve showed additional four peaks within the temperature interval of T = 100 to 200°C, where the water content sank by only a single $\{H_2O\}$ per Zn^{2+} cation, which leads to the conclusion, that at least temporary a crystal structure was formed which incorporated four zinc cations into a single unit cell. The corresponding temperatures and water contents are listed in Table 52.

Table 52 Estimated hydration stages of the {4$ZnCl_2$ + 7KCl} mixture at different temperatures

T [°C]	25	50	54	78	89	122	134	180	189
n {H_2O} per Zn^{2+}	6.00	5.00	4.50	4.00	3.50	3.25	3.00	2.75	2.50

The {8$ZnCl_2$ + 7KCl} mixture started out with n = 6.3 {H_2O} per Zn^{2+} cation but hydrated to up to n = 7.5 {H_2O} per Zn^{2+} cation. After only a single peak below T_{max} = 100°C the water content declined to n = 4.0 {H_2O} per Zn^{2+} cation. A partial melting of the mixture occurred at T ~ 194°C for a chemical composition of approximately {8$ZnCl_2$ + 7KCl + 24H_2O}, which hadn't been observed for either the untreated {$ZnCl_2$·nH_2O} nor for the samples with a higher percental {KCl} content. Aside from the melting peak there were only three peaks recorded in the temperature interval of T = 100 to 200°C, where the water content declined from n = 4.0 to 2.5 {H_2O} per Zn^{2+} cation as can be seen in Table 53. There is no indication that crystal structures requiring four zinc cations formed, like for the {4$ZnCl_2$ + 7KCl} mixture.

Table 53 Estimated hydration stages of the {8$ZnCl_2$ + 7KCl} mixture at different temperatures, including melting temperature

T [°C]	25	56 to 73	158	193	194	196
n {H_2O} per Zn^{2+}	6.30 to 7.50	4.0	3.50	3.00	melt	2.50

While the three tested zinc-potassium chloride mixtures all approached a water content of n = 2.5 {H_2O} per Zn^{2+} cation after heating to T_{max} = 200°C, it appears that the mixing ratio influenced the formation of different compounds with varying crystal structures and material properties.

8.3. Bromides

Several of the strontium-bromide -mixtures showed low temperature melting points in hydrated stage. Compared to untreated {$SrBr_2$}, a decline in heat storage density and reaction enthalpy output were observed for the mixtures. The exceptions were the three {$LiBr+SrBr_2$} samples but since lowering the material costs was the main aim for blending {$SrBr_2$} with other substances, an addition of the also costly lithium bromide was not going to achieve that goal.

TGA/DSC testing cross mixtures of strontium bromide with sulfates and chlorides, led to a multi-cycle analysis of the mixture {$5SrBr_2 + 8CaCl_2$}, which has no naturally occurring mineral equivalent, since no melting behavior was observed during dehydration. The heat storage density and reaction enthalpy values of the material were decent, if decreased in comparison to untreated {$SrBr_2$}.

The 10-cycles TGA analysis showed the reaction enthalpies, calculated from hydration and dehydration curves of {$5SrBr_2 + 8CaCl_2$}, settling after three cycles and then remaining stable over the remaining seven cycles.

The evaluation with the laboratory scale setup #3 however, showed mass loss of the m = 20g {$5SrBr_2 + 8CaCl_2$} sample, caused by melting during the dehydration.

8.4. Cross mixtures

The sulfate-chloride cross mixtures {$3MgSO_4 + 16KCl$} based on the mineral Kainite ($MgSO_4 \cdot KCl \cdot 3H_2O$) (Robinson, Fang, & Ohya, The crystal structure of kainite, 1972), (Anthony, Bideaux, Bladh, & Nichols, 2003) and {$ZnSO_4 + 36ZnCl_2$} which was planned to be synthesized as a zinc variation of the mineral Guarinoite ($((Zn,Co,Ni)_6(SO_4)(OH,Cl)_{10} \cdot 5H_2O$) (Sarp, 1993), (Mandarino, 1997), (Anthony, Bideaux, Bladh, & Nichols, 2003) showed some potential as heat storage materials.

While using hydrates instead of anhydrates caused a deviation in the mixing ratios away from the planned compositions, an improvement of the material properties of {$3MgSO_4 + 16KCl$} and {$ZnSO_4 + 36ZnCl_2$} over untreated {$MgSO_4$} or {$ZnCl_2$} was

observed. The {3$MgSO_4$ + 16KCl} showed a good cycle stability over the initial testing cycles. The powder pattern analyses indicated that indeed Kainite (4($KMg(SO_4)Cl$)·11H_2O) in the monoclinic form ($C\ 1\ \frac{2}{m}\ 1$) (Robinson, Fang, & Ohya, 1972), (Cambridge Crystallographic Data Centre (CCDC), 2016) had crystallized in the sample and existed alongside of Sylvite (KCl) in the cubic form ($F\ m\ \bar{3}\ m$) (Heinrich Heine Universität Düsseldorf , 2013). The low storage density relative to the sample mass was caused by that excess {KCl}. Reducing the amount of the additional unreactive material may increase the storage density without impacting the improved cycle stability.

And while the {$ZnSO_4$ + 36$ZnCl_2$} mixture can rather be treated as impure {$ZnCl_2$}, the sample shows an improved energy storage density compared to untreated {$ZnCl_2$}.

9. For future consideration

While the four mixed materials which had passed the initial TGA/DSC analysis all showed undesired material properties during the laboratory scale evaluation. However, low melting points as for the {$2MgCl_2$+$CaCl_2$} mixture can likely be circumvented by slower heating rates and the {$2MgCl_2$+KCl} may recover between hydrations, if the dehydration time is extended. Further testing with increased dehydration periods and slower heating rates respectively is suggested.

More evaluations of mixed salts for the {$5ZnCl_2$+$ZnSO_4$} cross mixture, samples blended with {NaCl} and {LiCl} and more different bromide mixtures or chloride-bromide intermixtures may lead to promising heat storage materials.

Storage of all samples at T = 60 to 70°C and preparation under a dry helium or nitrogen atmosphere coupled with reduced idle time on the sample tray in the TGA/DSC or using crucibles with a lid would eliminate the influence of air humidity on the starting hydration stage and lower the chance of sample liquefaction due to deliquescence.

To be able to accurately calculate the hydration stages of all materials, a high temperature dehydration should complement all the cycle measurements. Since several of the materials did not completely dry at T_{max} = 500°C and melting events weren't observed for all mixtures either, raising the maximum dehydration temperature to T_{max} = 700°C or higher is suggested. Preferably another high temperature dehydration should follow or replace the 2^{nd} T_{max} = 200°C dehydration of the cycle measurements and follow every multi cycle measurement.

More and longer multi-cycle measurements are also suggested for salt mixtures of interest.

For a more exact calculation of the specific heat capacity of all the tested salt mixtures, a larger number of spot samples needs to be taken from the measured dehydration curves, ideally the entire curves. These calculations should run parallel to calorimeter measurements of c_p of materials from the same mixture batch for a higher accuracy.

A realization and testing of the suggested laboratory scale setup #4 should, additionally to the parallel recording of sample and glass-standard temperatures, implement a method to directly control the applied heating rate and the water flow into the sample holder to avoid melting and dissolving events.

All samples should undergo XRPD evaluations at different stages of hydration. For the dehydration, the mixtures need to be either dried within a desiccator or in an oven with low heating and cooling rates respectively, to avoid melting and amorphous solidification. To ensure that the material is not altered by extended storage or exposure to air-humidity, the samples should either be vacuum sealed for transport or prepared directly at the institute where the XRPD analysis is supposed to take place.

10. Acknowledgements

I want to thank the following people whose commitment, encouragement and support made this work possible:

For their great help with setting up the measuring equipment in the laboratory and workshop, synthesizing the samples and their tolerance for me borrowing tools:

Karsten Neumann

and

Dagmar Schuchard

For teaching me as of how to handle the TGA/DSC analysis machines, how to interpret reaction curves, suggestions for laboratory setup improvements, help in the laboratory, workshop and with the evaluations and always having an open ear for my countless questions:

Melanie Böhme

Kathrin Korhammer,

Amanda Watts,

Armand Fopah-Lele,

N'Tsoukpoe Kokouvi Edem,

Dr. Holger Urs Rammelberg,

For encouraging me to do a doctorate and for being a great boss who showed zestful enthusiasm for the project:

Dr. Thomas Osterland,

For his advisory help with the doctorate thesis and university-administrative questions:

Professor Dr. Oliver Opel,

For accepting my expose and granting me the opportunity to do a doctorate

Professor Wolfgang Ruck

For a great working atmosphere:

The other members of the project “Thermochemical battery” of the innovation incubator at the Leuphana University Lüneburg

For all the backup I could wish for:

My family

11. Sources

(1873). *Accademia Napoli Atti 6*, S. 43.

(1951). *Mineralogical Magazine 29*, S. 667.

(1967). *Kali und Steinsalz 4*, S. 326.

(1969). *National Bureau of Standards, Monograph, 7*, S. 36.

(1987). *Neues Jahrbuch für Mineralogie, Monatshefte*, S. 171.

Abrahams, I., & Vordemvenne, E. (1995). Strontium Dibromide Hexahydrate. *Acta Crystallographica Section C, 51*, S. 183 - 185.

Ahtee, M. (1969). Lattice constants of some binary alkali halide solid solutions. *Annales Academiae Scientiarum Fennicae Series A6: Physica, 313*, S. 1-11.

Aljubouri, Z. A., & Aldabbach, S. M. (1980). Sinjarite a new mineral from Iraq. *Mineralogical Magazine 43*, S. 643 - 645.

American Elements. (05. 09 2017). *Magnesium Bromide Hexahydrate*. Von American Elements, The Advanced Materials Manufacturer: https://www.americanelements.com/magnesium-bromide-hexahydrate-13446-53-2 abgerufen

Andress, K. R., & Gundermann, J. (1934). Die Struktur von Magnesiumchlorid- und Magnesiumbromidhexahydrat. *Zeitschrift fuer Kristallographie, Kristallgeometrie, Kristallphysik, Kristallchemie (-144,1977), 87*, S. 345-369.

Andress, K. R., & Gundermann, J. (1934). Die Struktur von Magnesiumchlorid- und Magnesiumbromidhexahydrat. *Zeitschrift fuer Kristallographie, Kristallgeometrie, Kristallphysik, Kristallchemie (-144,1977), 87*, S. 345-369.

Anthony, J., Bideaux, R., Bladh, K., & Nichols, M. (1997). *Handbook of Minersalogy, vol. 3, Halides, Hydroxides, Oxides.*

Anthony, J., Bideaux, R., Bladh, K., & Nichols, M. (2003). *Handbook of Mineralogy, vol. 5, Borates, Carbonates, Sulfates.*

Armstrong, G., Dunham, K. C., Harvey, C. O., Sabine, P. A., & Waters, W. F. (1951). The Paragenesis of Sylvine, Carnallite, Polyhalite, and Kieserite in Eskdale Borings nos. 3, 4, and 6, North-East Yorkshire. *Mineralogical Magazine 29*, S. 667.

Barskii, J. A., & Egorov, G. M. (1993). Investigation of Heat Capacity of some Inorganic Salts. *Viniti*, S. 1-39.

Bassi, I. W., Polanto, F., Calcaterra, M., & Bart, J. J. (1982). A new layer structure of Mg Cl2 with hexagonal close packing of the chlorine atoms. *Zeitschrift fuer Kristallographie, 159* , S. 297-302.

Baur, W. H. (1964). On the crystal chemistry of salt hydrates. III. The determination of the crystal structure of FeSO4.7H2O (melanterite). *Acta Crystallographica 17*, S. 1167 - 1174.

Baur, W. H., & Rolin, J. L. (1972). Salt hydrates. IX. The comparison of the crystal structure of magnesium sulfate pentahydrate with copper sulfate pentahydrate and magnesium chromate pentahydrate. *Acta Crystallographica B28*, S. 1448 - 1455.

Biermann, M., Blanke, W., Dammermann, W., German, S., Gorski, W., Grigull, U., . . . Weiß, R. (1989). *Thermophysikalische Stoffgrößen.* New York: Springer Verlag Berlin Heidelberg.

Borchard-Ott, W. (2002). *Kristallographie.* Berlin Heidelberg New York: Springer.

Brackett, E. B., Brackett, T. E., & Sass, R. L. (1963). The crystal structure of calcium bromide. *Journal of Inorganic and Nuclear Chemistry,25*, S. 1295-1296.

Brehler, B. (1977). Kristallstrukturuntersuchungen an Zn Cl2. *Zeitschrift fuer Kristallographie, Kristallgeometrie, Kristallphysik, Kristallchemie (-144,1977), 145*, S. 146-154.

Brynestad, J., & Yakel, H. L. (1978). Preparation and structure of anhydrous zinc chloride. *Inorganic Chemistry, 17*, S. 1376-1377.

Burke, E. A. (2008). Tidying up mineral names: an IMA-CNMNC scheme for suffixes, hyphens and diacritical marks . *The Mineralogical Record 39/2*, S. 131.

Burns, J. A., & Verall, R. E. (1974). II. Heat Capacities of Solid State from 273 to 373 K. *Thermochim.Acta 9*, S. 277-287.

Busing, W. R. (1970). An interpretation of the structures of alkaline earth chlorides in terms of interionic forces. *Transactions of the American Crystallographic Association, 6*, S. 57-72.

Calleri, M., Gavetti, A., Ivaldi, G., & Rubbo, M. (1984). Synthetic epsomite, MgSO4.7H2O: absolute configuration and surface features of the complementary {111} forms. *Acta Crystallographica B40*, S. 218 - 222.

Cambridge Crystallographic Data Centre (CCDC). (05. 11 2016). Mercury - Crystal Structure Visualisation, Exploration and Analysis Made Easy . *Mercury 3.9 (Build RC1)*. Cambridge, UK.

Cemič, L. (2005). *Thermodynamics in Mineral Sciences, An Introduction.* Netherlands: Springer.

Černý, R., Ravnsbæk, D., Schouwink, P., Filinchuk, Y., Penin, N., Teyssier, J., . . . Jensen, T. (2012). Potassium Zinc Borohydrides Containing Triangular [Zn(BH4)3]−and Tetrahedral [Zn(BH4)xCl4–x]2–Anions. *The Journal of Physical Chemistry C, 116*, S. 1563.

Cesbron, F., & Sadrzadeh, M. (1973). NEW DATA ON ALUNOGEN AL2 (SO4) 3.18 H2O. *Bulletin de la Société Française de Minéralogie et de Cristallographie 96*, S. 385.

ChemicalBook. (05. 09 2017). *Magnesium bromide hexahydrate(13446-53-2)*. Von Chemical Book: http://www.chemicalbook.com/ProductMSDSDetailCB1733222_EN.htm abgerufen

Clark, J. R., Evans, H. T., & Erd, R. C. (1980). Tachyhydrite, dimagnesium calcium chloride 12-hydrate Locality: synthetic. *Acta Crystallographica, Section B, 36*, S. 2736-2739.

Clark, J. R., Evans, H. T., & Erd, R. C. (1980). Tachyhydrite, dimagnesium calcium chloride 12-hydrate Locality: synthetic. *Acta Crystallographica, Section B, 36*, S. 2736-2739.

Created with Mercury 3.1. (2015). Von http://www.ccdc.cam.ac.uk/mercury/# abgerufen

Cromer, D. T., Kay, M. I., & Larson, A. C. (1967). Refinement of the alum structures. II. X-ray and neutron diffraction of NaAl(SO4)2*12H2O, gamma alum Locality: synthetic. *Acta Crystallographica, 22*, S. 182-187.

CWK Bad Köstritz. (01 2013). Köstrolith. *Molecular Sieve Köstrolith 13XBFK*. Heinrichshall 2, 07586 Bad Köstritz, Germany.

CWK Bad Köstritz. (01 2013). Köstrolith. *Molecular Sieve Köstrolith 4ABFK*. Heinrichshall2, 07586 Bad Köstritz, Germany.

CWK Chemiewerk Bad Köstritz GmbH. (2017). *CWK*. Abgerufen am 23. 05 2017 von Because Chemistry Matters: http://www.cwk-bk.de/products/molecular-sieves/

Darapsky. (1890). *Neues Jahrbuch für Mineralogie, Geologie und Paleontologie, Heidelberg, Stuttgart: I: 49*.

Darapsky. (1890). *Neues Jahrbuch für Mineralogie, Geologie und Paleontologie.* Heidelberg, Stuttgart.

Day, N., & Murray-Rust, P. (02. 10 2017). *Crystallography Open Database*. Von COD: http://www.crystallography.net/cod/search.html abgerufen

Demartin, F., Castellano, C., Gramaccioli, M., & Campostrini, I. (2010). ALUMINUM-FOR-IRON SUBSTITUTION, HYDROGEN BONDING, AND A NOVEL STRUCTURE-TYPE IN COQUIMBITE-LIKE MINERALS. *Canadian Mineralogist 48*, S. 323 - 333.

Dinnebier, R. E., Freyer, D., Bette, S., & Oestreich, M. (2010). 9Mg(OH)2.MgCl2.4H2O, a High Temperature Phase of the Magnesia Binder System. *Inorganic Chemistry,49*, S. 9770-9776.

Donkers, P. (2015). *Experimental study on thermochemical heat storage materials.* Uitgeverij BOXPress.

Druske, M.-M., Fopah-Lele, A., Korhammer, K., Rammelberg, H. U., Wegscheider, N., Ruck, W., & Schmidt (Osterland), T. (2014). Developed materials for thermal energy storage: synthesis and characterization. *Energy Procedia 61 (2014), The 6th International Conference on Applied Energy – ICAE2014*, (S. 96 to 99).

EC POWER A/S. (2016). *BHKW-Anlagen auf dem Stand der Technik*. Abgerufen am 29. 03 2017 von Technische Daten: http://www.ecpower.eu/de/technische-daten.html

Energiewerkstatt. (2017). *Innovationen für Wärme und Strom*. Abgerufen am 29. 03 2017 von Technische Daten: http://www.energiewerkstatt.de/blockheizkraftwerke/technische-daten/

Erd, R. C., Clynne, M. A., Clark, J. R., & Potter, R. W. (1979). Crystal data for tachyhydrite, CaMg2Cl6.12H2O. *Journal of applied crystallography 12*, S. 481-482.

Ericksen, G. E., Mrose, M. E., & Fahey, J. J. (1970). Ice Clear Mirabilite from Chile. *The Mineralogical Record 1*, S. 12 - 15, 24 - 25.

Fang, J. H., & Robinson, P. D. (1970). CRYSTAL STRUCTURES AND MINERAL CHEMISTRY OF DOUBLE-SALT HYDRATES. 2. CRYSTAL STRUCTURE OF LOEWEITE. *American Mineralogist 55*, S. 378.

Fang, J. H., & Robinson, P. D. (1972). Crystal structures and mineral chemistry of double-salt hydrates: II. The crystal structure of mendozite, NaAl(SO4)2.11H2O. *American Mineralogist, 57*, S. 1081-1088.

Ferrrari, E. S., Roberts, K. J., Thomson, G. B., Gale, J. D., & Catlow, C. R. (2001). Interatomic potential parameters for potassium tetrachlorozincate and their

application to modelling its phase transformations. *Acta Crystallographica Section A, 57*, S. 264-271.

Fischer, W. (1973). Die kristallstruktur des carnallits KMgCl3*6H2O Locality: synthetic. *Neues Jahrbuch fur Mineralogie, Monatshefte*, S. 100-109.

Fischer, W. (1973). Die kristallstruktur des carnallits KMgCl3*6H2O Locality: synthetic. *Neues Jahrbuch fur Mineralogie, Monatshefte, 1973*, S. 100-109.

Fleischer, M. (1943). New Mineral Names. *American Mineralogist 28*, S. 61.

Fleischer, M. (1952). New mineral names. *American Mineralogist 37*, S. 1070-1073.

Fleischer, M. (1963). New Mineral Names. *American Mineralogist 48*, S. 433.

Floerke, O. W. (1952). Kristallographische und roentgenometrische Untersuchungen im System Ca S O4 - Ca S O4 (H2 O)2. *Neues Jahrbuch fuer Mineralogie. Abhandlungen (1950-), 84*, S. 189-240.

Fopah Lele, A. (2016). *Thermochemical Heat Storage System for Households: Thermal Transfers Coupled to Chemical Reaction Investigations.* Springer.

Fopah Lele, A., Korhammer, K., Wegscheider, N., Rammelberg, H. U., Schmidt (Osterland), T., & Ruck, W. K. (2013). THERMAL CONDUCTIVITY MEASUREMENT OF SALT HYDRATES AS POROUS MATERIAL USING CALORIMETRIC (DSC) METHOD. *8 th World Conference on Experimental Heat Transfer, Fluid Mechanics, and Thermodynamics.* Lisbon, Portugal.

Galan, M. A., Labrador, M. D., & Alvarez, J. R. (1980). Salt effect in liquid-vapor equilibrium: ethanol-water system saturated with strontium bromide, barium nitrate, and strontium nitrate. *J. Chem. Eng. Data, 25,(1)*, S. 7-9.

Galan, M. A., Labrador, M. D., & Alvarez, J. R. (1980). Salt effect in liquid-vapor equilibrium: ethanol-water system saturated with strontium bromide, barium nitrate, and strontium nitrate. *J. Chem. Eng. Data, 25 (1)*, S. 7-9.

Gardner, P. J., Finch, A., Steadman, C. J., & Crosby. (1971). Solvation studies. II. Alkaline earth halides in high dielectric solvents. *J. Phys. Chem., 75 (15)*, S. 2325-2329.

Georgia State University. (11. 09 2017). *Thermodynamic Properties of Selected Substances* . Von hyperphysics.info: http://hyperphysics.phy-astr.gsu.edu/hbase/Tables/therprop.html abgerufen

Giester, G., & Rieck, B. (1995). Mereiterite, K2Fe[SO4]2·4H2O, a new leonite-type mineral from the Lavrion Mining District, Greece. *European Journal of Mineralogy 7*, S. 559.

Hargittai, M., Tremmel, J., & Hargittai, I. (1986). Molecular structures of zinc dichloride, zinc dibromide, and zinc diiodide from electron diffraction reinvestigation. *Inorganic Chemistry 25*, S. 3163.

Harris, J. D., & Rusch, A. W. (2013). Identifying Hydrated Salts Using Simultaneous Thermogravimetric Analysis and Differential Scanning Calorimetry. *J. Chem. Educ., 90 (2)*, S. 235-238.

Hawthorne, F. C. (1985). Refinement of the crystal structure of bloedite; structural similarities in the [VI M(IV TPhi 4) 2 Phi n) finite-cluster minerals . *Canadian Mineralogist 23*, S. 669 - 674.

Hawthorne, F. C., & Ferguson, R. B. (1975). Anhydrous sulphates; I, Refinement of the crystal structure of celestite with an appendix on the structure of thenardite. *Canadian Mineralogist 13*, S. 181 to 187.

Hawthorne, F. C., Groat, L. A., Raudsepp, M., & Ercit, T. S. (1987). Kieserite, Mg(SO4)(H2O), a Titanite-Group Mineral. *Neues Jahrbuch für Mineralogie, Abhandlungen, 157*, S. 121 to 132.

Hayes, A. A. (1844). Description and Analysis of Pickeringite, a native Magnesian Alum. *American Journal of Science 46*, S. 360.

Haynes, W. M. (2011). *CRC Handbook of Chemistry and Physics (92nd ed.).* CRC Press.

Heinrich Heine Universität Düsseldorf . (2013).

Hennings, E., Schmidt, H., & Voigt, W. (2013). Crystal structures of hydrates of simple inorganic salts. I. Water-rich magnesium halide hydrates MgCl~2~·8H~2~O,

MgCl~2~·12H~2~O, MgBr~2~·6H~2~O, MgBr~2~·9H~2~O, MgI~2~·8H~2~O and MgI~2~·9H~2~O. *Acta Crystallographica Section C, 69*, S. 1292-1300.

Hennings, E., Schmidt, H., & Voigt, W. (01. 12 2014). Crystal structures of ZnCl2·2.5H2O, ZnCl2·3H2O and ZnCl2·4.5H2O. *Acta Chrystallogr. Section E Struct Rep Online; 70 (Pt 12)*, S. 515-518.

Hoennerscheid, A., Jansen, M., Nuss, J., & Muehle, C. (2003). Die Kristallstrukturen der Monohydrate von Lithiumchlorid und Lithiumbromid. *Zeitschrift fuer Anorganische und Allgemeine Chemie, 629*, S. 312-316.

Holleman, A. F., & Wiberg, E. (2001). *Inorganic Chemistry.* San Diego: Academic Press.

Hoppe, A. (26. 03 2018). *Das interaktive Periodensystem der Elemente (PSE)*. Von http://www.periodensystem.info abgerufen

Hudson Institute of Mineralogy 1993-2017. (02. 10 2017). *Mindat*. Von mindat.org: https://www.mindat.org/ abgerufen

IFA Institut für Arbeitsschutz Datenbank. (kein Datum). GESTIS-Stoffdatenbank. Sankt Augustin.

Institut für Arbeitsschutz der Deutschen Gesetzlichen Unfallversicherung. (05. 10 2017). *Magnesiumchlorid*. Von IFA Institut für Arbeitsschutz, GESTIS-Stoffdatenbank: http://gestis.itrust.de/nxt/gateway.dll/gestis_de/000000.xml?f=templates&fn=default.htm&vid=gestisdeu:sdbdeu abgerufen

International Programme on Chemical Safety and the European Commission. (2012). *CALCIUM BROMIDE.* Von Ilo: http://www.ilo.org/dyn/icsc/showcard.display?p_card_id=1628 abgerufen

Jambor, J. L., & Grew, E. S. (1992). New mineral names. *American Mineralogist 77*, S. 212.

Jambor, J. L., & Traill, R. J. (1963). On rozenite and siderotil. *Canadian Mineralogist 7 (5)*, S. 751 - 763.

Kaduk, J. A. (2002). Use of the Inorganic Crystal Structure Database as a problem solving tool. *Acta Crystallographica Section B, 58*, S. 370-379.

Kalaiselvam, S., & Parameshwaran, R. (2014). *Thermal Energy Storage Technologies For Sustainability.* London: Academic Press, Elsevier Inc.

Kamermans, M. A. (1939). The crystal structure of Sr Br~2~. *Zeitschrift fuer Kristallographie, Kristallgeometrie, Kristallphysik, Kristallchemie (-144,1977),101*, S. 406 - 411.

Kerkes, H., & et al. (2011). Thermochemische Energiespeicher. *Chemie Ingenieur Technik 83 No.11*, S. 2014-2026.

Khutia, A., Rammelberg, H. U., Schmidt (Osterland), T., Henniger, S., & Janiak, C. (2013). Water Sorption Cycle Measurements on Functionalized MIL-101Cr for Heat Transformation Application. *Chemistry of Materials 25 (5)*, S. 790-798.

Kipouros, G. J., & Sadoway, D. R. (2001). A thermochemical analysis of the production of anhydrous MgCl2. *Journal of Light Metals*, S. (1 - 7).

Kolesov, V. P., Paukov, I. E., & Skuratov, S. M. (1962). Free Energy Change in the Polymerisation of Lactams under Standard Conditions [Low Temperature Heat Capacities of Lactams and of Potassium Chloride]. *Russ.J.Phys.Chem. 36*, S. 400-405.

Kopp Glass; Galbraith, J. (2016). *GLASS TRANSFORMING LIGHT*. Von koppglass.com: http://www.koppglass.com/blog/glass-thermal-properties-and-their-role-in-product-design/ abgerufen

Korhammer, K., Apel, C., Osterland, T., & Ruck, W. K. (2016). Reaction of Calcium Chloride and Magnesium Chloride and their Mixed Salts with Ethanol for Thermal Energy Storage. *Energy Procedia 91*, S. 161 - 171.

Korhammer, K., Druske, M.-M., Fopah-Lele, A., Rammelberg, H. U., Wegscheider, N., Opel, O., . . . Ruck, W. (2015). Sorption and thermal characterization of composite materials based on chlorides for thermal energy storage. *Applied Energy*.

Korhammer, K., Neumann, K., Opel, O., & Ruck, W. K. (2017). Micro-scale thermodynamic and kinetic analysis of a calcium chloride methanol system for process cooling. *Energy Procedia 105*, S. 4363 to 4369.

Kunihisa, S., Dinnebier, R. E., & Schlecht, T. (2007). Structure determination of Mg~3~(OH)~5~Cl·4H~2~O (F5 phase) from laboratory powder diffraction data and its impact on the analysis of problematic magnesia floors. *Acta Crystallographica Section B, 63*, S. 805-811.

Leclair, A., & Borel, M. M. (1977). Le dichlorure de calcium dihydrate Locality: synthetic. *acta Crystallographica, Section B 33*, S. 1608-1610.

Leclaire, A., & Borel, M. M. (1977). Le dichlorure et le dibromure de calcium hexahydrates. *Acta Crystallographica B (24,1968-38,1982) 33*, S. 2938-2940.

Leclaire, A., & Borel, M. M. (1977). Le dichlorure et le dibromure de calcium hexahydrates. *Acta Crystallographica B (24,1968-38,1982), 33*, S. 2938-2940.

Leclaire, A., & Borel, M. M. (1980). La forme $-beta du dichlorure de calcium tetrahydrate. *Acta Crystallographica B (24,1968-38,1982) 36*, S. 2757-2759.

Leclaire, A., Borel, M. M., & Monier, J. C. (1980). Structure de la tachydrite. *Acta Crystallographica B (24,1968-38,1982) 36*, S. 1608-1610.

Leclaire, A., Borel, M. M., & Monier, J. C. (1980). Structure de la tachydrite. *Acta Crystallographica B (24,1968-38,1982) 36*, S. 2734-2735.

Lide, D. R. (2006). *CRC Handbook of Chemistry and Physics, 81st Edition.* CRC Press.

Lohninger, H. (08. 08 2013). *Anorganische Chemie*. Von Zinkchlorid: http://anorganik.chemie.vias.org/zinkchlorid.html abgerufen

Maiti, G., Kundu, P., & Guin, C. (2003). One-pot synthesis of dihydropyrimidinones catalysed by lithium bromide: an improved procedure for the Biginelli reaction. *Tetrahedron Lett., 44 (13)*, S. 2757-2758.

Malinko, S. V., Lisitsin, A. E., Purusova, S. P., Fitsev, B. P., & Khruleva, T. A. (1982). Korshunovskite Mg2Cl(OH) 3·nH2O a new hydrous chloride of magnesium. *Записки Всесоюзного минералогического общества (Zapiski Vsesoyuznovo*

Mineralogicheskovo Obshchestva, Zapiski Vserossiiskovo Mineralogicheskovo Obshchestva), 111, S. 324.

Mandarino, J. (1997). New Minerals 1990-1994. *Mineralogical record*.

Mandarino, J. A. (1999). Abstracts of New Mineral Descriptions (Department) . *The Mineralogical Record 30*, S. 399 - 405.

Mashiyama, H. (1993). Low-temperature commensurate phase of potassium tetrachlorozincate, K2 Zn Cl4. *Acta Crystallographica C (39,1983-), 49*, S. 9-12.

MaTecK. (2017). *Mateck Produkt Info*. Abgerufen am 09. 04 2017 von http://mateck.com/product_info.php?info=p3688_strontium-bromide-powder.html

Matsuo, M., Oguchi, H., Maekawa, H., Takamura, H., & Orimo, S.-I. (2007). Complex Hydrides: A New Category of Solid-state Lithium Fast-ion Conductors. *Material Matters Volume 5 Article 4*.

MatWeb, LLC. (11. 09 2017). *Strontium Bromide, SrBr2*. Von MatWeb, Material Property Data: http://www.matweb.com/search/datasheet.aspx?matguid=e3a1264b338b4a3c832b195457faaff1&ckck=1 abgerufen

Mc Ginnety, J. A. (1972). Redetermination of the Structures of Potassium Sulphate and Potassium Chromate: the Effect of Electrostatic Crystal Forces upon Observed Bond Lengths. *Acta Crystallographica B28*, S. 2845 to 2852.

Meek, K. M., Sharick, S., Winey, K. I., & Elabd, Y. A. (2015). Bromide and Hydroxide Conductivity-Morphology Relationships in Polymerized Ionic Liquid Block Copolymers. *Macromolecules, 48 (14)*, S. 4850-4862.

Merck & Co., Inc. (2006). *The Merck Index: An Encyclopedia of Chemicals, Drugs, and Biologicals, 14. Edition.* NJ, USA: Whitehouse Station.

Merck (formerly Sigma-Aldrich). (05. 09 2017). *Magnesium bromide* . Von Merck (Sigma-Alrich) : http://www.sigmaaldrich.com/catalog/product/ALDRICH/495093?lang=de&region=DE abgerufen

Mereiter, K. (2013). Redetermination of tamarugite, NaAl(SO~4~)~2~·6H~2~O. *Acta Crystallographica Section E, 69*, S. i63-i64.

Messerschmid-Energiesysteme. (2011). *Technisches Datenblatt des BHKW-Modul A-TRON Standa*. Abgerufen am 29. 03 2017 von http://www.messerschmid-energiesysteme.de/pdf/download88.pdf

N'Tsoukpoe, K. E., Schmidt (Osterland), T., Rammelberg, H. U., Watts, B. A., & Ruck, W. K. (2014). A systematic multi-step screening of numerous salt hydrates for low temperature thermochemical energy storage. *Applied Energy 124*, S. 1 to 16.

N'Tsoukpoe, K. E., Rammelberg, H. U., Lele, A. F., Korhammer, K., Watts, B. A., Schmidt (Osterland), T., & Ruck, W. K. (2015). A review on the use of calcium chloride in applied thermal engineering. *Applied Thermal Engineering 75*, S. 513 to 531.

Okada, K., & Ossaka, J. (1980). Structures of potassium sodium sulphate and tripotassium sodium disulphate. *Acta Crystallographica B36*, S. 919 - 921.

Opel, O., Rammelberg, H. U., Gérard, M., & Ruck, W. (2011). THERMOCHEMICAL STORAGE MATERIALS RESEARCH - TGA/DSC-HYDRATION STUDIES. *IC-SES.*

Oswald, H. R., & Jaggi, H. (1960). Zur Struktur der wasserfreien Zinkhalogenide. I. Die wasserfreien Zinkchloride. *Helvetica Chimica Acta,43*, S. 72-77.

Ott, H. (1923). Die Raumgitter der Lithiumhalogenide. *Physikalische Zeitschrift, 24*, S. 209-213.

Ott, H. (1926). Die Strukturen von Mn O, Mn S, Ag F, Ni S, Sn I~4~, Sr Cl~2~, Ba F~2~, Praezisionsmessungen einiger Alkalihalogenide. *Zeitschrift fuer Kristallographie, Kristallgeometrie, Kristallphysik, Kristallchemie (-144,1977), 63*, S. 222-230.

Palache, C., Berman, H., & Frondel, C. (1951). *The System of Mineralogy of James Dwight Dana and Edward Salisbury Dana, Yale University 1837-1892, Volume II., 7th edition, revised and enlarged.* New York: John Wiley and Sons, Inc.

Pauling, L. (1960). *The nature of the chemical bond and the structure of molecules and crystals; an introduction to modern structural chemistry (3rd ed.).* Ithaca (NY): Cornell University Press.

Perroud, P. (15. 11 2016). *ATHENA*. Von http://athena.unige.ch/athena/mineral/search.html abgerufen

Peterson, R. C., Nelson, W., Madu, B., & Shurvell, H. F. (2007). Meridianiite: A new mineral species observed on Earth and predicted to exist on Mars. *American Mineralogist 92*, S. 1756 - 1759.

Podder, J., Gao, S., Evitts, R. W., Besant, R. W., & Matthews, D. (03 2014). Synthesis of carnallite crystal from KCl – MgCl2 solutions and its characterization. *International Journal of Materials Research, Vol 105, No. 3*, S. 308-313.

Qiong-Zhu Huang, Gui-Min Lu, Jin Wang, & Jian-Guo Yu. (03 2010). Thermal Decomposition Mechanism of MgCl2·6H2O. *Journal of Inorganic Materials*.

Quartieri, S., Triscari, M., & Viani, A. (2000). Crystal structure of the hydrated sulphate pickeringite (MgAl2(SO4)4.22H2O): X-ray powder diffraction study. *European Journal of Mineralogy, 12*, S. 1131-1138.

R.A.H. (1999). *Mineralogical Abstracts 50/3*, S. 378.

Rammelberg, H. U. (07. 06 2015). Salt hydrates for thermochemical storage in a thermal battery. *Kumulative Dissertationsschrift zur Erlangung des akademischen Grades Doktor der Naturwissenschaften (Dr. rer. nat.)*. Lüneburg, Niedersachsen, Deutschland.

Rammelberg, H. U. (09. 10 2017). Internes Rundschreiben. *Waterflow waterpressure old system*. Lüneburg.

Rammelberg, H. U., Myrau, M., Schmidt (Osterland), T., & Ruck, W. (2013). AN OPTIMIZATION OF SALT HYDRATES FOR THERMOCHEMICAL HEAT STORAGE. *Paper No. IMPRES2013-117.* Fukuoka, Japan.

Rammelberg, H. U., Opel, O., Ross, S., & Ruck, W. (2011). *Hydration and Dehydration of CaO/ Ca(OH)2 and CaCl2 / CaCl2 * 6 H2O– TGA/ DSC studies.* IRES 2011.

Rammelberg, H. U., Opel, O., Ruck, W. K., & Ross, S. (2011). Hydration and Dehydration of CaO/ Ca(OH)2 and CaCl2 / CaCl2 * 6 H2O– TGA/ DSC studies. *Conference: 6th International Renewable Energy Storage Conference and Exhibition., Volume: 6th.*

Rammelberg, H. U., Osterland, T., Priehs, B., Opel, O., & Ruck, W. K. (2015). SALT HYDRATES FOR THE THERMOCHEMICAL HEAT STORAGE - OPTIMIZATION BY MIXING. *Solar Energy*.

Rammelberg, H. U., Osterland, T., Pries, B., Opel, O., & Ruck, W. K. (2016). Thermochemical heat storage materials - Performance of mixed salt hydrates. *Solar Energy 136*, S. 571 to 589.

Rammelberg, H. U., Schmidt (Osterland), T., & Ruck, W. (2012). Hydration and dehydration of salt hydrates and hydroxides for thermal energy storage - kinetics and energy release. *Energy Procedia 30*, S. 362 to 369.

Richest group. (30. 08 2017). *Strontium bromid hexahydrate CAS 7789-53-9*. Von Alibaba.com: https://german.alibaba.com/product-detail/strontium-bromide-hexahydrate-cas-7789-53-9-60646561000.html?spm=a2700.8699010.29.197.1a42b2efRI1dIi abgerufen

Riesen, R. (1 2008). Bestimmung der Wärmekapazität mittels TGA/DSC bei hohen Temperaturen Teil 1: DSC-Standardverfahren. *METTLER TOLEDO UserCom* , S. 4.

Robinson, P. D., & Fang, J. H. (1969). Crystal structures and mineral chemistry of double-salt hydrates: I. Direct determination of the crystal structure of tamarugite. *American Mineralogist, 54*, S. 19-30.

Robinson, P. D., Fang, J. H., & Ohya, Y. (1972). The crystal structure of kainite. *American Mineralogist 57*, S. 1325 - 1332.

Robinson, P., Fang, J., & Ohya, Y. (1972). The crystal structure of kainite Locality: Stassfurt, Germany. *American Mineralogist, 57*, S. 1325-1332.

Ropp, R. C. (2012). *Encyclopedia of the Alkaline Earth Compounds.* Newnes.

Roth. (19. 4 2017). *Carlroth.com.* Von Specification, Silica gel orange: https://www.carlroth.com/downloads/spez/en/P/SPEZ_P077_EN.pdf abgerufen

Sabelli, C., & Trosti-Ferroni, R. (1985). A structural classification of sulfate minerals. *Periodico di Mineralogia 54*, S. 1 - 46.

Sarp, H. (1993). Guarinoite (Zn,Co,Ni)6(SO4)(OH,Cl)10*5H2O et thérèsemagnanite (Co,Zn,Ni)6(SO4)(OH,Cl)10*8H2O, deux nouveaux minéraux de la mine de Cap Garonne, Var, France. *Arkives de Science, Genève 46 (1)*, S. 37 - 44.

Sass, R. L., Brackett, T. E., & Brackett, E. B. (1963). The crystal structure of strontium bromide. *Journal of Physical Chemistry, 67*, S. 2862 - 2863.

Sasvari, K., & Jeffrey, G. (1966). The crystal structure of magnesium chloride dodecahydrate, Mg Cl2 (H2 O)12. *Acta Crystallographica (1,1948-23,1967), 20*, S. 875-881.

Scapino, L., Zondag, H. A., Van Bael, J., Diriken, J., & Rindt, C. C. (15. March 2017). Sorption heat storage for long-term low-temperature applications: A review on the advancements at material and prototype scale. *Applied Energy, Volume 190*, S. 920 – 948.

Schlemper, E. O., Sen Gupta, P. K., & Zoltai, T. (1985). Refinement of the structure of carnallite, Mg(H2O)6KCl3. *American Mineralogist, 70*, S. 1309-1313.

Schlemper, E. O., Sen Gupta, P. K., & Zoltai, T. (1985). Refinement of the structure of carnallite, Mg(H2O)6KCl3. *American Mineralogist, 70*, S. 1309-1313.

Schlüter, J., Klaska, K.-H., & Gebhard, G. (1999). Changoite, Na2Zn(SO4)2·4H2O, the zinc analogue of blödite, a new mineral from Sierra Gorda, Antofagasta, Chile. *Neues Jahrbuch für Mineralogie, Monatshefte*, S. 97 - 103.

Siebel, E. (1941). *Die Prüfung nichtmetallischer Baustoffe.* Berlin: Springer-Verlag Berlin heidelberg GmbH.

Sigma-Aldrich. (2017). *Sigma-Aldrich Katalog*. Abgerufen am 09. 04 2017 von Strontium bromide hexahydrate:

http://www.sigmaaldrich.com/catalog/product/aldrich/433438?lang=de&region=DE&cm_sp=Insite-_-prodRecCold_xviews-_-prodRecCold10-1

Smeggil, J. G., & Eick, H. A. (1971). The crystal structure of strontium dibromide. *Inorganic Chemistry,10*, S. 1458 - 1460.

Snetsinger, K. G. (1975). What's in a Name: Starkeyite vs. Leonhardite. *The Mineralogical Record 6, No. 3*, S. 144 - 145.

Suesse, P., & Brehler, B. (1964). Die Kristallstruktur des K Zn Cl3 (H2 O)2. *Beitraege zur Mineralogie und Petrographie (-11,1965), 10*, S. 132-140.

Swanson, H. E., Gilfrich, N. T., Cook, M. I., Stinchfield, R., & Parks, P. C. (1959). Standard X-ray Diffraction Powder Patterns. *National Bureau of Standards, Circular 539/8*, S. 71.

Swanson, H. E., Mc Murdie, H. F., Morris, M. C., Evans, E. H., Paretzkin, B., (de Groot, J. H., & (Carmel, S. J. (1974). Standard X-ray Diffraction Powder Patterns; Section 11 - Data for 70 Substances. *National Bureau of Standards Monograph 11*, S. 37.

Torii, T., & Ossaka, J. (1965). Antarcticite: A New Mineral, Calcium Chloride Hexahydrate, Discovered in Antarctica. *Science 149, Issue 3687*, S. 975.

Vlassov, V. V., & Kusnetzov, A. B. (1962). On the melanterite and the products of its alteration. *Zapiski RMO (Proceedings of the Russian Mineralogical Society), Zapiski Vsesoyuznovo Mineralogicheskovo Obshchrstva, Zapiski Vserossiiskovo Mineralogicheskovo Obshchrstva 91*, S. 490-492.

Wagner&Co. (2007). *Wärmetauscher*. Abgerufen am 29. 03 2017 von Technische Information: http://old.wagner-solar.com/pdfs/deutsch/produkte/solarthermie/solarspeicher/D-Waermetauscher-TI-0512-11205000.pdf

Walenta, K. (1978). Boyleit, ein neues Sulfatmineral von Kropbach in Südlichen Schwarzwald. *Chemie der Erde 37*, S. 73 - 79.

Warren, J. (11. 09 2017). *Calcium Chloride (CaCl2), Article 1 of 2: Usage and brine chemistry* . Von Salty Matters: http://www.saltworkconsultants.com/blog/calcium-chloride-cacl2-article-1-of-2-usage-and-brine-chemistry abgerufen

Weiner, K.-L., & Hochleitner, R. (1987). Steckbrief Leonit. *Lapis 3*, S. 7.

Weiß, S. (2010). Neue Mineralien: Akaogiit, Alfredstelznerit, Arsenoflorencit-(La), Carbobystrit, Cranswickit, Cryptophyllit & Shlykovit: Edwardsit. *Lapis 10*, S. 65.

Welch, M. D., Smith, D. G., Camara, F., & Gatta, G. D. (2013). New Mineral Names. *American Mineralogist 98*, S. 279 - 282.

Wells, A. F. (1984). *Structural Inorganic Chemistry.* Oxford: Clarendon Press.

Wilcox, R. J., Losey, B. P., Folmer, J. C., Martin, J. D., Zeller, M., & Sommer, R. (2015). Crystalline and liquid structure of zinc chloride trihydrate: a unique ionic liquid. *Inorganic chemistry, 54*, S. 1109-1119.

Wildner, M., & Giester, G. (1991). The crystal structures of kieserite-type compounds. I. Crystal structures of Me(II)SO4×H2O [Me=Mn, Fe, Co, Ni, Zn]. *Neues Jahrbuch für Mineralogie, Monatshefte*, S. 296 - 306.

Wiley Information Services GmbH. (2016). *Chemgaroo, ChemgaPedia*. Abgerufen am 23. 05 2017 von Acide Katalysatoren: http://www.chemgapedia.de/vsengine/vlu/vsc/de/ch/10/heterogene_katalyse/acide_kat/acide_kat.vlu/Page/vsc/de/ch/10/heterogene_katalyse/acide_kat/zeolithe_in_der_katalyse/zeolithe_in_der_katalyse.vscml.html

Will, G. (1981). Energiedispersion und Synchrotronstrahlung: Eine neue Methode und eine neue Strahlenquelle für die Röntgenbeugung. *Fortschritte der Mineralogie, 59*, S. 31-94.

Williams, P. A., Hatert, F., Pasero, M., & Mills, S. (2010). New minerals and nomenclature modifications approved in 2010. *Mineralogical Magazine 74*, S. 376.

Williams, P. A., Hatert, F., Pasero, M., & Mills, S. J. (2010). New minerals and nomenclature modifications approved in 2010. *Mineralogical Magazine 74 (4)*, S. 798.

Winkler, H., & Brehler, B. (1959). Ueber das alpha- und beta-Zn Cl2. *Naturwissenschaften, 46*, S. 553-554.

Winter, M. (05. 09 2017). *Calcium: calcium dibromide hexahydrate.* Von WebElements: https://www.webelements.com/compounds/calcium/hexaaquocalcium_dibromide.html abgerufen

Wolf-Heiztechnik. (11 2005). *Aktive thermische Solargewinnung*. Abgerufen am 29. 03 2017 von Planungsunterlage: https://www.wolf-heiztechnik.de/fileadmin/content/Downloads/Archiv_Montage-Bedienungsanleitungen/Solarsysteme/3043703_1105_Sonnenkollektor_TopSon_TX_Planungsunterlage.pdf

Wyckoff, R. W. (1931). *Structure of Crystals, second edition.* New York: The Chemical Catalog Company, INC.

Wyckoff, R. W. (1963). Crystal Structures. In R. W. Wyckoff, *Crystal Structures* (S. 298 - 306). New York: Interscience Publishers.

Wyckoff, R. W. (1963). New York Note: Cadmium iodide structure. In R. W. Wyckoff, *Crystal structures, second edition* (S. 239-444). New York: Interscience Publishers.

Wyckoff, R. W. (1963). New York: rocksalt structure. In R. W. Wyckoff, *Crystal Structures, second edition.* New York: Interscience Publishers.

Wyckoff, R. W. (1963). Note: distorted rutile structure. *Crystal Structures*, S. 239-444.

Wyckoff, R. W. (1963). rocksalt structure. In R. W. Wyckoff, *Crystal Structures, 1, second edition* (S. 85 - 237). New York: Interscience Publishers.

Zalkin, A., Ruben, H., & Templeton, D. H. (1964). The crystal structure and hydrogen bonding of magnesium sulfate hexahydrate. *Acta Crystallographica 17*, S. 235 - 240.

Zodrow, E. L., & Mc Candlish, K. (1978). Hydrated sulfates in the Sydney Coalfield, Cape Breton, Nova Scotia. *Canadian Mineralogist 16 (1)*, S. 17 - 22.

12. Previous publications of my own

Korhammer, K.; Druske, M.-M.; Lele, A. F.; Rammelberg, H. U.; Wegschneider, N.; Opel, O.; Osterland, T.; Ruck, W. K. L.; (2015), Sorption and thermal characterization of composite materials based on chlorides for thermal energy storage; *Applied Energy*;

Druske, M.-M.; Neumann, K.; Rammelberg, H.U.; Korhammer, K.; Opel, O.; Ruck, W. K. L.; (2016); Mixed salts in thermochemical heat storage applications; *Conference: IRES 2016*;

Druske, M.-M.; Lele, A. F.; Korhammer, K.; Rammelberg, H. U.; Wegschneider, N.; Ruck, W. K. L.; Osterland, T.; (2014); Developed Materials for Thermal Energy Storage: Synthesis and Characterization; *Energy Procedia 61(2014)* S.: 96-99

Appendix

1. TGA/DSC measurement methods

Salt samples of m~10mg weight of the sulfates, chlorides and bromides were put through the following measurements:

Cycles of dehydration at T_{max} = 100°C, hydration, dehydration at T_{max} = 200°C, hydration at T_{max} = 25°C were implemented with the method named as 'MDKEN'.

Methode: S_Mineral_Be_1_MDKEN dt 1,00 s
[1] 25,0°C, 20,00 min
[2] 25,0 - 100,0°C, 1,00 K/min
[3] 100,0°C, 30,00 min
[4] 100,0 - 25,0°C, -10 K/min
[5] 25,0°C, 30,00 min
Synchronisation eingeschaltet

Methode: S_Mineral_Be_2_MDKEN dt 1,00 s
[1] 25,0°C, 20,00 min
[2] 25,0 - 100,0°C, 5,00 K/min
[3] 100,0°C, 30,00 min
[4] 100,0 - 200°C, 5,00 K/min
[5] 200,0°C, 30,00 min
[6] 200,0 - 25,0°C, -10 K/min
[7] 25,0°C, 30,00 min
Synchronisation eingeschaltet

Methode: Screening Entladung Cascade b dt 1,00 s
[1] 25,0°C, 30,00 min
[2] 25,0°C, 30,00 min N_2 25,0 ml/min
[3] 25,0°C, 45,00 min N_2 75,0 ml/min
[4] 25,0°C, 45,00 min N_2 125,0ml/min
[5] 25,0°C, 60,00 min
Synchronisation eingeschaltet

For the Bromides additional screening was conducted. The first of those consisting of a conditions-check that had combined heating and hydration steps to test up to which temperatures the samples still absorbed water.

The second screening consisted of heating the sample to T_{max} = 500°C to find the melting points of the materials and observe at which temperature the anhydrous state was reached.

Methode: S_T_conditions_check_KEN dt 1,00 s
[1] 25°C. 15,00 min
[2] 25,0 - 110°C, 1K/min N_2 150,0 ml/min
[3] 110,0°C, 30,00 min N_2 150,0 ml/min
[4] 110,0 - 62,5°C, -5,00 K/min N_2 150 ml/mim
[5] 62,5°C, 120,00 min N_2 150,00 ml/min
[6] 62,5°C, 60 min
[7] 62,5 - 25,0°C, -5,00 K/min
[8] 25,0°C, 15min
Synchronisation eingeschaltet

Methode: S_T_conditions_check_2_KEN dt 1,00 s
[1] 25°C. 15,00 min
[2] 25,0 - 110°C, 1K/min N_2 150,0 ml/min
[3] 110,0°C, 90,00 min N_2 150,0 ml/min
[4] 110,0 - 62,5°C, -50 K/min N_2 150 ml/mim
[5] 62,5°C, 120,00 min N_2 150,00 ml/min
[6] 62,5°C, 60 min
[7] 62,5 - 25,0°C, -5,00 K/min
[8] 25,0°C, 15min
Synchronisation eingeschaltet

Methode: Beladung 25-500-25°C 10K/min dt 1,00 s
[1] 25,0°C, 10,00 min
[2] 25,0 - 500,0°C, 10K/min
[3] 500,0°C, 20,00 min
[4] 500,0 - 25,0°C, -20 K/min
[5] 25,0 °C, 10,00 min
Synchronistion eingeschaltet

For the 25-cycles measurement of {2$MgCl_2$ + KCl} the temperature interval of the TGA was chosen as 35°C to 120°C to cover the expected reaction peaks within the interval and to shorten the cool-down period between cycles.

Methode: Beladen 35-120 +1°C; -5°C AlO-Blindwert
dt 1,00 s
[1] 35,0..120,0 °C, 1,00 K/min
[2] 120,0..35,0 °C, -5,00 K/min

Synchronisation eingeschaltet

The partial pressure of the water vapor e of the TGA/DSC measurement setup in use at the Leuphana University of Lüneburg within the timespan of the measurements from 2013 to 2016 was calculated by the formula (Rammelberg, Internes Rundschreiben, 2017):

$$e = 5.5986 \cdot \ln \dot{V} - 9.3708$$

$with$

$e := partial\ water\ vapor\ pressure\ [mbar]$

$\dot{V} := volume\ flow\ of\ N_2\ [ml\ min^{-1}]$

2. Minerals for Synthesis

Table 54 Naturally occurring sulfate evaporate minerals considered for synthesis and material evaluation. Cation-variations were added to Changoite and Mereiterite. Greyed out materials were not synthesized.

Mineral	Chemical formula	Educts	Mixtures synthesized for TGA/DSC
Aphthitalite (#1)	$KNa_3(SO_4)_2$	$3Na_2SO_4 + K_2SO_4$	$\{3Na_2SO_4 + K_2SO_4\}$
Aphthitalite (#2)	$K_2Na_2(SO_4)_2$	$Na_2SO_4 + K_2SO_4$	$\{Na_2SO_4 + K_2SO_4\}$
Aphthitalite (#3)	$K_3Na(SO_4)_2$	$Na_2SO_4 + 3K_2SO_4$	$\{Na_2SO_4 + 3K_2SO_4\}$
Leonite	$K_2Mg(SO_4)_2 \cdot 4H_2O$	$K_2SO_4 + MgSO_4$	$\{K_2SO_4 + MgSO_4\}$
Blödite	$Na_2Mg(SO_4)_2 \cdot 4H_2O$	$Na_2SO_4 + MgSO_4$	$\{Na_2SO_4 + MgSO_4\}$
Löweite	$Na_{12}Mg_7(SO_4)_{13} \cdot 15H_2O$	$6Na_2SO_4 + 7MgSO_4$	$\{6Na_2SO_4 + 7MgSO_4\}$
Syngenite	$K_2Ca(SO_4)_2 \cdot H_2O$	$K_2SO_4 + CaSO_4$	---
Görgeyite	$K_2Ca_5(SO_4)_6 \cdot H_2O$	$K_2SO_4 + 5CaSO_4$	---
Omongwaite (#1)	$NaKCa_5(SO_4)_6 \cdot 3H_2O$	$K_2SO_4 + Na_2SO_4 + 10CaSO_4$	---
Omongwaite (#2)	$Na_2Ca_5(SO_4)_6 \cdot 3H_2O$	$Na_2SO_4 + 5CaSO_4$	---
Changoite ---	$Na_2Zn(SO_4)_2 \cdot 4H_2O$ ---	$Na_2SO_4 + ZnSO_4$ $K_2SO_4 + ZnSO_4$	$\{Na_2SO_4 + ZnSO_4\}$ $\{K_2SO_4 + ZnSO_4\}$
Boyleite	$(Zn,Mg)SO_4 \cdot 4H_2O$	$ZnSO_4 + MgSO_4$	$\{MgSO_4 + ZnSO_4\}$
Mereiterite Amarillite ---	$K_2Fe^{2+}(SO_4)_2 \cdot 4H_2O$ $Na_2Fe^{2+}(SO_4)_2 \cdot 6H_2O$ ---	$K_2SO_4 + Fe^{2+}SO_4$ $Na_2SO_4 + Fe^{2+}SO_4$ $2Na_2SO_4 + Fe^{2+}SO_4$	$\{K_2SO_4 + Fe^{2+}SO_4\}$ $\{Na_2SO_4 + Fe^{2+}SO_4\}$ $\{2Na_2SO_4 + Fe^{2+}SO_4\}$
Alum-(Na)	$NaAl(SO_4)_2 \cdot 12H_2O$	$Na_2SO_4 + Al_2(SO_4)_3$	$\{Na_2SO_4 + Al_2(SO_4)_3\}$
Wupatkiite (1)	$CoAl_2(SO_4)_4 \cdot 22H_2O$	$CoSO_4 + Al_2(SO_4)_3$	---
Wupatkiite (2)	$NiAl_2(SO_4)_4 \cdot 22H_2O$	$NiSO_4 + A_{l2}(SO_4)_3$	---
Pickeringite	$MgAl_2(SO_4)_4 \cdot 22H_2O$	$MgSO_4 + Al_2(SO_4)_3$	$\{MgSO_4 + Al_2(SO_4)_3\}$
Aromite (oD)	$Mg_6Al_2(SO_4)_9 \cdot 54H_2O$	$6MgSO_4 + Al_2(SO_4)_3$	$\{6MgSO_4 + Al_2(SO_4)_3\}$
Halotrichite	$Fe^{2+}Al_2(SO_4)_4 \cdot 22H_2O$	$Fe^{2+}SO_4 + Al_2(SO_4)_3$	$\{Fe_n(SO_4)_m + Al_2(SO_4)_3\}$
Aluminocoquimbite	$AlFe^{3+}(SO_4)_3 \cdot 9H_2O$	$Al_2(SO_4)_3 + Fe^{3+}{}_2(SO_4)_3$	

Lausenite	$Fe^{3+}_2(SO_4)_3 \cdot 6H_2O$	$Fe^{3+}_2(SO_4)_3$	---
Calciocopiapite	$CaFe^{3+}_4(SO_4)_6(OH)_2 \cdot 19H_2O$	$CaO + 2Fe^{3+}_2(SO_4)_3$	---
Magnesiocopiapite	$MgFe^{3+}_4(SO_4)_6(OH)_2 \cdot 20H_2O$	$MgO + 2Fe^{3+}_2(SO_4)_3$	---
Aluminocopiapite	$(Al,Mg)Fe^{3+}_4(SO_4)_6(OH)_2 \cdot 20H_2O$	$Al_2O_3 + 2MgO + 8Fe^{3+}_2(SO_4)_3$	---
Metasideronatrite	$(4)Na_2Fe^{3+}(SO_4)_2(OH) \cdot H_2O$ $(+ 12H_2SO_4 + 5O_2)$	$4Na_2SO_4 + 2Fe^{3+}_2(SO_4)_3$ $(+ 15H_2O)$	---
Ferrinatrite	$Na_3Fe^{3+}(SO_4)_3 \cdot 3H_2O$	$3Na_2SO_4 + Fe^{3+}_2(SO_4)_3$	---

Table 55 Tachyhydrite and Carnallite of the chloride-series.

Mineral	Chemical formula	Educts	Untreated materials & mixtures synthesized for TGA/DSC
Sylvite	KCl	---	{KCl}
Bischofite	$MgCl_2 \cdot 6H_2O$	---	{$MgCl_2 \cdot 6H_2O$}
Sinjarite Antarcticite	$CaCl_2 \cdot 2H_2O$ $CaCl_2 \cdot 6H_2O$	--- ---	{$CaCl_2 \cdot 2H_2O$} {$CaCl_2 \cdot 6H_2O$}
---	---	---	{$ZnCl_2$}
--- --- Tachyhydrite	--- --- $CaMg_2Cl_6 \cdot 12H_2O$	$MgCl_2 + 2CaCl_2$ $MgCl_2 + CaCl_2$ $2MgCl_2 + CaCl_2$	{2CaCl2 + MgCl2} {CaCl2 + MgCl2} {CaCl2 + 2MgCl2}
--- --- ---	--- --- ---	$2MgCl_2 + ZnCl_2$ $MgCl_2 + ZnCl_2$ $MgCl_2 + 2ZnCl_2$	{2MgCl2 + ZnCl2} {MgCl2 + ZnCl2} {MgCl2 + 2ZnCl2}
--- --- ---	--- --- ---	$ZnCl_2 + 2CaCl_2$ $ZnCl_2 + CaCl_2$ $2ZnCl_2 + CaCl_2$	{2CaCl2 + ZnCl2} {CaCl2 + ZnCl2} {CaCl2 + 2ZnCl2}
---	---	MgCl2+ CaCl2 + ZnCl2	{MgCl2+ CaCl2 + ZnCl2}
--- Carnallite ---	--- $KMgCl_3 \cdot 6H_2O$ ---	$KCl + 2MgCl_2$ $KCl + MgCl_2$ $2KCl + MgCl_2$	{2MgCl2 + KCl} {MgCl2 + KCl} {MgCl2 + 2KCl}
--- Chlorocalcite ---	--- $KCaCl_3$ ---	--- $KCl + CaCl_2$ ---	{2CaCl2 + KCl} {CaCl2 + KCl} {CaCl2 + 2KCl}
--- Cryobostryxite Flinteite	--- $KZnCl_3 \cdot 2H_2O$ K_2ZnCl_4	--- $KCl + ZnCl_2$ $2KCl + ZnCl_2$	{2ZnCl2 + KCl} {ZnCl2 + KCl} {ZnCl2 + 2KCl}
---	---	$MgCl_2 + CaCl_2 + 2KCl$	{$MgCl_2 + CaCl_2 + 2KCl$}
---	---	$MgCl_2 + 2KCl + ZnCl_2$	{$MgCl_2 + 2KCl + ZnCl_2$}
---	---	$CaCl_2 + 2KCl + ZnCl_2$	{$CaCl_2 + 2KCl + ZnCl_2$}
---	---	$MgCl_2 + CaCl_2 + 3KCl + ZnCl_2$	{$MgCl_2 + CaCl_2 + 3KCl + ZnCl_2$}

Table 56 Naturally occurring Cl-SO4 compound minerals adapted and synthesized for TGA/DSC measurement.

Mineral	Chemical formula	Educts	Mixtures synthesized for TGA/DSC
(Anhydro-)Kainite	$MgSO_4KCl$	$KCL + MgSO_4$	$\{KCl + MgSO_4\}$
(Zn-) Guarinoite	$(Zn,Co,Ni)_6(SO_4)(OH,Cl)_{10}{\cdot}5H_2O$	$ZnSO_4 + 5ZnCl_2$	$\{5ZnCl_2 + ZnSO_4\}$

Table 57 $SrBr_2$ mixtures synthesized for the TGA/DSC analysis. As there are no known naturally occurring simple compound Sr-Bromide minerals, the listed mixtures are all synthetical.

TGA/DSC Bromides	{KBr}	{NaBr}	{LiBr}	$\{MgBr_2\}$	$\{CaBr_2\}$
$\{SrBr_2\}$	$\{2KBr + SrBr_2\}$ $\{KBr + SrBr_2\}$ $\{KBr + 2SrBr_2\}$	$\{2NaBr + SrBr_2\}$ $\{NaBr + SrBr_2\}$ $\{NaBr + 2SrBr_2\}$	$\{2LiBr + SrBr_2\}$ $\{LiBr + SrBr_2\}$ $\{LiBr + 2SrBr_2\}$	$\{2MgBr_2 + SrBr_2\}$ $\{MgBr_2 + SrBr_2\}$ $\{MgBr_2 + 2SrBr_2\}$	$\{5CaBr_2 + 4SrBr_2\}$ $\{5CaBr_2 + 8SrBr_2\}$ $\{5CaBr_2 + 16SrBr_2\}$ $\{2CaBr_2 + SrBr_2\}$ $\{CaBr_2 + SrBr_2\}$ $\{CaBr_2 + 2SrBr_2\}$

3. XRPD evaluations

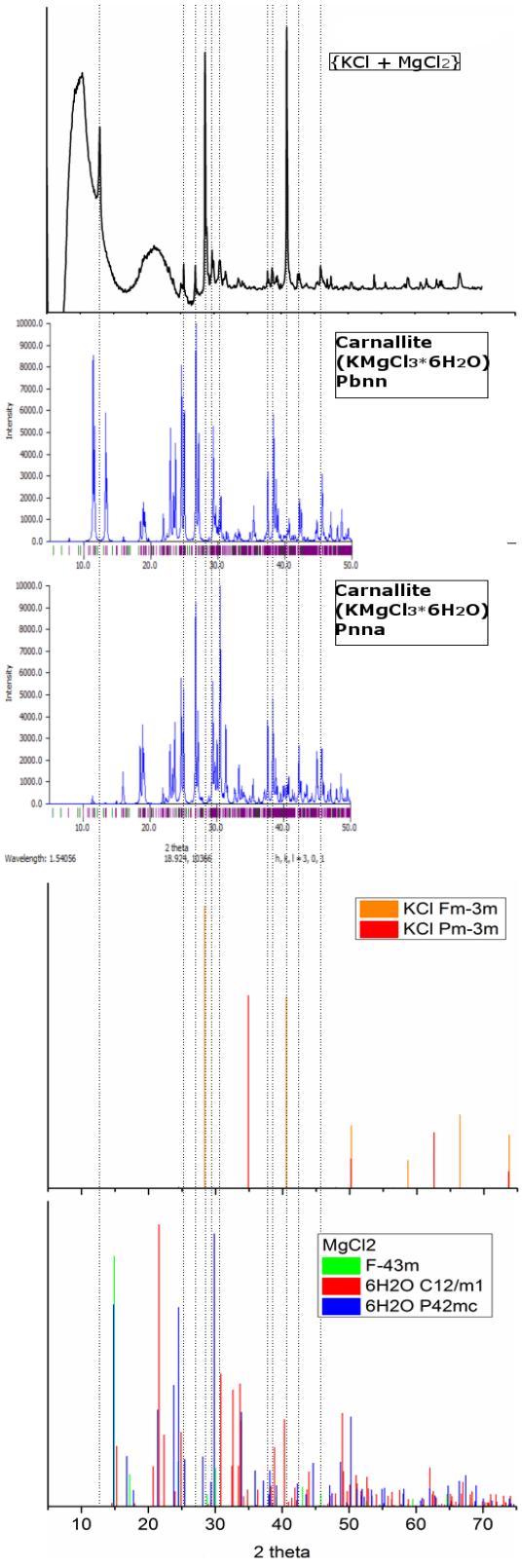

Figure 26 XRPD evaluation (Heinrich Heine Universität Düsseldorf , 2013) of an oven dried synthetic {$MgCl_2$ + KCl} mixture. While the sample appears to be only partially recrystallized after having been molten or dissolved previous to the measurement, there are several refraction peaks (2Θ between 25 to 30.5° and between 38 to 46.5°) that match the powder patterns of the two known forms of Carnallite ($KMgCl_3 \cdot 6H_2O$) (Fischer, 1973), (Schlemper, Sen Gupta, & Zoltai, 1985), (Cambridge Crystallographic Data Centre (CCDC), 2016) and one of the educts Sylvite (KCl) ($F\ m\ \bar{3}\ m$) (Heinrich Heine Universität Düsseldorf , 2013).

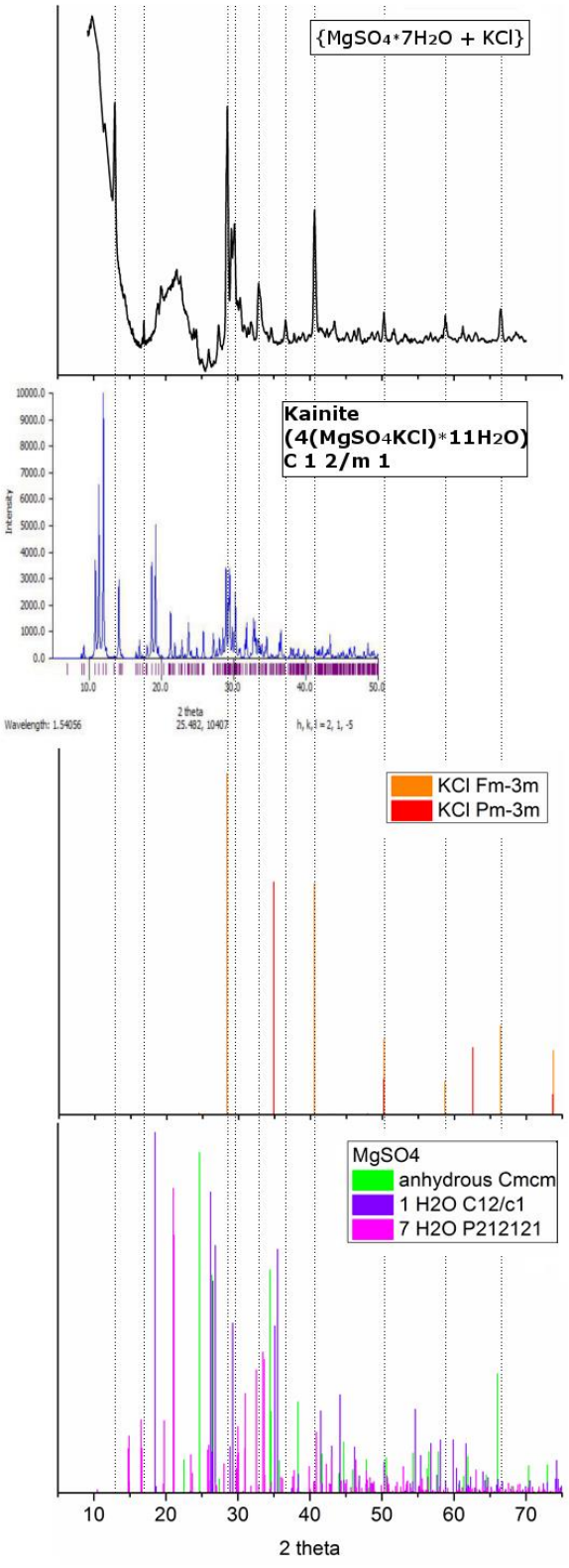

Figure 27 XRPD evaluation (Heinrich Heine Universität Düsseldorf , 2013) of an oven-dried synthetic {KCl + $Mg(SO_4)\cdot 7H_2O$} mixture. The observed powder pattern shows amorphous behavior, indicating a partial dissolving or melting of the sample, which didn't recrystallize completely upon solidifying. The sample peaks (between 2Θ = 28 to 36°) match with those of Kainite ($4(KMg(SO_4)Cl)\cdot 11H_2O$) (Robinson, Fang, & Ohya, 1972), (Cambridge Crystallographic Data Centre (CCDC), 2016) and (2Θ = 28, 40.5, 58 and 67°) with Sylvite (KCl) $F\,m\,\bar{3}\,m$ (Heinrich Heine Universität Düsseldorf , 2013).

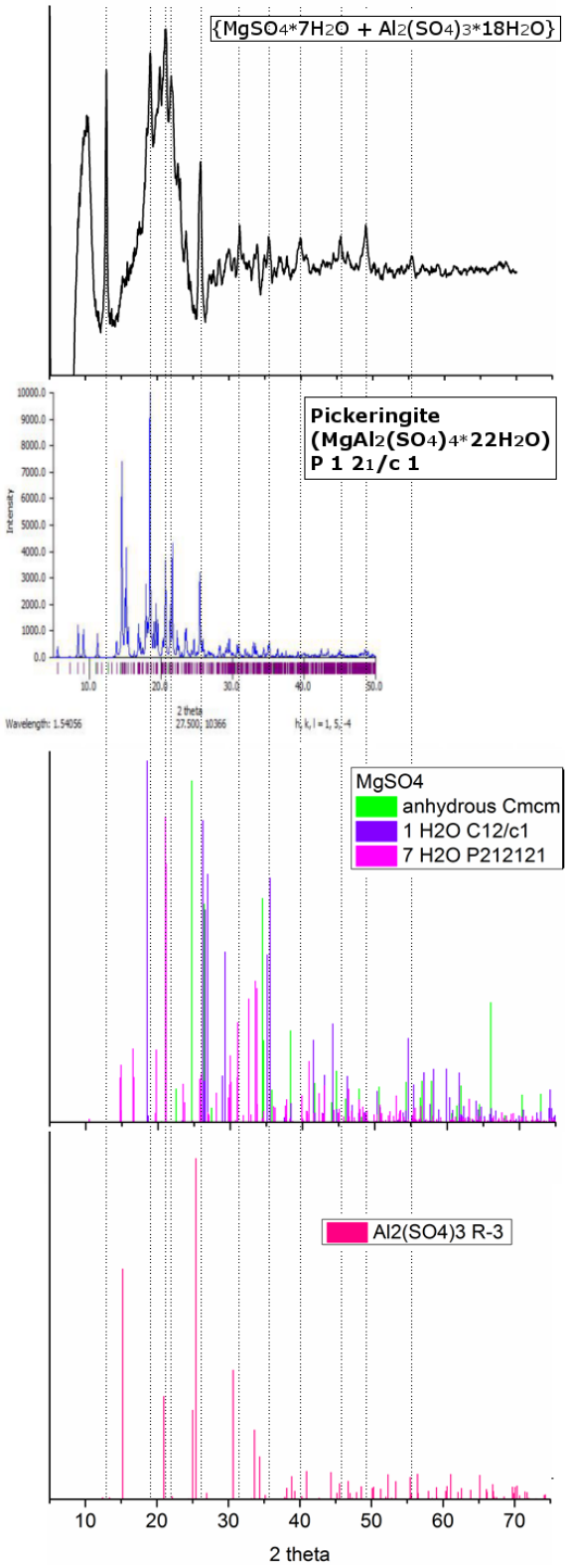

Figure 28 XRPD evaluation (Heinrich Heine Universität Düsseldorf , 2013) of an oven dried synthetic {$MgSO_4 \cdot 7H_2O + Al_2(SO_4)_3 \cdot 18H_2O$} mixture. The peaks (at 2Θ = 19, 21, 22 and 26°) match with those of the mineral Pickeringite ($(Mg_{0.93},Mn_{0.07})Al_2(SO_4)_4 \cdot 22H_2O$) (Quartieri, Triscari, & Viani, 2000), (Cambridge Crystallographic Data Centre (CCDC), 2016). No peak matches with the compared refraction peaks of the educts could be confirmed.

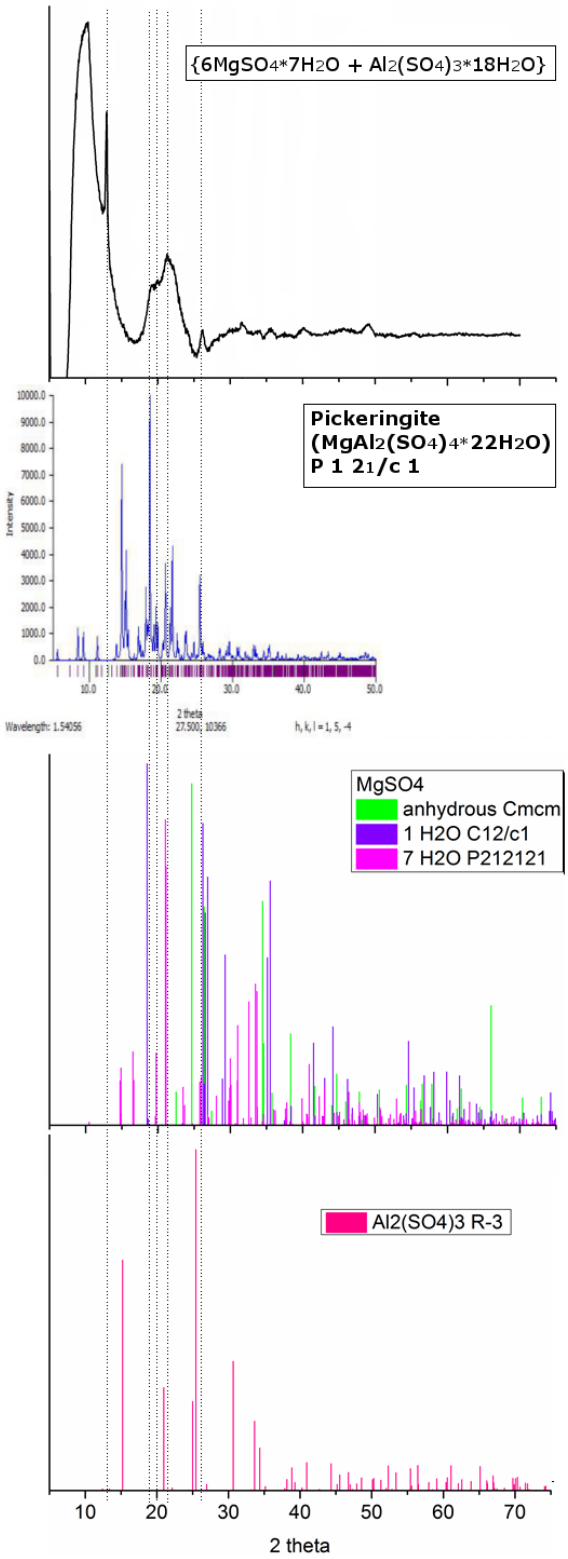

Figure 29 XRPD evaluation (Heinrich Heine Universität Düsseldorf , 2013) of an oven-dried synthetic {$6MgSO_4 \cdot 7H_2O + Al_2(SO_4)_3 \cdot 18H_2O$} mixture. While similarities to the refraction peaks of Pickeringite ($(Mg_{0.93},Mn_{0.07})Al_2(SO_4)_4 \cdot 22H_2O$), $P\ 1\ \frac{2_1}{c}\ 1$ (Quartieri, Triscari, & Viani, 2000), (Cambridge Crystallographic Data Centre (CCDC), 2016) can be seen, the powder pattern of the sample reads as too amorphous for a validation or for a comparison with the refraction peaks of the educts.

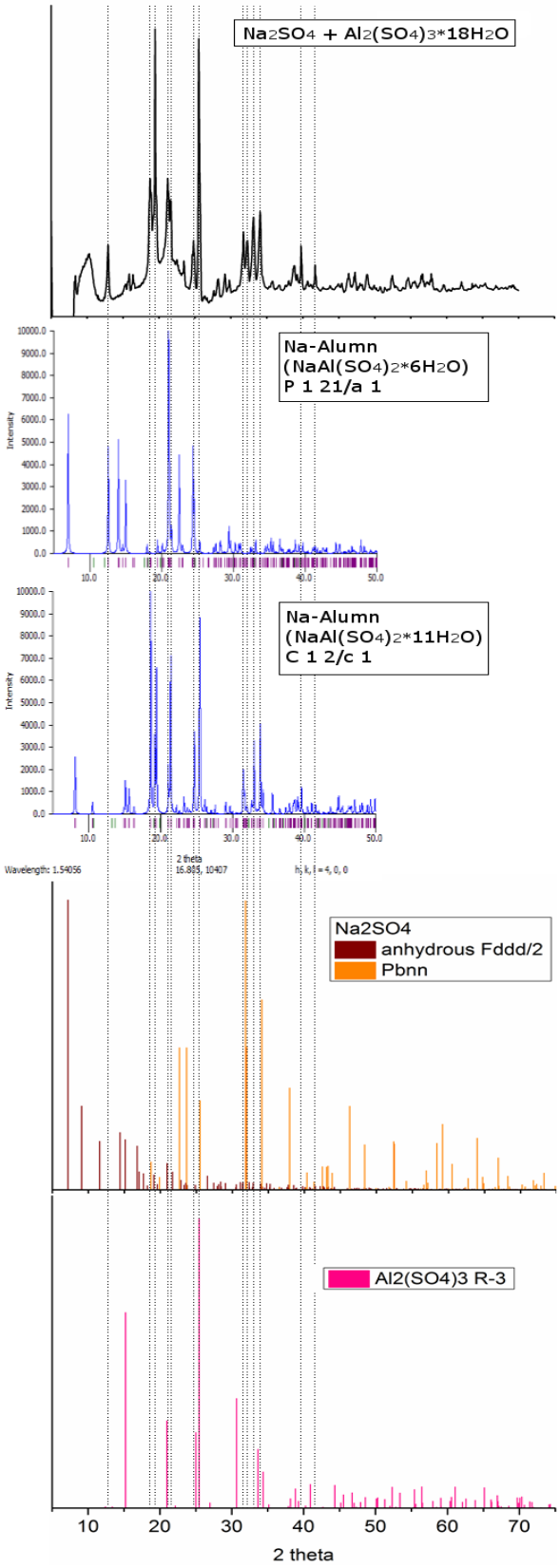

Figure 30 XRPD evaluation (Heinrich Heine Universität Düsseldorf , 2013) of an oven-dried synthetic {Na_2SO_4 + $Al_2(SO_4)_3 \cdot 18H_2O$} mixture. The sample peaks match with those of monoclinic ($NaAl(SO_4)_2 \cdot 6H_2O$) (Robinson & Fang, 1969) and monoclinic ($NaAl(SO_4)_2 \cdot 11H_2O$) (Fang & Robinson, 1972), (Cambridge Crystallographic Data Centre (CCDC), 2016) with no confirmed traces of the educts.

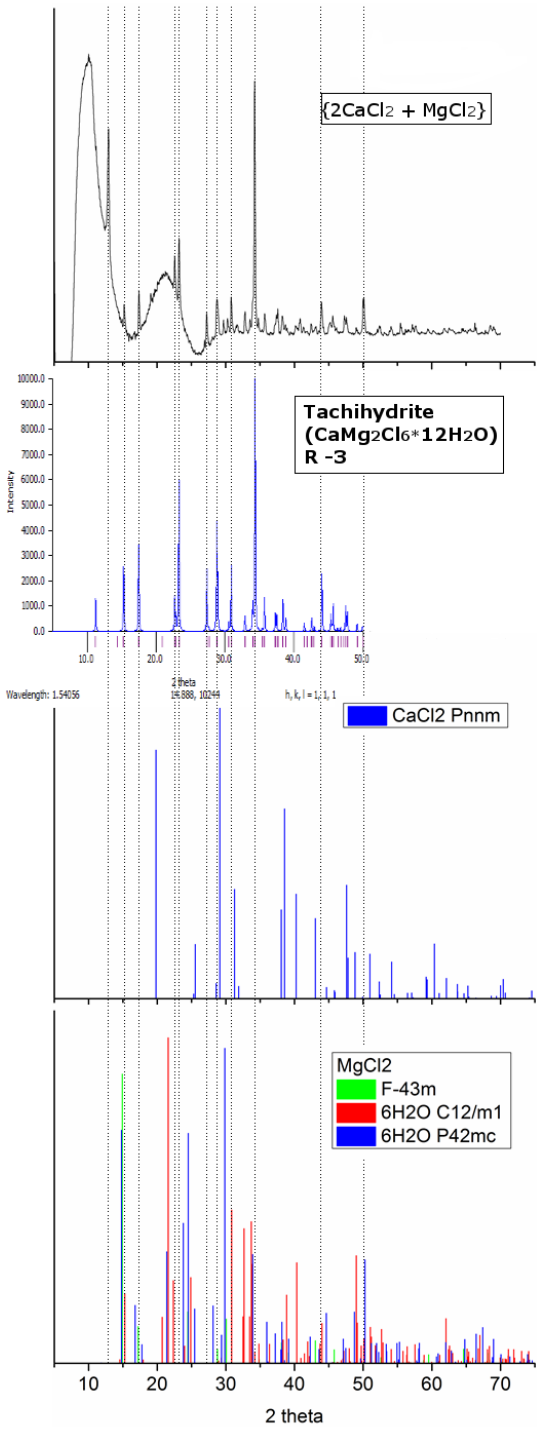

Figure 31 XRPD evaluation (Heinrich Heine Universität Düsseldorf , 2013) of an oven dried synthetic {$MgCl_2$ + $2CaCl_2$} mixture. The sample shows amorphous readings, indicating that the mixture was either partially dissolved during storage or molten when dried in the oven and recrystallized incompletely. The refraction peaks (at 2Θ = 15, 17, 23, 23.5, 26, 28, 31.5, 34 and 43.5°) match those of the powder pattern of Tachyhydrite ($CaMg_2Cl_6 \cdot 12H_2O$) (Leclaire, Borel, & Monier, 1980), (Clark, Evans, & Erd, 1980), (Cambridge Crystallographic Data Centre (CCDC), 2016). No match was found with the powder patterns of different phases of the educts (Heinrich Heine Universität Düsseldorf , 2013).

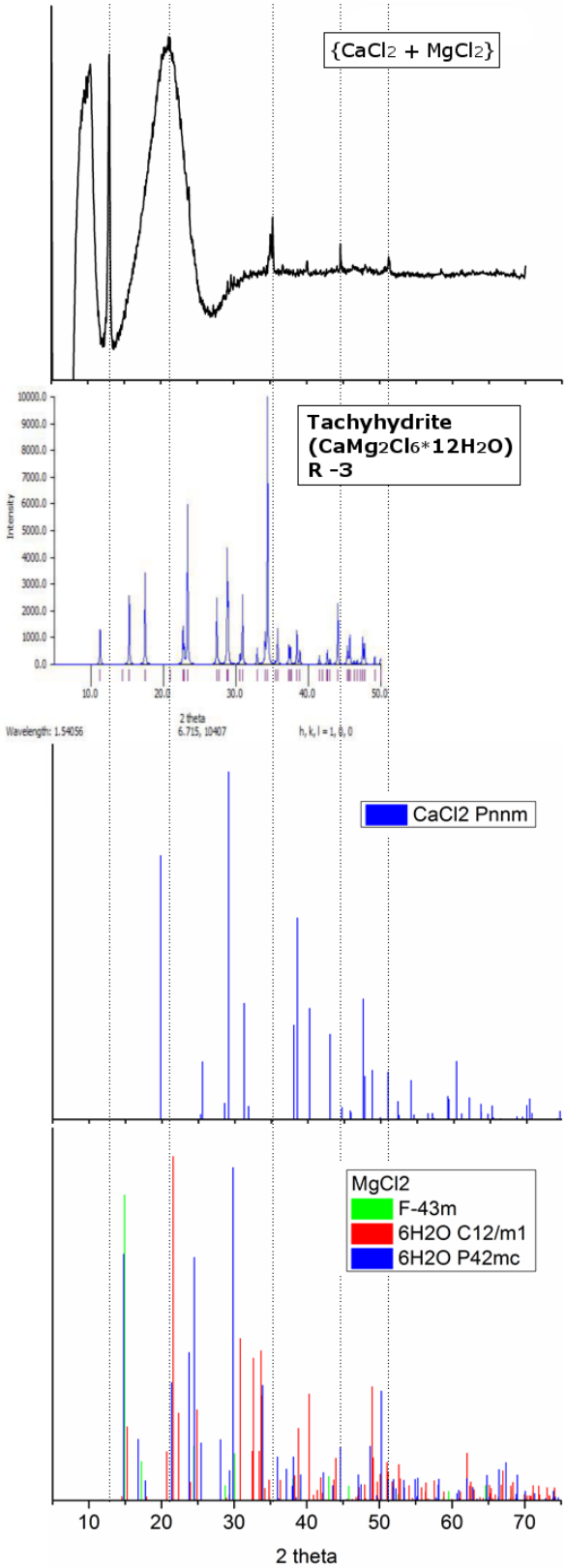

Figure 32 XRPD evaluation (Heinrich Heine Universität Düsseldorf , 2013) of an oven dried synthetic {$MgCl_2$ + $CaCl_2$} mixture. The sample shows amorphous readings, with only few refraction peaks. This indicates that the sample either dissolved or melted completely during storage or heating in the oven respectively and did not crystallize when solidifying after drying. No matching peaks to the powder pattern of Tachyhydrite ($CaMg_2Cl_6 \cdot 12H_2O$) (Leclaire, Borel, & Monier, 1980), (Clark, Evans, & Erd, 1980), (Cambridge Crystallographic Data Centre (CCDC), 2016) or different phases of the educts were found.

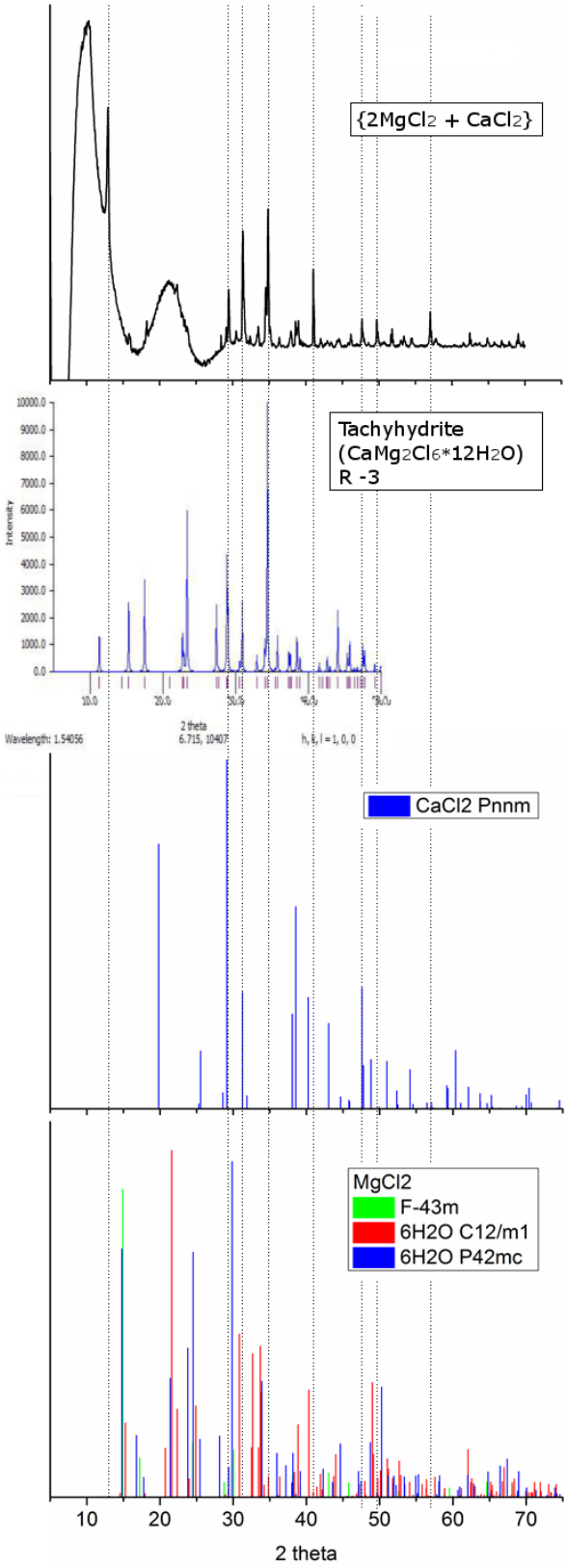

Figure 33 XRPD evaluation (Heinrich Heine Universität Düsseldorf , 2013) of an oven dried synthetic {$2MgCl_2$ + $CaCl_2$} mixture. The sample shows amorphous readings indicating partial melting or dissolving and incomplete recrystallisation during drying in the oven. The crystalline part of the mixture shows matching refraction peaks (at 2Θ = 29, 32, 35 and 47.5°) with Tachyhydrite ($CaMg_2Cl_6 \cdot 12H_2O$) (Leclaire, Borel, & Monier, 1980), (Clark, Evans, & Erd, 1980), (Cambridge Crystallographic Data Centre (CCDC), 2016) and three possibly matching peaks with anhydrate {$CaCl_2$} (Heinrich Heine Universität Düsseldorf , 2013) which however fall together with the matching peaks of Tachyhydrite (at 2Θ = 29, 32 and 47.5°).

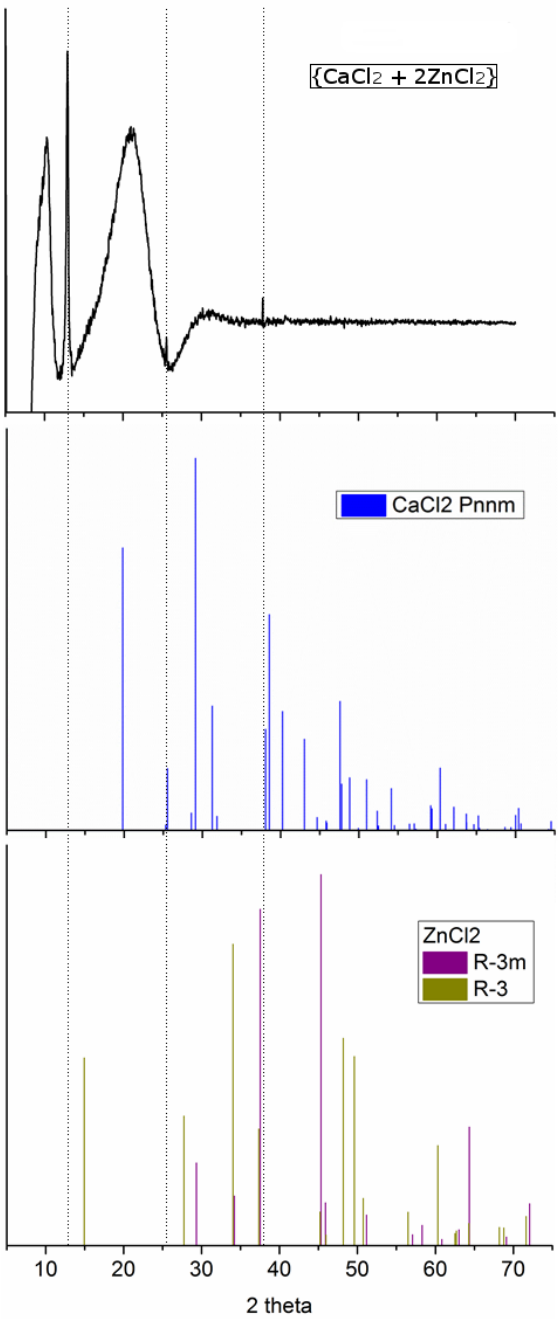

Figure 34 XRPD evaluation (Heinrich Heine Universität Düsseldorf , 2013) of an oven-dried {$CaCl_2$+2$ZnCl_2$} mixture. The material mixture has no similar naturally occurring minerals for comparison. The sample appears to have melted almost completely and not recrystallized, as most of the mixture reads as amorphous mass. Due to the lack of refraction peaks neither the presence of a potential compound nor that of excess educts was validated.

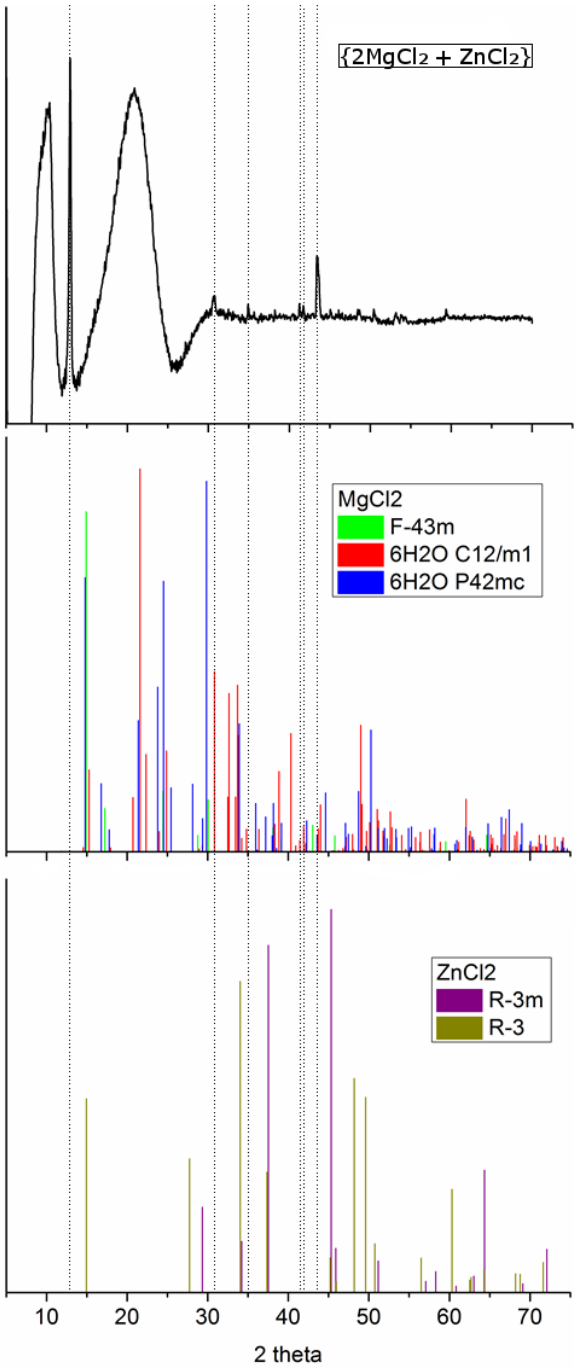

Figure 35 XRPD evaluation (Heinrich Heine Universität Düsseldorf , 2013) of an oven dried synthetic {2$MgCl_2$ + $ZnCl_2$} mixture, compared to peaks of different phases of the educts. The material mixture has no similar naturally occurring minerals for comparison. The sample shows only amorphous readings due to melting or dissolving before re-solidification without recrystallisation. No matching peaks for the educts or possible compounds were confirmed.

4. Chlorides TGA/DSC peak temperatures, melting points and {HCl}-emission comparison

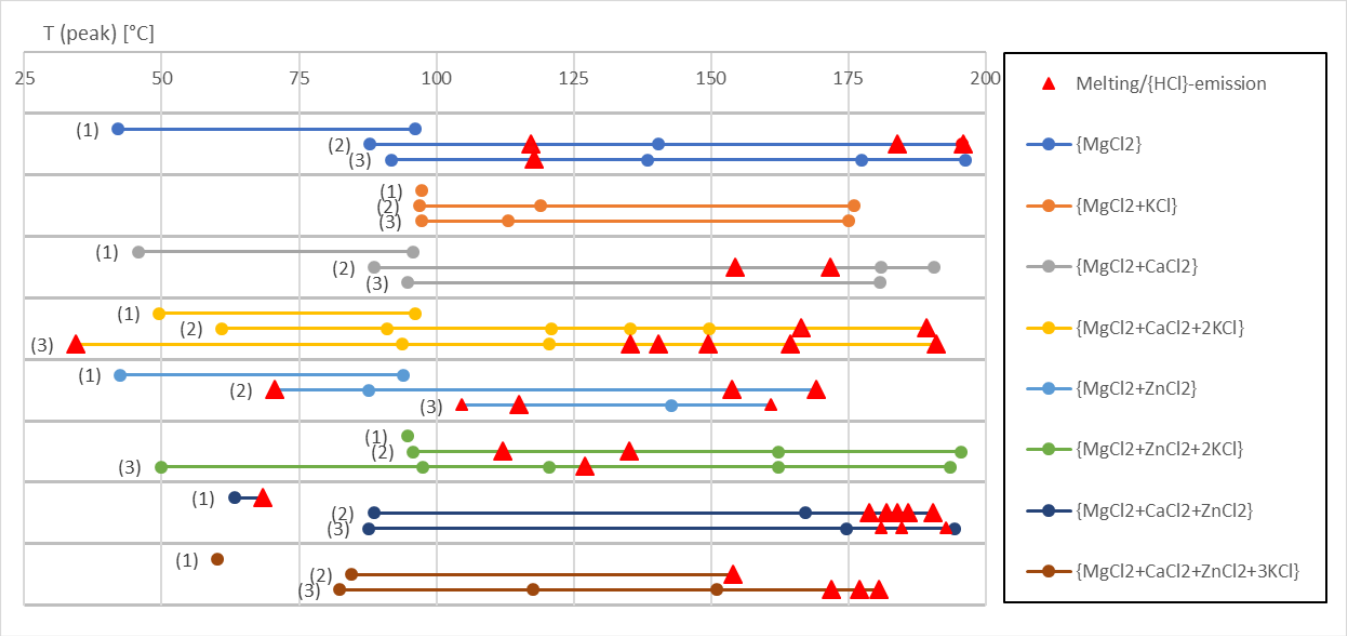

Figure 36 Peak temperatures for chloride samples containing {$MgCl_2$}, for three TGA/DSC dehydration stages each, showing the change in distribution of melting peaks, when a substance with a high melting point such as {KCl} is added. (1) T_{max} = 100°C, (2) & (3) T_{max} = 200°C.

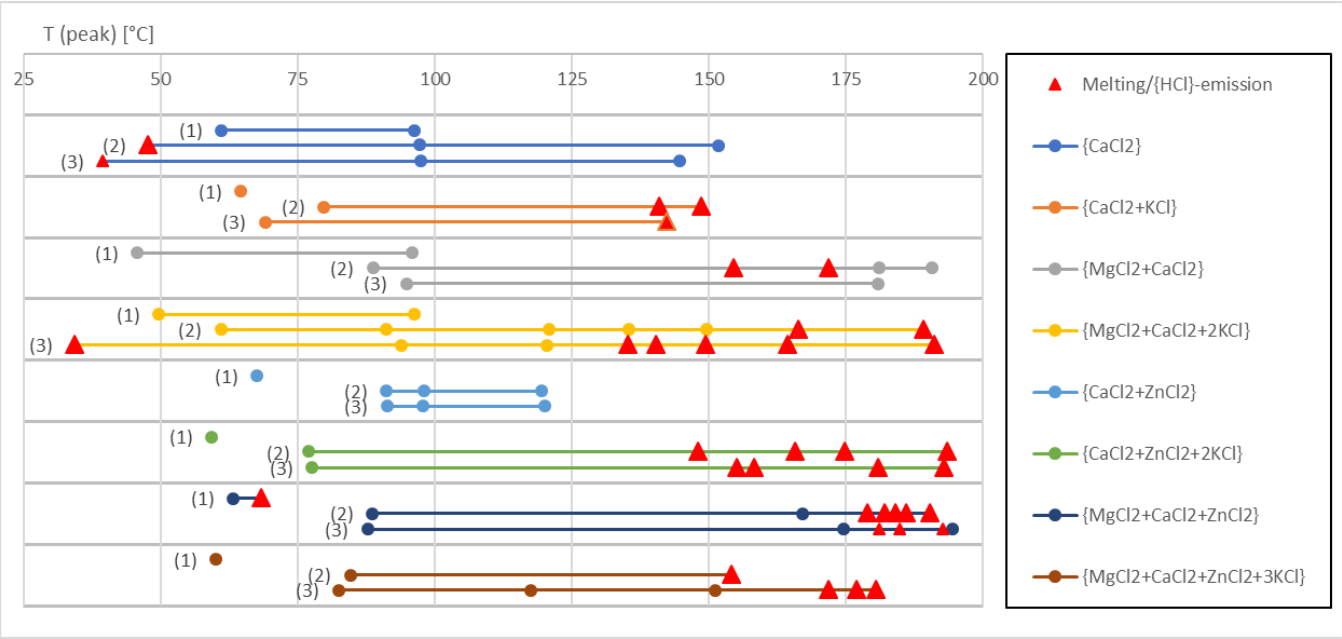

Figure 37 Peak temperatures for chloride samples containing {$CaCl_2$}, for three TGA/DSC dehydration stages each, showing the change in distribution of melting peaks, when a substance with a high melting point such as {KCl} is added. (1) T_{max} = 100°C, (2) & (3) T_{max} = 200°C.

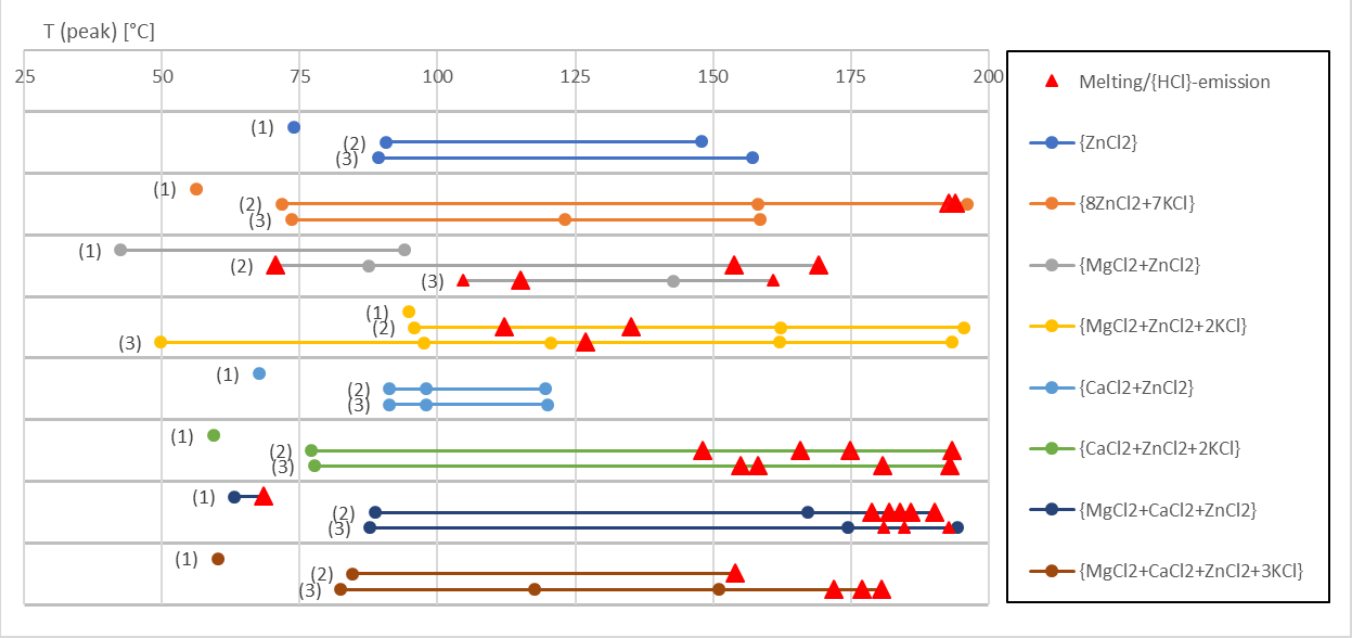

Figure 38 Peak temperatures for chloride samples containing {$ZnCl_2$}, for three TGA/DSC dehydration stages each, showing the change in distribution of melting peaks, when a substance with a high melting point such as {KCl} is added. (1) T_{max} = 100°C, (2) & (3) T_{max} = 200°C.

5. Specific heat capacities, comparison of literature values for {KCl}

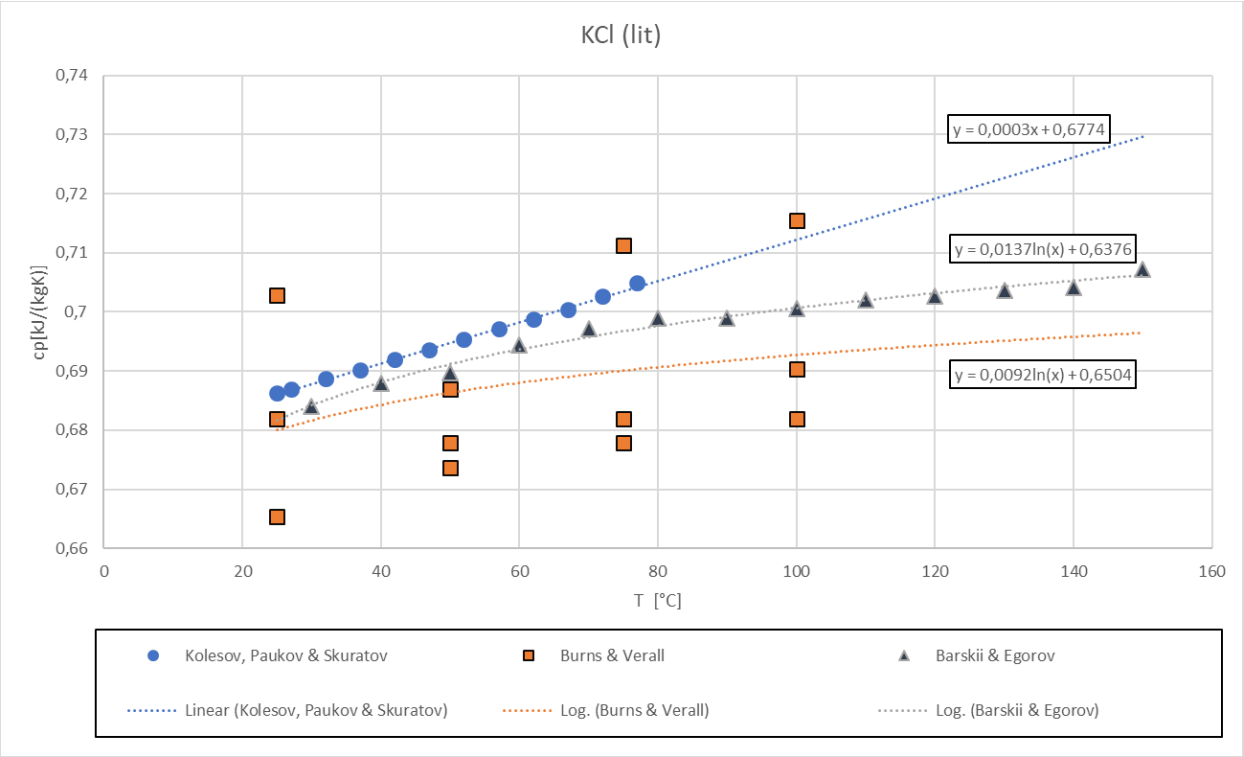

Figure 39 Specific heat capacity c_p [kJkg^{-1}K^{-1}] of {KCl} for the temperature range of T = 25 to 150°C. (Kolesov, Paukov, & Skuratov, 1962), (Burns & Verall, 1974), (Barskii & Egorov, 1993).

5.1. Calculated specific heat capacity $c_p(T)$ trends

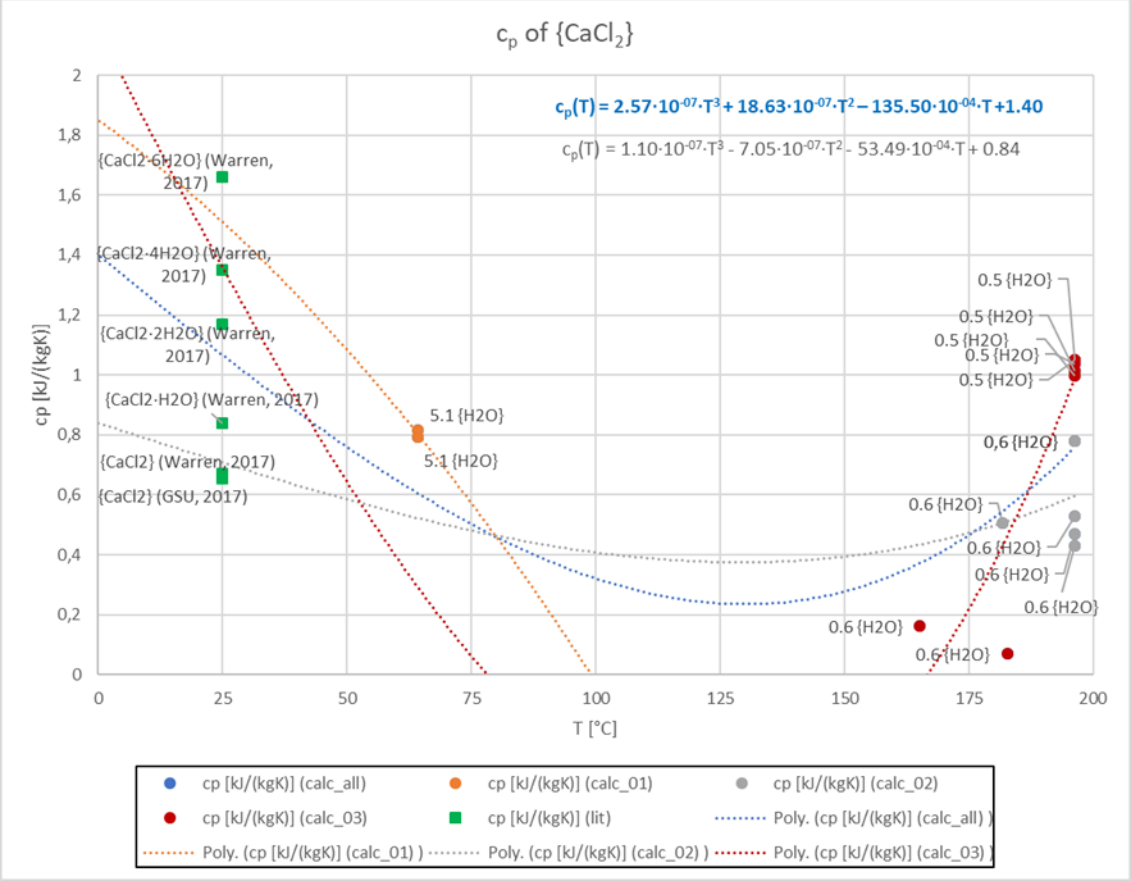

Figure 40 Specific heat capacity of {$CaCl_2 \cdot xH_2O$} from spot checks on three TGA/DSC dehydration curves and the literature value for T = 25°C (Georgia State University, 2017). The trend was calculated including the literature values, as during the hydrations an ongoing phase change was recorded for the temperature interval of T = 25 to 197°C for both the 2nd and 3rd dehydration. The higher hydrated the stage of the starting material, the higher is the c_p value at T = 25°C.

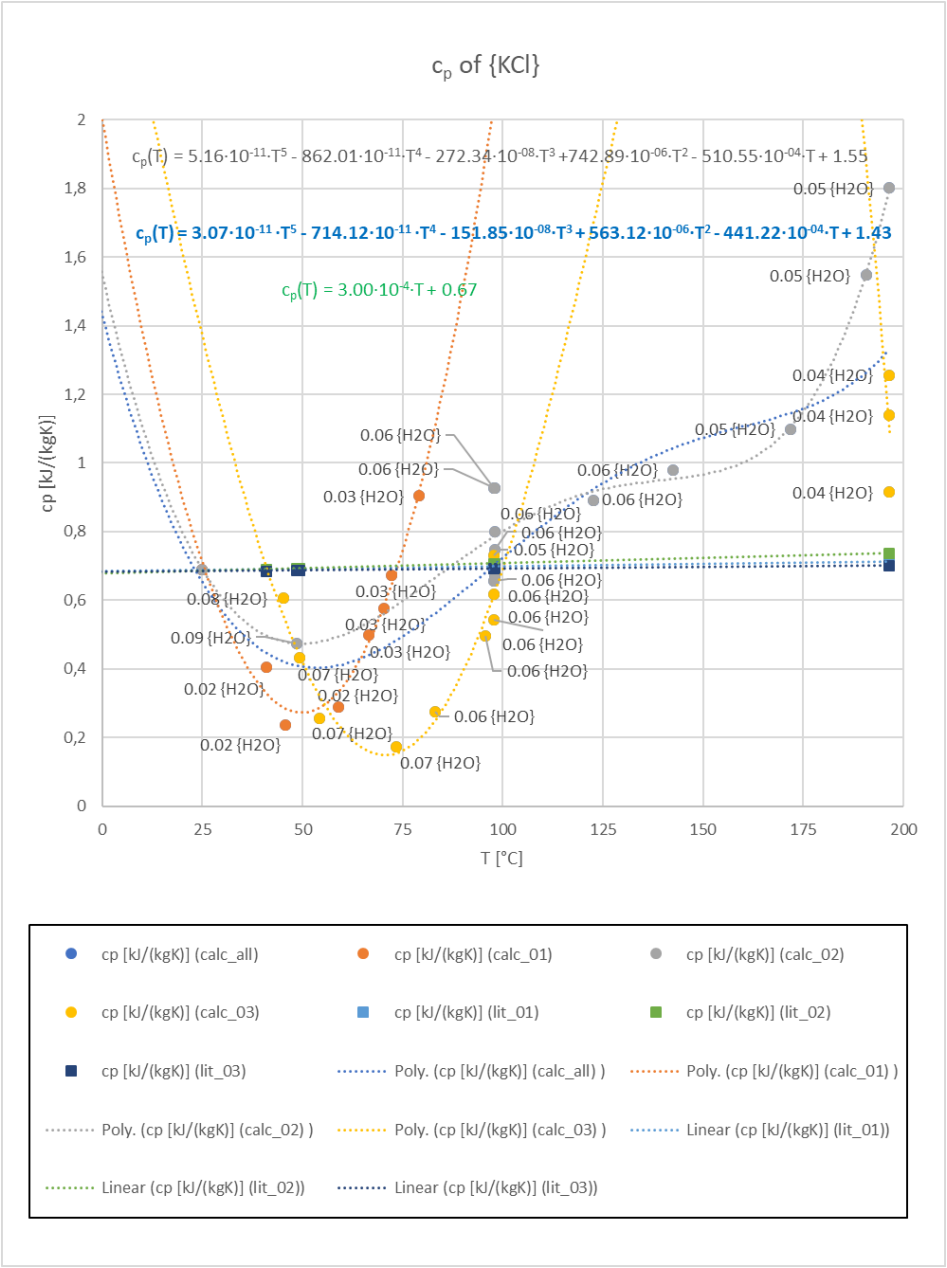

Figure 41 Specific heat capacity c_p for {KCl} from spot checks on three TGA/DSC dehydration curves and the literature value for different temperatures with calculated trends. The values calculated from the TGA/DSC evaluations do not correspond with either of the trends calculated from three different literature sources (Kolesov, Paukov, & Skuratov, 1962), (Burns & Verall, 1974) and (Barskii & Egorov, 1993). The material apparently undergoes a phase change in the interval between T = 25 to 100°C.

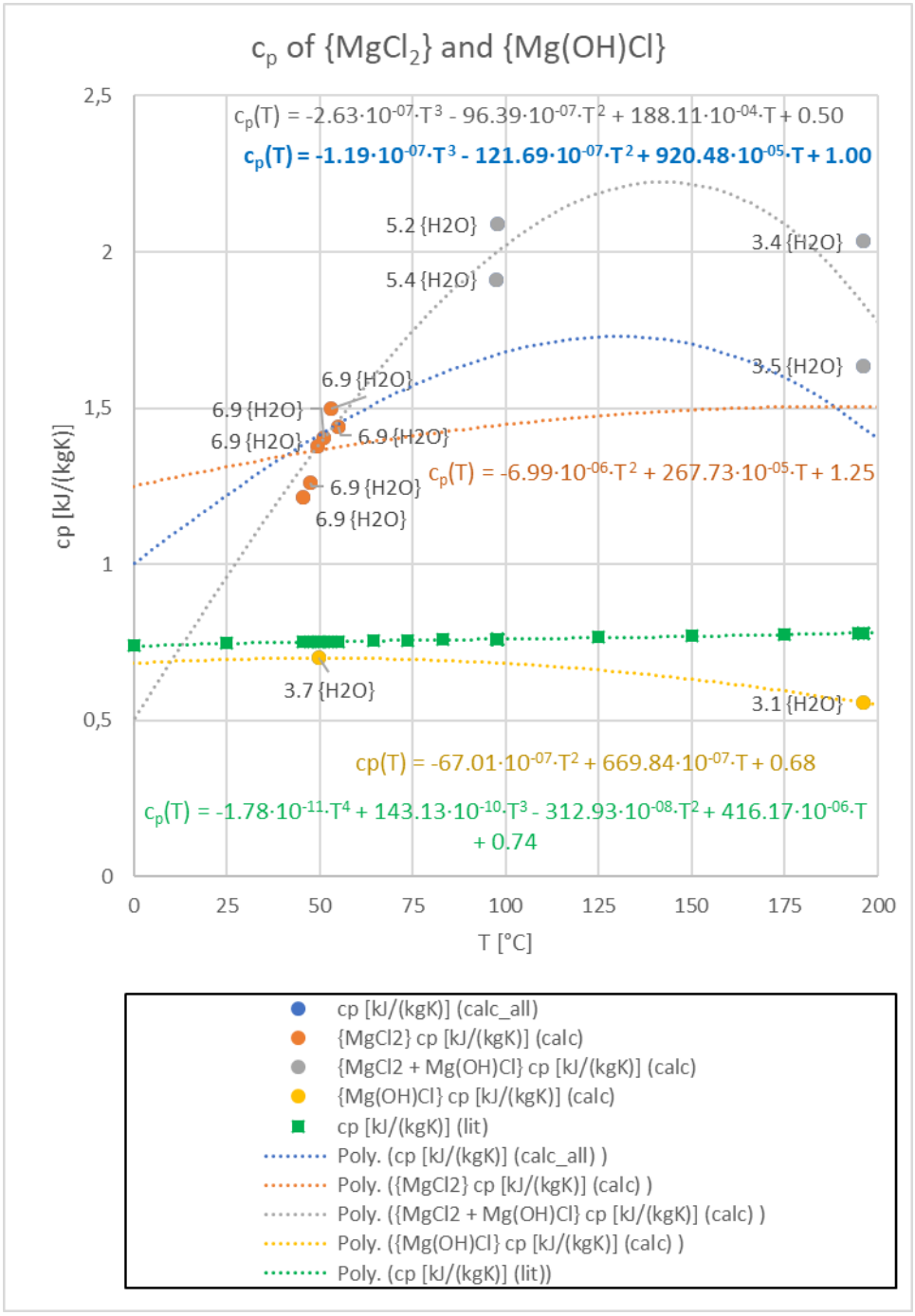

Figure 42 Specific heat capacity c_p for {$MgCl_2 \cdot xH_2O$} from spot checks on three TGA/DSC dehydration curves and the literature (Biermann, et al., 1989) values of anhydrate {$MgCl_2$} for different temperatures with calculated trends. It was assumed that the material undergoes a reaction to {$Mg(OH)Cl \cdot xH_2O$} at T > 110°C during the 2nd dehydration and is completely transformed to {$Mg(OH)Cl \cdot xH_2O$} at the start of the 3rd dehydration. The trend fitted to the values from all three dehydrations is influenced by the material transformation.

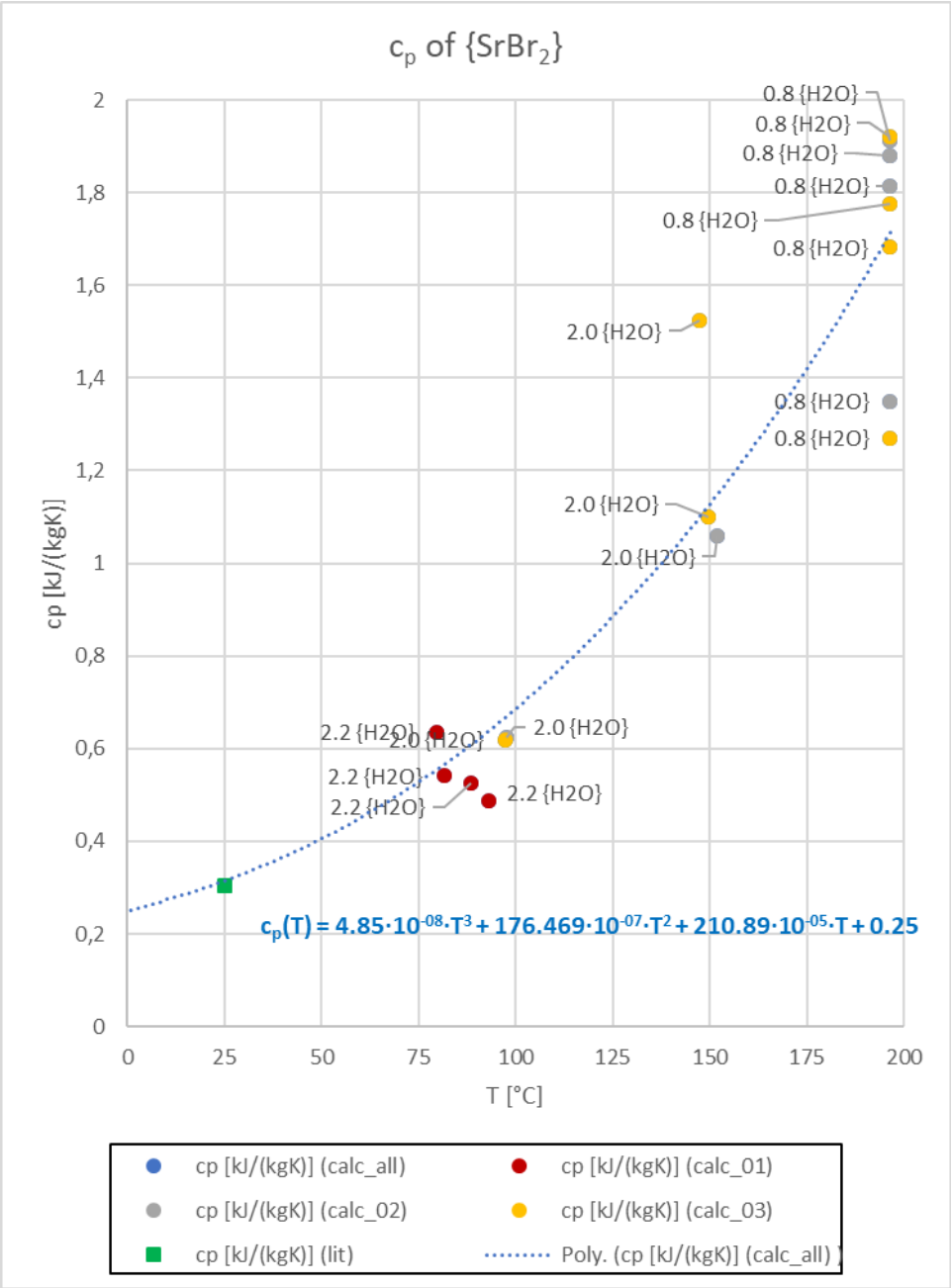

Figure 43 Specific heat capacity trend of an {$SrBr_2$+ xH_2O} sample, calculated from spot samples of dehydration curves from three different TGA/DSC cycles. As there were no valid values within the temperature range T =25 to 75°C to low temperature phase changes, a c_p value from literature for {$SrBr_2$} at T = 25°C (MatWeb, LLC, 2017) was added to calculate a temperature trend for the material.

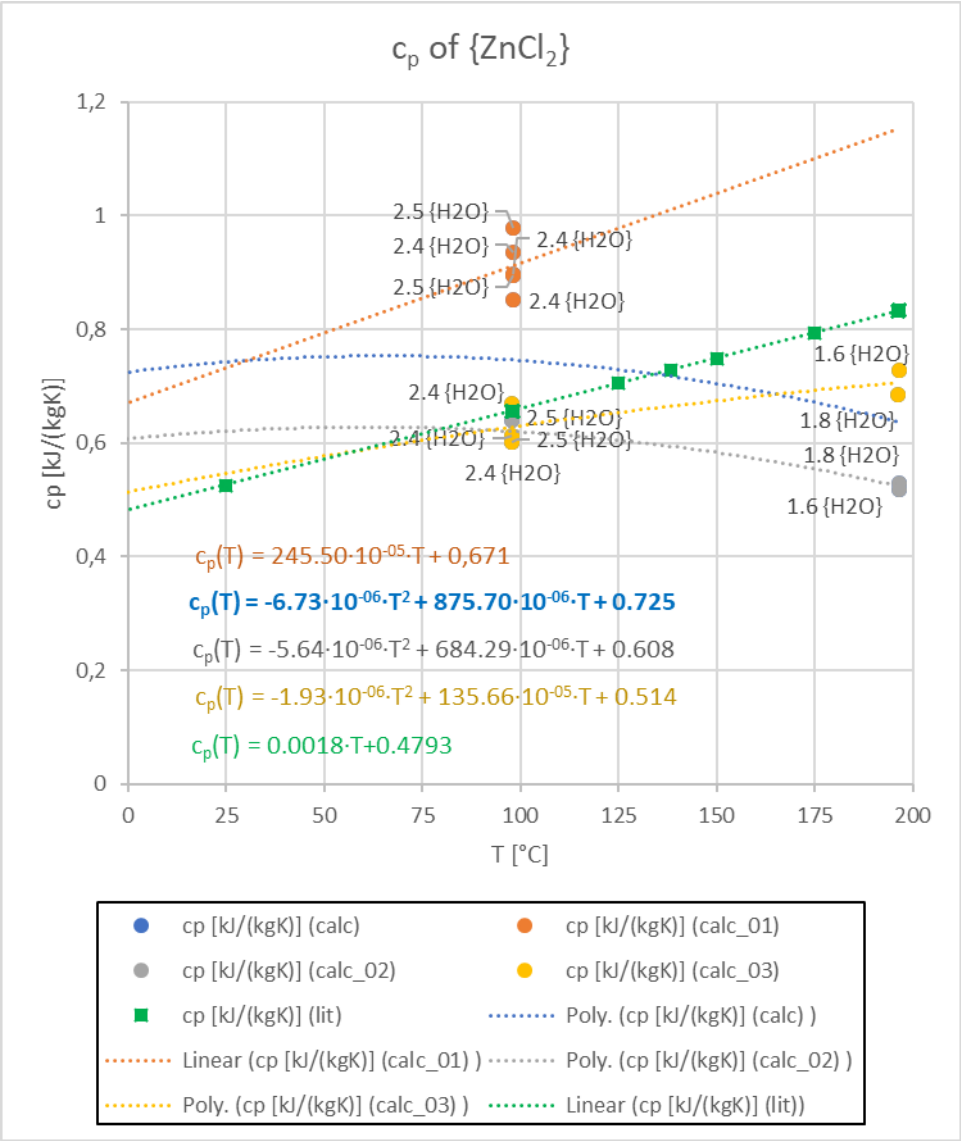

Figure 44 Specific heat capacity trends of a {$ZnCl_2$+ xH_2O} sample, calculated from spot samples of dehydration curves from three different TGA/DSC cycles. For comparison the trend for the anhydrate {ZnCl2} by (Hargittai, Tremmel, & Hargittai, 1986).

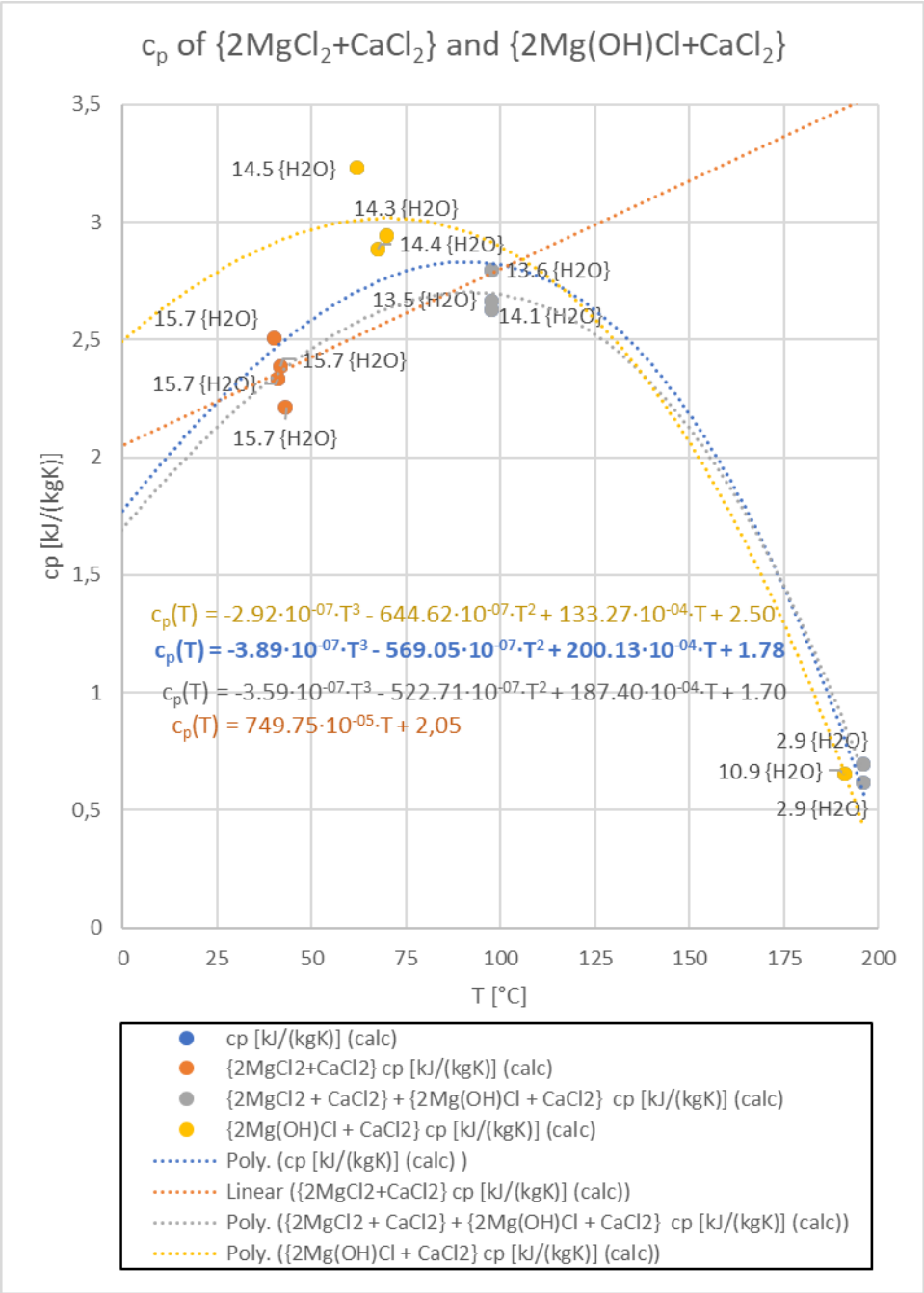

Figure 45 Specific heat capacity trends of a {$2MgCl_2 + CaCl_2 + xH_2O$} sample, calculated from spot samples of dehydration curves from three different TGA/DSC cycles. The water content was calculated under the assumption, that the {$MgCl_2 \cdot xH_2O$} component of the mixture emits {HCl} at temperatures of T > 110°C and transforms to {$Mg(OH)Cl \cdot (x-1)H_2O$} during the 2nd dehydration while the {$CaCl_2 \cdot xH_2O$} component remains unchanged. It was also assumed that the transformation was complete at the end of the 2nd dehydration and that the material is a {$2Mg(OH)Cl + CaCl_2 + xH_2O$} mixture at the start of the 3rd dehydration. The trend for all data-points represents an average c_p for both material mixtures.

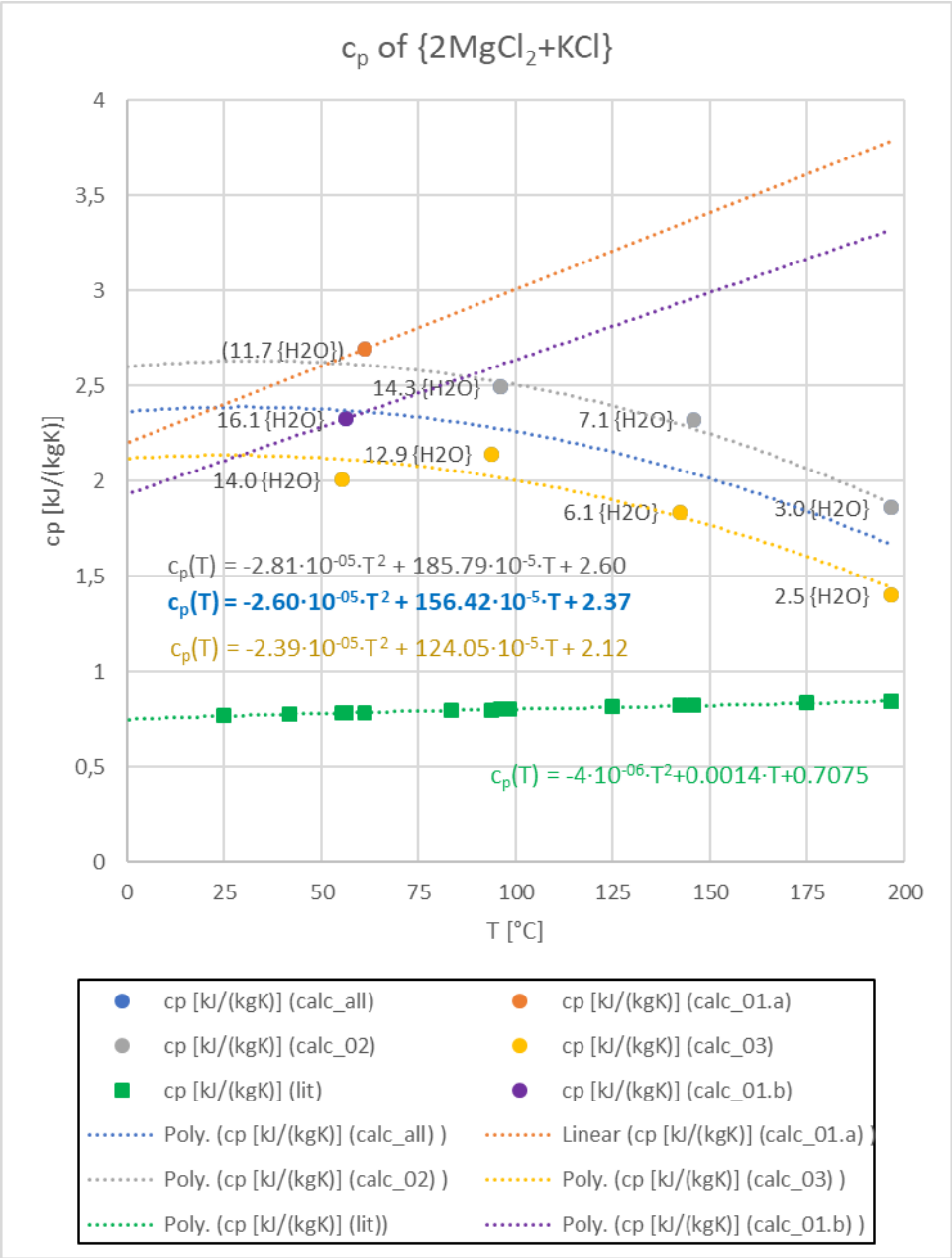

Figure 46 Specific heat capacity trends of a {2$MgCl_2$ + KCl+ xH_2O} sample, calculated from spot samples of dehydration curves from four different TGA/DSC cycles. Both trends calculated from the T_{max} = 100°C (calc_01.a and calc_01.b) measurements were discarded as they lack valid data for temperatures T > 75°C, leading to an overestimation of the c_p value at higher temperatures, where the material would have dehydrated to a lower hydration stage. As the weight measurement of dehydration 1.a failed, and had to be corrected by calculation, the water content was likely gauged too small. The trend for the average of the cp spot samples of all four curves was chosen for further calculations. The trend calculated from literature (Biermann, et al., 1989), was added for comparison and applies only to an anhydrate form of a {$MgCl_2$·KCl} mixture.

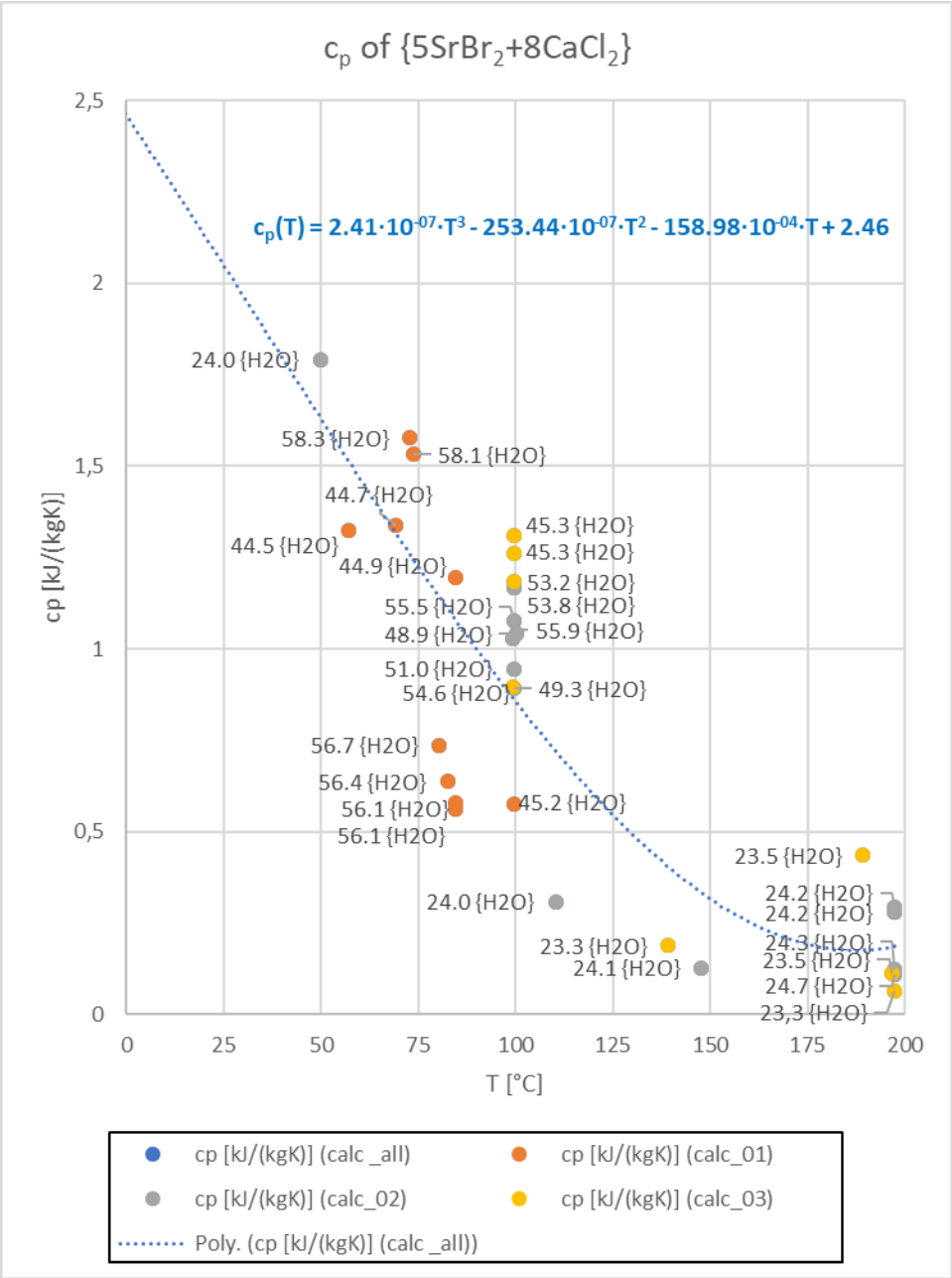

Figure 47 Specific heat capacity trend of an {5SrBr$_2$ + 8CaCl$_2$+ xH$_2$O} sample, calculated from spot samples of dehydration curves from three different TGA/DSC cycles.

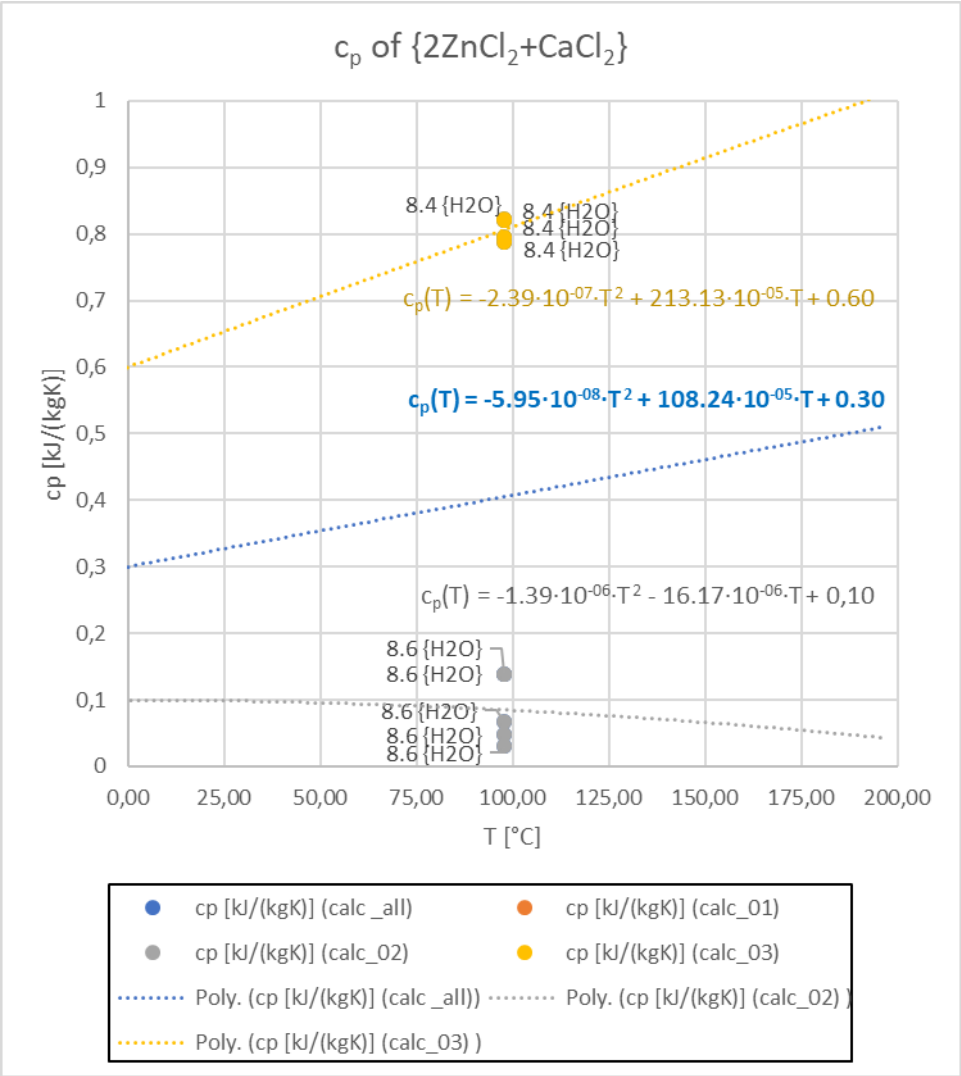

Figure 48 Specific heat capacity trends of a {$2ZnCl_2 + CaCl_2 + xH_2O$} sample, calculated from spot samples of dehydration curves from three different TGA/DSC cycles. Since the material showed phase changes within the temperature range of T = 25 to 75°C there are no valid values for low temperatures. There were no valid values calculated from the spot samples taken from the 1st dehydration curve. The calculated values from the 2nd and 3rd dehydration vary strongly due to a gap in measured heat flow, despite only small differences in measured sample weight. The difference is likely caused by a different degree of partial melting of the sample during the dehydrations.

6. Measured Temperature T(t) and calculated heat flow Δϕ(t) schematics

6.1. Temperature curves recorded with experimental setup #1 (liquid water supply)

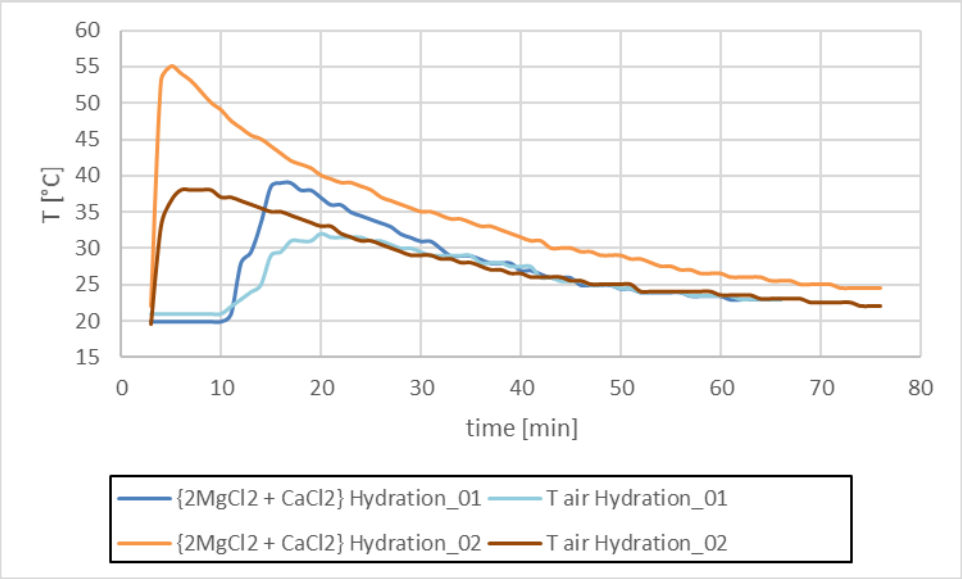

Figure 49 Setup #01 with liquid water supply. Hydration temperatures measured for a {2MgCl₂ + CaCl₂} sample during 1st and 2nd cycle. During hydration_01 it was observed that the thermometer T_1 was not reaching into the reaction and an extra quantity of 12ml water had to be applied to mitigate that. The measurement was interrupted after t = 1min and was restarted after a delay of t = 7min. The second measurement was undertaken with a larger amount of water from the beginning.

6.2. Temperature curves recorded with experimental setup #2 (liquid water supply)

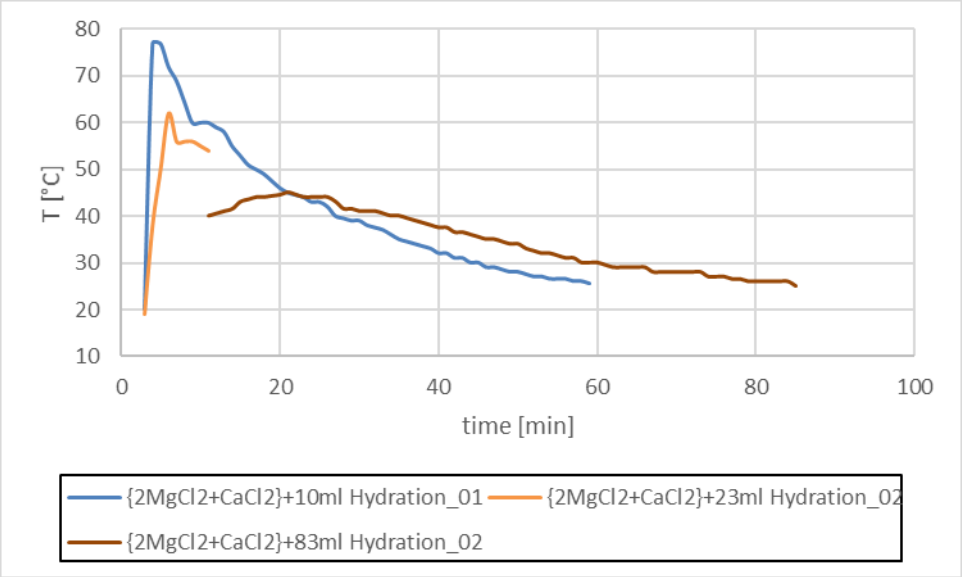

Figure 50 Setup #02 with a supply of liquid water, showing the hydration temperatures measured for a {2MgCl₂ + CaCl₂} sample during the 1st and 2nd cycle. During hydration_02 it was observed that the water was not reacting with the bulk of the sample which had accumulated in form of a ring around the sample bottle's surface above the waterline. An extra quantity of 50ml water had to be applied to mitigate that. The measurement was interrupted after t = min and was restarted after a delay of t = min.

6.3. Temperature curves recorded with experimental setup #1 (water vapor supply)

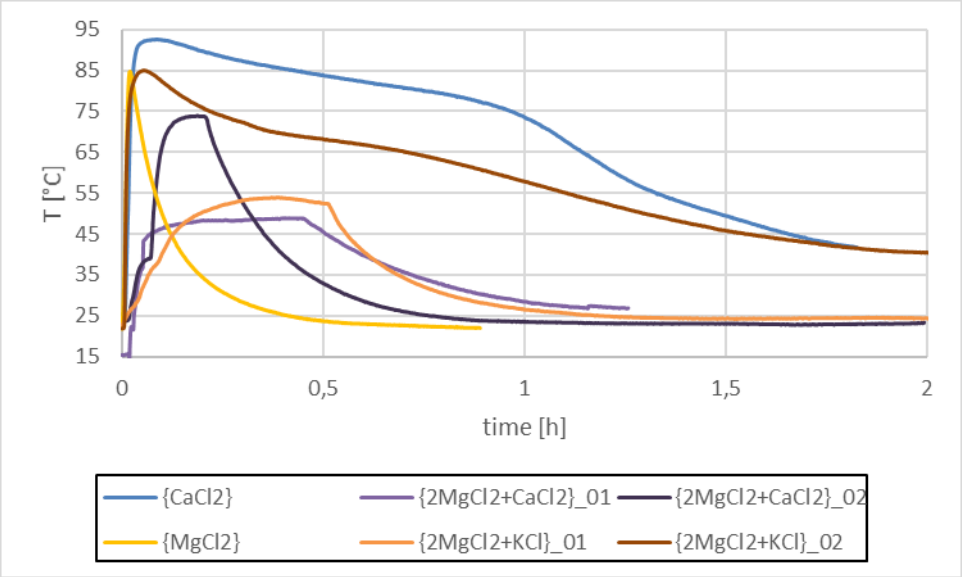

Figure 51 Hydration behavior of {MgCl2}, {CaCl2}, {2MgCl2+CaCl2} and {2MgCl2+KCl}, measured in experimental setup #1. Sudden drops in temperature here indicate the failing of the vacuum seal of the apparatus. Samples of same material were removed and dried in the oven at T=120°C for t= 2h and then cooled down in a desiccator between measurements.

6.4. Temperature curves recorded with experimental setup #2 (water vapor supply), specific heat capacity values and heat flow curves

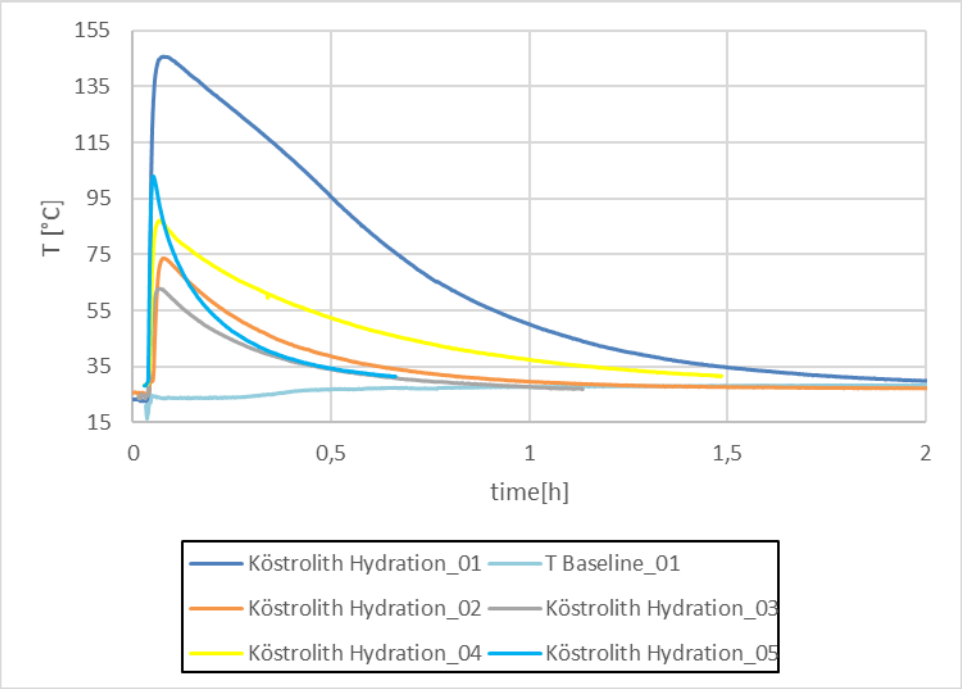

Figure 52 Hydration temperatures of Köstrolith over time for #1 factory dried material, #2 dried for t_2 = 160min at T_{max2}= 127°C, #3 dried for t_3= 360min at T_{max3} = 127°C, #4 oven dried for t_4 = 360min at T_{max4} = 120°C and #5 dried for t_5 = 230min at T_{max5} = 140°C.

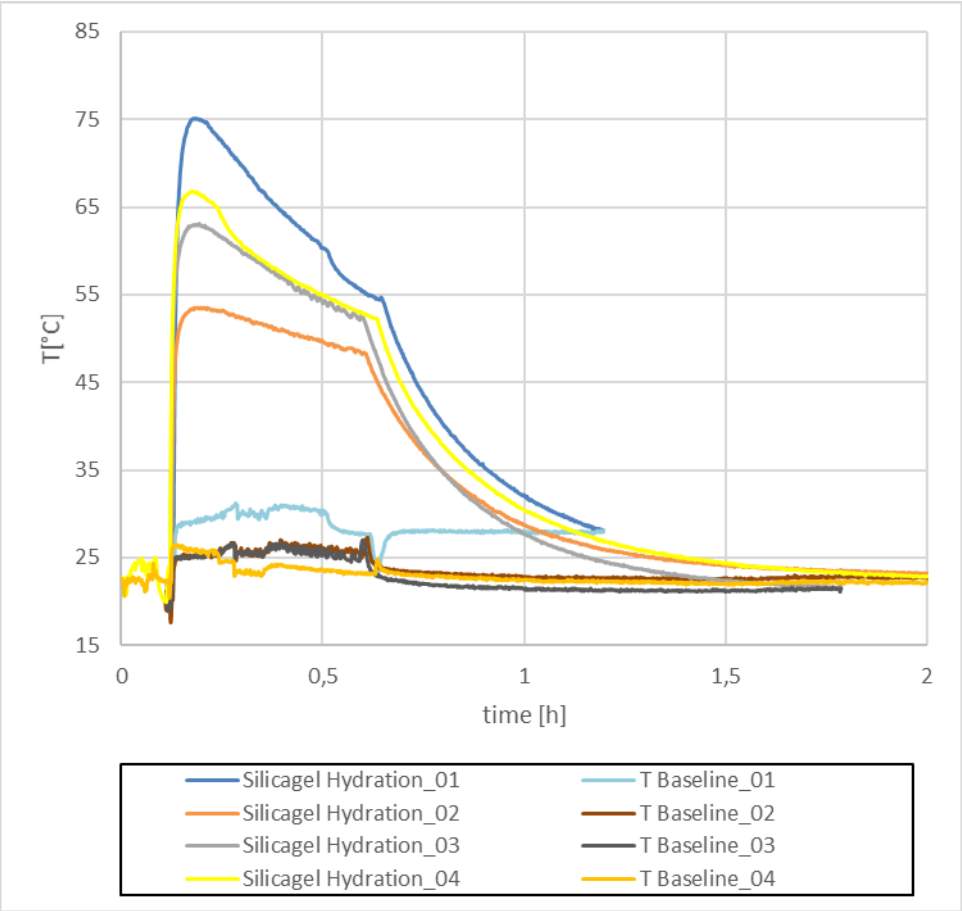

Figure 53 Temperature curves for four hydrations of an m = 20g Silicagel sample, evaluated with experimental setup #2 (with water vapor). There is a strong decline between the 1st and the 2nd hydration. The temperature output recovers during the 3rd hydration. Before the 4th hydration, the sample was not dried in-situ but in the oven. The 3rd and the 4th hydration show a similar temperature output. The vacuum for the water supply was shut off after about 40 minutes of hydration time during each measurement.

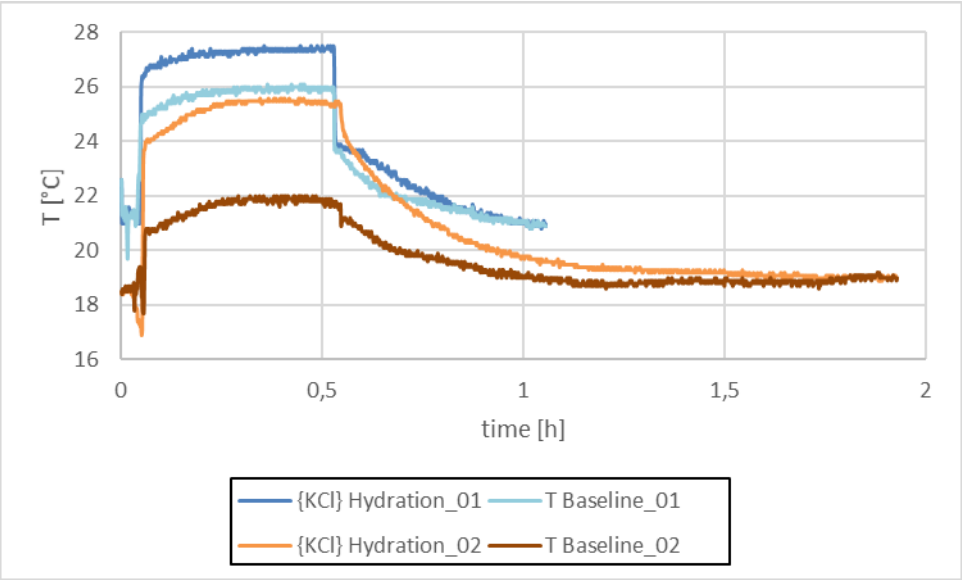

Figure 54 Experimental setup #2, hydration curves of {KCl} for two cycles. The vacuum was turned off after t ~ 30 to 35min.

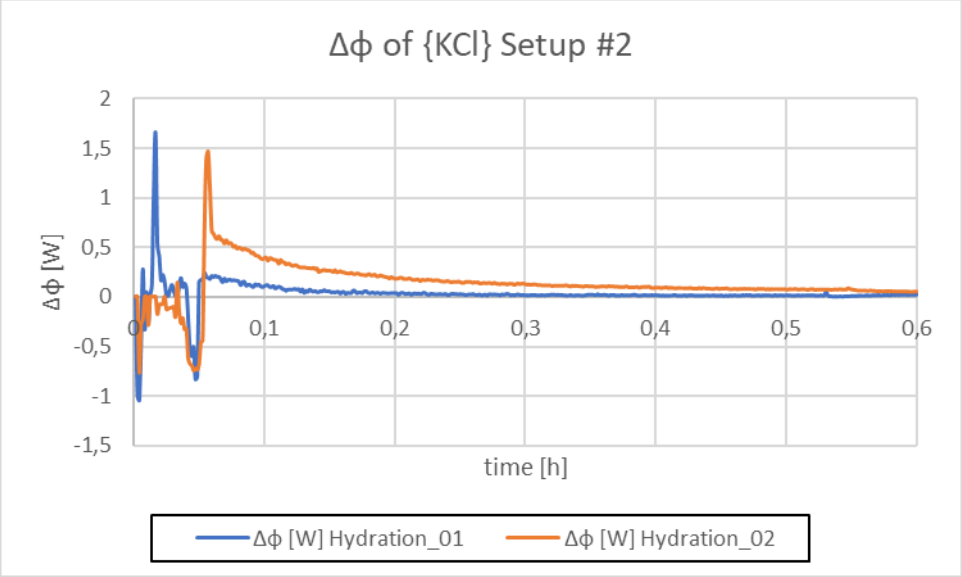

Figure 55 Calculated hydration heat ΔΦ from two cycle measurements of a m_{start} = 20g {KCl·xH_2O} sample evaluated with laboratory scale setup #2 (with water vapor) for a 30 minutes measurement interval. The endothermic peaks at the start of the measurement are an indicator for a phase change from cubic {KCl} to being partially dissolved.

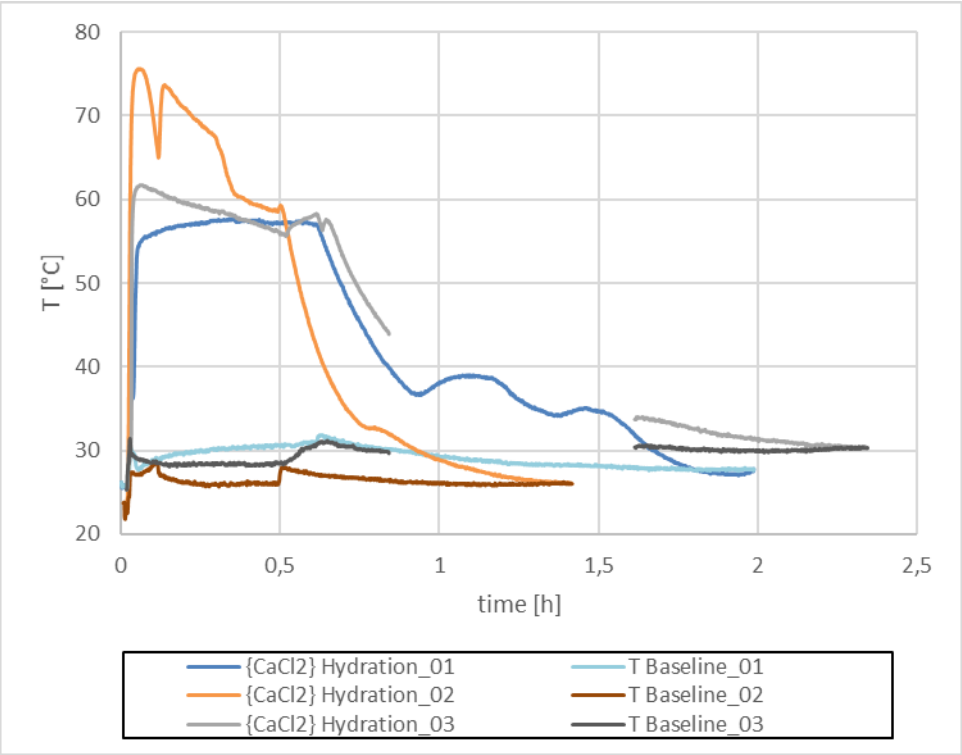

Figure 56 Experimental setup #2, hydration curves of {$CaCl_2 \cdot 6H_2O$} for three cycles. The vacuum was turned off after t ~ 30 to 40min. During the 3rd hydration, the measurement equipment failed to record for a timespan of Δt = 46min before it was reenabled, for that reason there is a gap in the temperature curve and the related baseline.

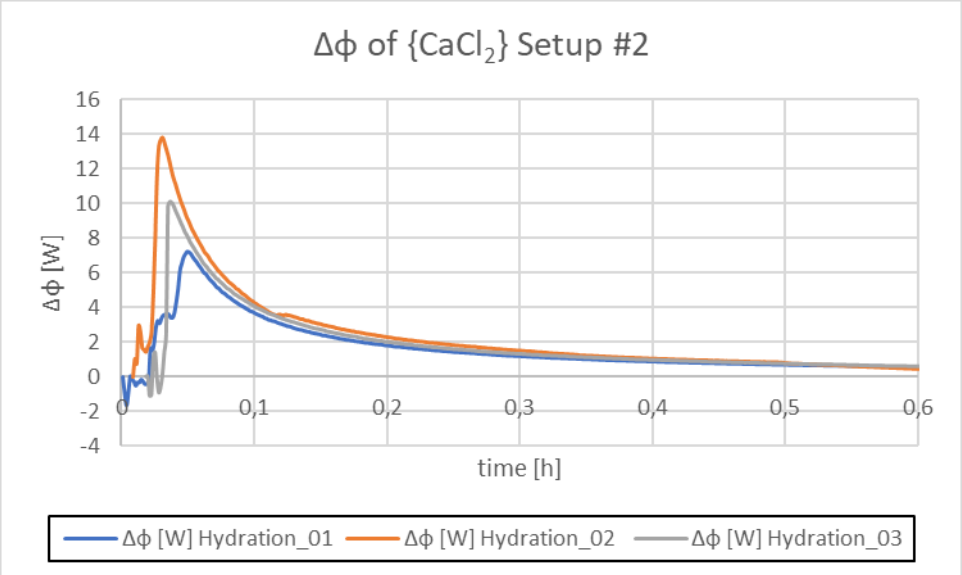

Figure 57 Calculated hydration heat ΔΦ from three cycle measurements of a m_{start} = 20g {$CaCl_2 \cdot xH_2O$} sample evaluated with laboratory scale setup #2 (with water vapor) for a 30 minutes measurement interval. The weak endothermic peaks at the start of the hydration curves are likely artifacts from applying the baseline.

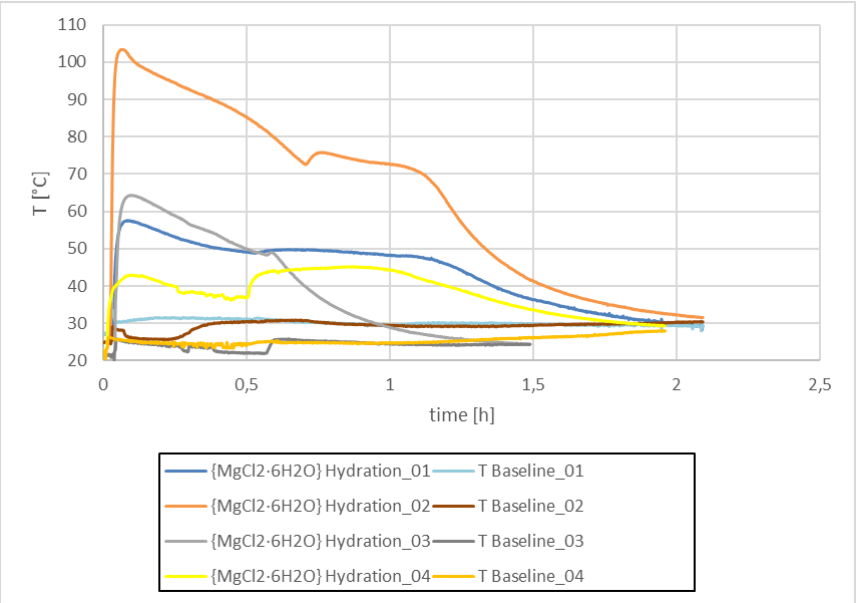

Figure 58 Experimental setup #2, hydration curves of {$MgCl_2 \cdot 6H_2O$} for four cycles. The baseline for the 4th hydration was calculated with the difference in water-temperature between beginning and the end of the measurement instead of difference in sample temperature between start and end, since the material was still reacting at the end of the measurement.

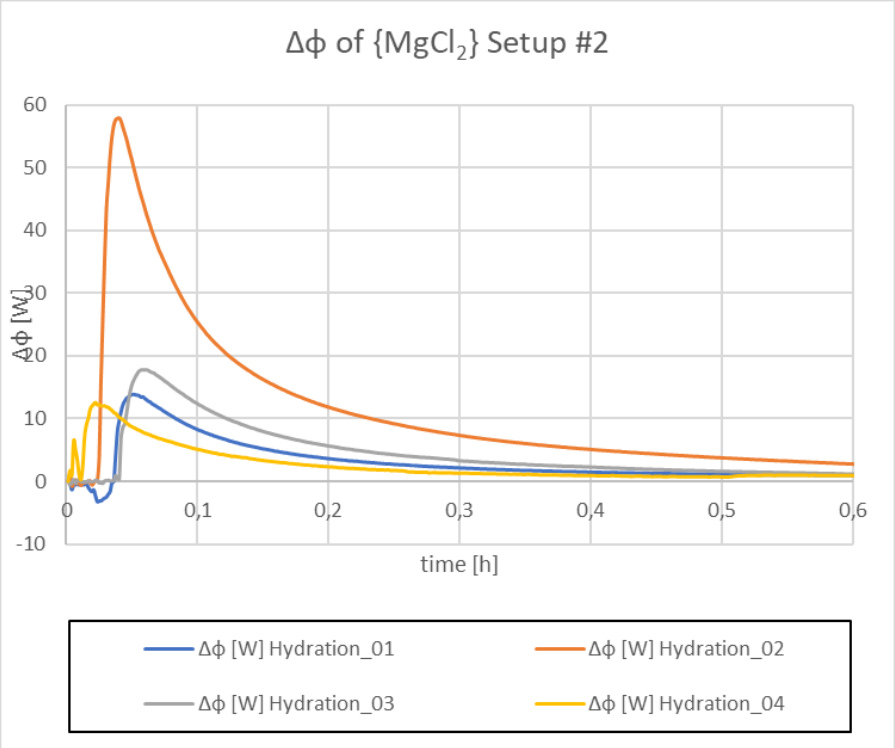

Figure 59 Calculated hydration heat-flow ΔΦ from four cycle measurements of a m_{start} = 20g {$MgCl_2 \cdot 6H_2O$} sample evaluated with laboratory scale setup #2 (with water vapor) for a 30 minutes measurement interval.

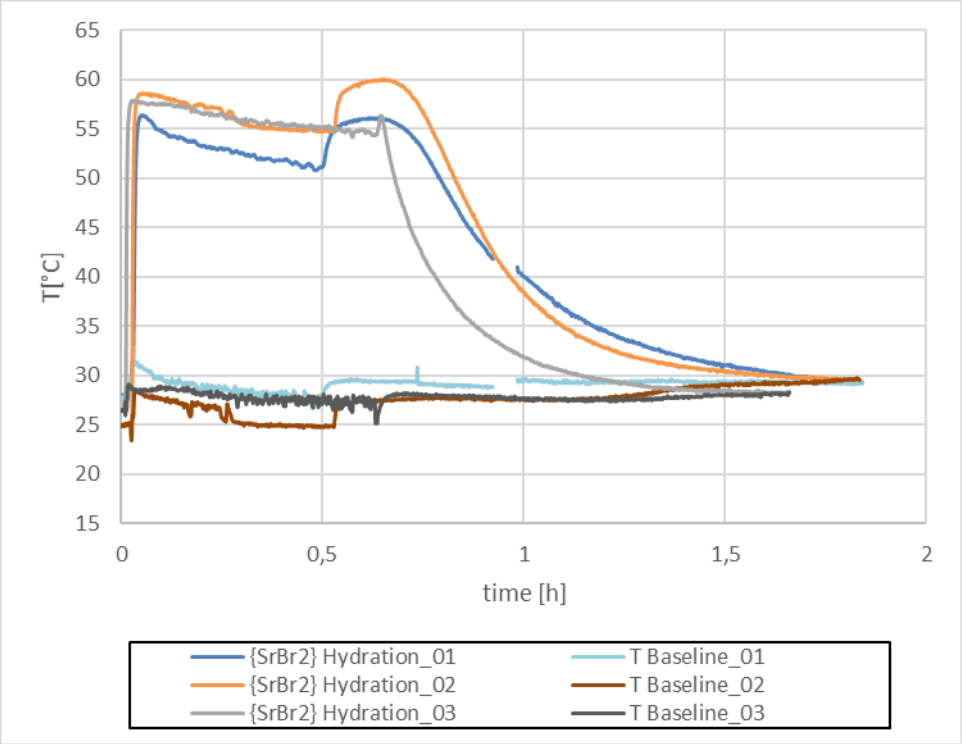

Figure 60 Experimental setup #2, hydration curves of {$SrBr_2 \cdot 6H_2O$} for three cycles.

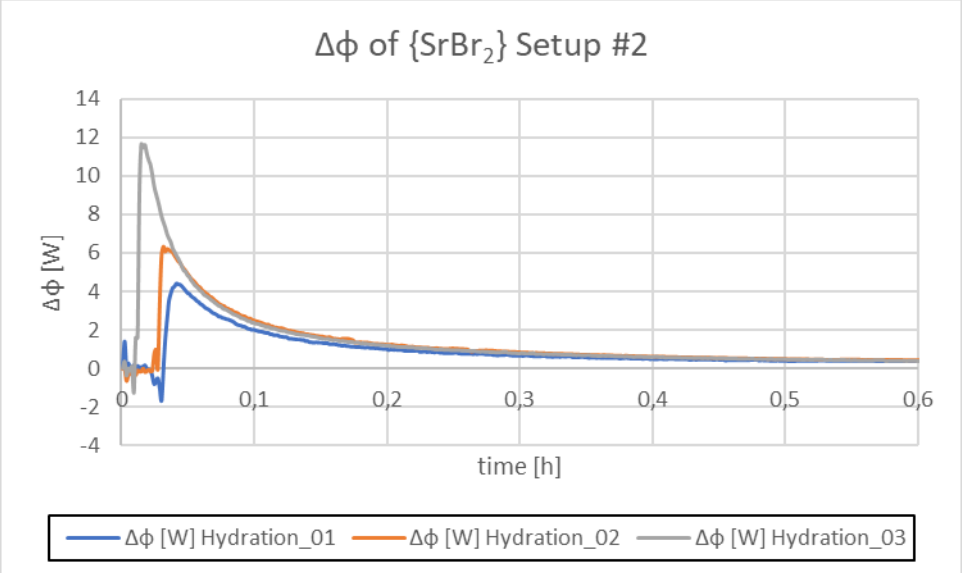

Figure 61 Calculated hydration heat-flow ΔΦ from four cycle measurements of a m_{start} = 20g {$Srbr2_2 \cdot 6H_2O$} sample evaluated with laboratory scale setup #2 (with water vapor) for a 30 minutes measurement interval. The low heat yield is caused by the low specific heat capacity of the {$SrBr_2$}. Distinct endothermic reactions can be seen at the start of each of the hydration curves, which had not been as obvious from the observation of the temperature curves alone.

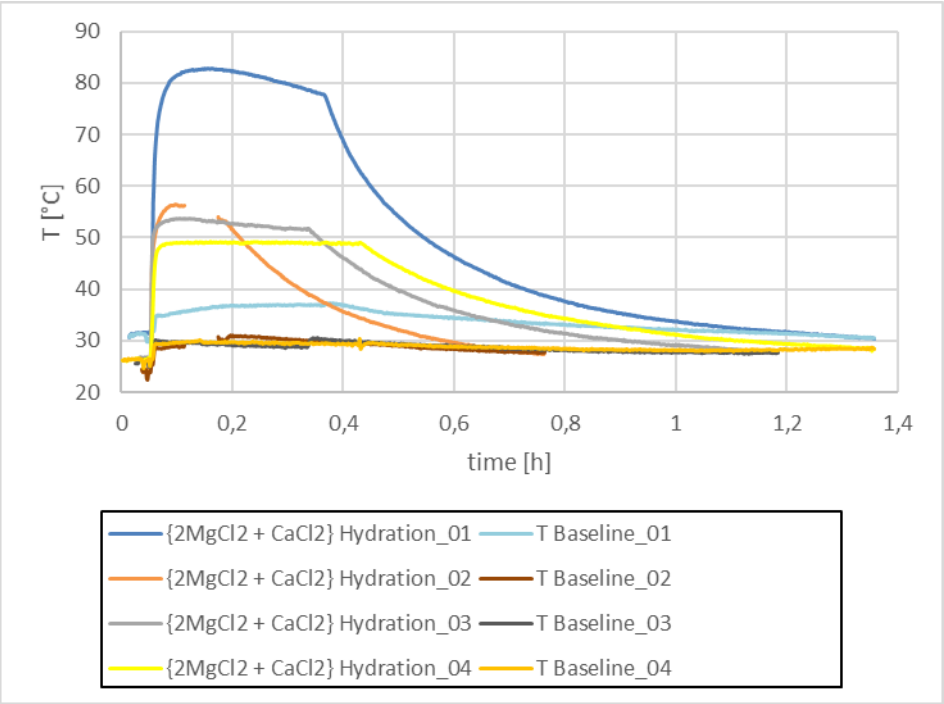

Figure 62 Experimental setup #2, hydration curves of {2MgCl₂ + CaCl₂} for four cycles. The vacuum was turned off after t ~ 30 to 35min.

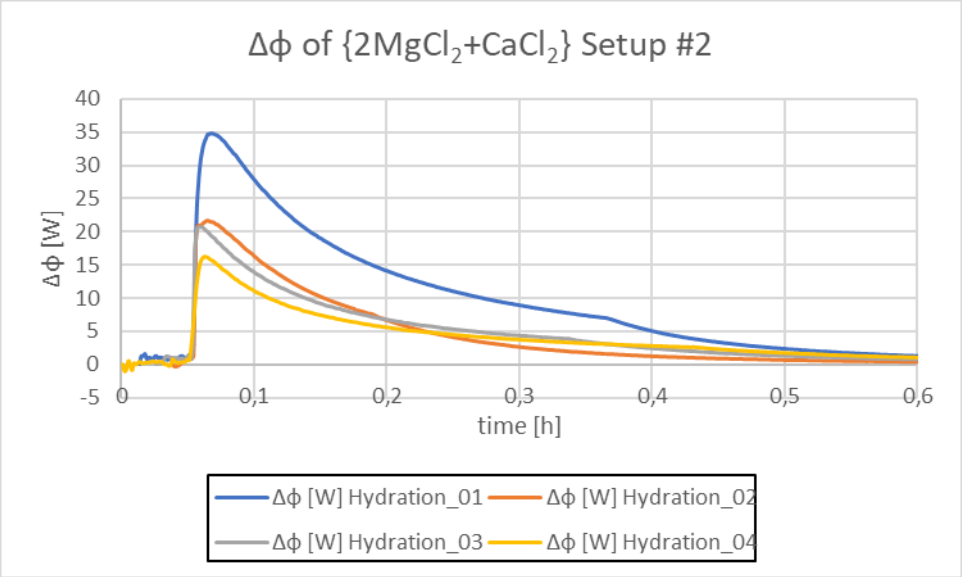

Figure 63 Calculated hydration heat-flow ΔΦ from four cycle measurements of a m_{start} = 20g {2MgCl₂ + CaCl₂ + xH₂O} sample evaluated with laboratory scale setup #2 (with water vapor) for a 30 minutes measurement interval. The low heat yield is caused by the low specific heat capacity of the {SrBr₂}. Distinct endothermic reactions can be seen at the start of each of the hydration curves, which had not been as obvious from the observation of the temperature curves alone.

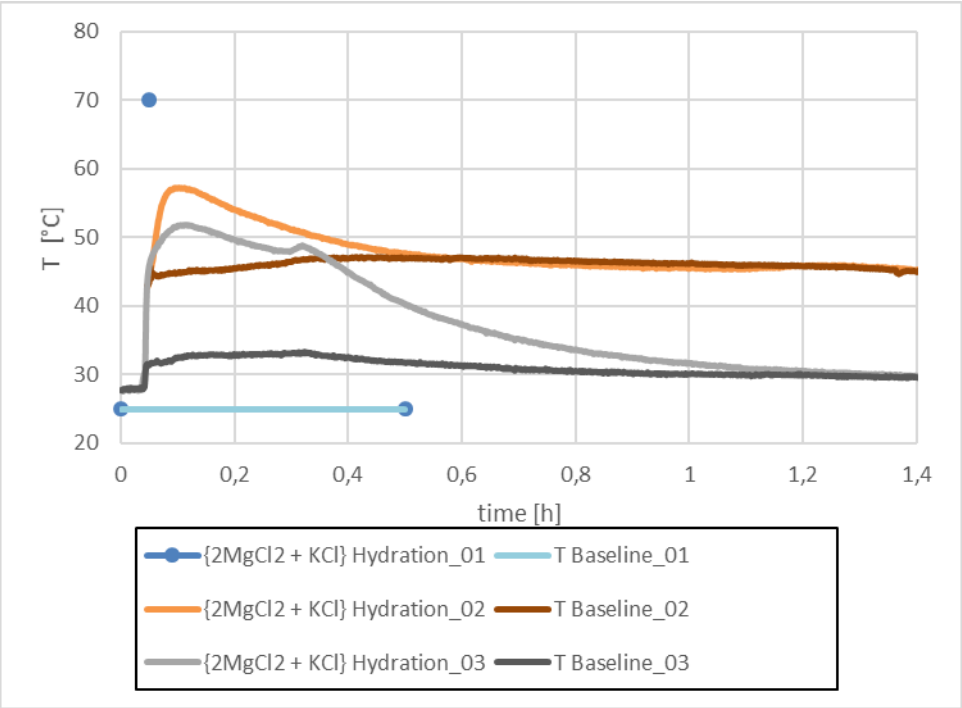

Figure 64 Experimental setup #2, hydration curves of {2MgCl$_2$ + KCl} for three cycles. The vacuum was turned off after t ~ 30 to 35min. During the 1st hydration, the automatic recording of the measurement failed, however the maximum temperature was observed to be T$_{max}$ ~ 70°C. The 2nd hydration shows an unusually high baseline temperature.

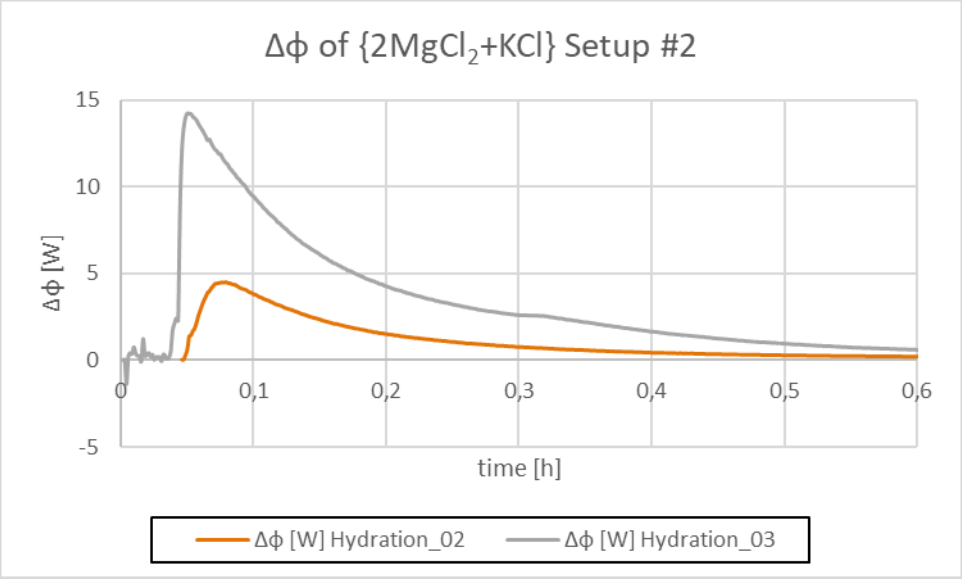

Figure 65 Calculated hydration heat-flow ΔΦ from the 2nd and 3rd cycle measurement of a m$_{start}$ = 20g {2MgCl$_2$ + KCl + xH$_2$O} sample evaluated with laboratory scale setup #2 (with water vapor) for a 30 minutes measurement interval. The recording of data during the hydration of the 1st cycle failed. The heat yield of the 2nd hydration was low because the room temperature and with it the baseline temperature was unusually high.

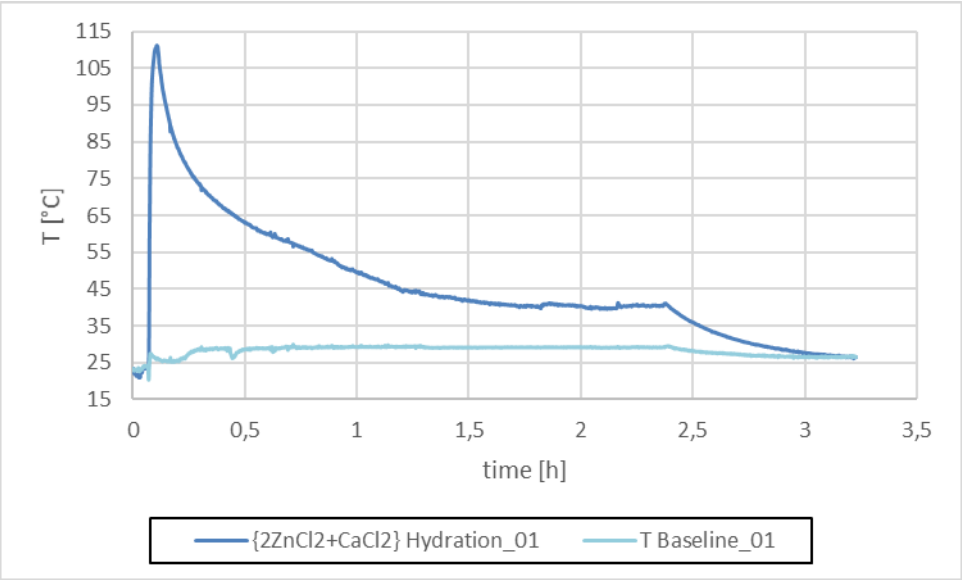

Figure 66 Experimental setup #2, hydration curve of {2ZnCl2+$CaCl_2$}. The vacuum was turned off after t ~ 145min. Only a single cycle could be measured, as the sample dissolved during the 1st hydration and the remaining sample mass melted during the 2nd dehydration.

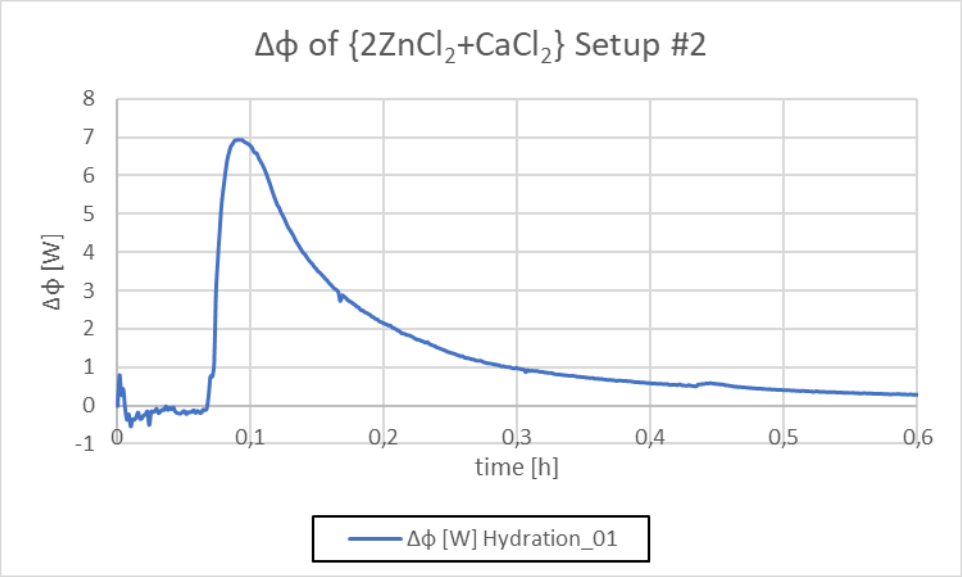

Figure 67 Calculated hydration heat ΔΦ from a single cycle measurement of a m_{start} = 20g {2$ZnCl_2$ + $CaCl_2$ + xH_2O} sample evaluated with laboratory scale setup #2 (with water vapor) for a 30 minutes measurement interval. The relatively strong endothermic peak at the beginning of the hydration event hints at a part of the material having crystallized in a structure of high order like a cubic or hexagonal spacegroup.

6.5. Temperature curves recorded with experimental setup #3 (water vapor supply), specific heat capacity values and heat flow curves

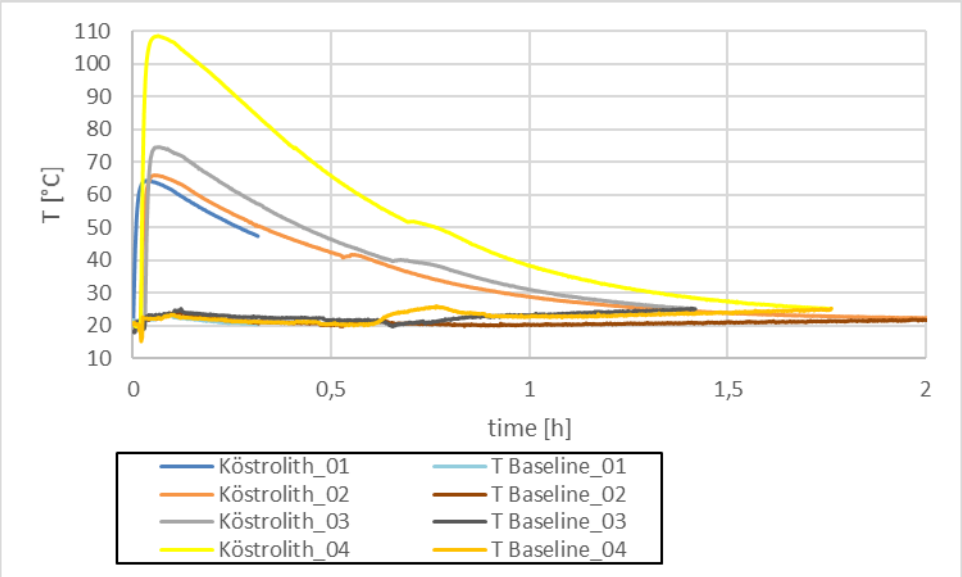

Figure 68 Hydration curves of a Köstrolith sample #1 to #4. The discharged sample was dried in-situ at temperatures of T_{max}= 125°C during measurements #1 to #3. It was dried in the oven at T_{max} = 120°C before measurement #4.

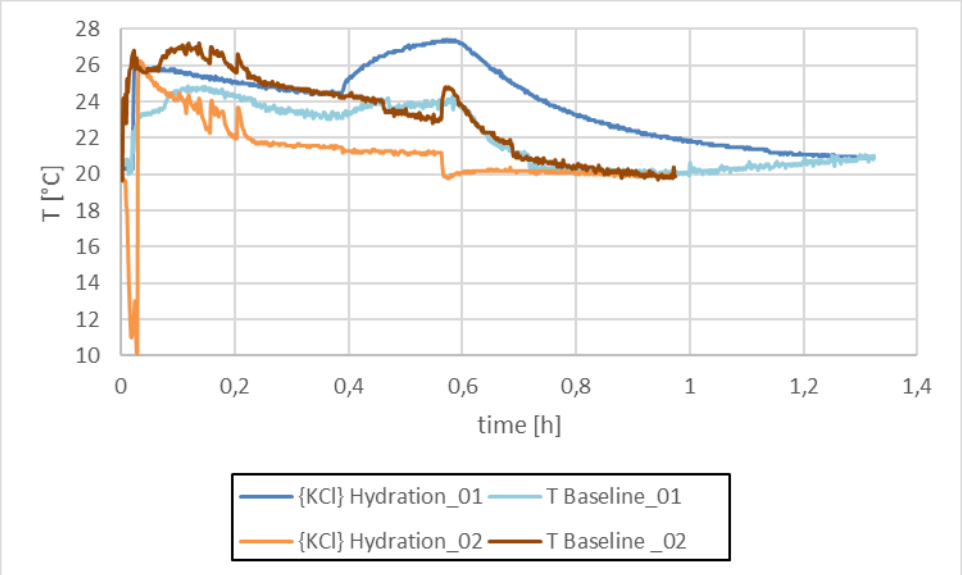

Figure 69 Experimental setup #3, 1st and 2nd hydration of {KCl}. The temperature increased only by a small margin during both hydrations. During the 2nd hydration, a sudden drop in temperature upon initializing the vacuum was observed, this happened before the valve to the water supply was opened.

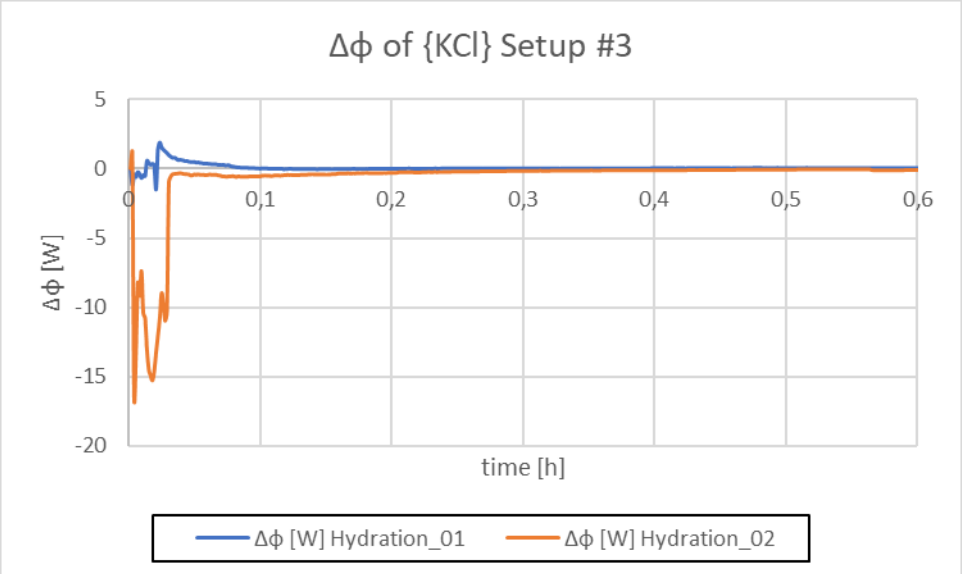

Figure 70 Calculated hydration heat ΔΦ of a m_{start} = 20g {KCl} sample for two cycles, evaluated with laboratory scale setup #3 (with water vapor) for a 30 minutes measurement interval. Only a weak reaction was recorded during the 1st hydration, the reaction during the 2nd hydration was endothermic.

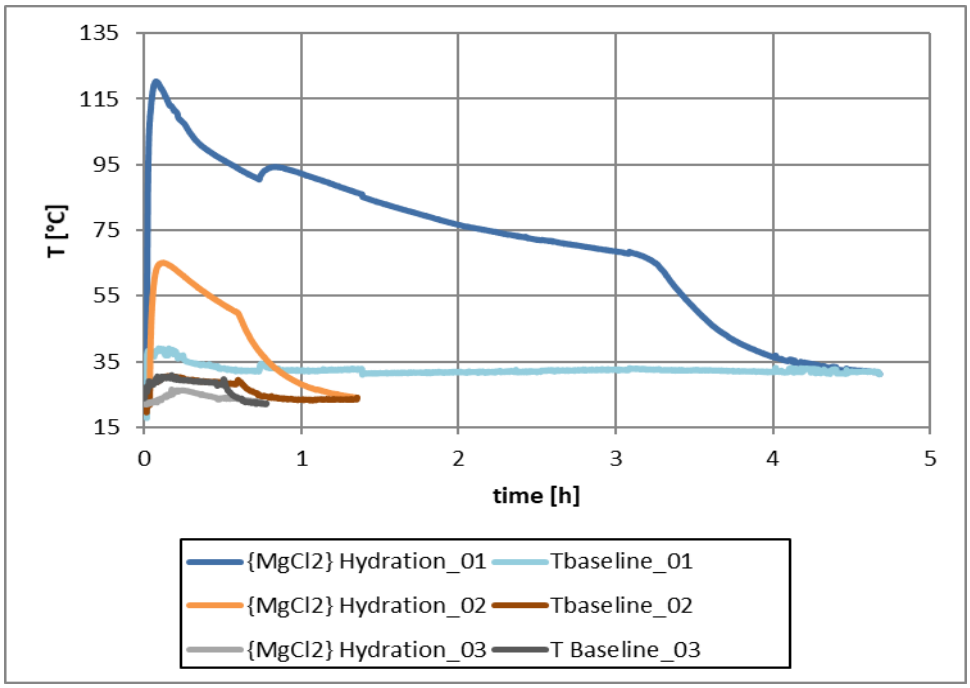

Figure 71 Experimental setup #3, hydration curves #1 to #3 of {$MgCl_2$}. The sample was factory dried at unknown temperature before the 1st hydration. During the 3rd hydration, no vacuum could be established within the apparatus which caused a limitation to the supply of water vapor. Without the vacuum to support the reaction or draw water into the sample-holder, the measured curve of the 3rd hydration is below its corresponding Baseline.

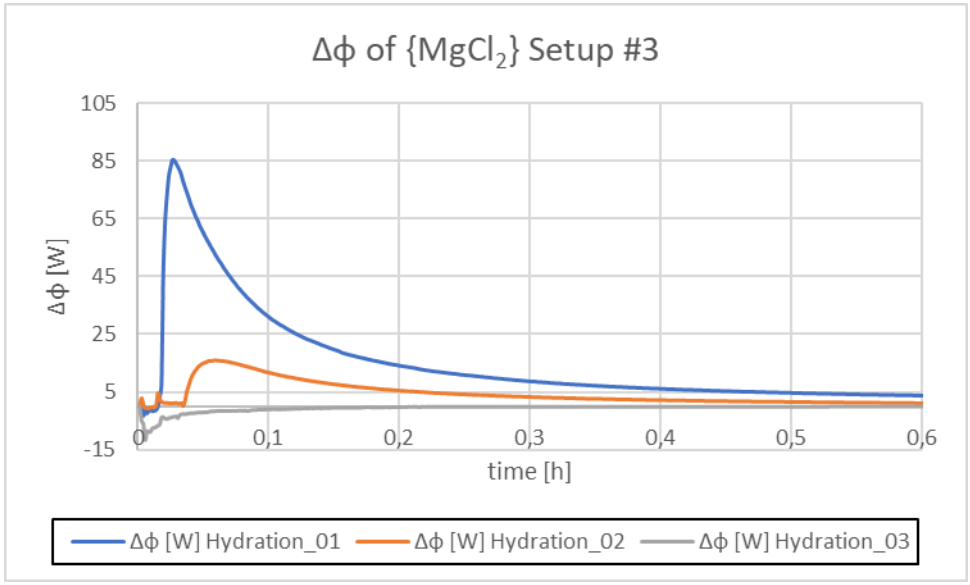

Figure 72 Calculated hydration heat ΔΦ of a m_{start} = 20g {$MgCl_2 \cdot xH_2O$} sample for three cycles, evaluated with laboratory scale setup #3 (with water vapor) for a 30 minutes measurement interval. A decline in heat output can be observed between the 1st and 2nd hydration. A damaged sample holder caused a breach in the vacuum during the 3rd hydration, which resulted in a too low water vapor pressure and a possible emission of excess water from the sample resulting in an endothermic peak.

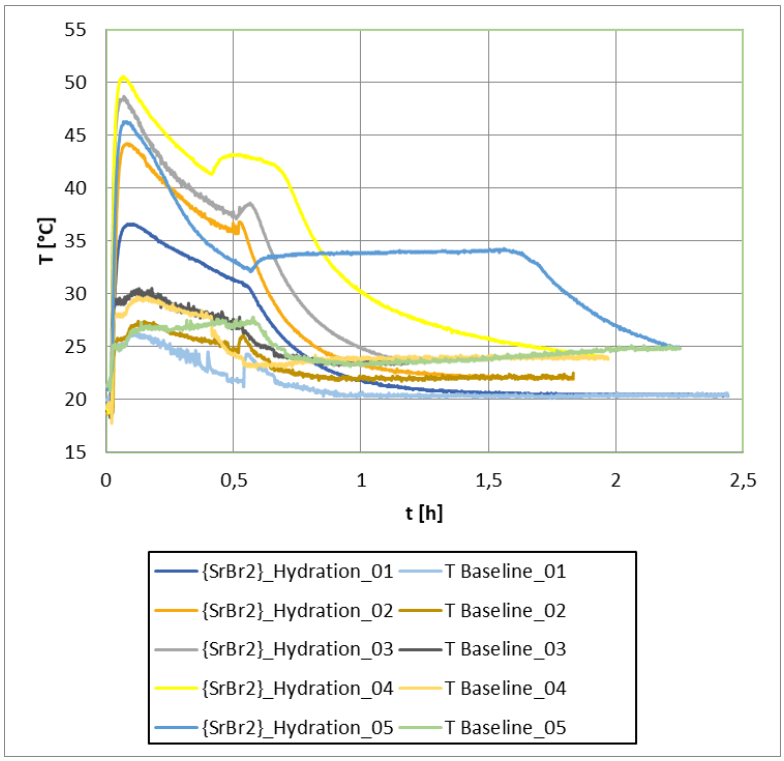

Figure 73 Experimental setup #3, hydration curves #1 to #5 of a {$SrBr_2$} sample. The sample's reaction temperatures and reaction time improves with the progressing cycles.

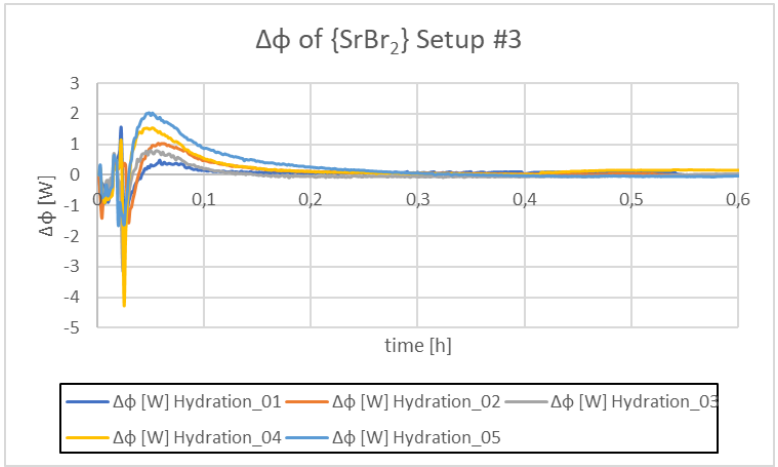

Figure 74 Calculated hydration heat ΔΦ from five cycle measurements of a m_{start} = 20g {$SrBr_2$ + xH_2O} sample evaluated with laboratory scale setup #3 (with water vapor) for a 30 minutes measurement interval. While there is a minor loss of mass between hydrations, it coincides with the material's heat output increasing, indicating that the material is dehydrating to lower stages of hydration rather than melting or dissolving. All curves show four peaks at the start of the hydration. While the first endothermic peak is likely artificial, caused by application of the baselines, the 1st exothermic, followed by the second endothermic peak indicate a phase change to first higher, and then lower order in quick succession, which could explain the halting reaction of the material with water supplied at low water vapor pressures, as the endothermic stage is a hurdle that has to be overcome first.

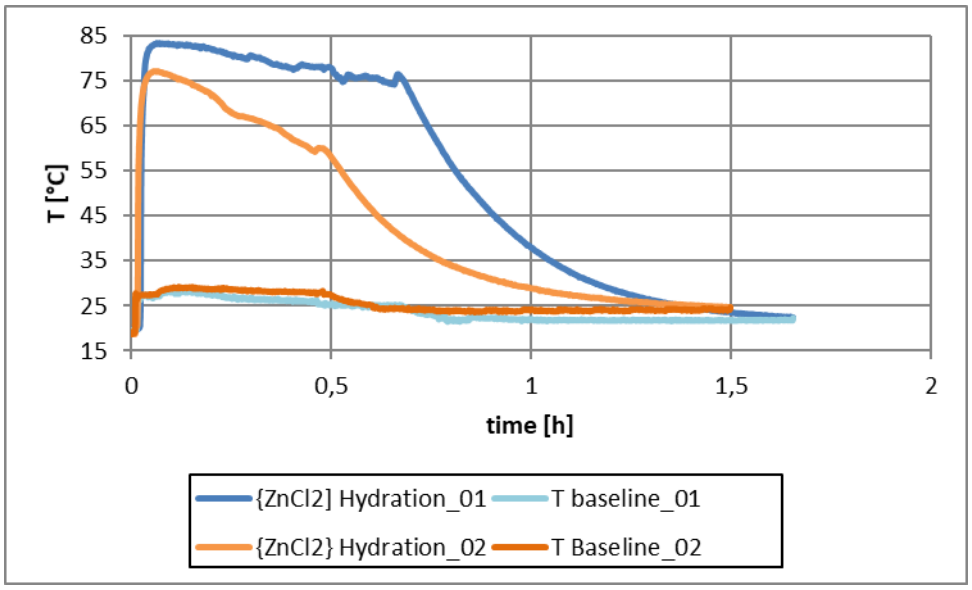

Figure 75 Experimental setup #3, hydration curves #1 and #2 of a {$ZnCl_2$} sample. The sample proved to be unstable at hydration, the deliquescence causing material loss during measurement. This caused a decline in temperature and reaction time between hydration #1 and #2.

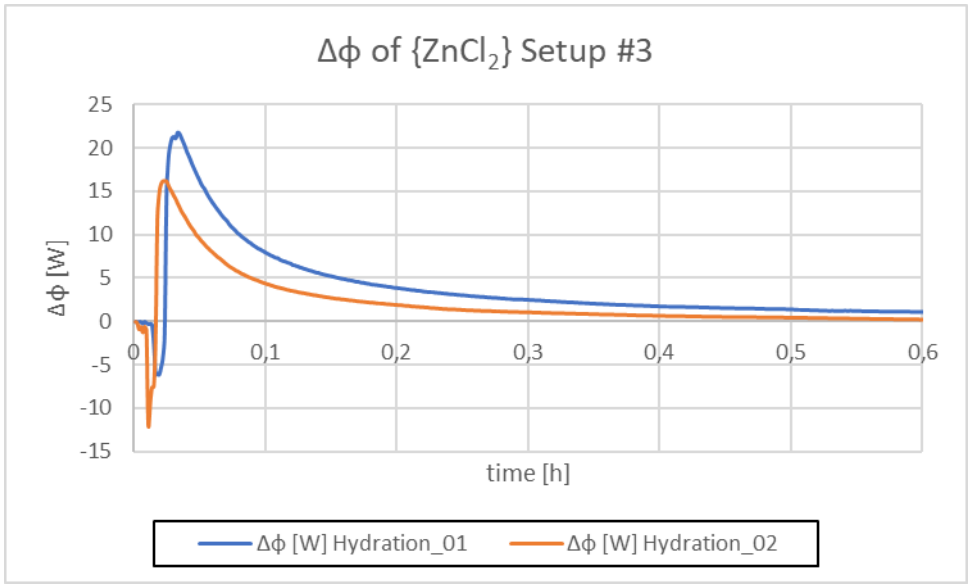

Figure 76 Calculated hydration heat ΔΦ from two cycle measurements of a m_{start} = 20g {$ZnCl_2$ + xH_2O} sample evaluated with laboratory scale setup #3 (with water vapor) for a 30 minutes measurement interval. A decline in heat output can be observed between the two hydrations, it coincides with a massive mass loss due to melting. Two strong endothermic peaks can be observed at the start of both hydration curves, indicating that the material had partially crystallized in a structure of high order such as cubic or hexagonal during the previous dehydrations.

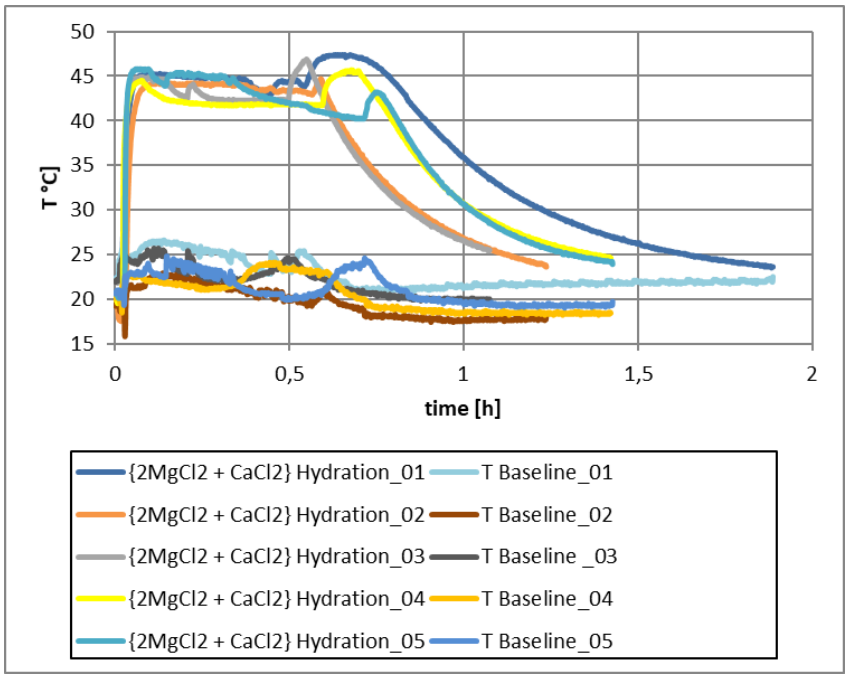

Figure 77 Experimental setup #3, hydration curves of {2MgCl2+CaCl₂} for 5 cycles. The temperature yield remains stable over five cycles, only declining once the vacuum pump and with it the constant supply of water vapor are turned off. The recordings ended before the material completely cooled down to room temperature.

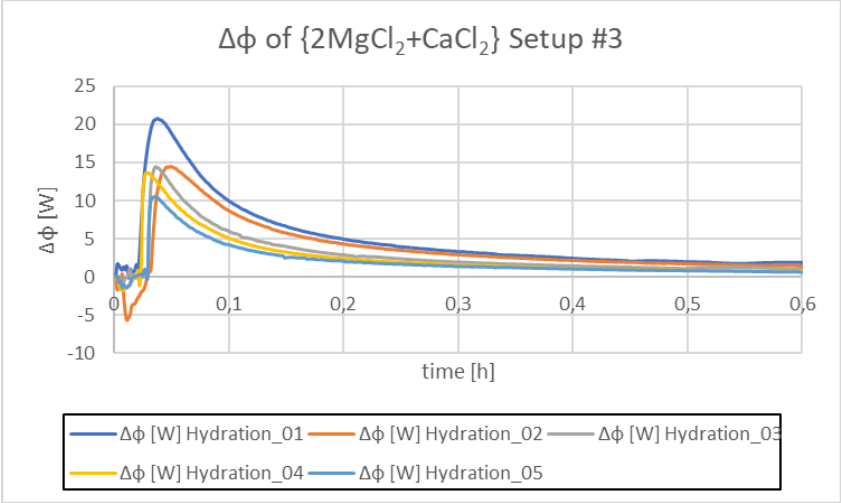

Figure 78 Calculated hydration heat ΔΦ from five cycle measurements of a m_{start} = 20g {$MgCl_2$ + KCl + xH_2O} sample evaluated with laboratory scale setup #3 (with water vapor) for a 30 minutes measurement interval. While most of the endothermic activity calculated for the five curves is likely an artifact from applying the baseline, the curve from the 2nd hydration shows a distinct endothermic peak, indicating that the material had partially crystallized in a structure of high order like cubic or hexagonal during the previous dehydration. While the heat output remained relatively stable between the cycles #2 to #4, the output rapidly decreases during the 5th hydration. As a distinct material loss due to melting was recorded and observed, it is possible, that the material, reduced to below half its original weight was able to expel heat to the environment faster while less densely packed.

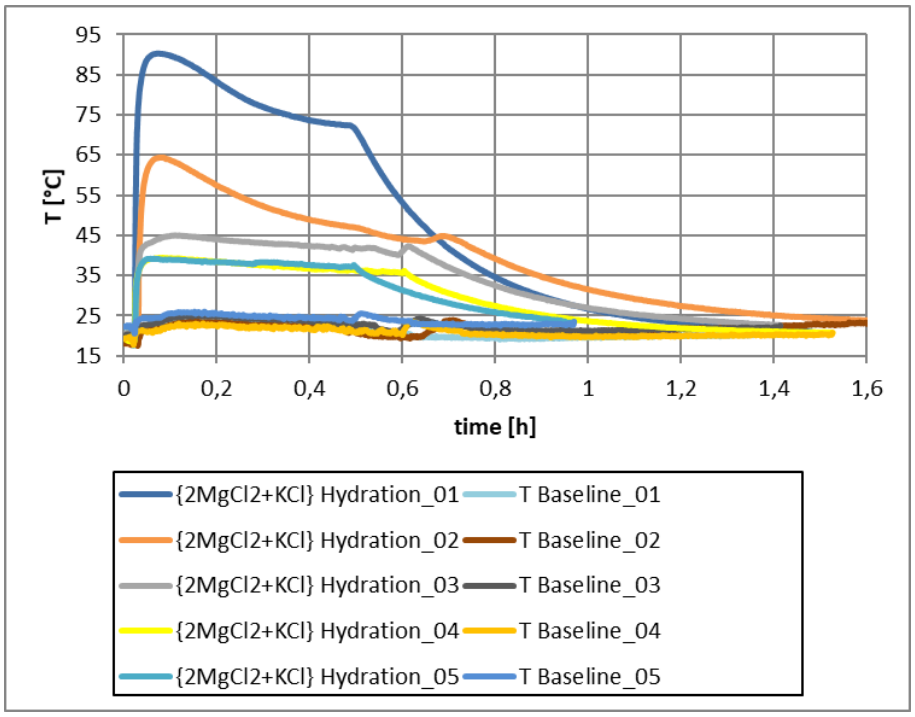

Figure 79 Experimental setup #3, hydration curves of {2MgCl2+KCl} for 5 cycles. The temperature yield decreases with each measurement until it stabilizes at the 4th cycle.

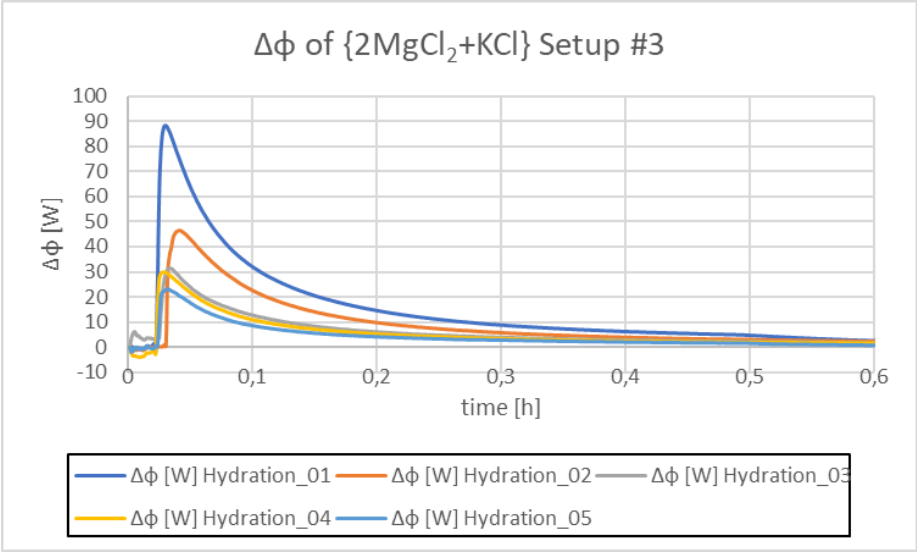

Figure 80 Calculated hydration heat ΔΦ from five cycle measurements of a m_{start} = 20g {$MgCl_2$ + KCl + xH_2O} sample evaluated with laboratory scale setup #3 (with water vapor) for a 30 minutes measurement interval. The material's heat output declined with every cycle until it stabilized at the 4th cycle. A steady gain of sample weight indicated an incomplete dehydration. The material didn't show any melting behavior and did not agglomerate as strongly as the untreated {$MgCl_2$} sample did.

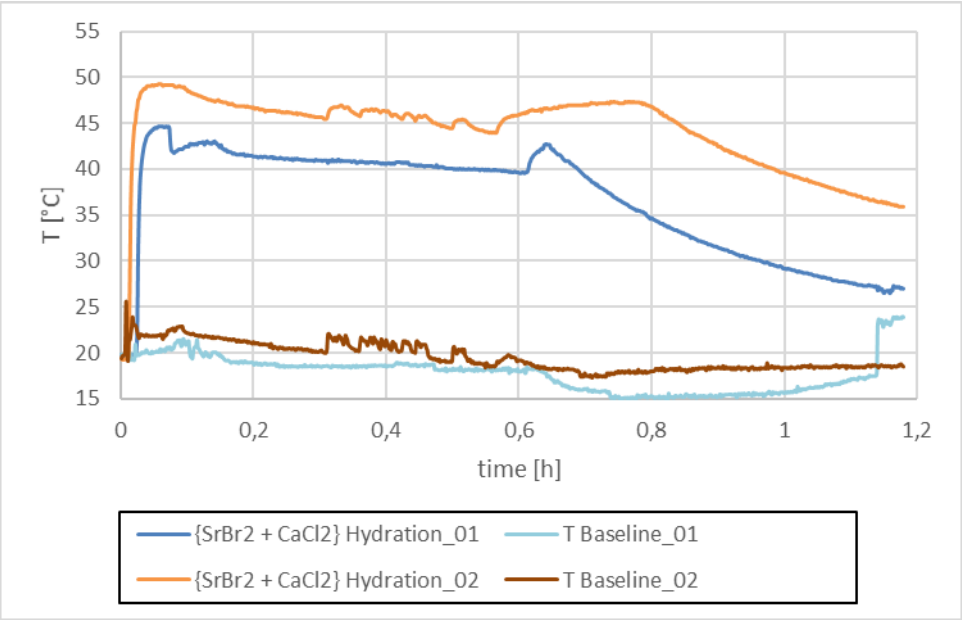

Figure 81 Experimental setup #3, hydration curves #1 and #2 of a {5$SrBr_2$ + 8$CaCl_2$} sample. During the 2nd hydration the automatic temperature recording ended before the sample was completely cooled down.

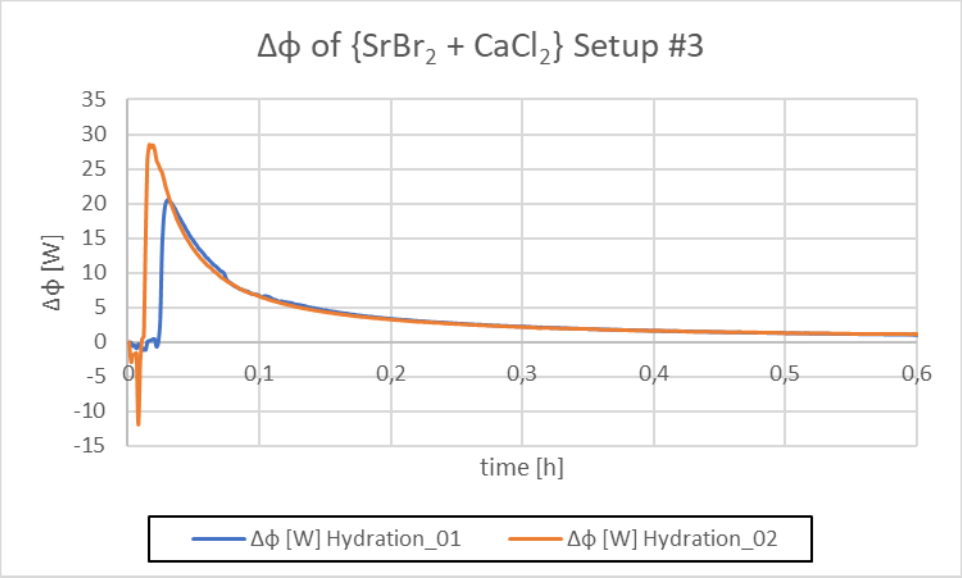

Figure 82 Calculated hydration heat ΔΦ from two cycle measurements of a m_{start} = 20g {5$SrBr_2$ + 8$CaCl_2$ + xH_2O} sample evaluated with laboratory scale setup #3 (with water vapor) for a 30 minutes measurement interval. The material increases its heat output between measurements, this may have been caused by partial material loss due to melting, resulting in an easier dehydration of the material remaining within the sample holder. There are short but strong endothermic peaks at the beginning of both hydration events, they hint at a part of the material having crystallized in a structure of high order like a cubic or hexagonal spacegroup.

Table 58 Calculated Enthalpy ΔH for the materials evaluated in the laboratory scale setups #2 and #3.

Material	n of cycles	Setup #2		Setup #3	
		T_{peak} [°C]	ΔH [Jg^{-1}]	T_{peak} [°C]	ΔH [Jg^{-1}]
{$CaCl_2 \cdot xH_2O$}	#1	25.5 57.7	-1.60 172.21	---	---
	#2	75.6	244.52	---	---
	#3	25.3 61.7	-0.27 194.82	---	---
{KCl}	#1	21.0 21.6 21.0 27.5	-0.70 1.29 -0.85 3.18	20.3 25.9 25.0 27.0	-1.03 6.47 -0.21 1.75
	#2	16.9 25.6	-2.37 15.71	10.1	-78.01
{$MgCl_2 \cdot xH_2O$}	#1	27.1 30.3	-8.58 328.79	20.0 120.4	-3.83 1612.13
	#2	103.4	1217.94	23.3 65.2	5.66 458.52
	#3	64.3	480.39	21.9	-70.01
	#4	22.8 42.9	4.67 259.13	---	---
{$SrBr_2 \cdot xH_2O$}	#1	28.0 27.9 56.4	0.48 -1.37 94.25	19.3 21.7 22.3	-1.33 1.06 -1.98

				36.6	8.90
	#2	24.8	-0.66	18.6	-1.75
		58.6	140.65	19.7	0.65
				19.8	-1.73
				44.2	17.15
	#3	26.4	-0.21	18.7	-0.70
		57.9	57.40	19.1	0.42
				19.7	-3.05
				48.7	8.19
	#4	---	---	18.7	-1.58
				19.4	0.48
				19.4	-2.31
				50.6	25.06
	#5	---	---	20.9	-1.12
				22	0.32
				22.1	-2.33
				46.3	33.94
{$ZnCl_2 \cdot xH_2O$}	#1	---	---	19.6	-6.33
				83.3	412.27
	#2	---	---	18.7	-14.60
				77.1	332.86
{$2MgCl_2 + CaCl_2 + xH_2O$}	#1	82.9	1020.42	45.3	548.44
	#2	56.5	593.70	17.5	-13.49
				44.2	528.07
	#3	53.6	846.11	21.8	-1.44

				44.9	515.61
	#4	49.2	890.79	19.5 44.5	-4.83 563.88
	#5	---	---	20.1 45.8	-5.27 556.72
{2$MgCl_2$ + KCl + xH_2O}	#1	~70.0	---	18.2 90.3	0.37 1603.45
	#2	57.3	106.48	17.9 64.4	-2.50 903.45
	#3	51.7	312.63	45.0	569.58
	#4	---	---	18.5 39.4	-8.92 472.13
	#5	---	---	22.0 39.2	-1.42 392.88
{5$SrBr_2$ + 8$CaCl_2$ + xH_2O}	#1	---	---	44.7	429.85
	#2	---	---	19.3 49.2	-7.87 564.74
{2$ZnCl_2$ + $CaCl_2$ + xH_2O}	#1	21.1 111.3	-1.96 150.07	---	---

7. List of used chemicals

Table 59 Materials used for TGA/DSC analysis, laboratory scale experiments and material synthesis

Substance	CAS No.	Article No.	Manufacturer	Purity	Amount	M [gmol^{-1}]
Aluminiumsulfat-18-Hydrat		1102	Merck	Reinst DAB, Ph Eur, BP	1,000g	666.42
Zinc Sulfate heptahydrate $ZnSO4{\cdot}7H2O$	7446-20-0	1088831000	Sigma-Aldrich (Merck)	ACS, ISO, Reag. Ph Eur 99.5 - 103.0 %	1,000g	287.54
Iron(II) sulfate heptahydrate	7782-63-0	A3586.1000	Applichem	p.A. 99,5%	1,000g	278.02
Kaliumsulfat		X889.2	Roth	>= 99% krist.	1,000g	174.27
Magnesiumsulfat heptahydtrat		A677186615	Merck	p.A. Ph Eur	500g	246.48
Natriumsulfat wasserfrei		A924886 803	Merck	Wasserfrei zur Synthese >=99,0%	1,000g	142.04
Magnesiumchlorid		KK36.2	Roth	>= 98,5%	500g	95.22
Calcium chloride	10043-52-4	K44296278	Merck	Reag. Ph Eur 98,0%	500g	110.98
Calcium chloride-Hexahydrate reinst		A693072	Merck	DAB, Ph Eur 98.0-101.0%	1,000g	219.09
Potassium chloride	7447-40-7	LCL.L4292.1000	Scharlau	Ph Eur, BP USP Extra pure 99-100.5%	1,000g	74.56
Zinc chloride $ZnCl_2$	7646-85-7	B974916 230	Merck	p.A. ACS, ISO 98%	250g	136.28
Magnesium bromide hexahydrate	13446-53-2	LCL.L5800.1000 A0306103	Acros organics	99+% for analysis	1,000g	292.21
Calciumbromide hydrate $CaBr_2 \cdot xH_2O$	71626-99-8	MKBP7919V	Sigma-Aldrich (Merck)	98%	100g	199.89
Lithiumbromid LiBr		5669	Merck	Erg. B. 6	100g	86.85
Natriumbromid NaBr		K30615060225	Merck	reinst Ph Eur, BP 98-100.5%	1,000g	102.9

Kaliumbromid KBr		K28151805 049	Merck	p.A. ACS 99.5%	500g	119.01
Strontium bromide hexahydrate $SrBr_2 \cdot 6H_2O$	7789-53-9	B22553	Alfa Aesar	99%	100g	
Strontium bromide hexahydrate	7789-53-9	143214	Chemos GmbH		25,000g	

Table 60 Drying agents

Substance	CAS No.	Article No.	Manufacturer	Purity	Amount
Silica Gel orange		P077.2	Roth	2-5mm, with Indikator beads	2,500g
Köstrolith			CWK-Bad Köstritz	2.5 – 5.0mm beads	Sample package
Calciumchlorid wasserfrei	10043-52-4		Lolab	Reinst-Chemie 97.0% powder	5,000g
Zinkchlorid	7646-85-7		Lolab	Reinst Min. 97.0%	5,000g

7.1. Köstrolith

Köstrolith is a zeolithic compact molded molecular sieve with a 100% active component ratio (CWK Chemiewerk Bad Köstritz GmbH, 2017).

Zeolithes crystallize in the form of $\{M_{x/m} \cdot Al_xSi_{y-x}O_4 \cdot nH_2O\}$ (Wiley Information Services GmbH, 2016).

Table 61 Köstrolith material data (CWK Bad Köstritz, 2013)

Köstrolith	Pore size [Å]	Chemical formula	Molecular sieve type
13XBFK	9	$\{Na_2O \cdot Al_2O_3 \cdot mSiO_2 \cdot nH_2O\}$	NaMSX (FAU)
4ABFK	4	$\{Na_2O \cdot Al_2O_3 \cdot 2SiO_2 \cdot nH_2O\}$	A (LTA)

8. Index of figures

9. Index of tables